PASSIVE SOLAR ENERGY:

MODIFICATIONS OF EXISTING MASONRY WALLS

TO IMPROVE THERMAL PERFORMANCE

By

P.M. Boyle

Submitted in fulfilment of the requirements
for the degree of Doctor of Philosophy

THE UNIVERSITY OF LEEDS
DEPARTMENT OF CIVIL ENGINEERING

JANUARY 1986

To

my

Parents

Abstract

Existing brick walls usually have a high U value. One method of improvement is by insulation, but if the wall faces approximately south, it is possible that greater benefits could be obtained by improving the wall's performance as a solar collector. Three solid 225 mm walls were constructed: one glazed, one unglazed, and (since glazing prevents rain penetration) one waterproofed unglazed wall. Two glazed cavity walls were also constructed one glazed with a fan to recover heat from the cavity by forced convection, and one unglazed, with no fan. These walls gave small heat gains.

The walls behind the glazing were then insulated on their outer faces, and warm air collected by natural convection. Such a collector was built using a selective surface, a maximum efficiency of about 50% was observed. A theoretical model was developed based on simple steady state theory, this was found to correlate well with experimental data. The theory could be used for any system of low thermal storage, including forced flow collectors.

Fainally these walls, and others, are compared and their reletive merits discussed.

ACKNOWLEDGEMENTS

The author would like to thank Professor A.R. Cusens, head of the Department of Civil Engineering, and particular thanks are due to Dr D. Fitzgerald and Dr W. Houghton-Evans for their help and encouragement.

He also wishes to thank the staff of the Civil Engineering workshop, particularly Mr R. Keene, Mr P. Richards and Mr J. Howarth.

Mr G. Broadhead for his electrical expertise.

Mr R. Duxbury for the photographic work.

Mr A. Butler and Mr R. Allinson, of the University Maintenance department, for building the brick walls for this project.

The Science and Engineering Research Council for providing financial support.

Friends and colleagues for their encouragement.

Lastly the author would like to thank his wife whose patience and encouragement has been a continual help.

Contents

Chapter 1 -	Introduction	1
Chapter 2 -	Review of Related Work	17
Chapter 3 -	Masonry Walls - Experimental Work	29
Chapter 4 -	Masonry Walls - Experimental Results, the Effect of Reduced Rain Penetration due to Glazing.	43
Chapter 5 -	Masonry Walls - Experimental Results, Effect of Glazing on Solar Gain.	53
Chapter 6 -	Natural Convection Collectors - Theory	68
Chapter 7 -	Description of Natural Convction Computer Model	97
Chapter 8 -	Natural Convection Experimental work and Results	1Ø2
Chapter 9 -	Comparison of Wall Types	125
Chapter 1Ø -	General Conclusions	159
Appendix 1 -	Data File for NATCONV Programs	167
Appendix 2 -	Rehabilitation Using Forced Convection	168
Appendix 3 -	Calculation of Radiation Heat Transfer Co-efficients	195
References		199

Nomenclature

a	absorptivity	
b	breadth	m
c	specific heat capacity	J kg^{-1} K^{-1}
d	overall thickness, gapwidth	m
dt	time interval	s
dx,dt	co-ordinate distance intervals	m
f	friction factor	
g	acceleration due to gravity	m s^{-2}
h	heat transfer co-efficient	W m^{-2} K^{-1}
k	thermal conductivity	W m^{-1} K^{-1}
p	pressure	N m^{-2}
q	heat flow	W m^{-2}
s	transmission factor	
t	time	s
tai	inside air temperature	C
tao	outside air temperature	C
teo	solair temperature	C
v	velocity	m s^{-1}
x,y	co-ordinate distances	m
A	area	m^2
Gr	Grashof number	
L	height	m
Pr	Prandtl number	
Q	insolation	W m^{-2}
Ra	Rayleigh number	

Re	Reynolds number	
R	thermal resistance	$m^2 K W^{-1}$
U	thermal transmittance	$W\ m^{-2}\ K^{-1}$
V	ventilation loss	$W\ K^{-1}$

Greek symbols

α	thermal diffusivity	$m^2\ s^{-1}$
β	co-efficient of volumetric expansion	K^{-1}
δ	depth of boundary layer	m
ε	emissivity	
μ	dynamic viscosity	$kg\ m^{-1}\ s^{-1}$
ν	kinematic viscosity	$m^2\ s^{-1}$
ϕ	phase lag	h

Subscripts

e	equivalent
i	input
g	glass, window
lam	laminar
si	inside surface
so	outside surface
th	thermal
turb	turbulent
vel	velocity

Other symbols are defined in the text. Many of the equations are valid only for SI units.

Chapter 1

Introduction

Building regulations for the thermal insulation of new buildings are stringent and are likely to become more so. There are, however, no similar regulations covering older buildings and it is difficult to design effective ways of improving them.

A survey of housing by the Department of the Environment, 1980-81, (1) shows that 50% of the houses in Great Britain, date from before 1945 and 30% from before 1918. Older houses will mostly have brick or masonry walls. Insulation for such houses is becoming available, but outside insulation is difficult to weatherproof and inside insulation greatly disturbs inside finishes and decorations and excludes any benefit from the thermal storage in the fabric. Both methods are expensive.

Houses built after 1945 until about ten years ago will again be mostly of brick but are likely to have cavity walls. Insulating cavity walls is relatively easy and is reasonably effective.

It may be that the thermal storage of masonry, whether single leaf or cavity, could be utilised in passive solar heating. Systems such as the Trombe wall are now fairly well developed for buildings in appropriate

climates, and more sophisticated versions can be used in Britain, for example as shown by Lee (14). It might well be that such systems would be suitable for rehabilitation of older buildings. To be worthwhile such systems would not only have to give adequate heat savings but also be simple, maintainance free, long-lasting and cheap. The aim of this thesis is to look at some of the possibilities of using passive solar energy for rehabilitation.

1.2 - Potential of Passive Solar Heating in the United Kingdom

10 year average data from the Meteorological Office, show that the global solar input on a south facing vertical surface, during a heating season between October and April is 1400 MJ/m^2. For a single glazed, dark surface the average solair temperature, over the heating season, would be 18.6°C, but in March, April and October the average solair temperature would be above 20°C. This would also be true of May and September when heating is also frequently required. The significance of these figures is that for an inside temperature of 18°C a wall protected by external clear glazing would be a net gainer over the whole of the heating season. For an inside temperature of 20°C the wall would still be a net gainer for half of the heating season. Such an arrangement clearly has potential, worthy of more detailed calculations which will be presented later.

The above calculations are 24 hour averages but buildings are not occupied or heated continuously. Fig 1.1 shows the typical behaviour of a glazed masonry wall on a sunny day. Between 1800 and midnight the room will gain heat when it is most required in domestic buildings. In order to assess this effect the use of unsteady state calculations is required, this will be done below.

1.3 - Possible Passive Solar Systems

The simplest passive solar device would consist of glazing on the outside of the masonry wall to utilise the greenhouse effect to increase the solar gain, fig 1.2 shows two of the possibilities.

In section 1.2 above a value for the global solar radiation over the heating season of 1400 MJ/m^2 (average insolation 60 W/m^2 [Q_{24}]) was used. Most of this is diffuse radiation. During the time when there is direct radiation (average 3 h/day), the global radiation incident on a south facing wall is only 300 MJ/m^2 (average insolation for the 3 hours direct radiation 103 W/m^2 [Q_S]). With this amount of solar radiation the contribution by convection from a Trombe wall would not be worthwhile, unless a more efficient convection collector were to be used. However, an advantage of the conduction component is that there is a phase lag of several hours between the solar input and the gain to the room. This is useful for houses occupied

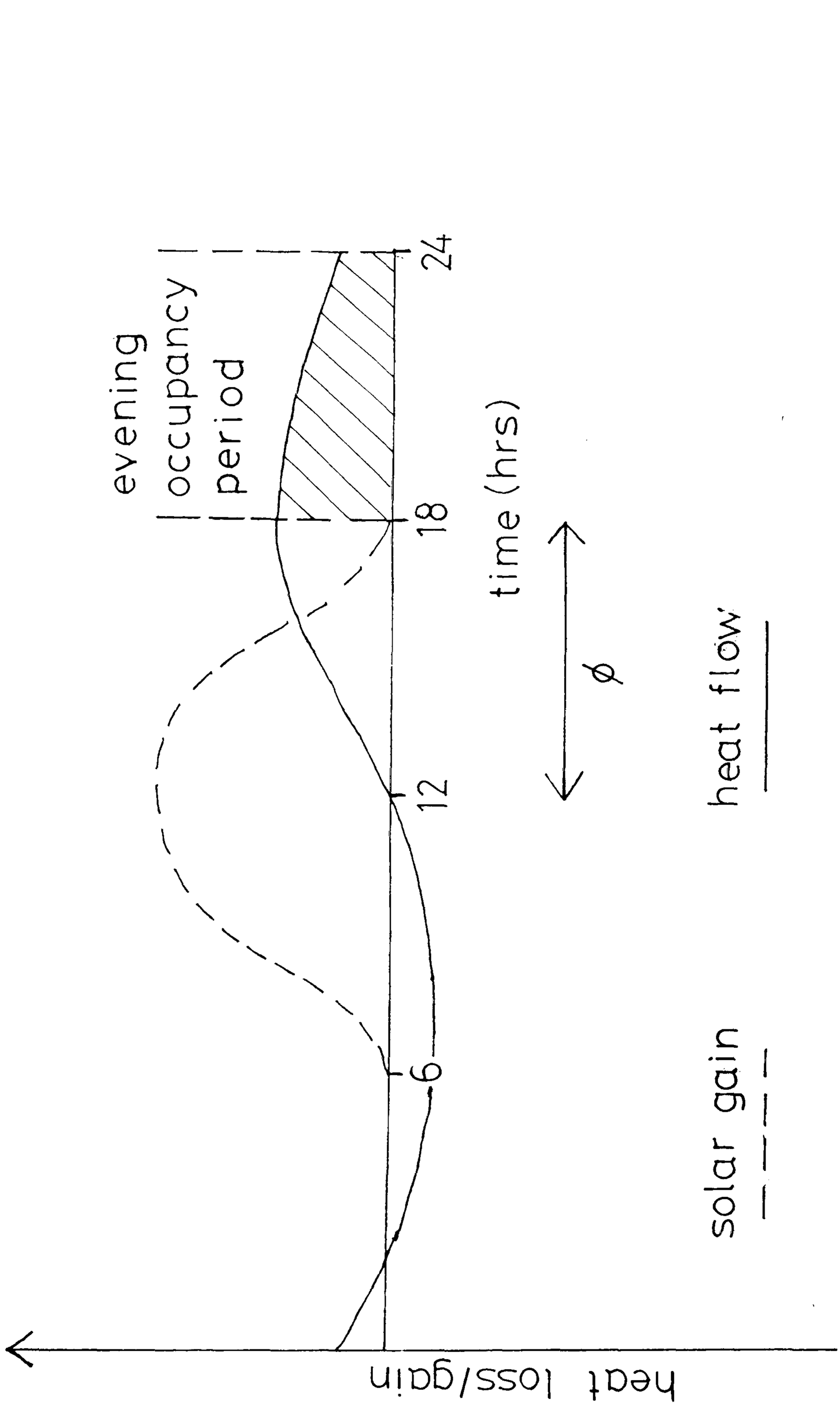

Fig 1.1 - Heat flow through a masonry wall of a domestic building under solar loading

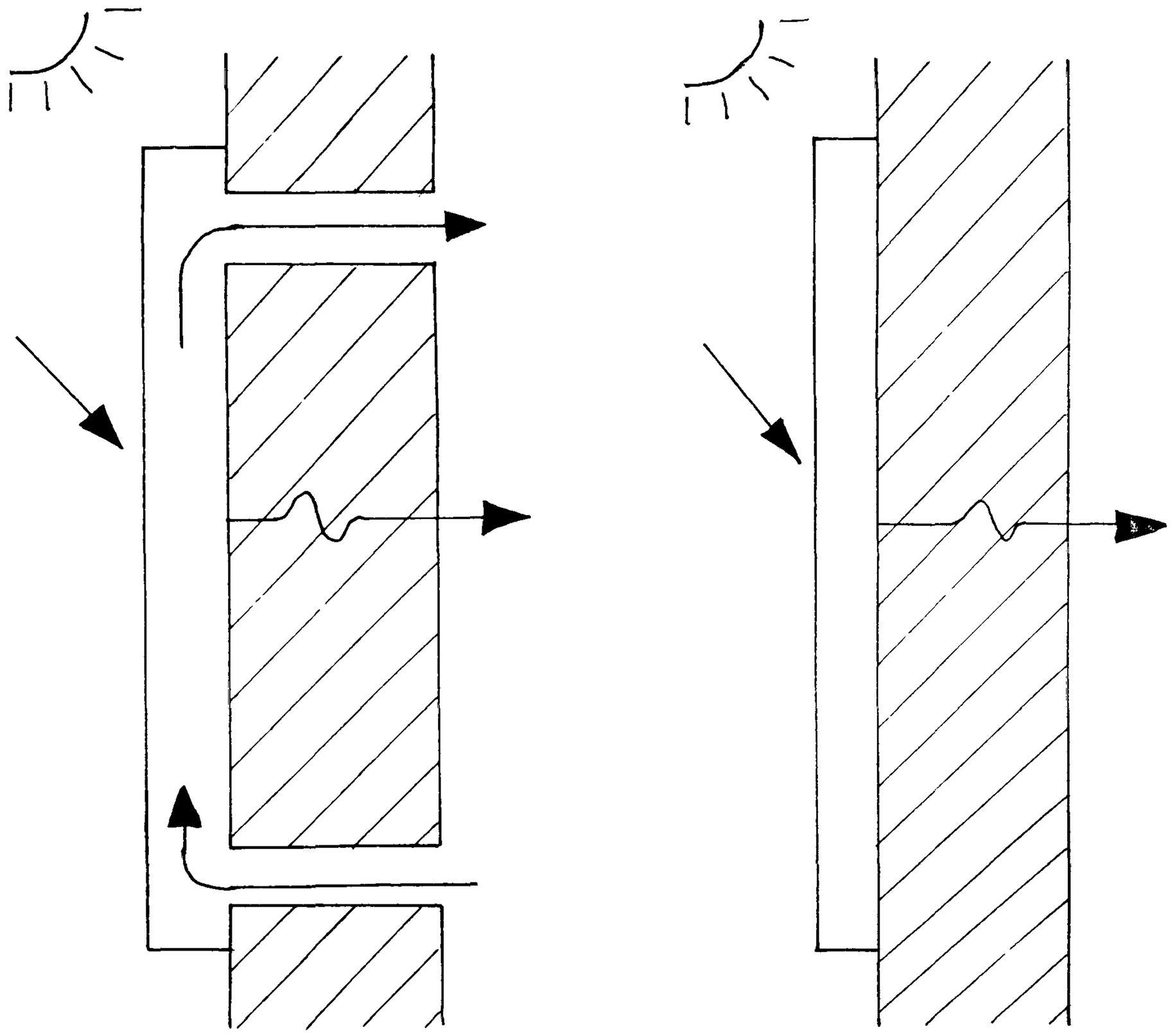

Fig 1.2 - Use of a solid masonry wall as a passive solar collector.

(a) the Trombe wall

(b) the conduction only wall

mainly in the evening. A disadvantage is that much of the heat initially stored in the outer parts of the wall is later lost to the outside. It would be an advantage, therefore, if the outside of the wall could be insulated and the heat gained transferred into the wall or the room in some way other than by conduction.

Two possible arrangements are shown in fig 1.3. The insulation on the outer face of the wall prevents the solar radiation from entering the wall directly, but now the outer gap could be used as an efficient convection collector (because of the increased surface temperature due to the insulation). In fig 1.3(a) the storage of the wall is not used and the warmed air enters the room directly. In fig 1.3(b) there is a useful phase lag when the heat is required later.

1.3(a) would be useful for buildings occupied in the daytime (between 0900 and 1800 hours), wheras 1.3(b) would be useful for domestic buildings occupied in the evening (between 1800 and 2300).

The description so far has concentrated on solid walls. Similar systems can be devised for cavity walls. These will be discussed below.

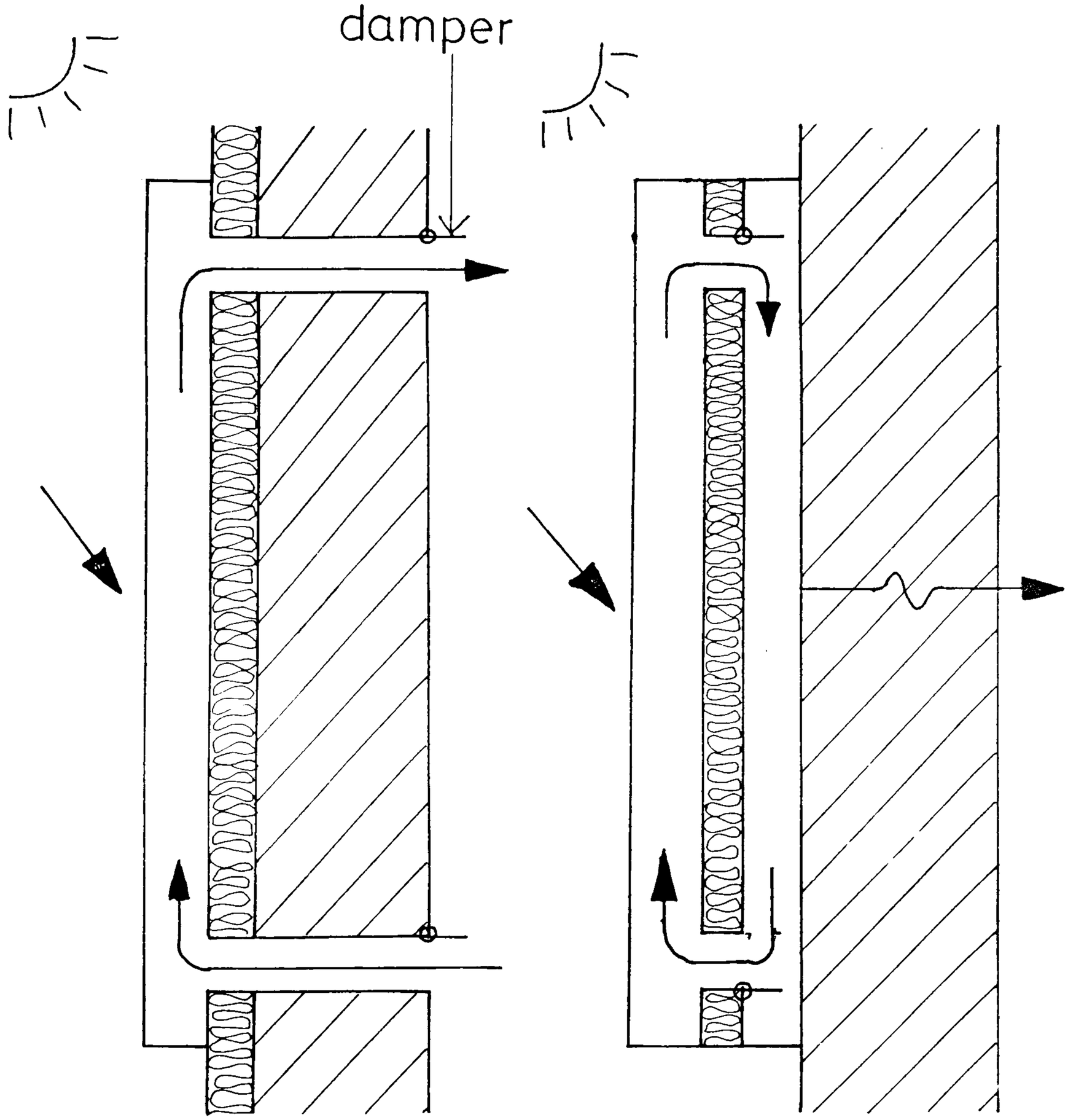

Fig 1.3 - Insulated solid walls with solar gain by convection, back flow prevented by thermostatically controlled dampers.

1.4 - Preliminary Calculations

1.4.1 - Effect of room environment

The aim of this project is primarily to look at a single building component, i.e a masonry wall, and how it can be improved. In the experimental and theoretical work in later chapters the environment of the room will be standardised in order to make comparisons between various wall configurations. At this stage, however, it is essential to see how significantly variations in the room environment affect the performance of the wall.

Fig 1.4(a) shows a typical room and the various heat losses/gains normally encountered. Also shown are values for the various parameters which will be used for the calculations performed in the next section. The masonry wall, under study, occupies the whole of the south facing wall, except for the window.

1.4.2 - Steady state calculations

Although a steady-state calculation is inadequate it is a useful indicator of the amount of heat which might be gained.

The steady state gain through the collector and through any other walls is

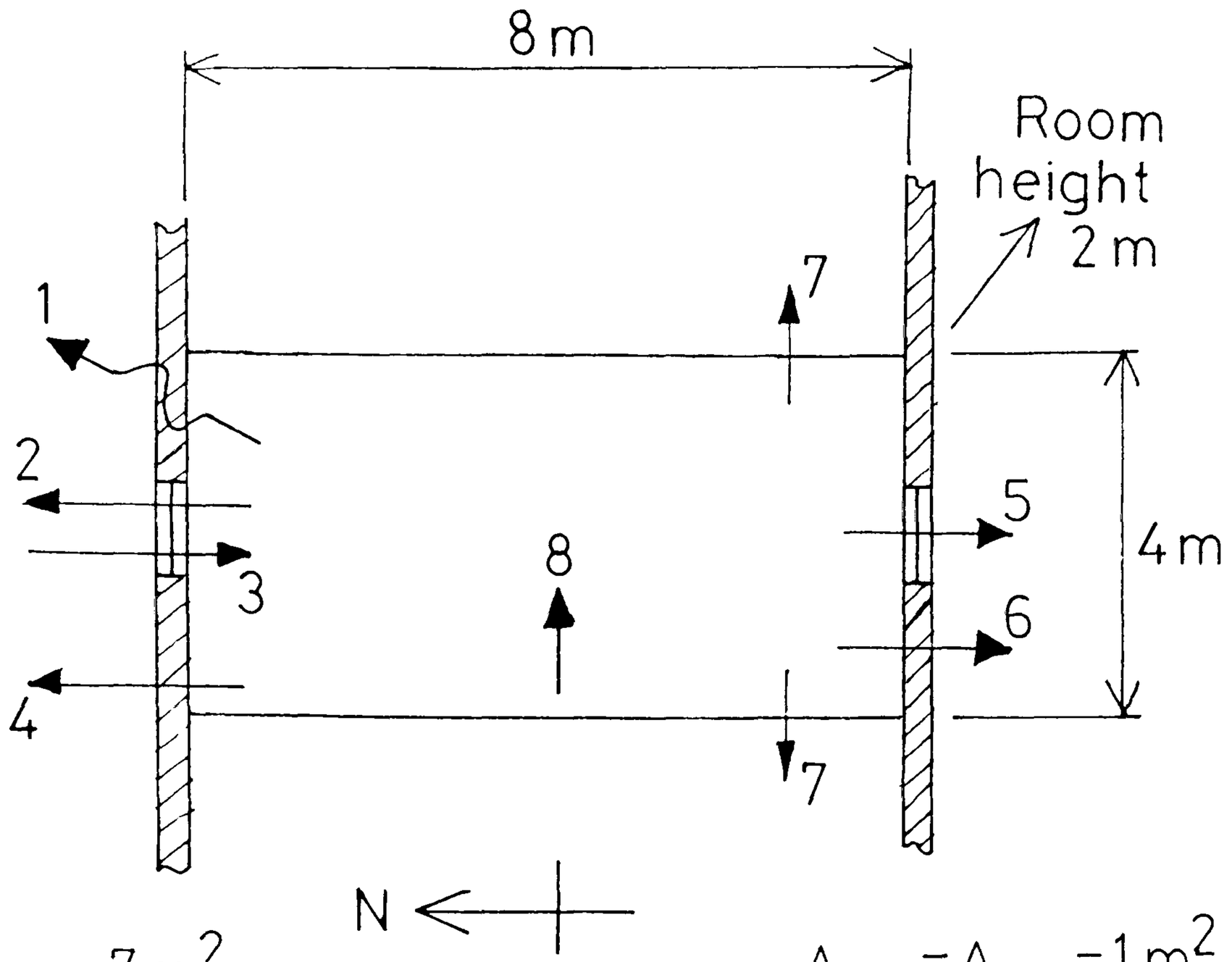

$A_c = A_n = 7\,m^2$
$U_n = 2\,W/m^2K$

$A_{g,2} = A_{g,5} = 1\,m^2$
$U_g = 5.6\,W/m^2K$

Heat loss/gain key

1 - Ventilation	$\rho cv = V$		
2 - Window	$A_g U_g$		
3 - Direct solar gain	$s_w Q$	$s_w = 0.80$	
4 - Collector	$A_c U_c$		
5 - As 3			
6 - North wall	$A_n U_n$		
7 - Ceiling, floor, partitions	$= 0$		

Climatic data

$\overline{tao} = 7°C$ $\quad \bar{Q} = 60\ W/m^2$

Fig 1.4 (a) - Data for steady state calculation, results shown in Fig 1.4 (b)

$$q_w = \sum AU(teo-tei) \qquad (1.1)$$

where $teo = tao + asQ_{24}R_{so}$ (1.2)

This must be calculated using the average 24 hour total Q (6MJ/m2) and the 24 hour average of tao (7 C), for the heating season. If convection is utilised, as suggested in fig 1.3, the daily convected total will consist of heat collected only during the hours of sunshine (average 3 hours) for which the average daily total is 1.3 MJ/m2. The gain from convection to the room is

$$q_c = \eta Q_s \qquad (1.3)$$

where η is the efficiency of the convection collector

There is also a loss from the room due to ventilation

$$q_v = \rho cV(tao-tai) \qquad (1.4)$$

Taking tai = tei which at this level of calculation is valid, the necessary heat input to the room is

$$q_h = \underbrace{(tei-tao)(V+W) + (tei-tao-asQ_{24}R_{so})*U}_{\text{Independent of collector}} + \underbrace{\eta Q_s}_{\text{Dependent only on collector}} \qquad (1.5)$$

W is the wall conductance excluding the collector area.

For a room with the given properties

$$q_h = f(V,tai) \qquad (1.6)$$

Fig 1.4(b) shows how the part of q dependent on the collector would vary for a typical room.

SOLID WALLS

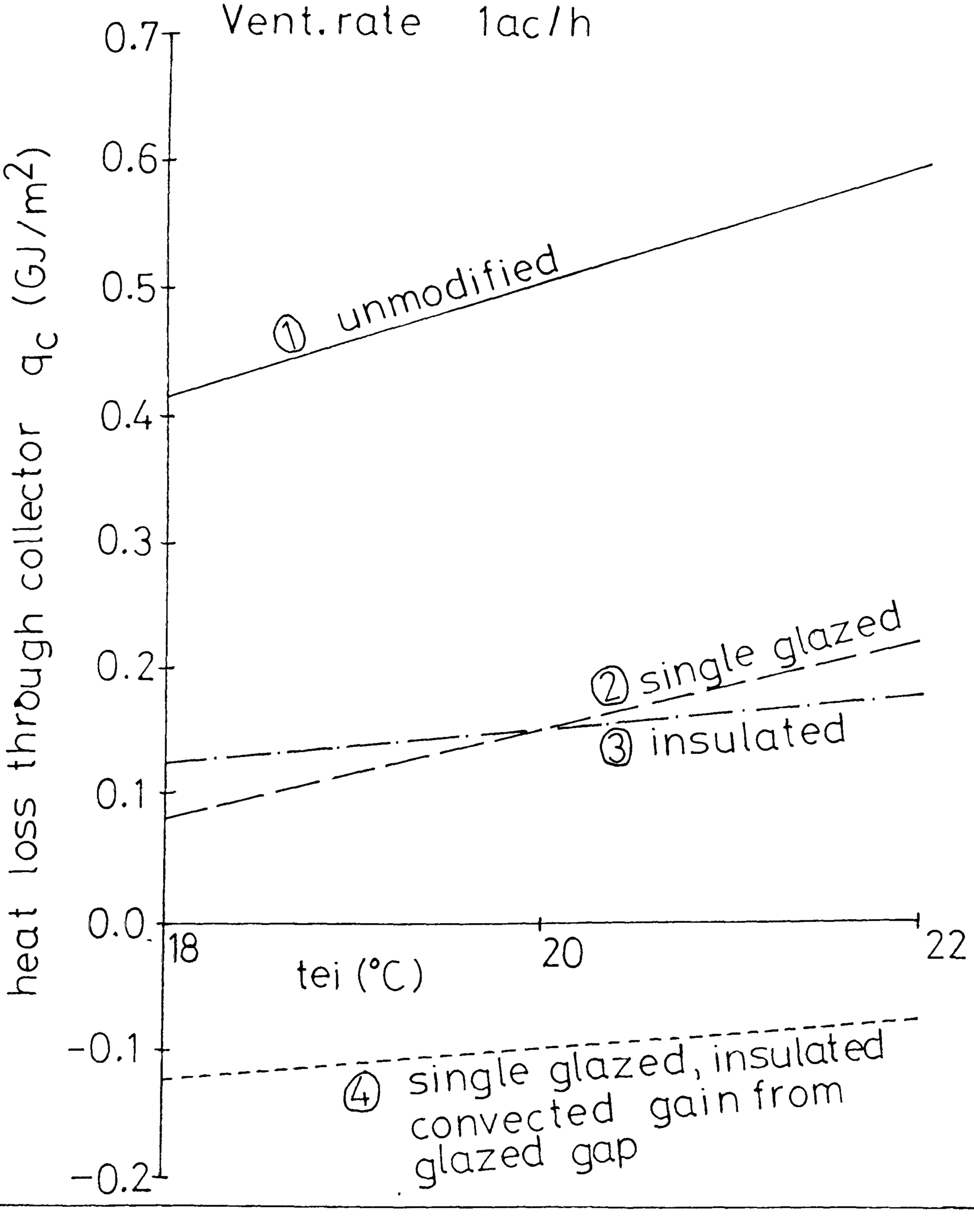

$U_{C1} = 2.0$ $U_{C2} = 1.5$ $U_{C3} = 0.6$ $U_{C4} = 0.5$ W/m²K

s_c - solar gain factor

$s_c1 = s_c3 = 0.70$ $s_c2 = s_c4 = 0.72$

Fig 1.4(b) - Heat loss through various collectors over heating season (Oct. to April)

1.5 - Further Solar Systems for Rehabilitation

1.5.1 - Cavity walls

As mentioned above, cavity walls are relatively easy to insulate. They could, however, be made into passive solar collectors. Fig 1.5 shows some possibilities. Some preliminary observations can be made of these systems.

1.5(a) is likely to be less effective than the equivalent solid wall due to the extra thermal resistance.

1.5(b) although not strictly passive, has a fan which need not consume much power.

1.5(c) would be difficult to build but may be effective.

For the room described in section 1.4, fig 1.6 shows the variation in heat flow through cavity walls, (1) unmodified wall, (2) glazed wall, (3) insulated wall.

The walls with air recovery cannot be readily modelled in this way. From fig 1.6 and fig 1.4 for solid walls, it can be seen that a single glazed wall has approximately the same performance as an insulated wall. From this it can be noted that (1) with diurnal variation, the sunlit glazed wall will be better than the insulated wall, (2) for cavity walls, the insulated wall will be more cost effective, due to its cheap capital cost, and if, for sunlit solid walls, glazing and insulation are equally expensive, glazing may

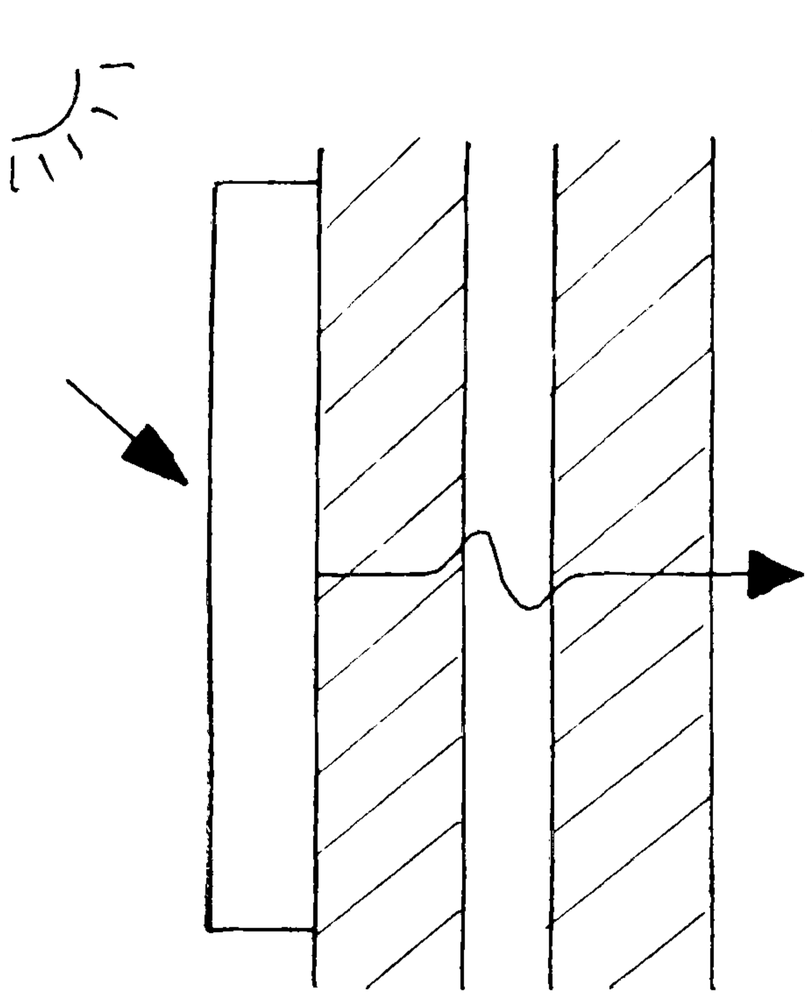

(a) conduction only

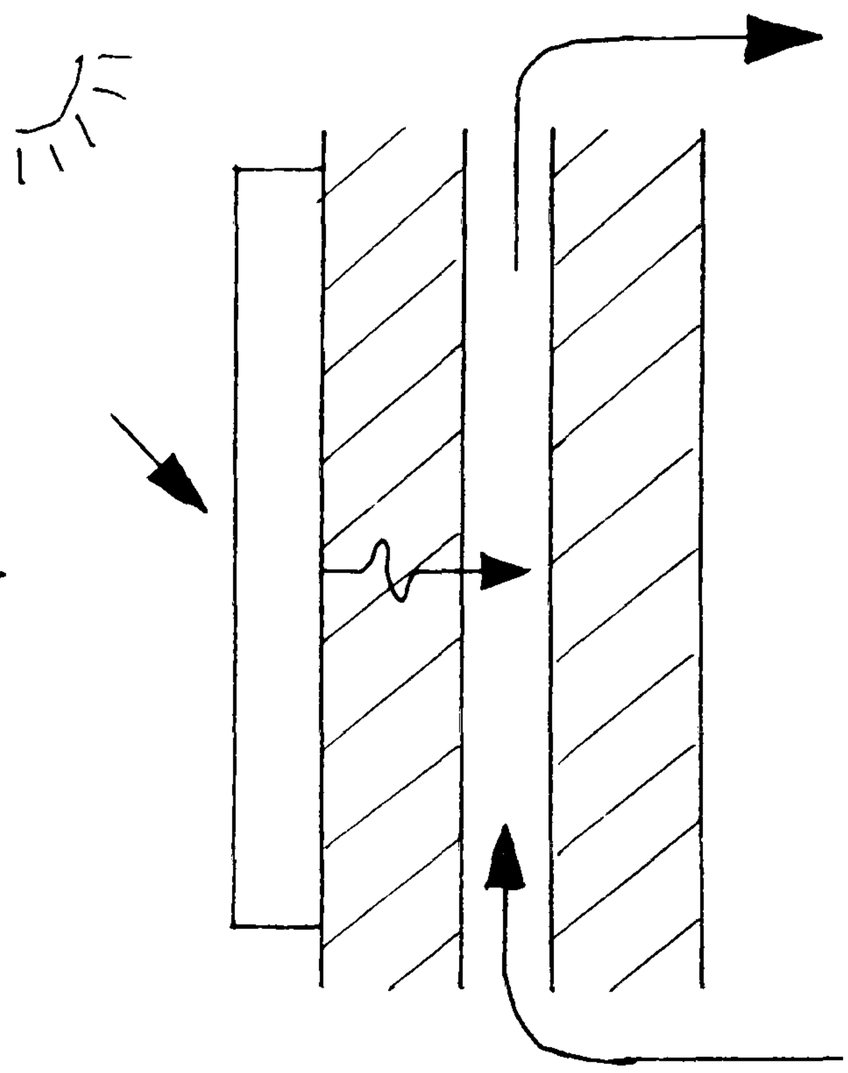

(b) fan assisted recovery from cavity in evening.

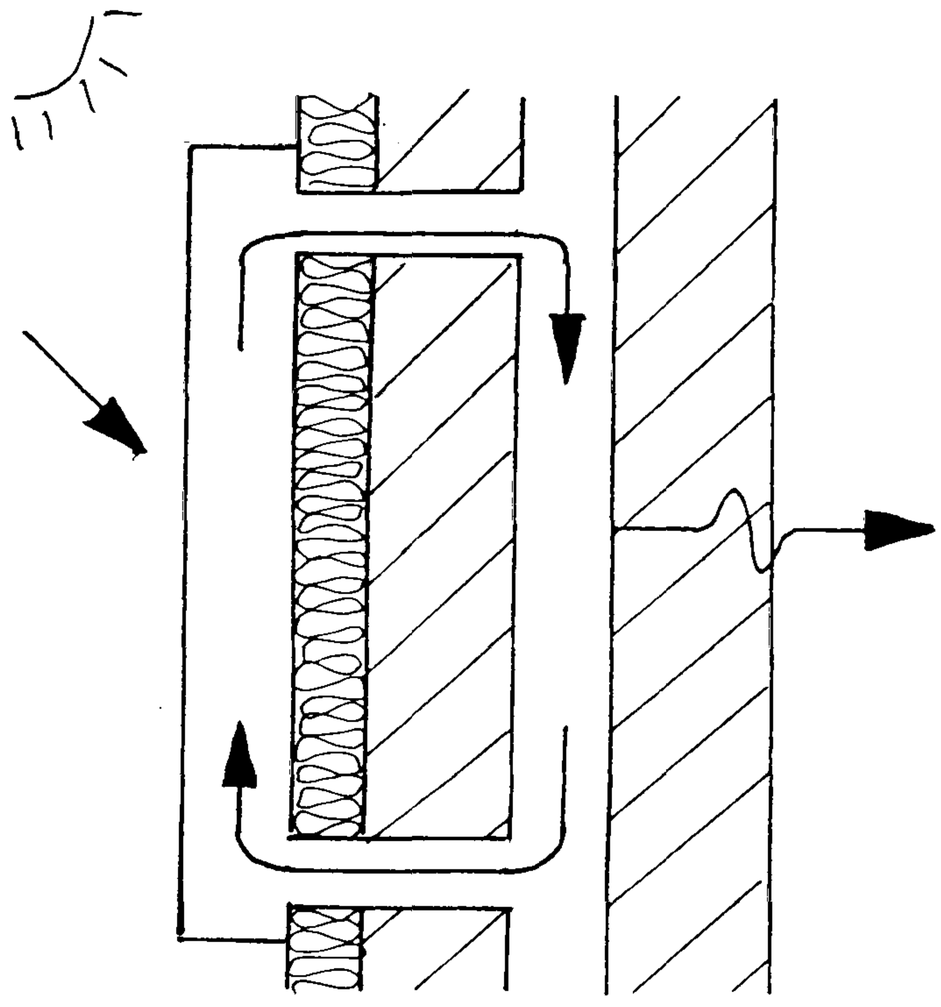

(c) natural convection into cavity causing conduction through inner leaf

Fig 1.5 - Cavity walls as passive solar collectors

CAVITY WALLS

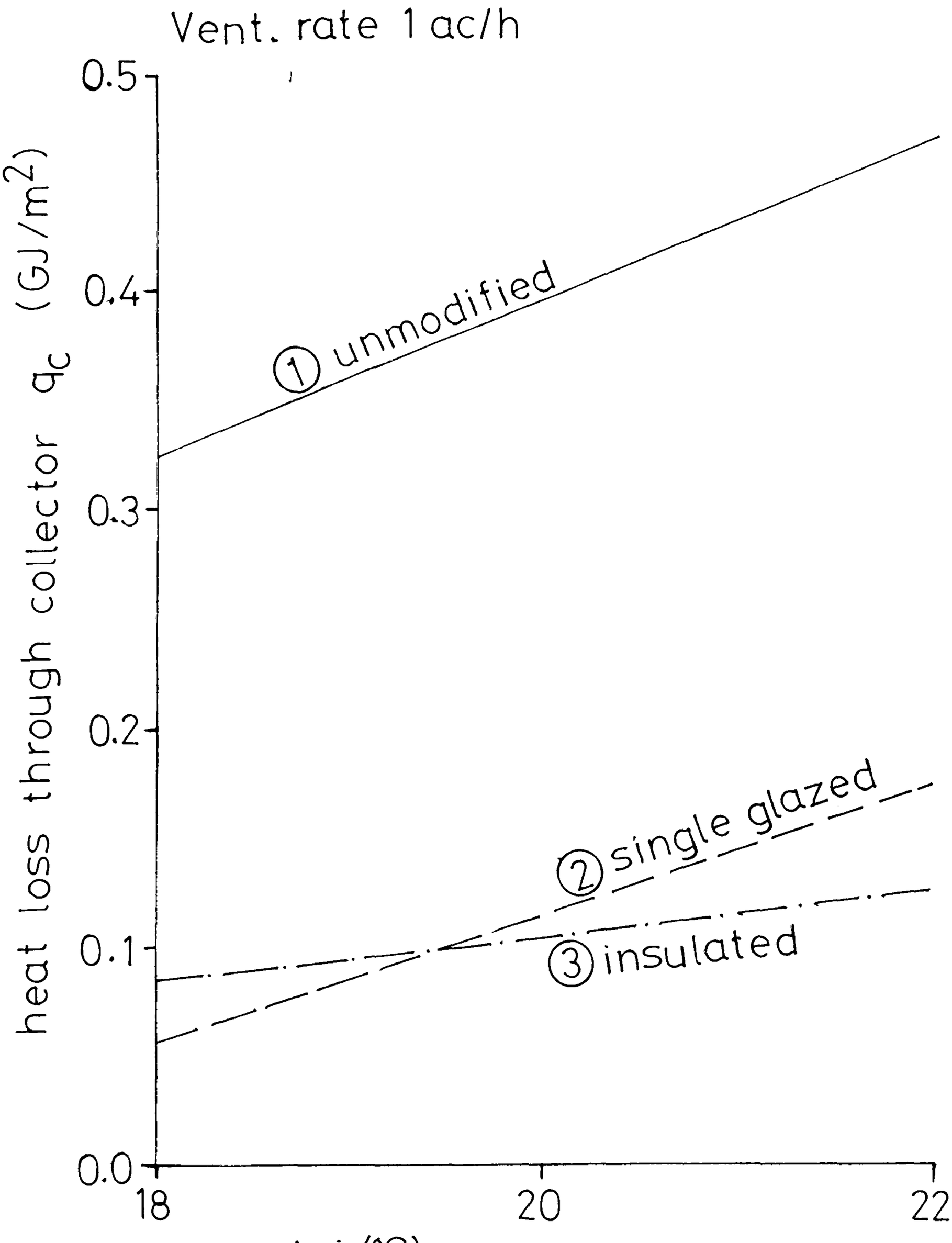

$U_{c1} = 1.6$ $U_{c2} = 1.3$ $U_{c3} = 0.4$ W/m²K

s_c – solar gain factor

$s_{c1} = s_{c3} = 0.70$ $s_{c2} = 0.72$

Fig 1.6 – Heat loss through various collectors over heating season (Oct. to April)

be better than insulation.

1.5.2 - Forced convection for rehabilitation

The main interest of this project is passive solar energy, but certain active systems are worthy of note. One such active system is the forced air collector which is fairly familiar in the USA, where air is forced through a glazed solar panel and the warmed air is used to heat a remote store. Experience of rehabilitation shows that it is often necessary to replace both the roof and ground floor of old buildings. It may be possible that the roof be rebuilt as a forced air collector and the floor as a concrete slab suitable for use as a heat store.

Although at an unfavourable angle, the roof collector has the major advantage that it will rarely be overshadowed, hence could be used on a greater number of buildings, particularly close rows of terraced housing.

1.6 - Problems Requiring Investigation

The discussion of heat transfer through a glazed solid wall (section 1.4) and a glazed wall with a cavity (section 1.5) shows that the two principal mechanisms requiring investigation are (1) the conduction of heat through a glazed wall and (2) the performance of a vertical glazed gap as a natural convection collector.

Some other secondary problems will also be considered.

1.7 - Sequence of Study

The following will be studied in detail

(1) Unglazed solid and cavity walls.

(2) A waterproofed, but unglazed, solid wall to study how rain affects heat flow. (1) and (2) are to provide control data.

(3) Glazed solid and cavity walls

(4) Glazed cavity wall with fan assisted heat recovery from the cavity.

(5) A natural convection collector, consisting of a glazed insulated gap. The use of ordinary and selective surfaces will be studied.

(6) Experimental results and theory will be used to compare the above walls and some others not studied in detail, conclusions of significance for future practice in the rehabilitation of older buildings will be drawn.

Chapter 2

Review of Related Work

The deliberate use of passive solar energy for the rehabilitation of existing buildings is virtually unknown in this country, although there are several examples in the USA. These are described along with British examples of passive solar energy for newly constructed buildings where the techniques used could be applied to rehabilitation. (The American examples may be relevant to Britain but obviously the climate in much of America is very different from that in Britain).

2.1 - Passive Solar Energy for Rehabilitation

Some American examples are summarised in (2). Most of these have Trombe walls with natural convection in the glazed airgap. The Starwood House, Rocky Mountains, Colorado, (lat.40 N), (pp 274-7) gains heat by convection in the day, and by conduction through the wall in the evening. It is interesting to note that Trombe's original wall provided heat by convection in the evening. At night an insulated shutter is used and in the summer the vents are arranged to cool the house.

A similar system is used at the Upper Black Eddy House, Bucks County, Pennsylvania, (lat.40 N), this has 475 mm stone walls with double glazing. However, because of

the thickness of the wall little heat is gained by conduction, and to increase the convected gain, forced air heat recovery is used.

One of the most famous examples of passive solar rehabilitation is the Keller Products factory in Manchester, Massachusetts, (lat.43 N), (pp 286-9) also described in (3). This building has a very large area of glazed south wall (183 sq m) of a special insulating double glazed sandwich. Most of the heat is gained by convection during the day to suit the occupancy of a factory. It is interesting to note that it is claimed that this building has no problems with expansion of the brickwork.

An unusual system is used at the Beatrice-Mongeau House, Pittsboro, North Carolina, (lat.36 N), where a masonry wall has been constructed behind existing glazing. The Wickel House, Bloomsbury, New Jersey, (lat.41 N), (pp 289-93) is of lightweight wall construction and the glazing forms a natural convection air collector with no deliberate heat recovery by conduction. Both these houses use insulating double glazed sandwiches.

Some general observations can be made about these buildings and the potential of using such systems in Britain. The major problem is that the British climate is not as favourable as that in most parts of the USA, e.g a typical annual total global radiation on the horizontal for

Britain is 3000 MJ/m^2 for Bebbington (lat. 53°N), whereas it is 4800 MJ/m^2 for Manchester, Massachusetts (lat. 43°N).

As will be shown below, in this country, natural convection in the gap between glazing and a masonry wall would not be sufficient to collect a worthwhile amount of heat. Hence either the effect must be increased by insulating the outside of the wall (to reduce the heat absorbed by the masonry) or the wall must collect heat by conduction alone. This would not be practicable for very thick masonry walls such as that in the Upper Black Eddy House.

At present the special insulating glazings mentioned above (products such as 'Kalwall') are not readily available in Britain, and hence until they are, it would not be economical to use them. These consist of double glazing with a transparent fluid or gel in the gap, giving the glazing a low U value.

One major British work on passive solar energy for rehabilitation is by R Lebens (4) which is summarised in (5). This is based on work done at Massachusetts Institute of Technology (MIT) for the MIT V solar house, described in (6). Lebens applied these techniques to a typical Victorian terrace house.

As much of the south facing wall as possible is

glazed, the rest of the outside wall is insulated on the outside, to keep the thermal storage on the inside. Sunlight entering through the glazing is reflected by solar modulator blinds onto the ceiling, where the radiation is absorbed by phase change tiles which later in the day release their heat to the room, when the insulating blinds are shut. The heat is circulated to the other rooms of the house by a fan and ducting.

Calculations show that this technique is quite promising, but at present, because some of the products used are not readily available, it would probably not be economic to use them.

Recently, the Centre for Alternative Technology in Wales, has added a hybrid system to an old house which is fairly close to the work described below in chapter 8 (35). The construction is fairly complicated and is shown in Fig 2.1, with the modes of operation. The heat exchanger on the outside of the existing wall is to increase heat transfer from the air to the wall. The combination of double glazing and selective surface would make the system expensive, but will certainly improve the efficiency of collection. The area of the glazed collector is 13.4 m^2. The volume of the store is 6.5 m^3. The area of the heat exchanger is 6 m^2.

The modes of operation shown in Fig 2.1 are

(a)

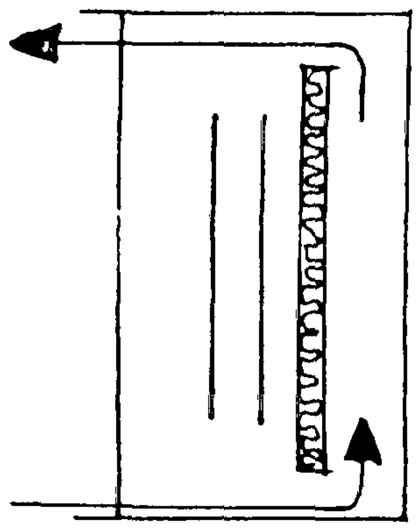

bright day
cold rooms

solar heated air
direct to room

(b)

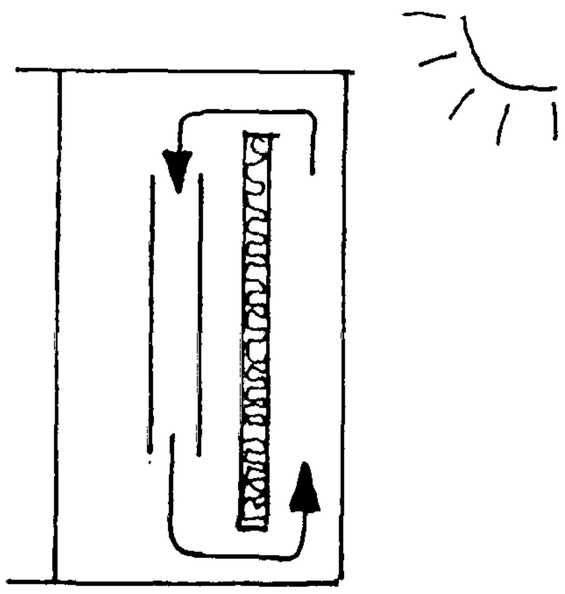

bright day
warm rooms

charging the
heat store

(c)

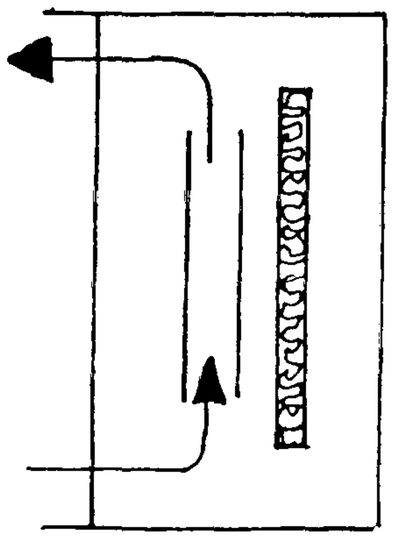

dull day or
night

recovering
stored heat

Fig 2.1 – Principle of operation of solar wall at the Centre for Alternative Technology – Machynlleth.

(1) Sunny day, house occupied - warm air passed directly into the house. (2) Sunny day, house unoccupied - air passed from collector over the heat exchanger to store the heat until needed in the existing wall. (3) Night or dull day, house occupied - air drawn from room over the heat exchanger to recover heat from the store, and then returned to the room.

The entire system cost about £1500, in 1983, but this is very much lower than if it had been built commercially. It is likely that a realistic figure for the average house owner would be much more than this.

The 'First European Passive Solar Competition - 1980' had a category for rehabilitation. The most interesting of the entries was for the improvement of a terrace house in Bath. The solution was very elegant, and the construction details are described at some length. The house is covered with a combination of Trombe walls, window-box greenhouses and a conservatory on the ground floor. The Trombe wall is conventional. It is double glazed and has a 'heat mirror' layer between the two pieces of glass. The conservatories work by allowing warm air from the top to enter the room behind. Although not an efficient method of collecting heat, this is probably worthwhile. One criticism of this is that it is somewhat extravagant, although the result is pleasing in appearance. Such a solution would be

practicable if the components could be mass produced.

Important experimental and theoretical work has been done by MacGregor at Napier College, Edinburgh (7). He compared an unmodified masonry wall with one with outside insulation and another with glazing. Using simple steady state theory he showed that the insulated wall would give an annual total improvement of 160 MJ/m^2, where as the glazed wall would give a improvement of 540 MJ/m^2. He examined three pieces of existing concrete wall, with thermocouples on their inside and outside faces. The results agreed well with the theory, although it could not predict the diurnal variations.

Davies, at Liverpool University, has made many theoretical studies of glazed masonry walls (36). These are mainly using steady-state theory, but are informative as to the gains that might be expected from such walls. This work is particularly useful for new buildings, for example, in suggesting an optimum thickness of wall. The main results give the necessary heat inputs to a room in order to maintain the design air temperature. The improvement per m^2 of wall of approximately 0.2m thickness is 280 MJ/m^2 for October to April, or for example, 42 MJ/m^2 for March. The method enables the user to calculate the performance of a wall from tables.

2.2 - Examples of Passive Solar Energy in Britain

St George's school in Wallasey (8), has proved that passive solar energy can work in this country. This building works by direct solar gain, a very difficult technique to apply to existing buildings since it may involve demolition of existing walls. However, this may be practicable where the walls are non-structural, as for example, using Lebens' technique of replacing much of the south facing wall with glazing. For a dwelling, it will often be desired that the heat gained be stored until the evening, as in Lebens' project. In this country, simple direct gain systems, such as that at St Georges school, are mainly suitable for buildings occupied in the day.

One of the most interesting recent buildings is also in the Wirral, at Poulton Lancelyn primary school in Bebbington (9). The main solar collector is essentially a conventional cavity wall, double glazed on the outside and insulated on the inside. In the evening, if the wall is warm enough, air is blown, through the cavity and into the building. No heat is to be gained by conduction because of the internal insulation. The building is highly insulated, and has a heat wheel to recover heat from the ventilation air.

It would be interesting to study this building in detail since it would be possible to convert the cavity

wall of an existing house into such a collector, except that it may be difficult to insulate the inside of the wall.

Normal occupancy of a school is during the day and not in the evening or at night. Because of the conduction phase lag of the brick wall the fan recovers heat in the evening when the building may be unoccupied. This is the reverse in the case of a dwelling where the phase lag would work to advantage. For a school, or other building with similar occupancy, it may well be more efficient to insulate the outer face of the wall, and blow air from the gap between glazing and insulation, directly into the building's warm air system. It may well be shown that most of the benefits of this building result from its high insulation combined with heat recovery from the waste air, and that the solar collector is almost redundant.

Also in Bebbington are some old people's homes (10,11) bungalows double glazed on the south with a large gap (600 mm) between wall and glass. Heat is collected by conduction through the wall and by natural convection from the gap.

This system could well be used for rehabilitation although the provision of ductwork to move air from the collector to the rest of the house could prove difficult. The large gapwidth makes natural convection less efficient

but does make cleaning the glass easier. Forced recovery might improve the collector's performance, without the need to reduce the gapwidth.

The problem of cleaning the glass is one to which there is no completely satisfactory solution. If the gap is sufficiently wide to allow easy cleaning, its efficiency as an air collector will be reduced. If the glazing is openable, this makes cleaning possible, but also increases capital cost and the risk of leakage.

The simplest method of using passive solar energy for rehabilitation is undoubtedly the conservatory without deliberate heat recovery by convection. Some proposed schemes are described briefly by Turrent et al. (11), who suggests that the cost may be prohibitive for a new dwelling (pp 64-6). An example is given of a lean to conservatory on an existing terrace house in Milton Keynes (pp 69-70). This seems to have been reasonably cheap and it is thought that this simple technique could have great potential, even though the thermal improvements may be slight, because it also provides an extension to the living area. In practice this may well be a realistic method of passive solar rehabilitation. Cleaning of the glass should prove no problem.

B. Berrett (33) provides a good survey of possible techniques, and further British examples of passive and

hybrid systems, one of which will be described in section 2.4.

2.3 - Potential of Active Systems for Rehabilitation

Chapter 9 of this study will describe a joint proposal by Leeds University and the Cynon Taf Housing Association, to rehabilitate some terraced housing in Aberdare, South Wales (33). Lack of space meant that such structures as conservatories were not possible, the only large area available being the roof, which will be reconstructed as a forced air collector. Such systems are very common in the USA both for new housing and for rehabilitation, the usual thermal storage being a bin of stones in a basement. Many examples are described by Shurcliff (6). For a small terrace house it may be feasible to use the basement for a store but if there is no basement, then the masonry parts of the house must be used i.e the walls or the ground floor slab. This is also discussed in chapter 9.

Forced air collectors, even for new housing, are rare in Britain, the most important example being the Building Research Station's experimental heat pump house (12). The collector is of profiled metal cladding insulated on the rear, air being blown through the enclosed channels of the profiling. No deliberate thermal storage is used in the house, the heat is immediately upgraded by an electric heat

pump and passed into the house. The use of forced air collectors seems very much cheaper than passive systems, especially for rehabilitation, since the roof of the house would probably be renewed anyway. The use of both heat pumps and thermal storage have potential, but must be left as a matter for further research and development.

2.4 - Conclusions

At present simple techniques will be the most practicable, but products described in work by Lebens may well become available soon, and hence increase the number of options. Certainly the simple conservatory seems feasible, its likely performance is therefore assessed later (chapter 5).

More complicated Trombe walls and natural convection collectors may well be possible but need careful design to make them cost effective for the British climate. Some examples of these walls form the main body of the present work and will be discussed in much greater detail. Forced air collectors have potential, but full size demonstrations are needed to prove their value fully.

Chapter 3

Masonry Walls - Experimental Work

The site for the experimental work was that used by J Lee, described fully by him (14). The data logging equipment is also described by him detail in (14), but will be discussed with reference to this work in 3.2. Reusing the site and some of the equipment proved to be no problem and saved much time in beginning experimental work.

3.1 - Description of Walls

Five walls were built:

(a) Cavity wall glazed, at first with a sealed cavity, later with fan assisted recovery.

(b) Cavity wall unmodified.

(c) Solid wall glazed.

(d) Solid wall waterproofed on outer face.

(e) Solid wall unmodified.

(c), (d) and (e) are all double thickness brickwork. These are shown in Fig 3.1. Walls (b),(d) and (e) are built on top of each other. Vertical conduction between them is negligible because of the low temperature difference. The glazed cavity wall (a), is built over a manifold with a fan which allows air to be blown through the cavity. Fig 3.2 shows a plan of the room in which the walls are sited.

None of the walls is painted dark, so that they can

Approx. scale - 1:25

+ thermocouple blocks

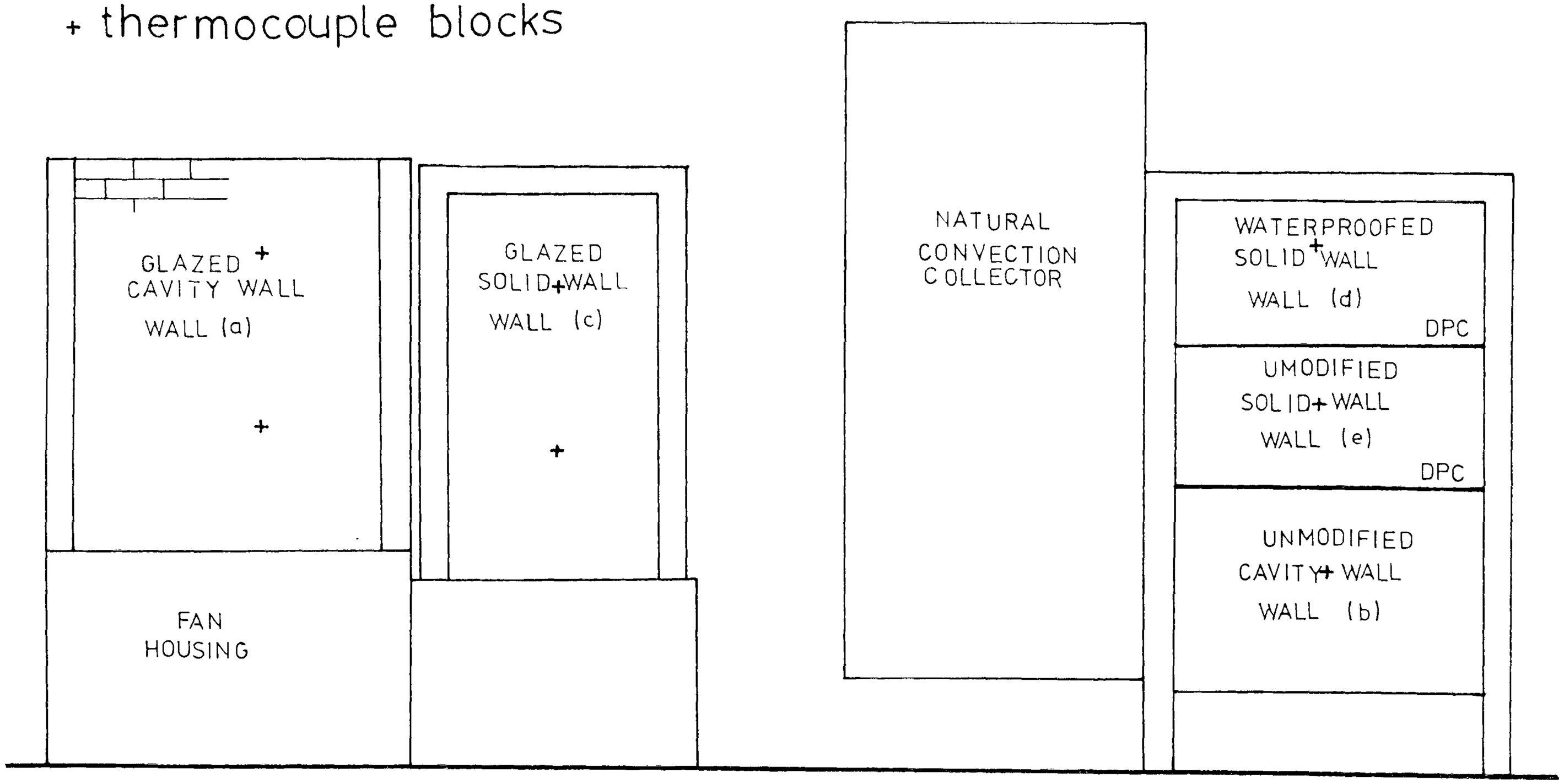

Fig 3.1 - Interior View of Walls

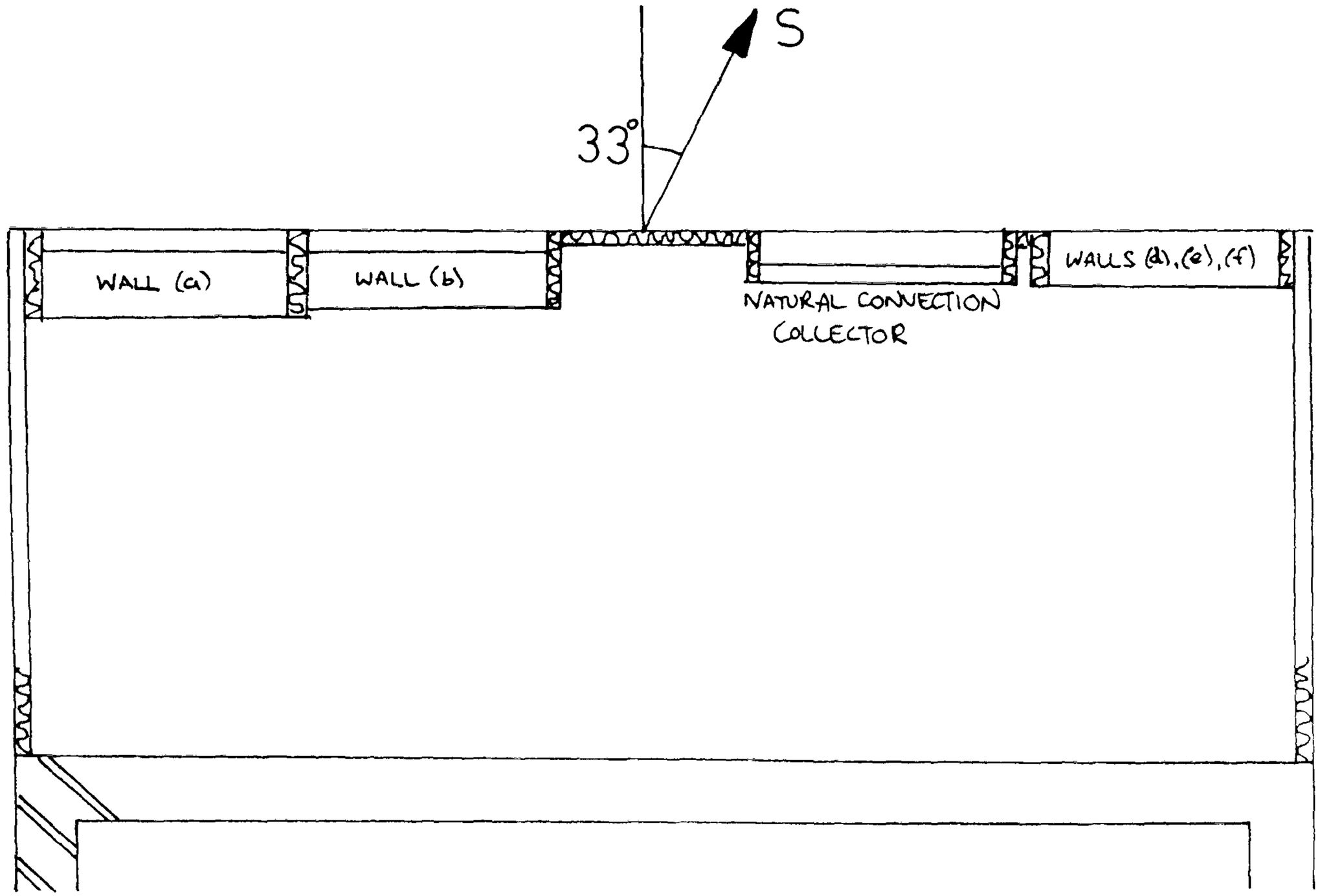

Scale 1:100

Fig 3.2– Plan of Experimental Room Showing Test Walls

be compared without having to measure the surface absorptivity. In practice the glazed walls may be darkened, which would give an improved performance. The waterproofed wall is painted with a transparent sealant.

The solid wall (c) is glazed whereas the cavity wall (a) is covered with perspex. The two materials have similar properties and since comparisons of (a) and (c) are not necessary, any difference can be ignored.

All the bricks are LBC 'Regency' facing bricks. These have an average density of 1640 kg/m^3. Most existing walls would not be entirely built of facing bricks, but this was done to simplify comparisons. The mortar used is three parts sand to one part of cement.

No difficulties were encountered in constructing the walls. The cavities were kept as clear as possible, cavity ties were inserted at standard intervals. The solid walls could not realistically be constructed of either 'Flemish bond' or 'English bond' hence they were constructed in stretcher bond with a single header at alternate ends on each course.

The walls were insulated at the edges with 50 mm expanded polystyrene. The walls (b),(d) and (e) are separated by bituminous felt. Originally they were to be separated by insulation but this proved difficult to

construct.

An important point to stress is that the walls face 33 east of south. This means that the wall may be less efficient than a wall facing due south, but is realistic in that existing walls do not all face south. The peak wall temperatures will occur earlier than with a south facing wall. The room air temperature is maintained at 20 C by a simple thermostat, controlling an electric warm air heater.

3.2 - Monitoring of Walls

Temperatures within the walls are measured with calibrated copper/constantan thermocouples set into the bricks as shown in Fig 3.3. The thermocouples are grouted into 12 mm deep, 3 mm diameter holes with cement. The series of thermocouples, across the wall, is to give a clearer idea of how the heat is flowing within the wall, particularly due to the warming and cooling caused by the solar gain. The spacing of the thermocouples was governed by the total number that could reasonably be monitored. Calibration of the thermocouples is described by Lee (14). The two glazed walls have thermocouples at two levels, the other walls have only one set. The reason for measuring the temperature distributions is to observe, qualitatively, the behaviour of the heat flow in the wall.

Also measured were the temperatures of the room and

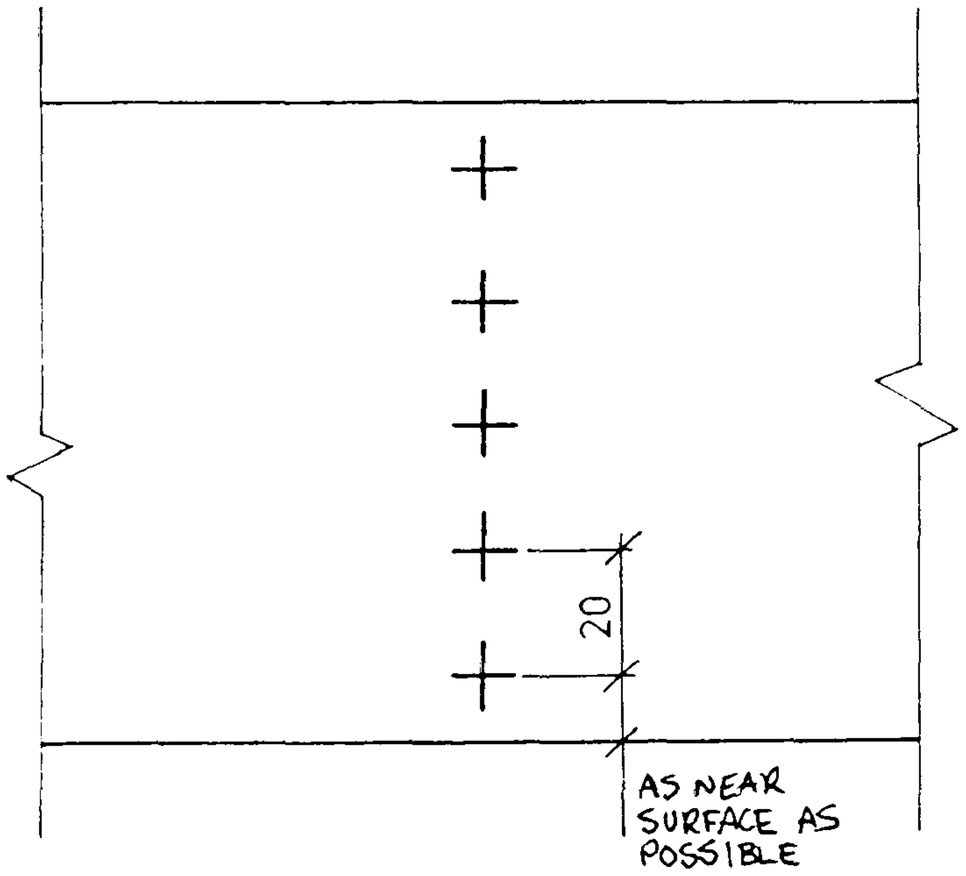

Single Brick

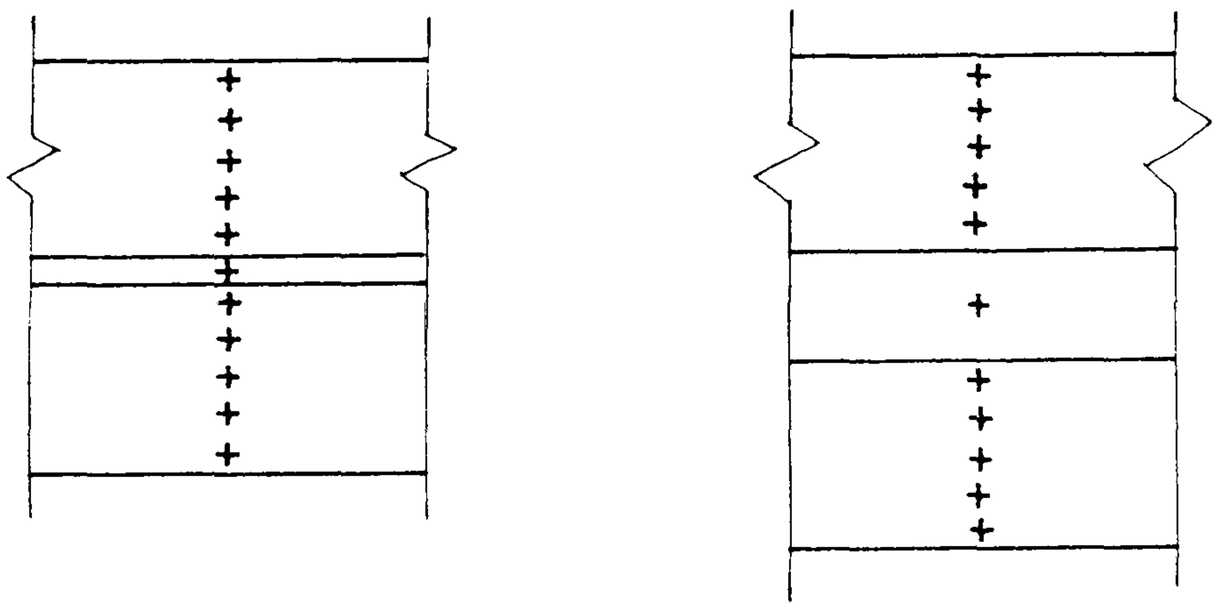

Solid Wall

Cavity Wall

Fig 3.3 - Thermocouple Locations

the outside air, the thermocouple used for the outside air is in an aluminium radiation screen. The insolation is measured with a solarimeter (calibrated at 11.5 $\mu V/(W/m^2)$).

The inputs are scanned by the data logger and recorded in μV on paper tape. The logger has at times been unreliable, and for a long period in 1981 it was not working at all. At other times it has suffered from electrical interference the consequence of which has been irregular output files. Much time was needed to correct these output files manually, which meant that it was impossible to record as much data as was originally desired.

There were some problems in monitoring the glazed cavity wall with forced air recovery. Originally it was controlled by a differential switch which very soon broke and proved impossible to repair. Another control system was designed which was simpler but less flexible. A central heating timer switches the fan on at 1600 hrs and the thermostat which is set at 20°C, switches the fan off if the air is below this temperature. The timer switches the fan off at 2300 hrs. This system has worked without any trouble.

The air flow was measured with a heated thermistor which was not suitable for continuous monitoring, so it could only be used manually. No significant changes in the

airflow were observed, the air flow was 0.07 m^3/s. To determine whether the fan was switched on at any time, the exact set temperature of the thermostat was found (20.4 °C) and if the recorded temperature was above this, then the fan was assumed to be on. Observations showed that the thermostat was consistent and this technique was reliable. The heat gain by the air is given by

$$q(conv) = \rho cV(tout-tai) \qquad (3.1)$$

3.3 - Heat Flow From Wall Surfaces

For all the walls except (a) the only mechanisms of heat transfer from the room are by convection and radiation to the wall surfaces (which also occur in wall (a)). It was essential that this heat flow should be monitored with some accuracy.

Originally it was intended to build some form of 'heat box' on the inside of all the walls. This would have been difficult and would give unrealistic results, since under real conditions the heat transfer is affected by draughts and radiation from other walls (i.e heat transfer can be considered dependent on the environmental temperature). Having tested the air flow around the room with a heated thermistor, the velocity of any draughts varied little from place to place, and rarely exceeded 0.1 m/s.

Hence to keep the results realistic the walls need to be left unaltered and some value for the internal surface resistance was needed to use the relation

$$qtot = (ts-tei)/R_{SI} \qquad (3.2)$$

It was decided to analyse theoretically how much Rsi could be expected to vary. The value is made up of three components, natural convection (due to temperature gradient), forced convection (due to draughts) and radiation. The radiation component can be considered constant at

$$h_{RAD} = 5.8 \not{\mathcal{F}} \; W/m\,K \qquad (3.3)$$

For verification of this see appendix 3. The emissivity of all walls for long wave radiation is 0.9. The calculation of the configuration factor , which includes the emissivity is also given in appendix3. For the room in question the configuration factor is 0.98. The natural convection component is a function of the wall height and the temperature gradient and is given by O'Callaghan (15), these are

$$\text{Laminar} \quad h_{LAM} = 1.37((ts-tai)/L)^{0.25} \qquad (3.4)$$

$$\text{Turbulent} \quad h_{TURB} = 1.75(ts-tai)^{0.33} \qquad (3.5)$$

$$\text{Average} \quad h_{AV} = (h_{LAM} * L_{LAM} + h_{TURB}(L-L_{LAM}))/L \qquad (3.6)$$

$$\text{where} \quad L_{LAM} = (6/(ts-tai)) \qquad (3.7)$$

These equations require the use of SI units.

L_{LAM} is the distance along the plate at which transition

occurs. The forced convection component is a function of the local air velocity over the surface and is given by

Laminar $h = 0.5913(Re^{0.5})/(40L)$ (3.8)

where Re is the Reynolds number, a function of v the average velocity, and L is the length of collector.

A variation of v from 0 to some high value is used in equation (3.8).

The convection components are a function of the difference in temperature between the wall surface and the air temperature, whereas the radiative component is dependent on the difference in temperature between two wall surfaces. The floor and wall opposite are adjoined by rooms also maintained at a fairly high temperature, and these surfaces were observed to vary little from the air temperature. All the other outer walls have 50mm of insulation on their surfaces. For an outside temperature of $-1^{\circ}C$, the inside surface temperature of these walls would be $18.8^{\circ}C$, hence, simplyfying the radiative heat transfer to be dependent on the air temperature would lead to an error of about 5%.

As it has been shown that all the heat transfer mechanisms can be considered dependent on the difference between the wall surface temperature and the air temperature the total heat transfer co-efficient is the sum of the three and, R is the reciprocal of this value. Fig 3.4 shows the variation of Rsi against various parameters.

Variations of Inside Surface Resistance

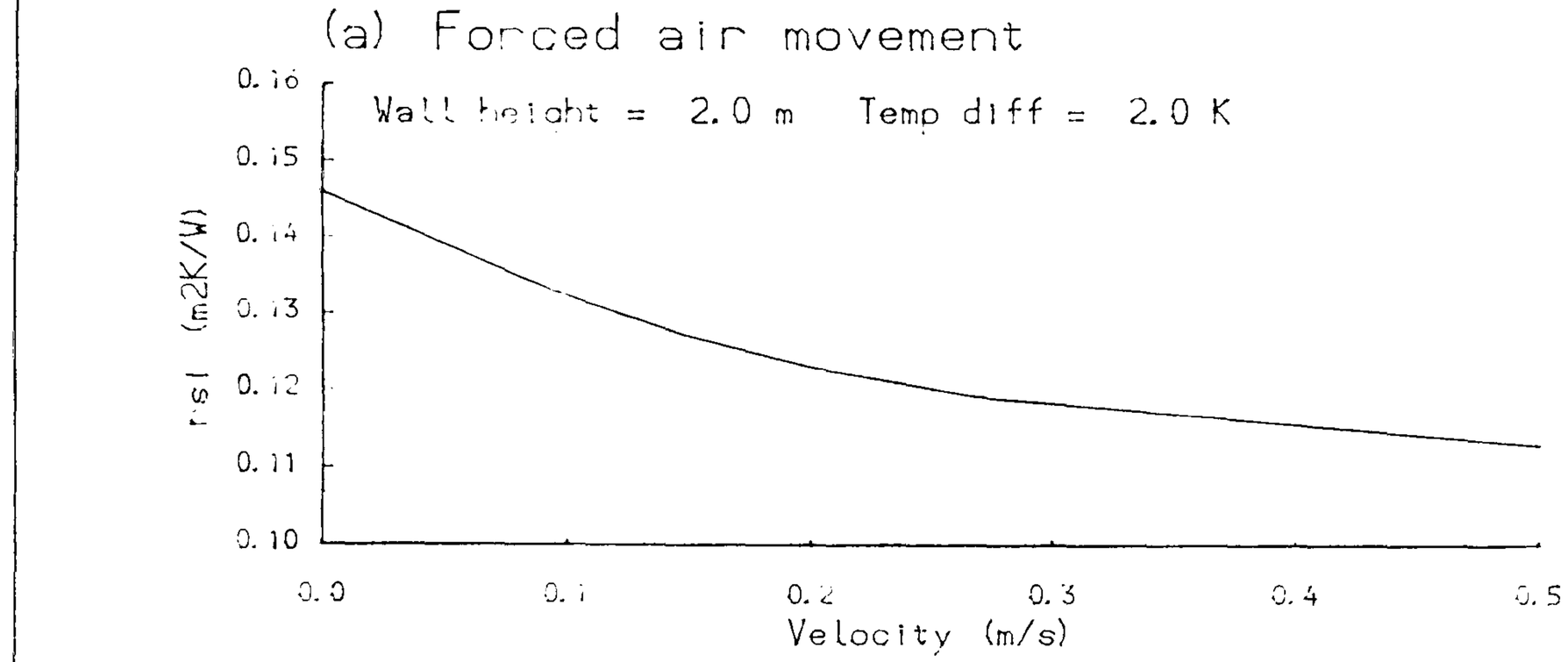

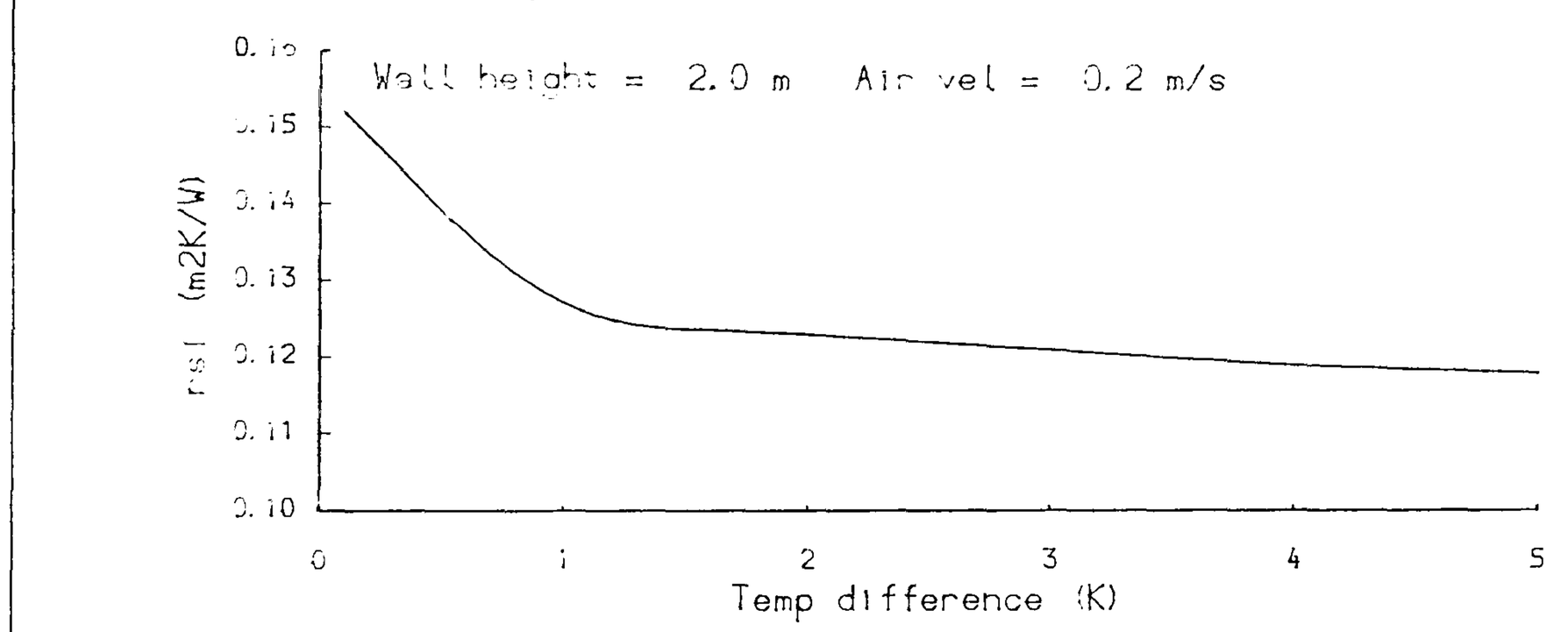

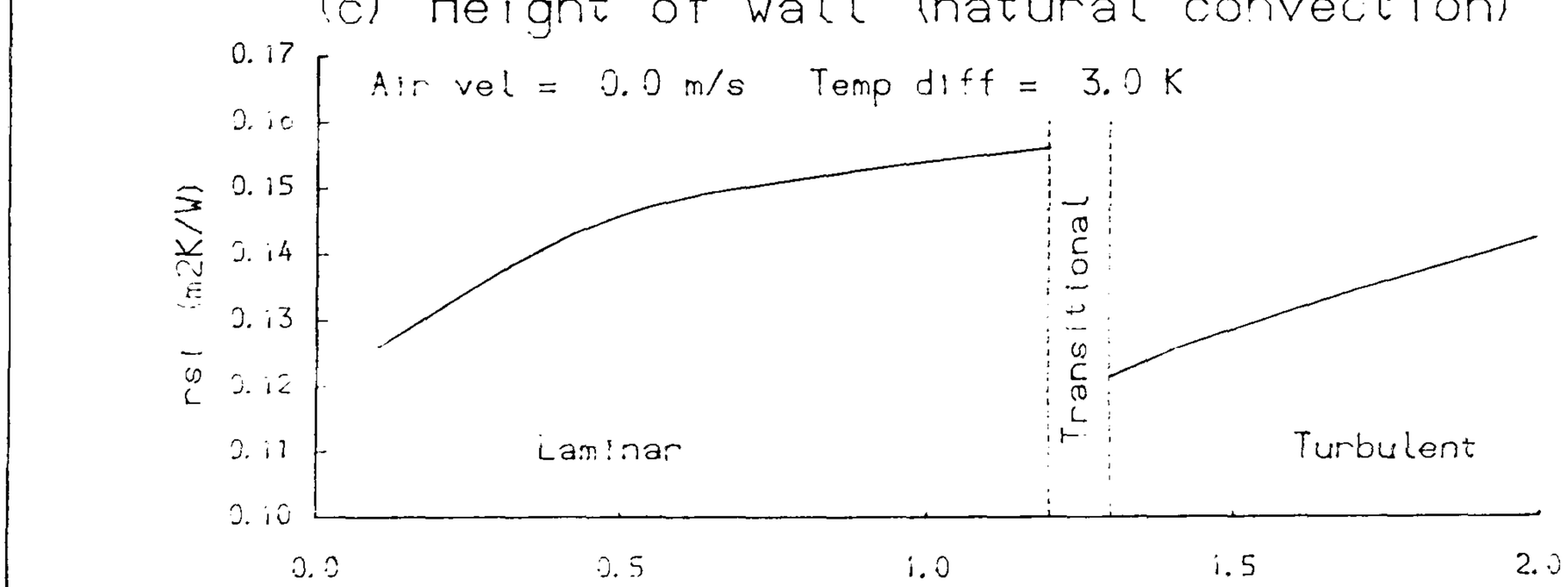

$h_{rad} = 5.7\ W/m^2K$

Fig 3.4

In these calculations it has been assumed that tei is equal to tai to simplify comparisons further.

It can be seen that the value of the internal surface resistance does not vary much even if the parameters it depends on are varied to extreme values. For practical values of the above parameters the internal surface resistance does not vary much from the 0.12 m,K/W recommended by the CIBS guide (Table A3.4) (16). Hence for consistency and simplicity this is the value used to calculate all subsequent heat flows. The errors arising from this would be no greater than in any experimental measurement.

3.4 - Monitoring Proceedure

Since so many channels need to be scanned (up to 90) it was only possible to record a full day at 20 minute intervals. This is only a disadvantage in recording the insolation, since the value recorded at any instant may not be typical of that period. All the temperatures vary sufficiently slowly for this to be no problem. The effect on the values of insolation will clearly be seen in the results and hence these must not be relied on too heavily.

The glazed cavity wall was run up to March 1982 without forced air heat recovery. This left a relatively short time for results to be obtained with forced air heat

recovery but this was sufficient to give reasonable results.

Paper tapes were changed manually and read into the Leeds University Amdahl computer for analysis. This was found to be time comsuming because the University has only one paper tape reader which was frequently out of action which caused delays.

3.5 - Tape Analysis

After the tapes were read into the computer and corrected where necessary by hand, they were analysed by a computer program of which the flow chart is shown in Fig 3.5. Many of the problems of analysis are the same as those of J Lee and are described by him (14).

The main part of the program allocates channels to walls, recognises the innermost thermocouple of each and calculates the heat flow. The channels 82-85 are recognised individually as special functions (insolation, room temperature, outside air temperature and temperature of glazed cavity wall air output). The results are put into various output files and can then be displayed on a line printer or by a graphical output program.

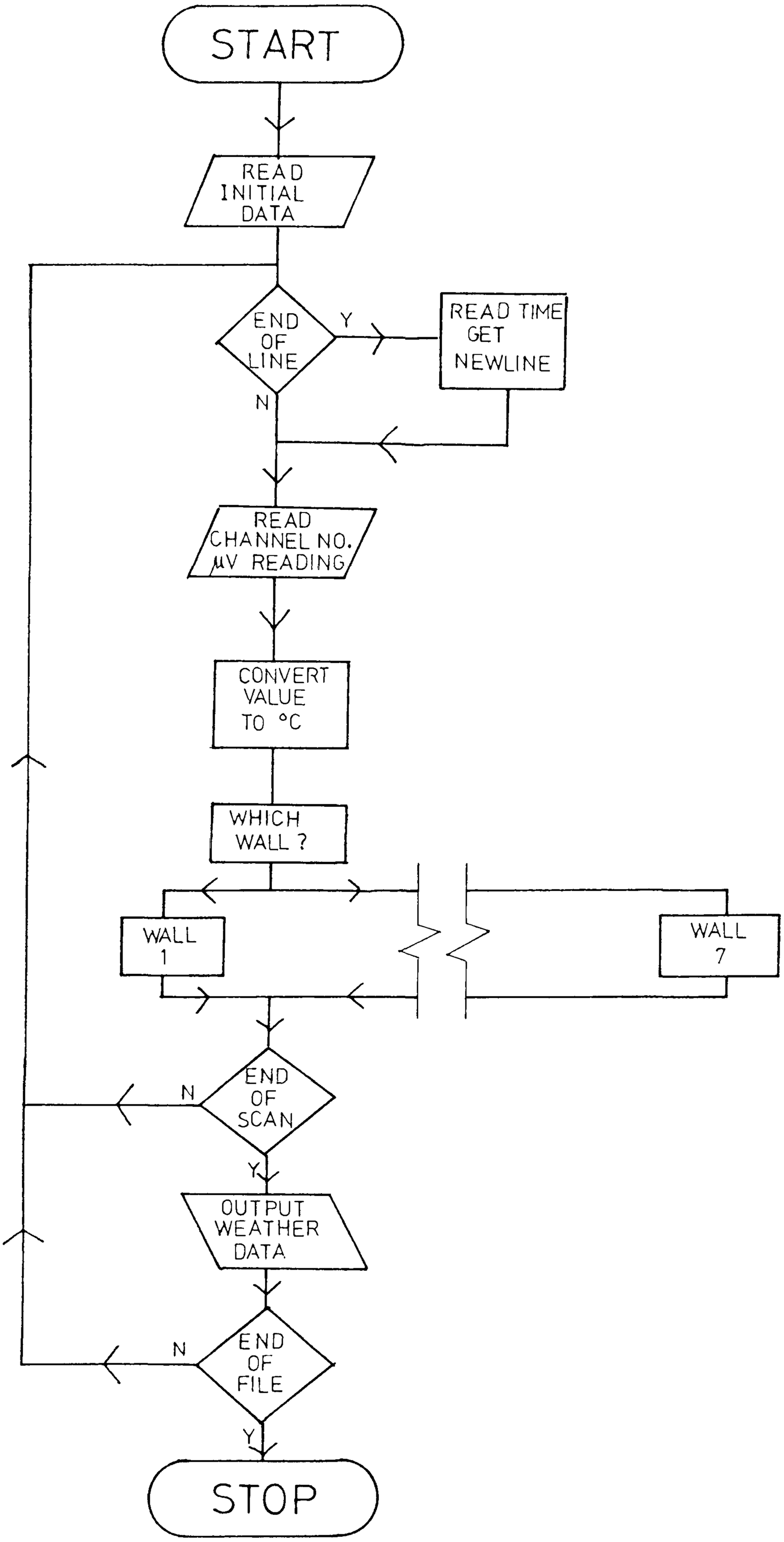

Fig 3.5 - Flow Chart for Tape Reader Program

Chapter 4

Masonry Walls - Experimental Results, the Effect of Reduced Rain Penetration due to Glazing

As mentioned above, glazing a brick wall will prevent rain penetration which in turn will alter the heat flow characteristics. To test this effect a solid wall was built which was coated on the outside with a transparent waterproof varnish. Its performance was compared with that of the unmodified solid brick wall. This is a control experiment to check what proportion of the improvement is due to preventing rain penetration. No attempt will be made to analyse this effect theoretically in this thesis.

4.1 - Theory

The way in which rainfall and moisture absorption affects the heat loss through a wall is complicated. A summary of the various mechanisms would include,

(1) evaporation from the outside surface

(2) condensation within the wall

(3) water flowing down the outer face.

These in turn would alter the wall properties i.e the thermal capacity and the specific heat capacity.

The theory of the combined effect of moisture and heat flow is complicated. There was insufficient time to

do a rigorous theoretical analysis of this problem, although it would be very difficult to justify any hypothesis from experimental work alone.

This problem was partly solved by Vahid of Newcastle School of Architecture (17). This work was a completely theoretical analysis largely covering the experimental work outlined above. Comparisons with this work will be made below. Vahid's work is a modification of Basnett's 'HOUSE' computer model (18) for simulating the thermal performance of buildings, based on unsteady state theory. A typical house is simulated which has intermittent heating. The model begins with all the walls dry, and is run for 12 hours model time to allow the model to steady. Then the house is subjected to heavy rain for 6 hours, after which the model is run for a further 72 hours with no further rain. Vahid studies the effect the rainfall has on the wall and room temperatures.

4.2 - Experimental Results

4.2.1 - Experimental measurement

The measurement consists simply of comparing the heat loss of the two walls. The values plotted on the following graphs are

$$q(\text{unmodified}) - q(\text{waterproofed}) \qquad (4.1)$$

The monitoring of these heat flows is as described in

section 3.3. No continuous measurement of rainfall or wind speed was made, but for each day the insolation and outside air temperature is given.

4.2.2 - Results

This section describes the experimental observations made, comparing the waterproofed and unmodified walls.

Results fall into two catogories, those from long periods of cold, wet weather, and those from long periods of warm, dry weather. In periods of changeable weather the results tend to be a combination of these two extremes. The positive values on the following graphs show the waterproofed wall with a lower heat loss than the unmodified wall.

Fig 4.1 shows results for a day in the first category. The period was cold, with little sun and much, often heavy, rainfall. The curve consistently shows a 6-8 W/m^2 (0.8-1.0 K) difference. It is important to note that a period of heavy rain does not cause any rapid change in heat flow on the inner face.

One exception to this is if the sun shone for a appreciable time in an otherwise cold, wet period. Results for such a day are shown in Fig 4.2. After the period of sunshine the difference between the two walls approaches

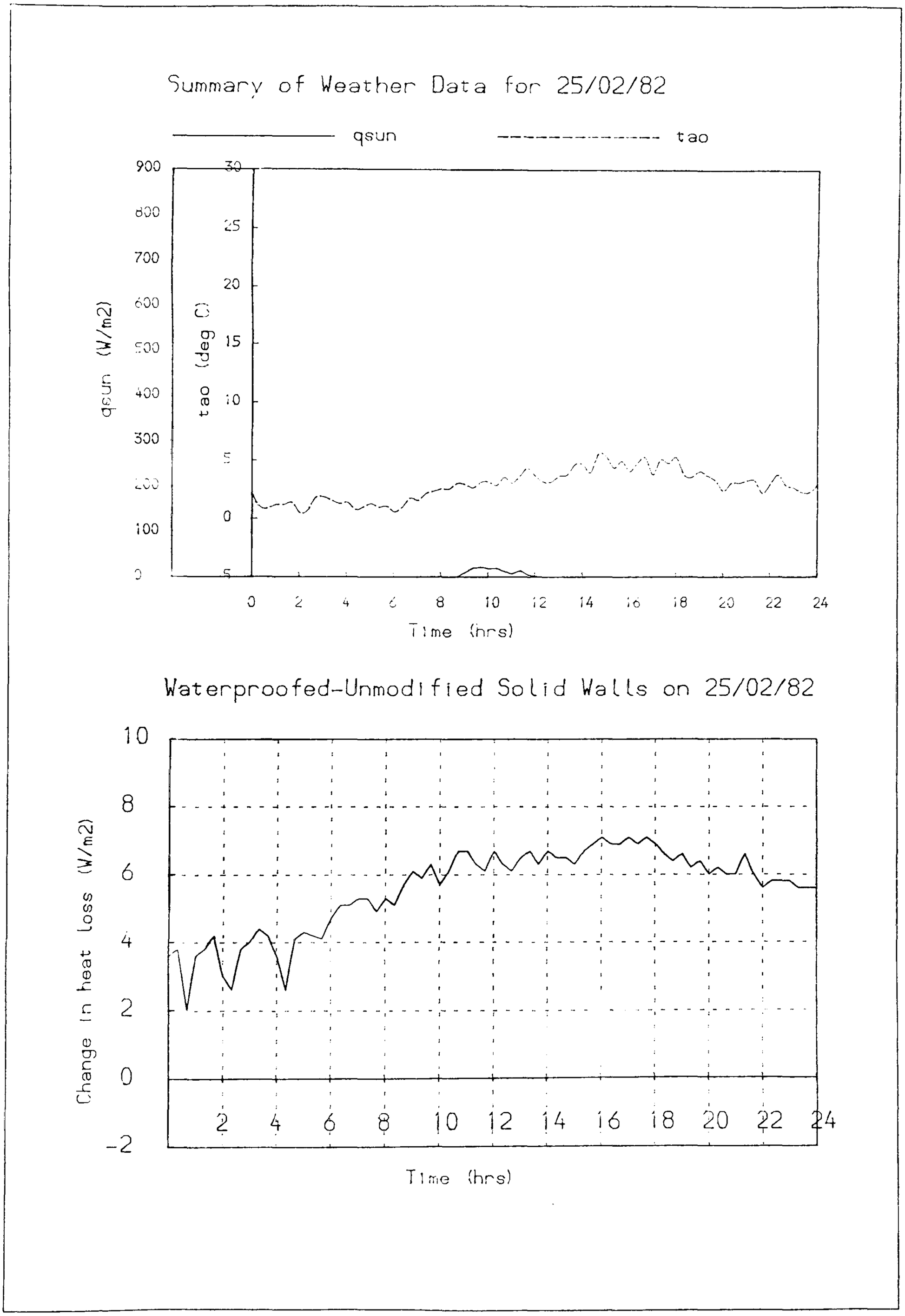

Results for cold rainy day. Fig 4.1

Shows waterproofed wall steadily better than unmodified wall.

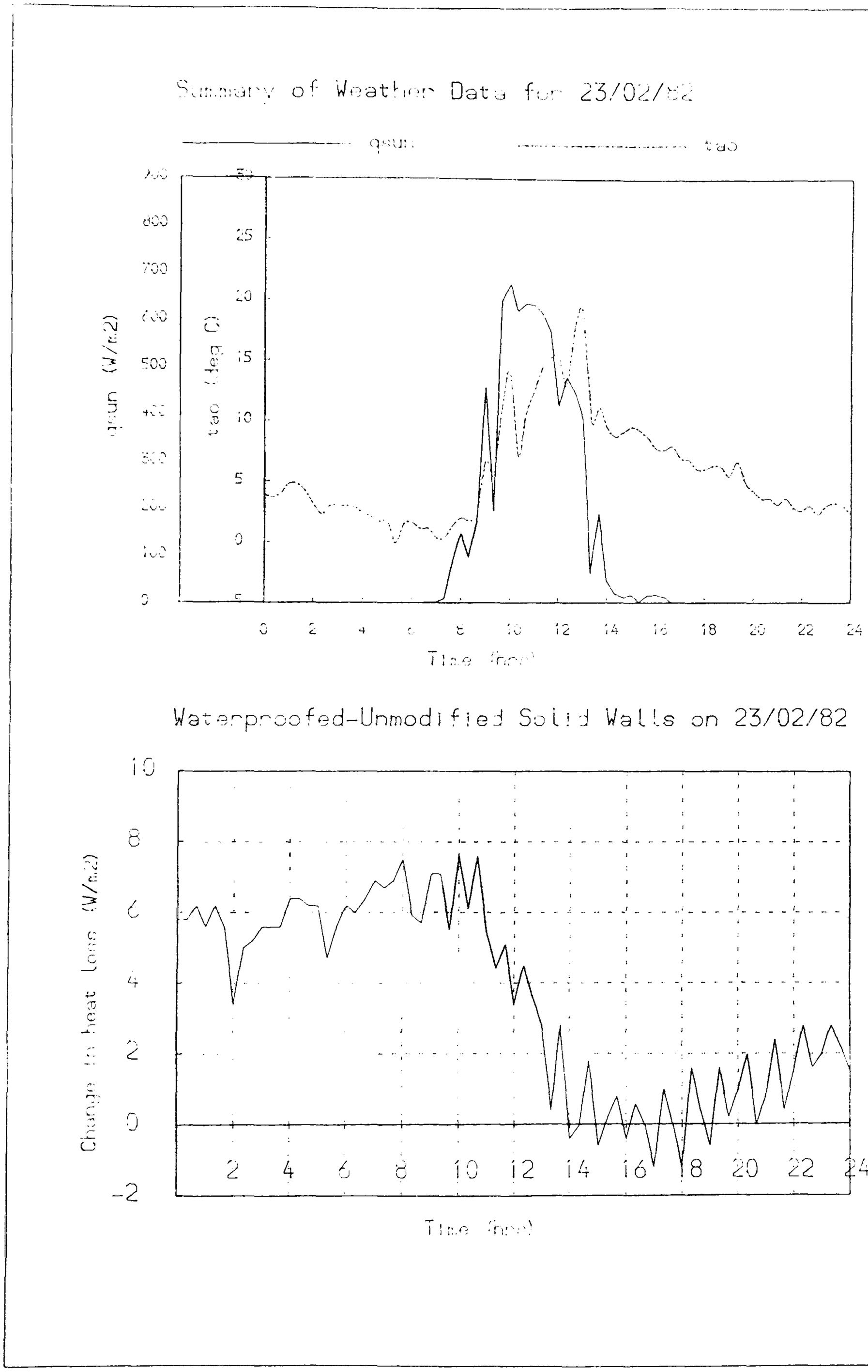

Results for cold, rainless and sunny day.

Fig 4.2

Shows walls having equal heat flows after period of sunshine

zero, as the evening progresses the difference reappears although there had been no further rain that day.

An example of the second catagory is given in Fig 4.3. This period was very dry and even though it was relatively dull, there is no great difference between the two walls. Any small amounts of rain in such a period have no noticable effect on the heat loss of the unmodified wall.

4.2.3 - Discussion of results

Having made some observations, it is necessary to provide some explanations. Clearly, without more detailed results these explanations can only be hypotheses.

During the winter when the weather is cold and wet with little sunshine it is quite clear that the wall has very little chance to dry. To support this Fig 4.4 shows the time taken for a brick to dry at room temperature. The brick was first saturated, and moisture was allowed to escape from all surfaces. Drying is very slow. The experiment was not monitored after the end of the graph on fig 4.4.

It is interesting to compare observations with predictions from Vahid's theoretical work. He expects a rapid variation in the internal surface temperature during

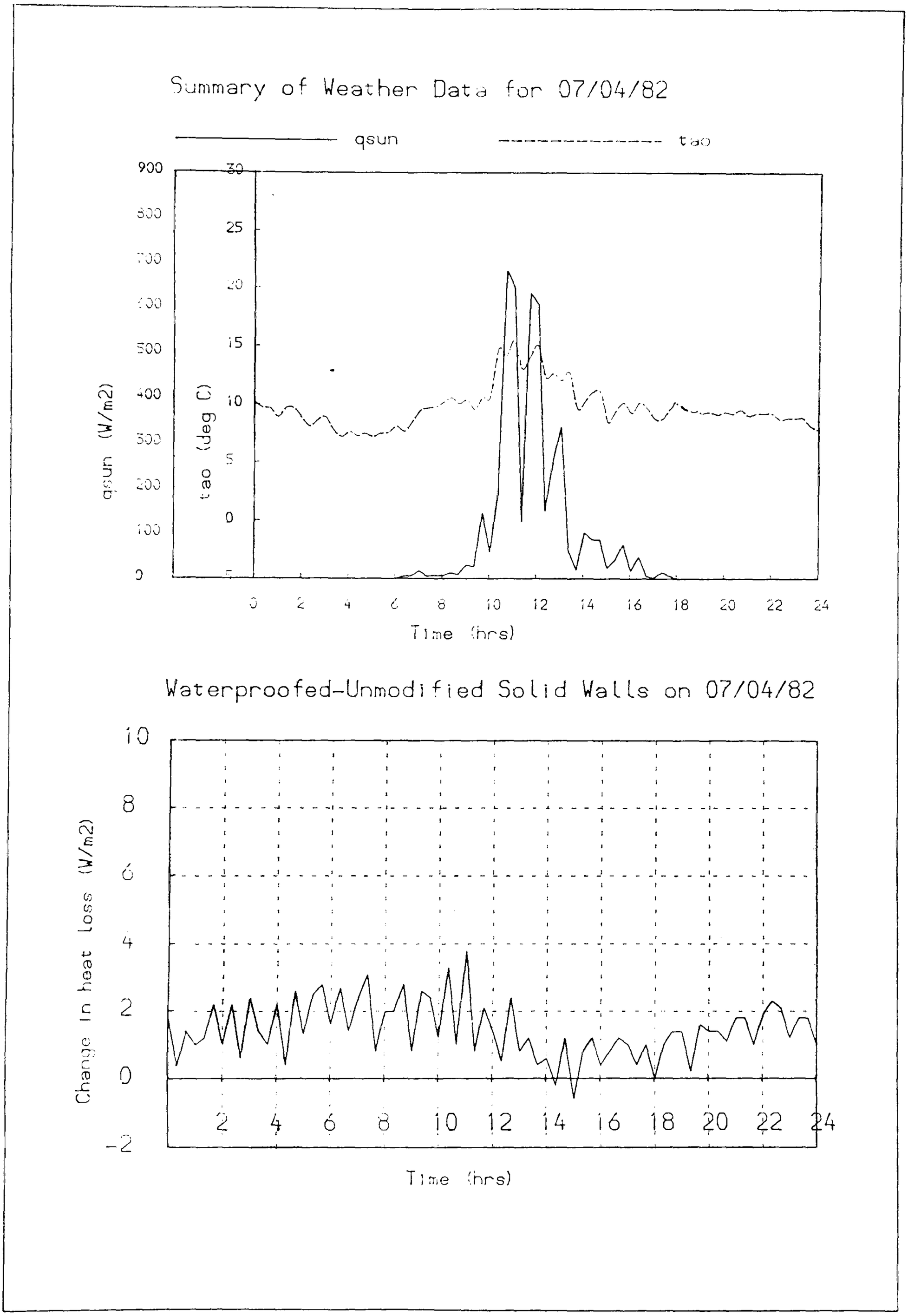

Results for warm dry day, after a prolonged dry spell.

Fig 4.3

Shows walls steadily equal during prolonged dry spell

Moisture Content v Drying Time For Brick at Room Temp

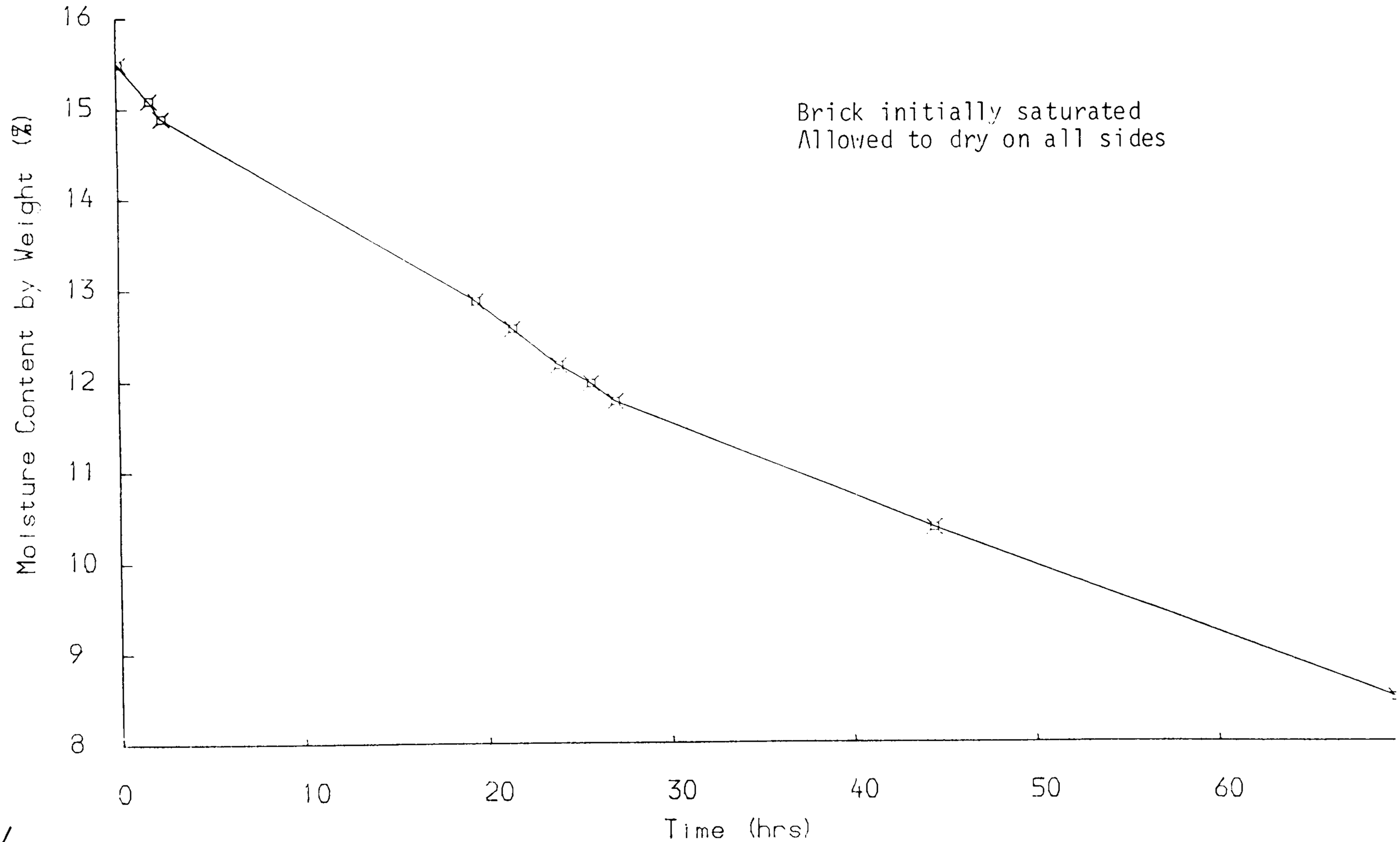

Brick initially saturated
Allowed to dry on all sides

Fig 4.4

the period of rain. Such an effect was never observed, but in the period immediately after the end of rainfall, Vahid's results compare well with the experimental results given in Fig 4.1, both show a difference of about 0.7-0.8 °C. Vahid's results also show that the difference disappears when the outside air temperature rises. Vahid's model takes about 36 hours after the end of the rainfall for the difference to disappear permanently.

In the winter, on a sunny day, as summarised in Fig 4.2, the outer parts of the wall dry, so that there can be no evaporation from the surface. After the period of sun, moisture from the inside of the wall will have diffused to the surface, and evaporation will again take place cooling the wall. The fall in the graph 4.2 from 1100 to 1600 hours, followed by the difference reappearing seems consistent with this hypothesis, (the maximum solar radiation is at 1000, the minimum difference is at 1700, the phase lag is hence 5 hours, which is what would be expected for a double thickness brickwall).

For very dry periods, such as April 1982, the unmodified wall will dry almost completely and any small amounts of rain will soon evaporate and have little or no effect on the heat loss. In such a period the thermal conductivity will also be lower.

4.3 - Conclusions

The experimental results obtained seem consistent with Vahid's theoretical work, except during the period of rain. Vahid expects a rapid change in the wall internal surface temperature of up to 2 K. Such a change was never observed in the experimental work described above. The difference may be caused by the fact that the model was begun with dry walls which is rarely true in real walls. In winter a temperature drop of about 1 K could be expected on the inside of a solid brick wall which is equivalent to about 8 W/m^2

$$qtot = dT/R_{SI} = 1/0.125 = 8\ W/m^2 \qquad (4.2)$$

Although the experimental results discussed above cannot show why this difference occurs, Vahid suggests that the major affect is the evaporation from the outer surface. Vahid's work compares well with the observed results. The effect of rain penetration can be significant, but provided the wall is well pointed, it would not be worthwhile, thermally, to waterproof a solid wall.

Chapter 5

Masonry Walls - Experimental Results, effect of Glazing on Solar Gain

The results fall into two sections - those for solid walls and those for cavity walls. Theoretical comparisons are made only where it helps to explain the experimental results. More detailed theoretical results are described in chapter 10. The important parameter considered is the 'improvement', this is the reduction in heat loss through the wall, comparing the modified wall with the unmodified wall. The previous chapter eliminated the improvement due to the prevention of rain penetration. This chapter discusses the improvement due to the increased solar gain caused by glazing of the walls.

5.1 - Solid Walls

5.1.1 - Experimental results

The heat gain or loss from the solid brick walls was only by convection and radiation from the wall's inner surface to the room. The effect of moisture was examined in chapter 4, hence the two typical situations to consider are a sunny day and a dull day. For comparison the performance of the waterproofed wall is given with that of the glazed wall and the unmodified wall.

Fig 5.1 shows the heatflows and the weather data for a typical sunny day in late February (23/02/82). In the evening the glazing gives an improvement of about 20 W/m^2 (2.5 K), this means that between 1800 and 2300h the glazed wall loses no net heat, (i.e the evening occupation period discussed in chapter 1). Over the day the glazing gives an improvement of 1.7 MJ/m^2.

Fig 5.2 shows the temperature gradients in the wall at various times of the day. It is obvious that of the heat stored most is lost to the outside and little enters the room.

Fig 5.3 shows results for a dull day in February (19/02/82), (the dip at 1600 hrs is a logging fault). There was no measurable sunshine and the outside air temperature dropped slowly and steadily. The result is that the wall almost reaches a steady state: this can be seen in the temperature distributions in Fig 5.4. The average improvement is about 11 W/m^2, and is totally due to the extra thermal resistance provided by the glass along with the wall being drier.

The most complete period analysed is February, March and April 1982, a total of 92 days. Fig 5.5 gives a summary of results for this period for the various solid walls. MacGregor (7) gives a average monthly improvement of 45.3 MJ/m^2, (monitored over a whole year), in comparing

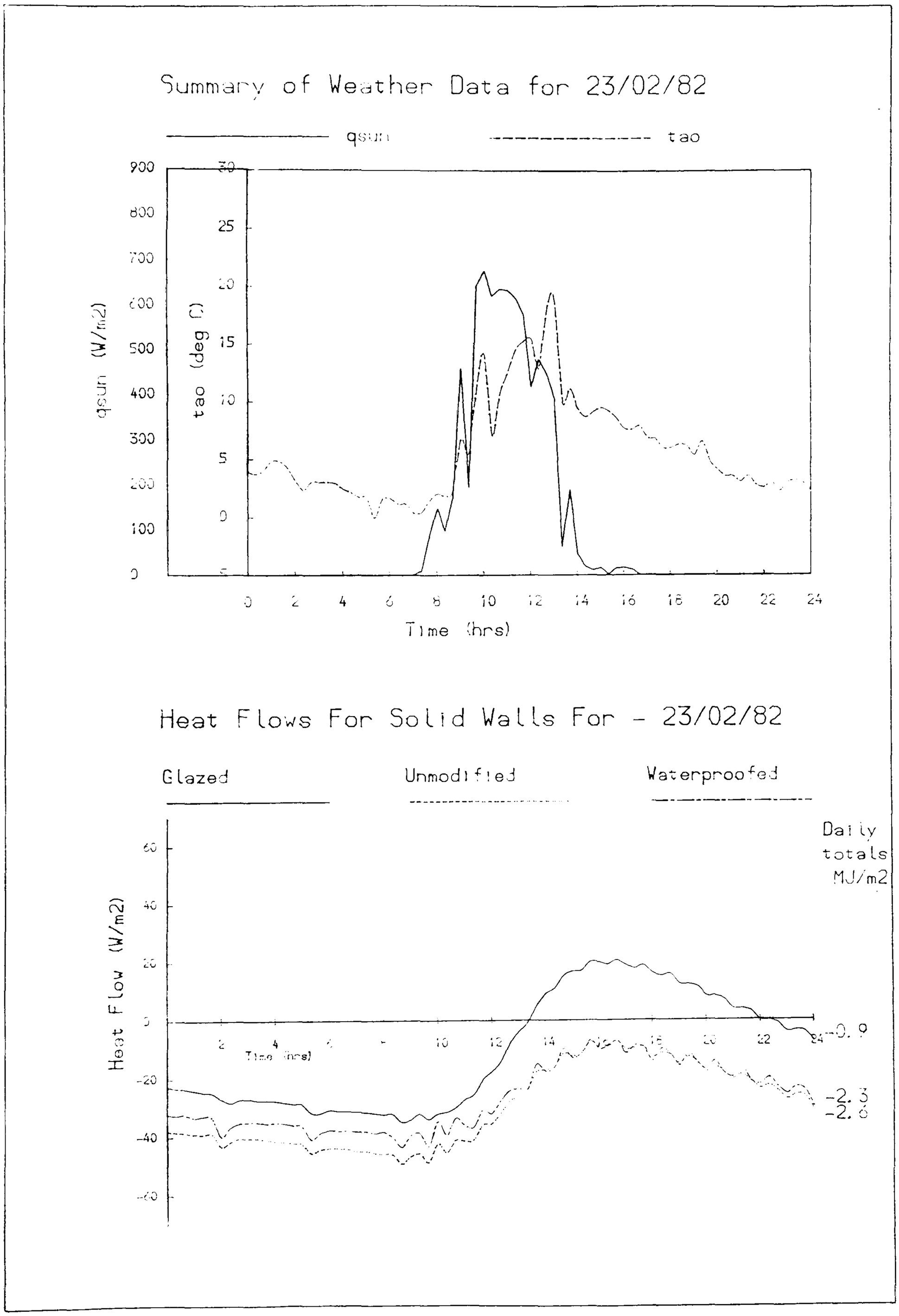

Shows walls on a sunny day in late winter

Fig 5.1

EXPERIMENTAL RESULTS FOR SOLID WALLS FOR 23/02/82 ROOM TEMP=20 DEG C

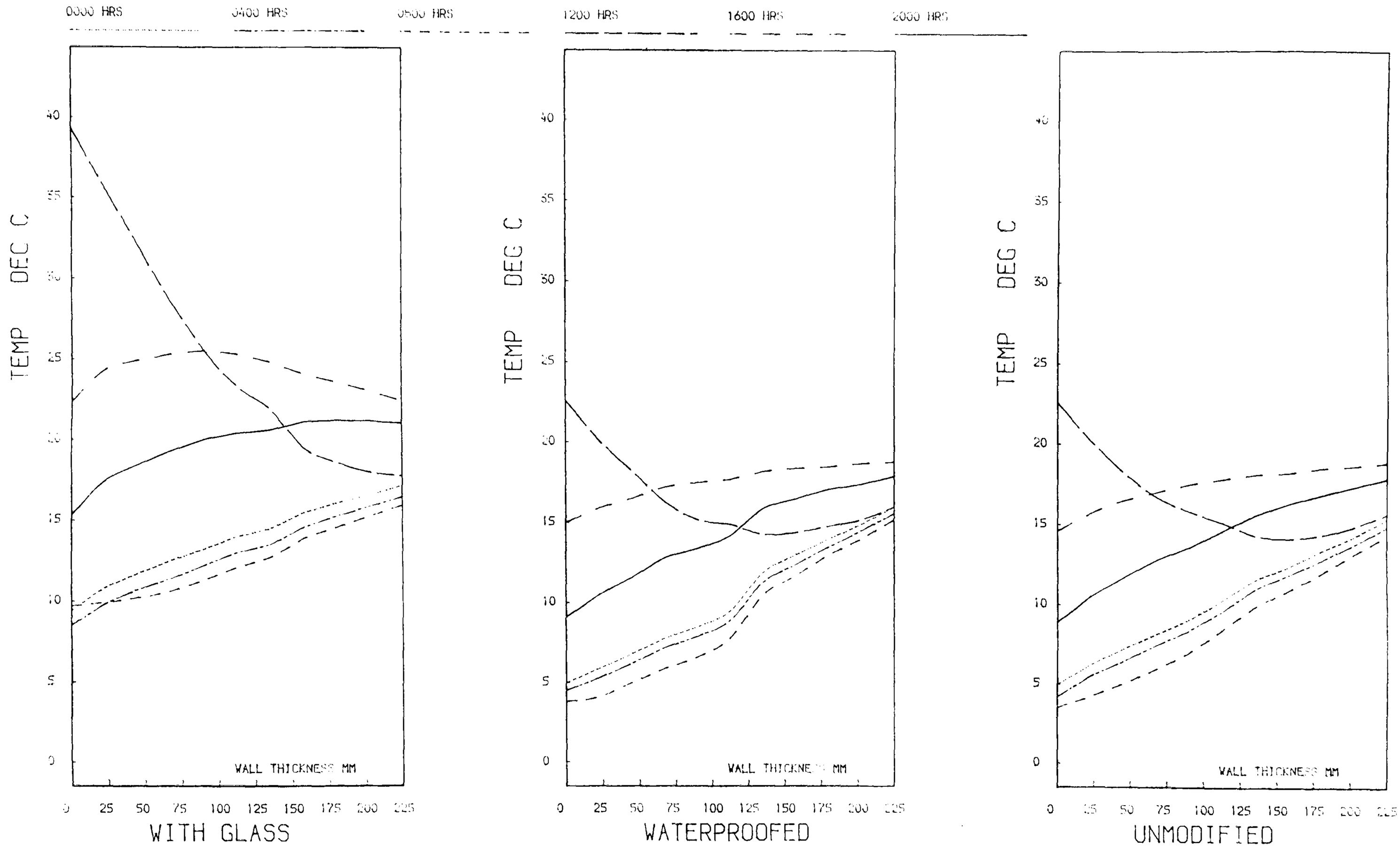

Fig 5.2 Shows temperature profiles for a sunny day in winter, showing the movement of stored heat in the walls

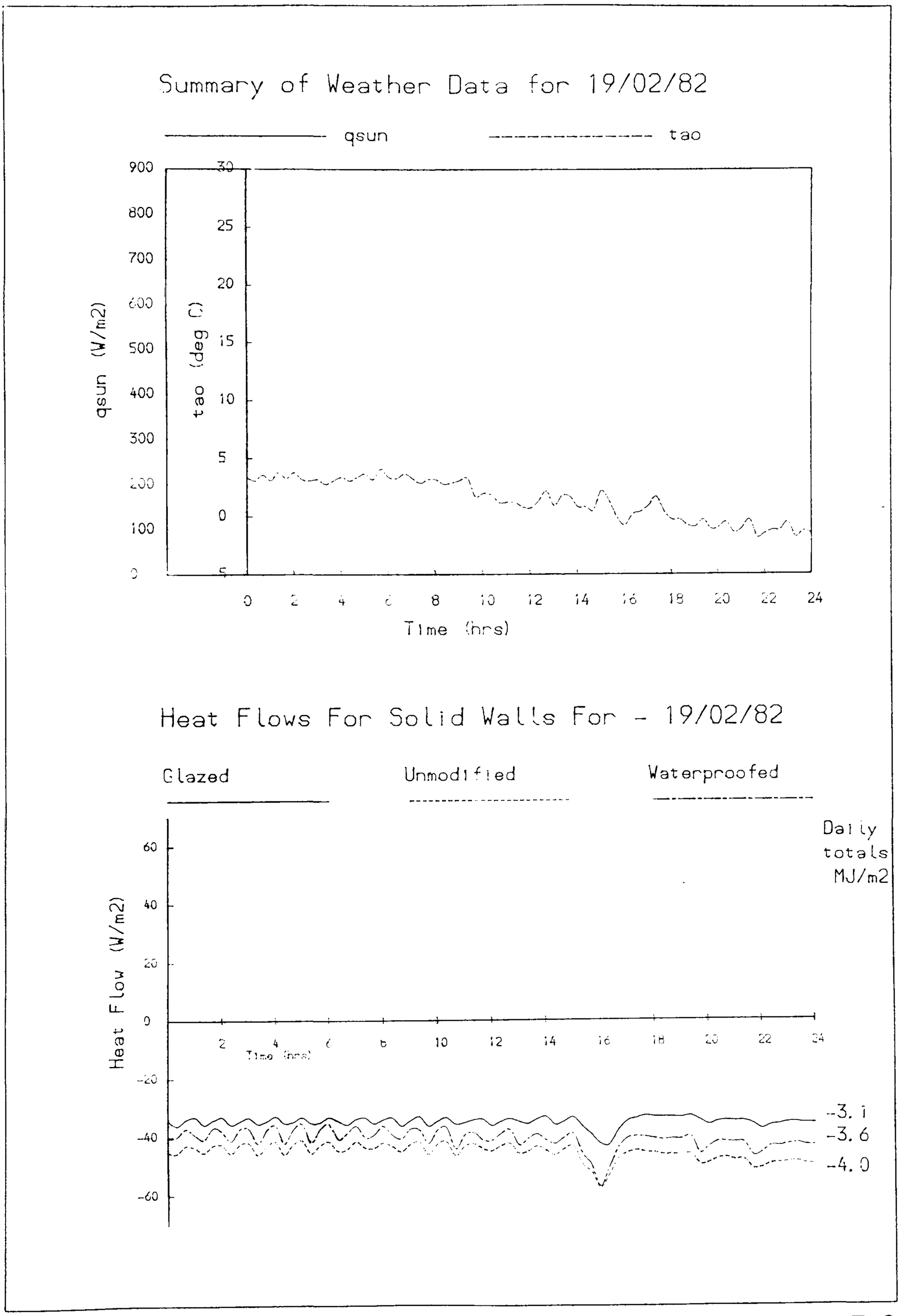

Fig 5.3

Shows performance for a cold sunless winter day.

This shows the improvement in U value due to the glass alone.

EXPERIMENTAL RESULTS FOR SOLID WALLS FOR 19/02/82 ROOM TEMP=20 DEG C

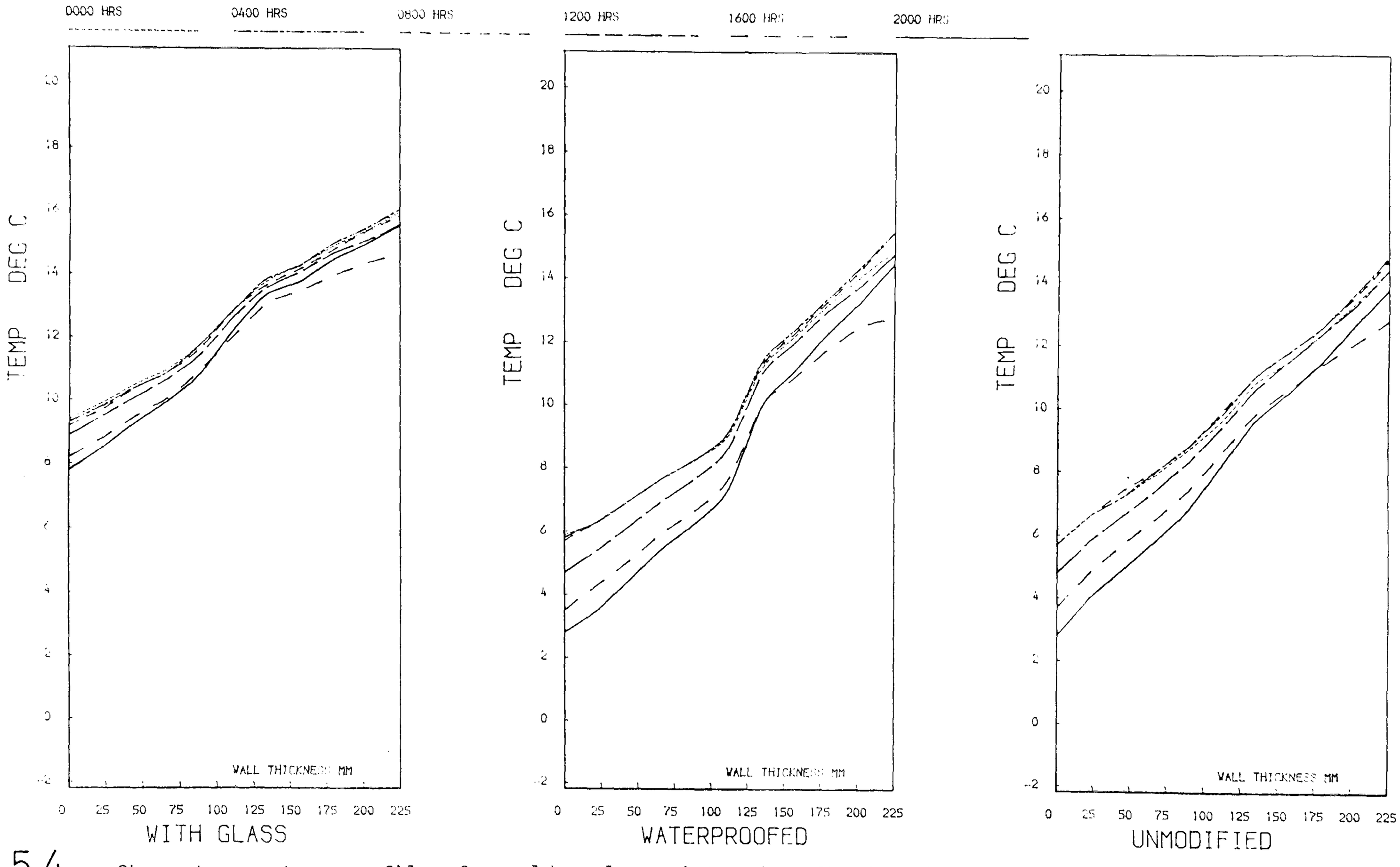

Fig 5.4 Shows temperature profiles for cold sunless winter day. Showing the walls approaching steady state.

Wall	month / Period	FEB Heat flow MJ/m²	FEB Improvement MJ/m²	MAR Heat flow MJ/m²	MAR Improvement MJ/m²	APR Heat flow MJ/m²	APR Improvement MJ/m²
Glazed	full day	-53.2	38.5	-46.5	40.3	-30.4	24.8
	18-23	-8.0	10.2	-6.2	11.2	-4.8	6.6
Water-proofed	full day	-80.5	11.2	-83.7	3.1	-52.1	3.1
	18-23	-16.1	2.1	-17.1	0.3	-10.8	0.6
Un-glazed	full day	-91.7	0.0	-86.8	0.0	-55.2	0.0
	18-23	-18.2	0.0	-17.4	0.0	-11.4	0.0
No. of days		28		31		30	
Q MJ/m²		125		162		151	

Fig 5.5 - Summary of Solid Walls' Performance 1982

a glazed and unglazed wall. Davis (36) from steady state calculations outlined in section 2.1, predicts an improvement of 42 MJ/m^2 for March. These compare well with the figures in Fig 5.5, e.g 40.3 MJ/m^2 for March. The improvement calculated using steady state theory and the experimental weather data gives an improvement of only 33.8 MJ/m^2.

It is interesting to note that the improvement in March is more than in April. This is because of more incident solar radiation, which is partly due to the lower solar altitude in March.

5.2 - Cavity Walls

In this section, the results of the cavity walls are discussed. Firstly a glazed wall with sealed cavity (no air heat recovery) is compared with an unmodified, unglazed cavity wall. Then in the second section a glazed cavity wall, with fan assisted air heat recovery is compared with the unglazed cavity wall.

5.2.1 - Without air heat recovery

This wall has a sealed cavity, no convective heat recovery is used. Fig 5.6 shows the performance of the cavity walls and Fig 5.7 shows the temperature distributions and the weather data for 23rd Feb 1982. The

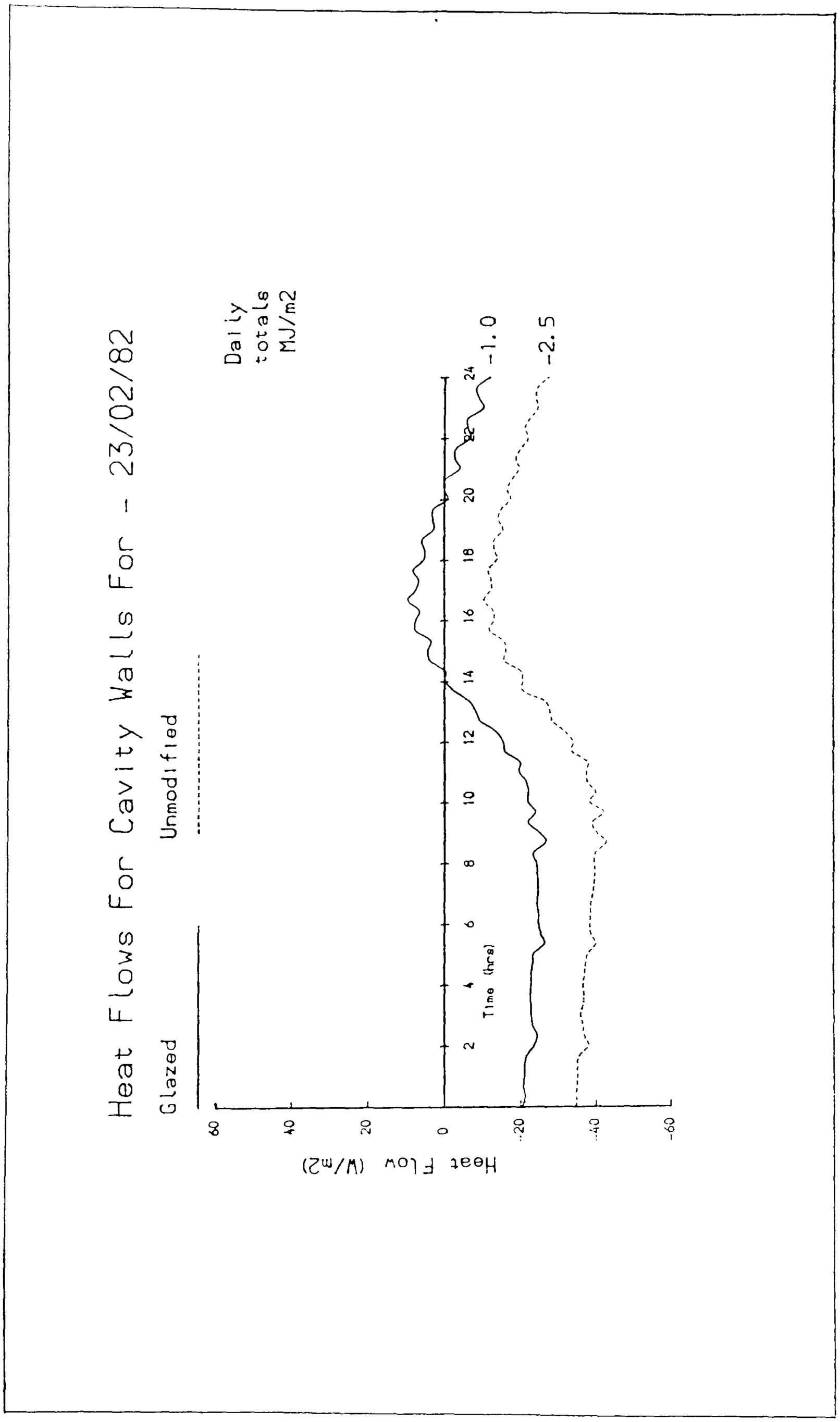

Shows performance for sunny winter day. No convected gain from cavity.

Fig 5.6

EXPERIMENTAL RESULTS FOR CAVITY WALLS FOR 23/02/82

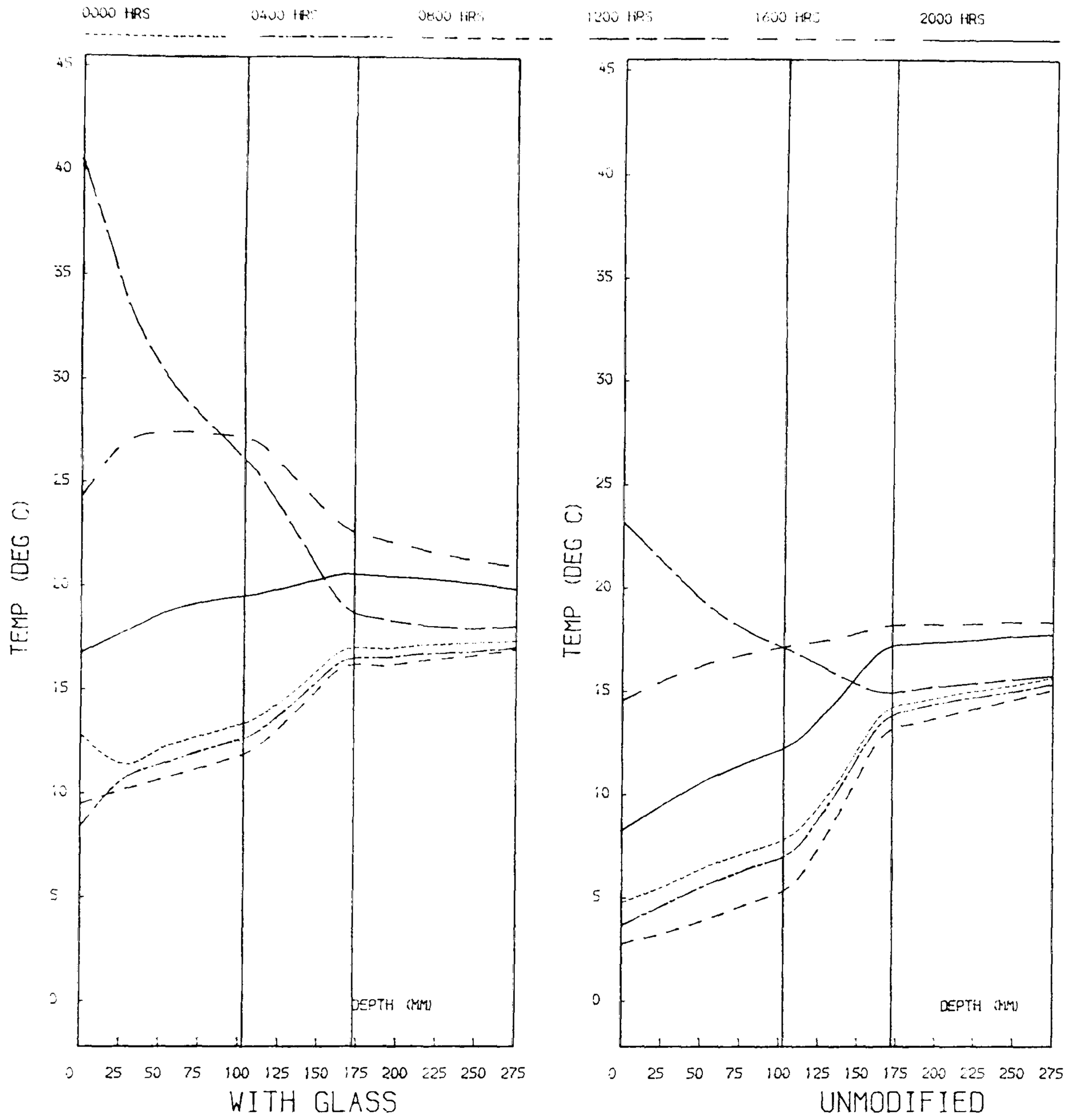

SUMMARY OF WEATHER DATA FOR 23/02/82

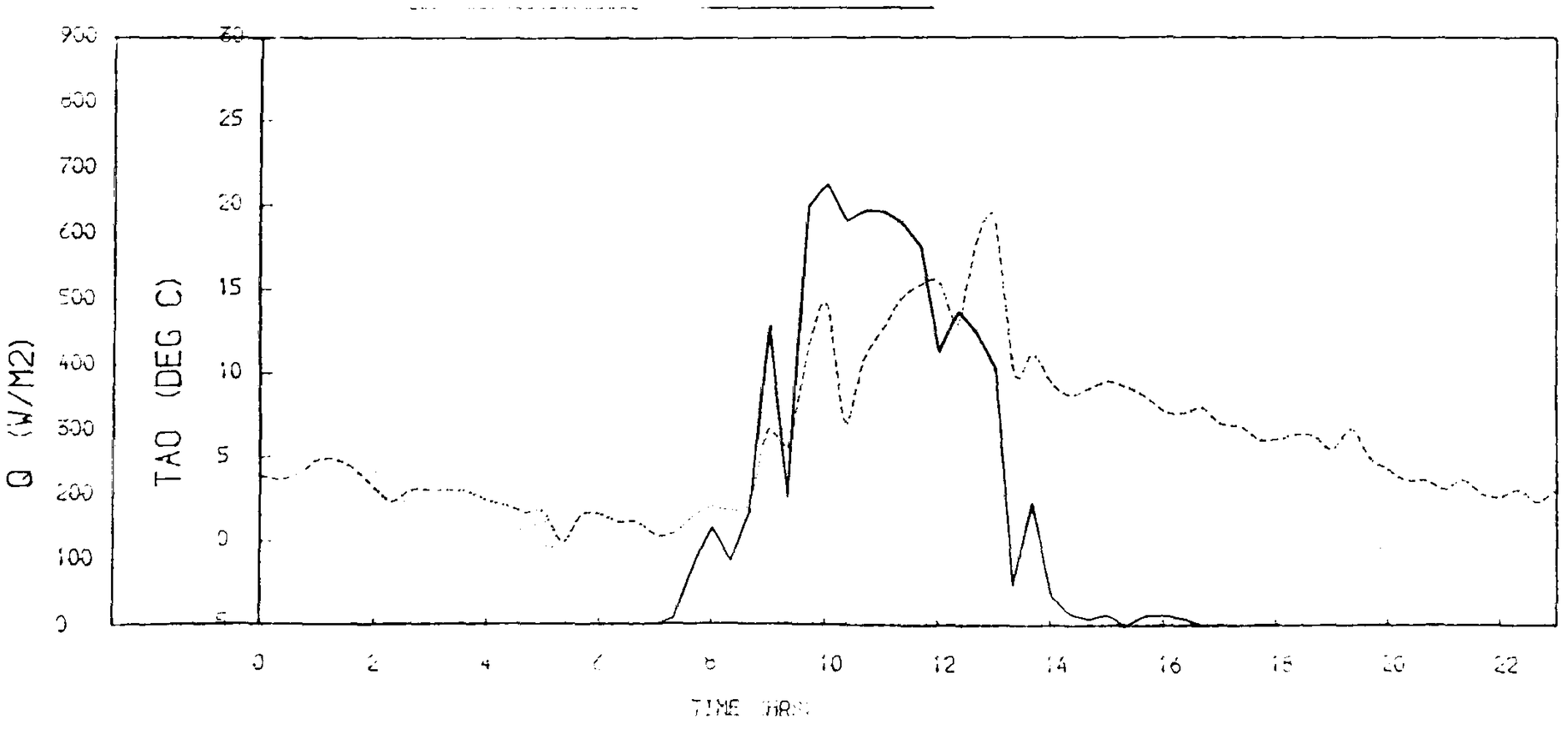

Shows temperature profiles for sunny winter day.
Shows the effect of the cavity resistance.

Fig 5.7

effect of the thermal resistance of the cavity can be seen, especially when compared with the results for the solid walls on the same day Figs 5.1 and 5.2. The daily variation of temperature on the wall's inner surface is smaller for a cavity wall than for a solid wall.

In the CIBS Guide A (16), equation A8.8 gives the periodic heat flow through a wall due to solar loading. This is given by

$$q_f = fUA(teo - tei) \qquad (5.1)$$

where f is the decrement factor calculated from the admittance method, (f=0.46 for a solid wall, and f=0.39 for a cavity wall). Since the temperature difference is the same for both the glazed solid wall and the glazed cavity wall, the ratio of fU(cav)/fU(sol) should represent the comparison of the two heat flows. This ratio is 0.63. From the experimental results the ratio of the 'improvements' is 0.61 for February and 0.63 for March. This shows that the lower the value of fU, the poorer the performance.

5.2.2 - With forced air heat recovery

This is the same glazed wall as 5.2.1 but with fan assisted air heat recovery. The airflow was 0.07 m^3/s, giving an airspeed of 1.4 m/s in the cavity. As discussed in chapter 3 the fan operates when the air in the cavity is warm enough. Fig 5.8 shows the performance of the cavity

EXPERIMENTAL RESULTS FOR CAVITY WALLS FOR 15/04/82

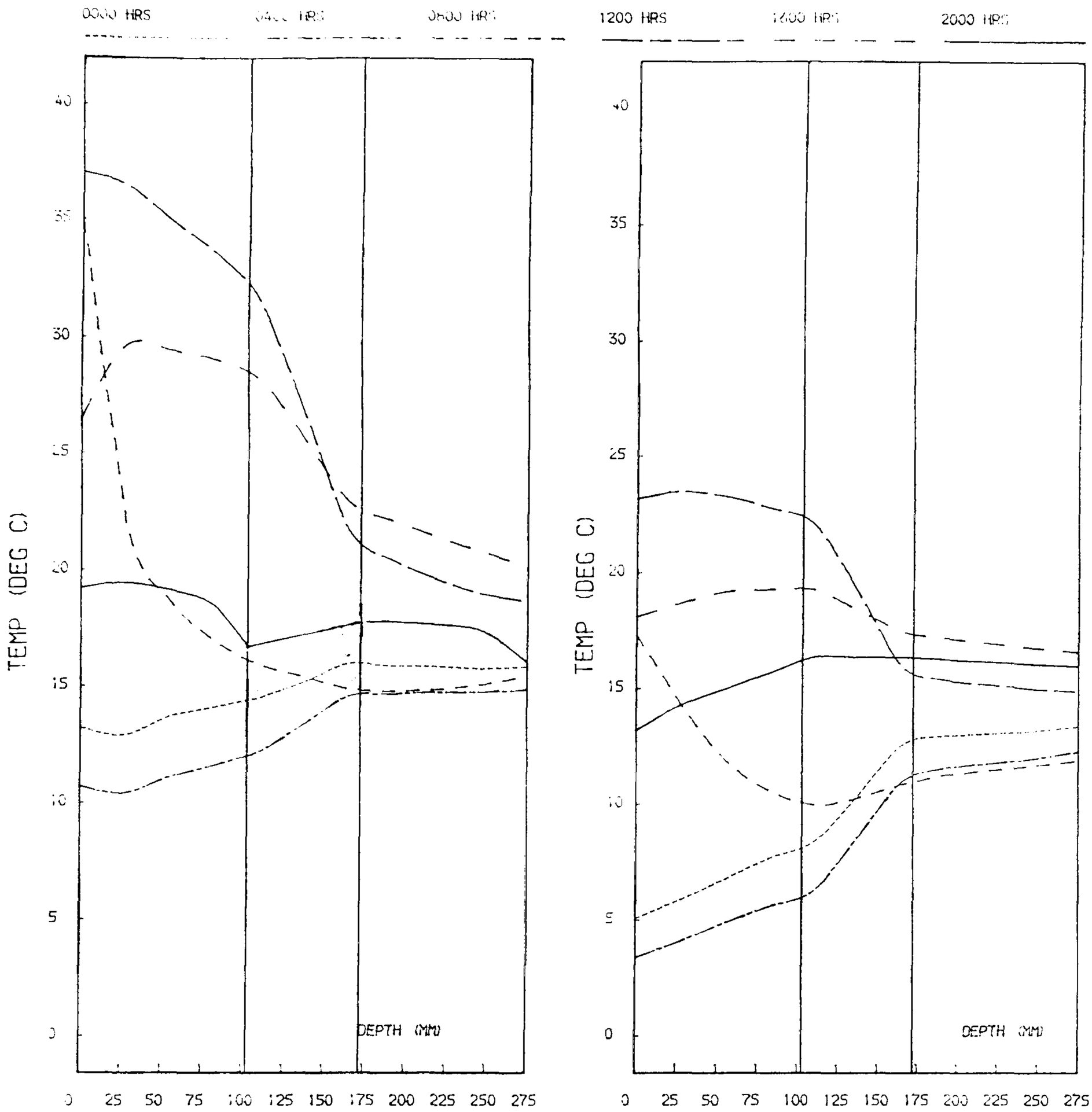

SUMMARY OF WEATHER DATA FOR 15/04/82

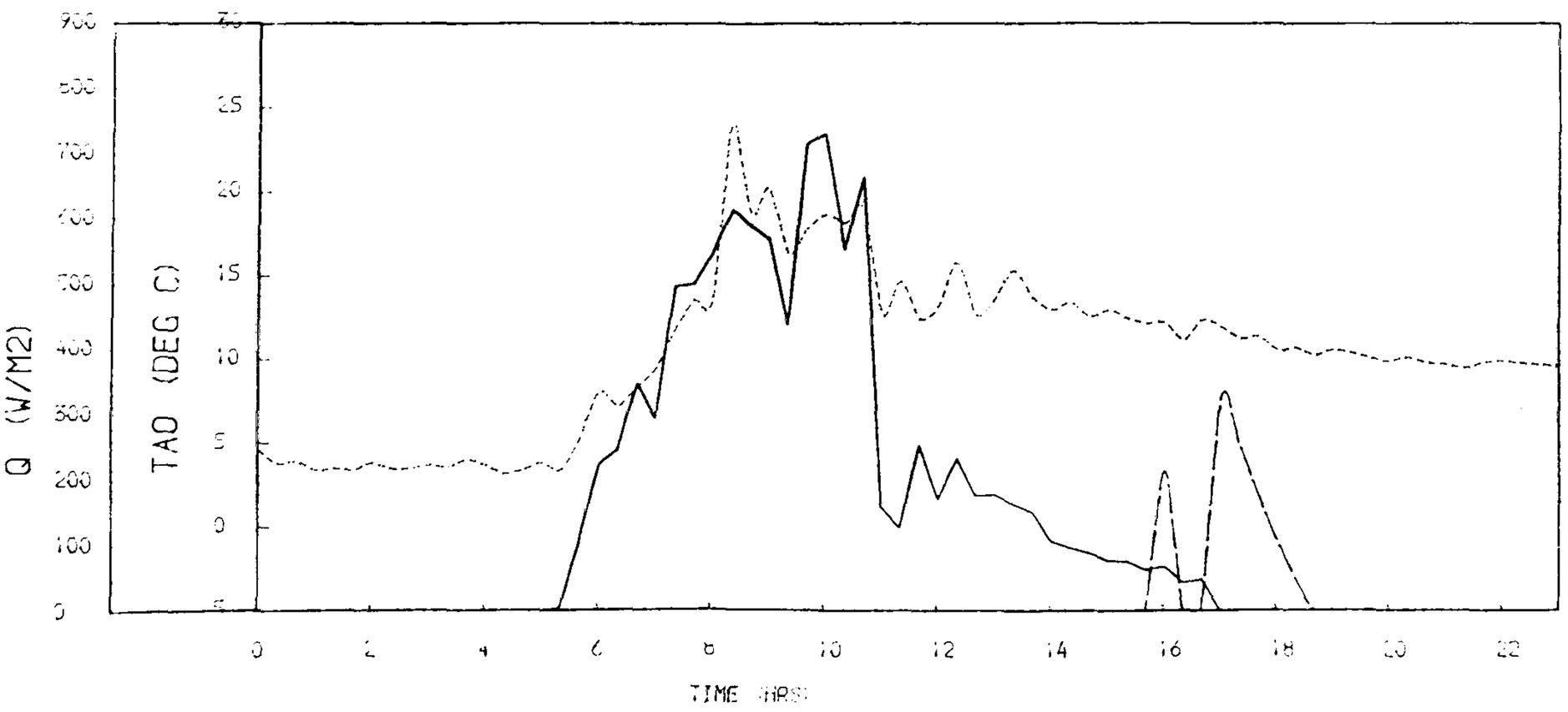

Shows performance on a sunny spring day.
Wall has convected gain from cavity (forced)

Fig 5.8

walls along with weather data for 15th Apr 1982. The maximum heat output from the circulated air is 436 W, the total heat recovered over the evening is 1.5 MJ. The fan consumes a constant 180 W which for the period considered gives a total of 1.3 MJ, this gives a net gain of only 0.2 MJ. Since the fan works from peak rate electricity and the energy saved may well be from gas, clearly this is not an efficient collector, however, the fan was not specifically sized for this system. The comparison with the walls described in section 5.2.1 is not reliable. The incident solar radiation on the walls is actually a little less in April although the average outside air temperature is higher.

Figs 5.9 and 5.10 give summaries of the total period described in section 5.2.1. Fig 5.9 is for the walls without forced air heat recovery, and Fig 5.10 is with forced air heat recovery from the glazed wall. Comparison with the results for solid walls shows that the use of glazing is less efficient for cavity walls. Also it is clear that the use of fan assisted heat recovery from a cavity wall is hardly worthwhile.

Wall	month / Period	FEB Heat flow MJ/m^2	FEB Improvement MJ/m^2	MAR Heat flow	MAR Improvement MJ/m^2
Glazed	full day	-56.3	23.3	-49.0	25.3
	18-23	-9.5	6.2	-7.1	6.1
Un-glazed	full day	-79.8	0.0	-74.3	0.0
	18-23	-15.6	0.0	-13.2	0.0
No. of days		28		31	
Q MJ/m^2		125		162	

Fig 5.9 - Summary of Cavity Walls' Performance 1982
(No Air Recovery)

Wall	Period	Gain from inner surface MJ/m^2	Convected gain MJ/m^2	Total gain MJ/m^2	Improve-ment MJ/m^2
Glazed	full day	-39.3	10.6	-28.7	28.8
	18 - 23	-7.4	1.0	-6.4	5.8
Un-glazed	full day	-57.5	0.0	-57.5	0.0
	18 - 23	-12.2	0.0	-12.2	0.0

Fig 5.10- Cavity Walls' Performance - April 1982

(Forced Air Recovery)

Chapter 6

Natural Convection Collectors - Theory

This chapter and chapters 7 and 8 describe the second main section outlined in the introduction. This work develops a theoretical model for natural convection collectors and shows the validity of the model with some experimental work.

The main disadvantage of a masonry wall with only a piece of glass on its outer face, is that at night or in prolonged dull periods, it loses most of any stored heat to the outside. If in such periods, a piece of insulation could be inserted in the gap between glass and wall, then the heat loss would be reduced.

It would be difficult to move insulation into the gap. Possible arrangements with a conservatory are described below in section 9.5.1. The original 'Trombe Wall' Fig 6.1(a), partly depends on natural convection between glass and wall to recover heat. As shown by Lee (14), this would be impracticable in a northern climate, since much heat would be absorbed in the wall and not enough would be available to cause sufficient convection. The Trombe wall could work with 'heat mirror' glass in place of ordinary glass, since this type of glazing would reduce the heat loss to the outside and may increase the air temperature enough to cause sufficient convection.

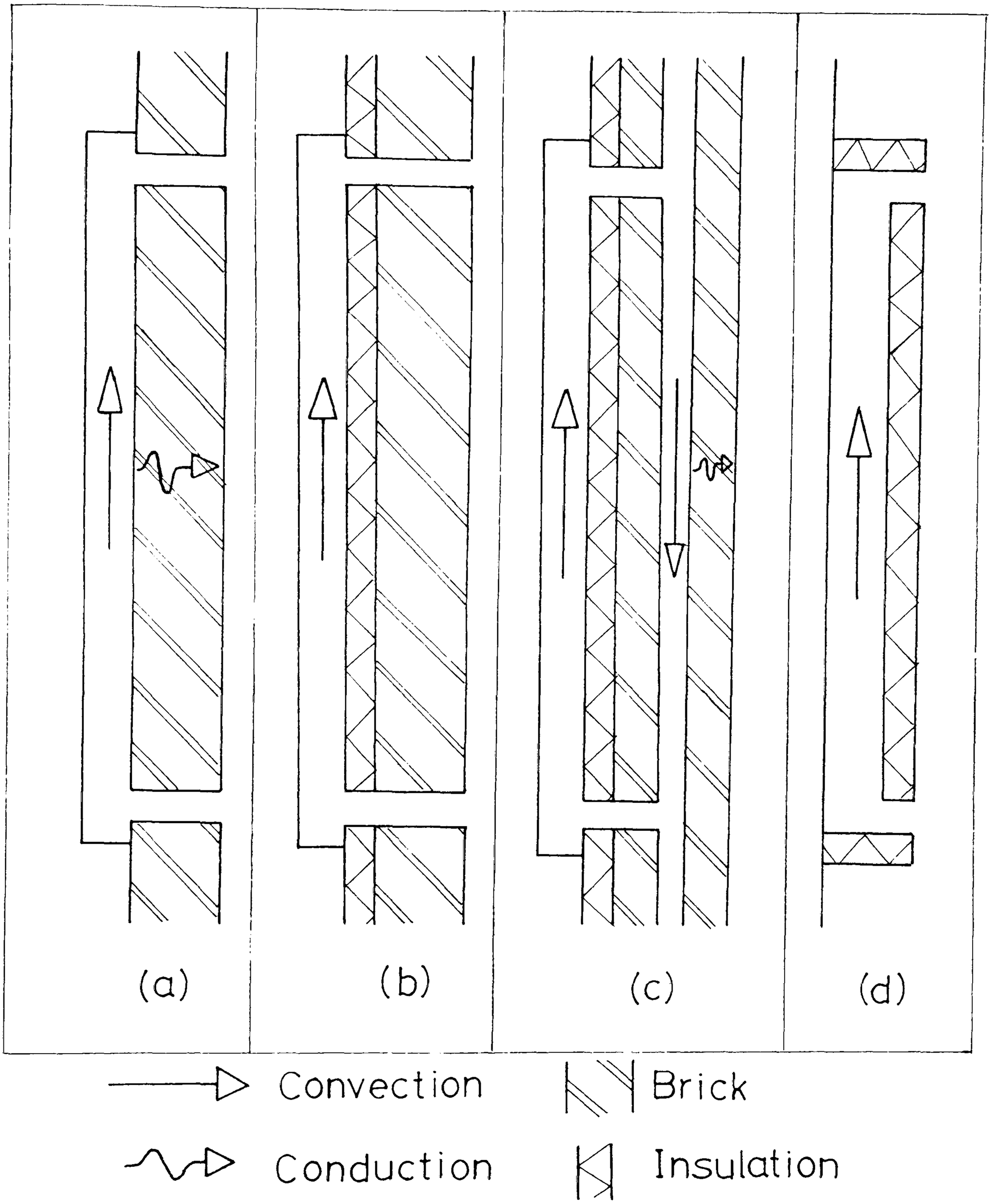

Fig 6.1- Walls with natural convection heat recovery

The poor performance of a Trombe wall could be improved by fixing insulation between the glass and the wall which while increasing the convection would also reduce the heat absorbed by the wall, a possible construction is shown in fig 6.1(b). The main disadvantage of this is that the storage of the wall is no longer used. Some warmed air may become available for immediate use, and this may be appropriate in a building occupied during the day, such as a school, where solar heating might be combined with a warmed air system. Storage would otherwise be required.

If the wall being modified is a masonry wall, then there is already storage available and this could be used, for example, as in Fig 6.1(c). When there is insufficient solar radiation available to cause convection, dampers could be closed at top and bottom, effectively insulating the wall from the outside. The dampers could be operated automatically by devices similar to the window openers used in greenhouses, thus introducing the minimum of mechanical devices and removing the need for manual intervention. These devices would open the dampers, given sufficient solar radiation, and heat would be collected by the wall. Because of the complexity of the theory of natural convection, the wall shown in Fig 6.1(d) is analysed initially and then the analysis extended to cover the wall shown in Fig 6.1(c).

6.1 - Introduction to theory

The main problem in designing a vertical air collector for natural convection is to find the optimum value for the gapwidth. If, for example, the gap is too small, friction will dominate and suppress the flow. If the gap is too wide, circulation will occur and again the efficiency will drop. So it is necessary to develop theory that will predict optimum gapwidth and provide simple guidelines to facilitate design. Since the study of boundary layers is difficult, the solution will be imprecise.

6.2 - Flow in Gaps of Varying Width

If a vertical surface is at a different temperature from the adjoining air, a flow will result along the surface due to the increased or decreased buoyancy of the air. For a completely free vertical surface the development of the boundary layer is relatively simple to predict, but if another parallel vertical surface is placed nearby, the two surface boundary layers will interact, resulting in a rather more complicated flow pattern.

Even if the flow were laminar, a thorough analytical study of flow between two parallel plates would be exceedingly difficult, but if the flow were turbulent (which is most likely) a solution would be nearly

impossible. In this section use will be made of previous studies, qualitative observations and simple theory in order to derive a workable method for analysing natural convection flow between two parallel plates.

6.2.1 - Boundary layer theory for a free vertical surface

Fig 6.2 shows the growth of boundary layer along a free vertical surface. Also shown is the variation of the surface convective heat transfer co-efficient where the surface is warmer than the air. (If the air is warmer than the surface, the figure would be inverted). The figure also shows the velocity and temperature profiles across the boundary layer.

Although not shown in figure 6.2 there is a distinction between the velocity layer and the thermal layer, the relationship of the two is given by

$$\delta_{TH} = (1/1.075Pr)^{0.33}\,\delta_{VEL} \qquad (6.1)$$

where $Pr = \frac{\mu}{\rho\alpha}$ is the Prandtl number, 0.7 for air (6.2)

$$\alpha = k/\rho c \quad \text{is the diffusivity} \qquad (6.3)$$

For air $\delta_{TH}/\delta_{VEL} = 1.1 \sim 1$ (6.4)

For air the two boundary layers will therefore have a very similar depth, but a conversion factor of 1.1 will be used. As the curves are so close together it is unnecessary to show both in fig 6.2.

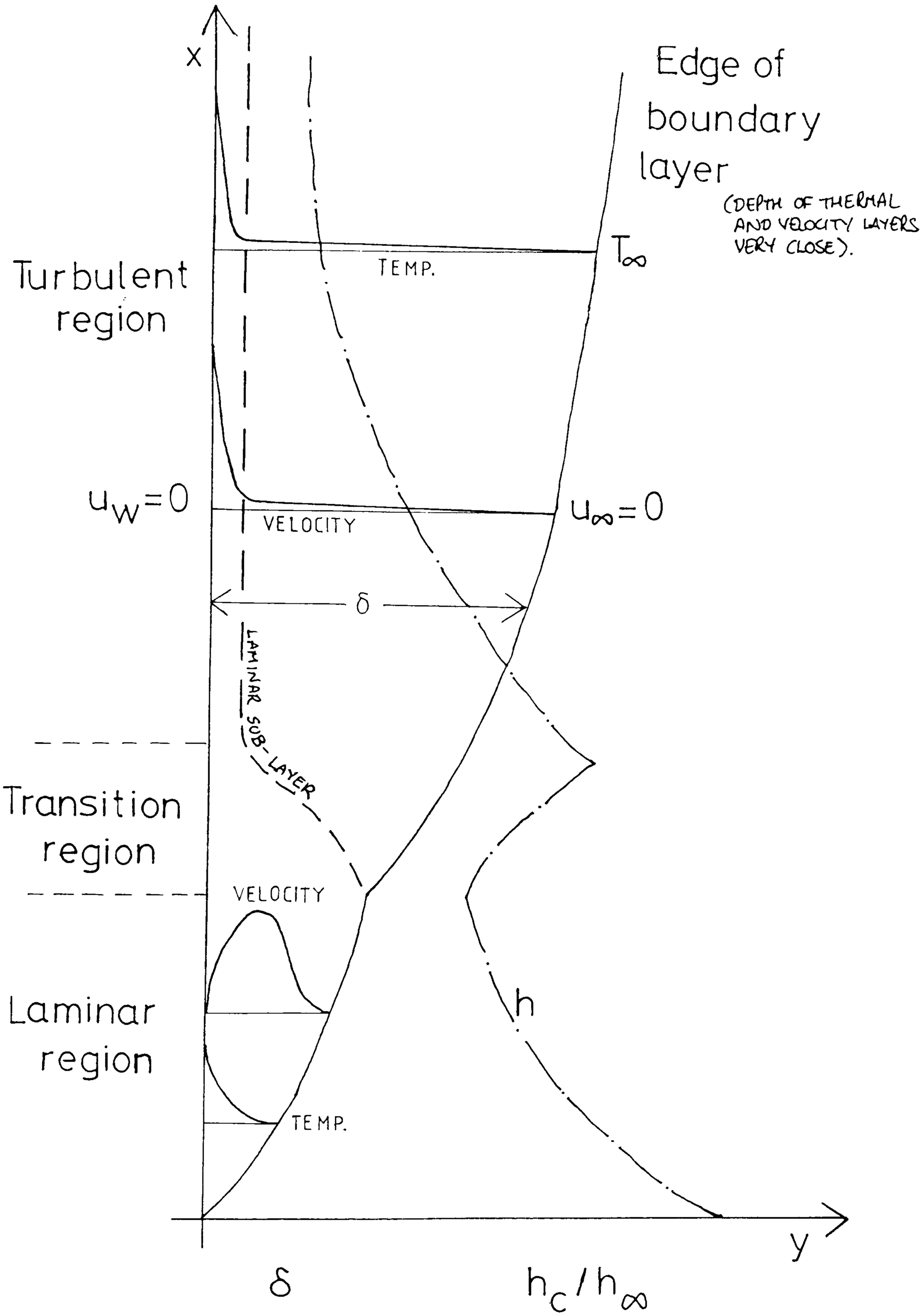

Fig 6.2 – Growth of a boundary layer along an isothermally heated vertical wall due to natural convection.

As mentioned in section 6.1, analysis of flow over a free surface is relatively simple, one such analysis is summarised by Rosenhow et al. (20). The depth of the velocity boundary layer is

$$\delta_{LAM} = 3.93Pr^{-1/2}(0.952+Pr)^{1/4}Gr^{-1/4}\,x \qquad (6.5)$$

$$\delta_{TURB} = 0.565Pr^{-8/15}(1+0.494Pr)^{1/10}Gr^{-1/10}\,x \qquad (6.6)$$

where the transition to turbulence occurs at

$$x = (6/dT)^{0.33} \qquad (6.7)$$

and where $Gr = \rho^2 g\beta\, dT x^3/\mu^2$ is the Grashof number (6.8)

It is next necessary to show how this relatively simple situation is altered for the more complicated situation of flow between parallel plates.

6.2.2 - Flow between parallel plates

Flow between parallel plates will only be looked at qualitatively because of the difficulty of the necessary analysis. Yaluria (19) states that for an aspect ratio (height/gapwidth), of less than three, the two surfaces act independently. The two surfaces can hence be considered as free surfaces, and will be governed by the theory outlined in 6.2.1. Such a circumstance would arise in using a conservatory as an air collector. It is possible that the warmed air would be forced to circulate around the conservatory rather than pass through ducts into the room behind the heated wall.

For an aspect ratio of three and upwards the two

boundary layers will interact. The resulting velocity and temperature profiles will be a product of this interaction. Fig 6.3 shows approximate velocity profiles for increasing aspect ratio.

6.2.3 - Criteria for a narrow gap

It is clear that if the velocity profile is as in Fig 6.3(a) or 6.3(b) that the collector would be working inefficiently. These profiles could occur if the gap were too wide or if the solar radiation were too small. The collector would, therefore, work most efficiently if the velocity profile was as in Fig 6.3(d) or possibly as in Fig 6.3(c). In both these the flow is all upwards. This is desirable.

With an aspect ratio of less than three, the surfaces can be considered independently, i.e as in Fig 6.3(a). The other three profiles illustrated are more difficult to predict, and it is only possible to give an approximate calculation. This will be done using equation 6.6 to give the depth of the free boundary layer.

When there is sufficient solar radiation the boundary layer on the warm surface will dominate since dT between the surface and the air will be greater. If δ for the warm surface is greater than the gapwidth for most of the time, the velocity profile will be as in Fig 6.3(c) or 6.3(d).

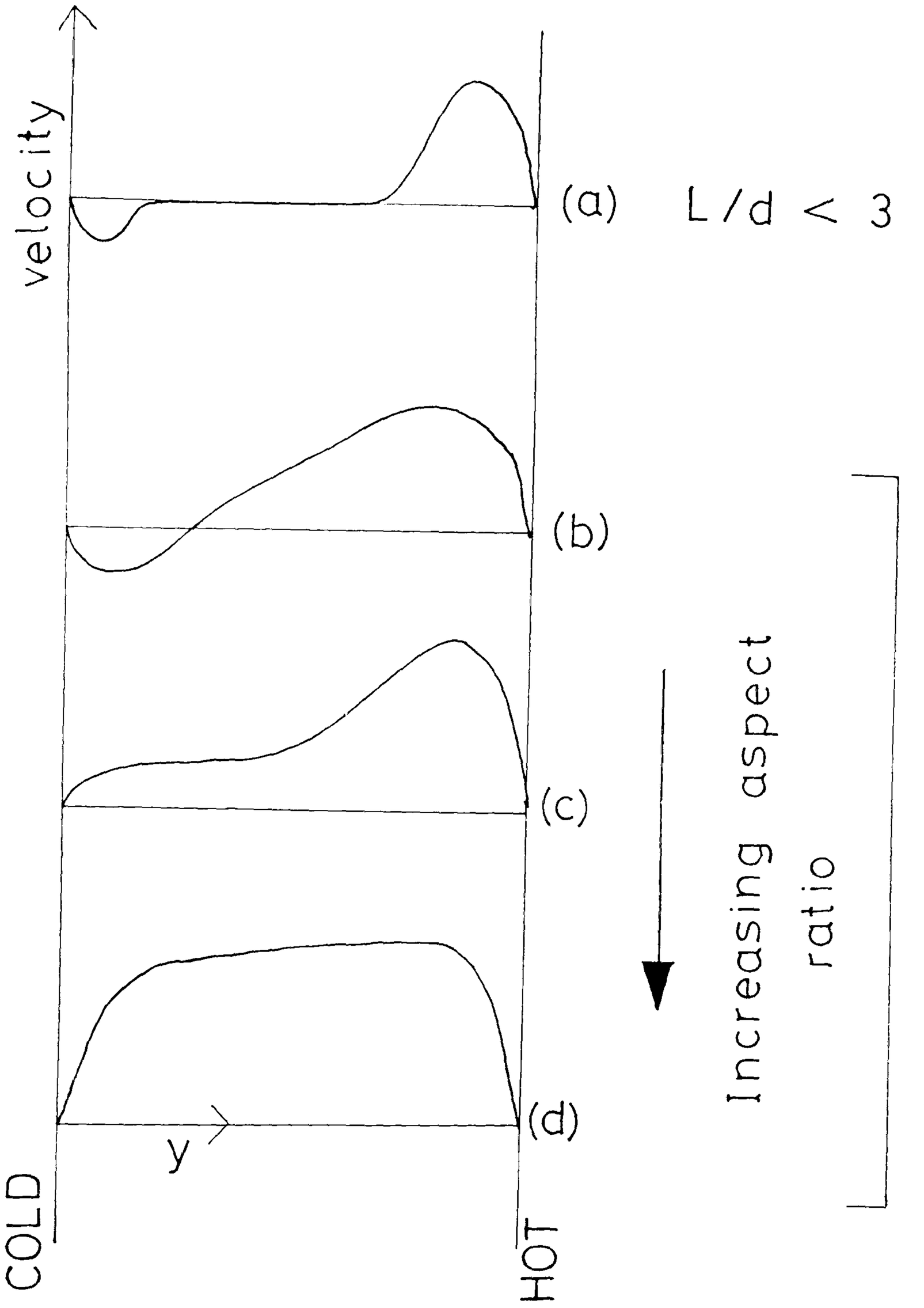

Fig 6.3 - Velocity profiles for various aspect ratios fo natural convection between two parallel plates.

The velocity profile shown in Fig 6.3(b) will occur when the aspect ratio is greater than three, and δ for the warm surface is less than the gapwidth. Fig 6.4 shows how δ would vary for various values of dT for a collector 3m high and for various gapwidths. Choice of a suitable value for dT will give the maximum allowable value for the gapwidth.

There will also be problems if the gapwidth is too small. For natural convection, the pressure causing flow will be very small and will be very susceptible to increased loss due to friction. It is necessary, therefore, to keep the gapwidth as wide as possible within the limit specified above.

6.3 - Other Conditions and Possible Methods of Solution

6.3.1 - Laminar or turbulent flow

The amount of heat transferred from the heated wall to the rising column of air depends upon whether the flow in the gap is laminar or turbulent. This may not be important if reasonable values for the heat transfer coefficients are used. Most previous studies have ignored this. Pratt and Karaki (23) for example assume the flow is laminar all the way up the duct. Others give the point of transition for liquids rather than for gases. Firstly a new dimensionless group must be defined. It is usual, at

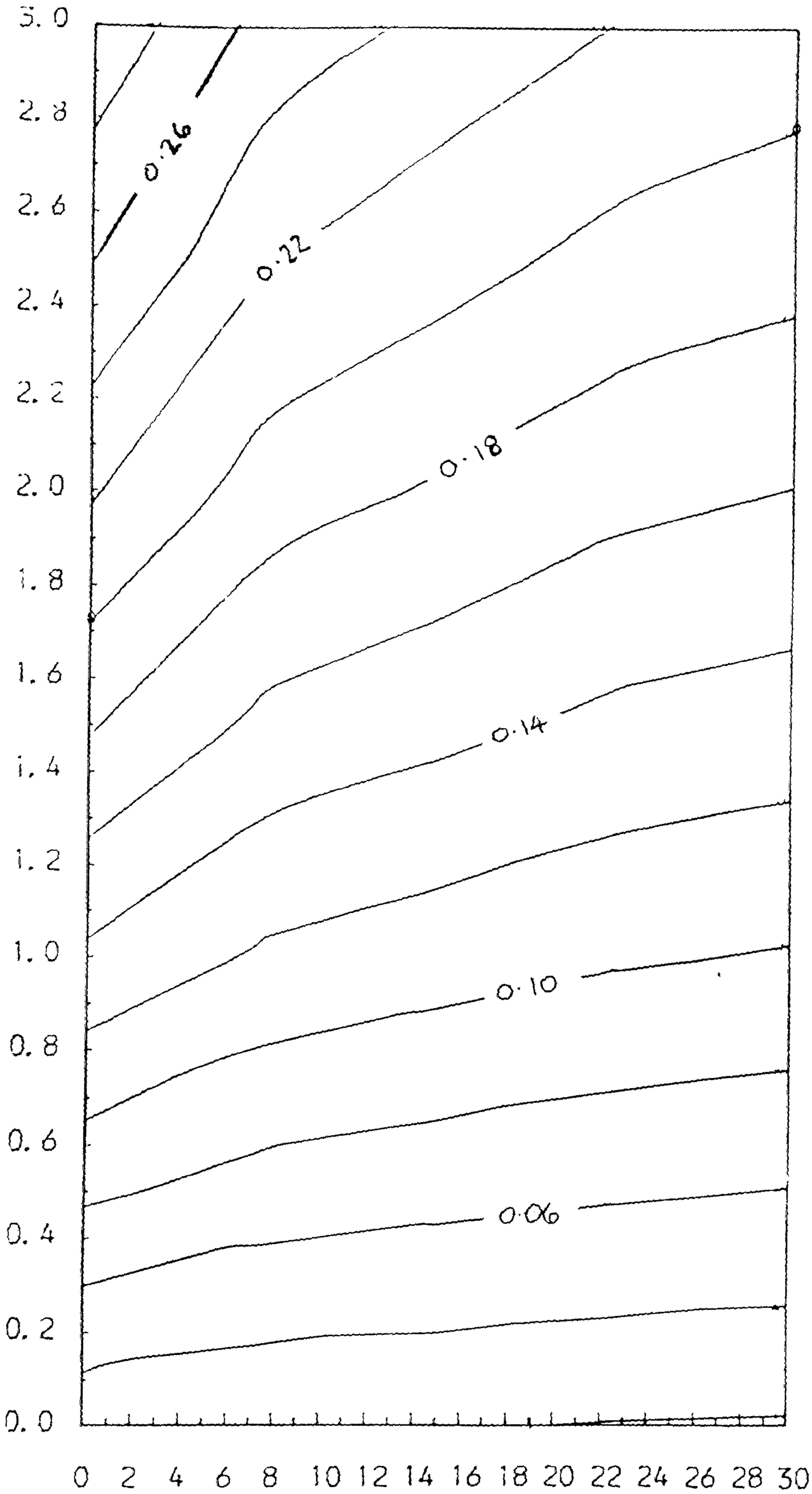

Fig 6.4 - Depth of free surface, natural convection boundary layer as a function of distance along surface and temp. gradient.

(turbulent flow)

present, to group the Grashof number and the Prandtl number to give the Rayleigh number.

$$Ra = Gr.Pr = \rho g \beta dT d^3 / \mu \alpha \qquad (6.9)$$

Elder (21) and (22) assumes the transition occurs at approximately $Ra = 1.0*10^6$. Jaluria (19) gives the transition at $Ra = 1.4*10^5$ wheras Kettleborough (24) only considers flow below $Ra = 1.0*10^4$. Gebhart (32) analyses flow between vertical parallel plates, and gives the transition to turbulence at $Ra = 1.4*10^5$.

For air, O'Callaghan (15) calculates that transition occurs when

$$dT.d^3 > 2*10$$

For a 0.1m gap with a temperature difference of 30 K , this parameter is $30*10^{-3}$ ($Ra = 3.5*10^5$) so that turbulence is complete. This result agrees well with the value given by Gebhart. The figures given by the various workers show that transition occurs over a large range.

Most work done on this problem shows that for a collector of typical dimensions the flow will be turbulent. This is also shown by observations in this project (section 8.1.1). The main assumption made by Pratt and Karaki (23) is that the flow is laminar. Schlicting (34) states that the Navier-Stokes equations can only be solved analytically for laminar flow. For turbulent flow, a completely theoretical model cannot be derived from the Navier-Stokes

equations.

6.3.2 - Possible methods of solution

The usual way of modelling such systems is by attempting to solve the Navier-Stokes equations. As mentioned above this is considered impossible for turbulent flow. To attempt such a solution, the flow must be assumed to be laminar. For a natural convection collector this is unlikely, but the assumption may not necessarily lead to a large error.

For example, Pratt and Karaki assume laminar flow and then use finite differences to solve the Navier-Stokes equations. Apart from the assumption of laminar flow, which may lead to error, the method is still exceedingly complicated which tends to mean that any computer model must be inflexible to keep runtime to a minimum.

Borgers and Akarbi (37) derive a solution for turbulent flow using Prandtl's mixing length hypothesis and empirical equations for parameters such as the turbulent Prandtl number.

Pacetti et al. (35) assume the equation of the velocity profile (i.e the variation of velocity across the gap) to be governed by a 1/7th power equation which is based on work by Nickuradse, which is summarised by

Schlicting (34). An explanation of this is given in fig 6.5. This power varies little with velocity and can be assumed to represent a wide range of velocities. This simplifies the solution and does not exclude the assumption of turbulent flow. Even using this approach the resulting solution is still complicated. It appears that if assumptions can be made that can be shown to be valid (such as the 1/7th power equation) then it may be that the solution can be simplified to the point where it is no longer necessary to solve the Navier-Stokes equations.

Another approach is to reduce the solution to a few general equations and use an average temperature over the height of the collector. Such a solution is given by Rea et al. (36) which is simple but probably too simple. Clearly some compromise is necessary.

6.3.3 - General solution and assumptions

A thorough solution would need to cover at least the following: (1) laminar or turbulent flow, (2) any possible velocity profile, (3) possible unsteady state conduction in the wall. For this, an integration method must be used. It must also be iterative, as the velocity is not initially known. Making use of the previous theoretical and empirical solutions, the following section will discuss the development of a simplified general theory for modelling air collectors.

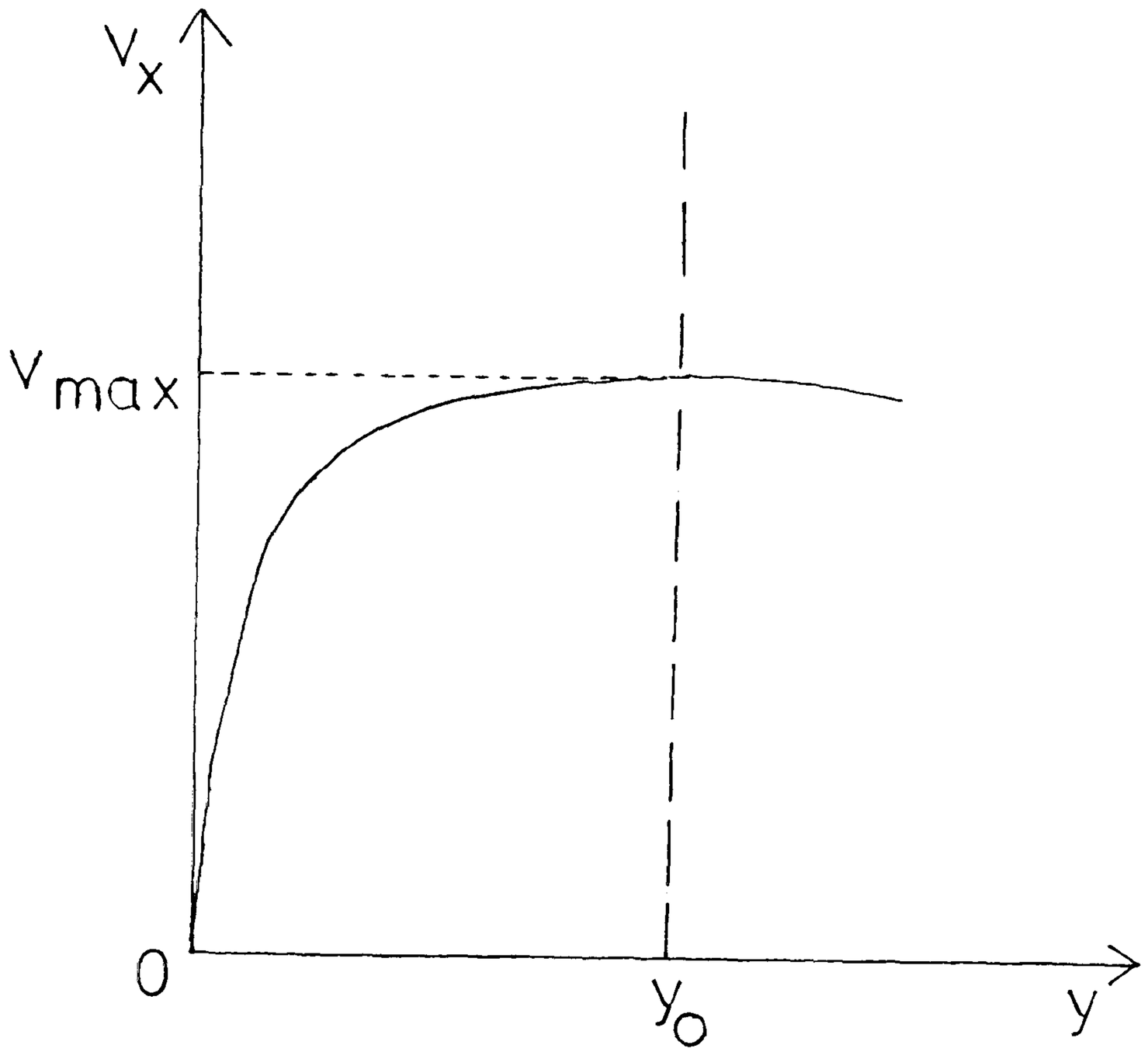

$$V_y = V_{max}\left(\frac{y}{y_o}\right)^{1/7}$$

$y_o = d/2$ where d is the gapwidth

Fig 6.5 – Explanation of the 1/7 power velocity distribution

The situation where the air is warmer than the surface has not been discussed in any detail. The velocity profiles in this case would be the inverse of those shown in fig 6.3. This situation could be modelled using this theory but this will not be done in the model proposed here. A test within the model will check wether the buoyancy pressure is negative, and if so halt any further calculation.

For solving the collector shown in Fig 6.1(d) it will be assumed that the collector will operate at a steady state. Since the surface is insulated this should be valid. As will be shown the model can be extended to cover the unsteady state, although this is outside the scope of this project.

6.4 - Assumptions and Solution

6.4.1 - Basic nodes

Fig 6.6 shows the two basic nodes necessary for the solution. In Fig 6.6(a) it is indicated that if the flow is not unidirectional it could be solved provided the x and y vectors of the velocity could be specified at every node. In the solution of a vertical air collector the y vector will be zero (i.e $v_y = 0$).

In Fig 6.6(b) the unsteady state term would have to

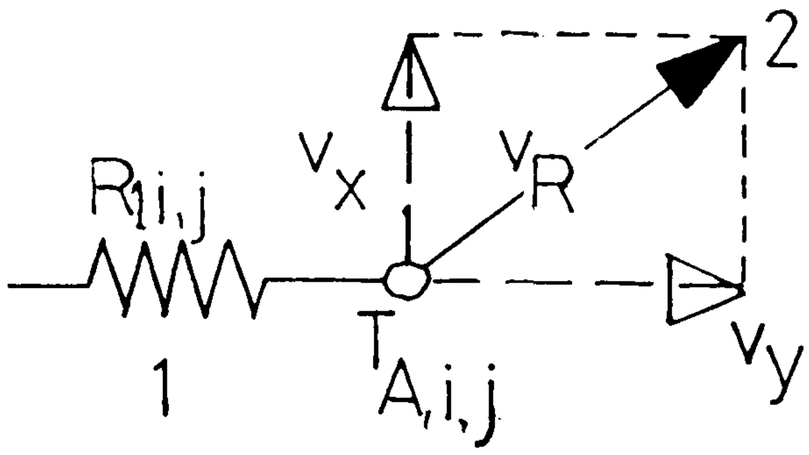

(a)

j - 1,n
j - 1,m

1 - resistance across boundary layer

2 - convected transfer

i-vertical j- horizontal interval

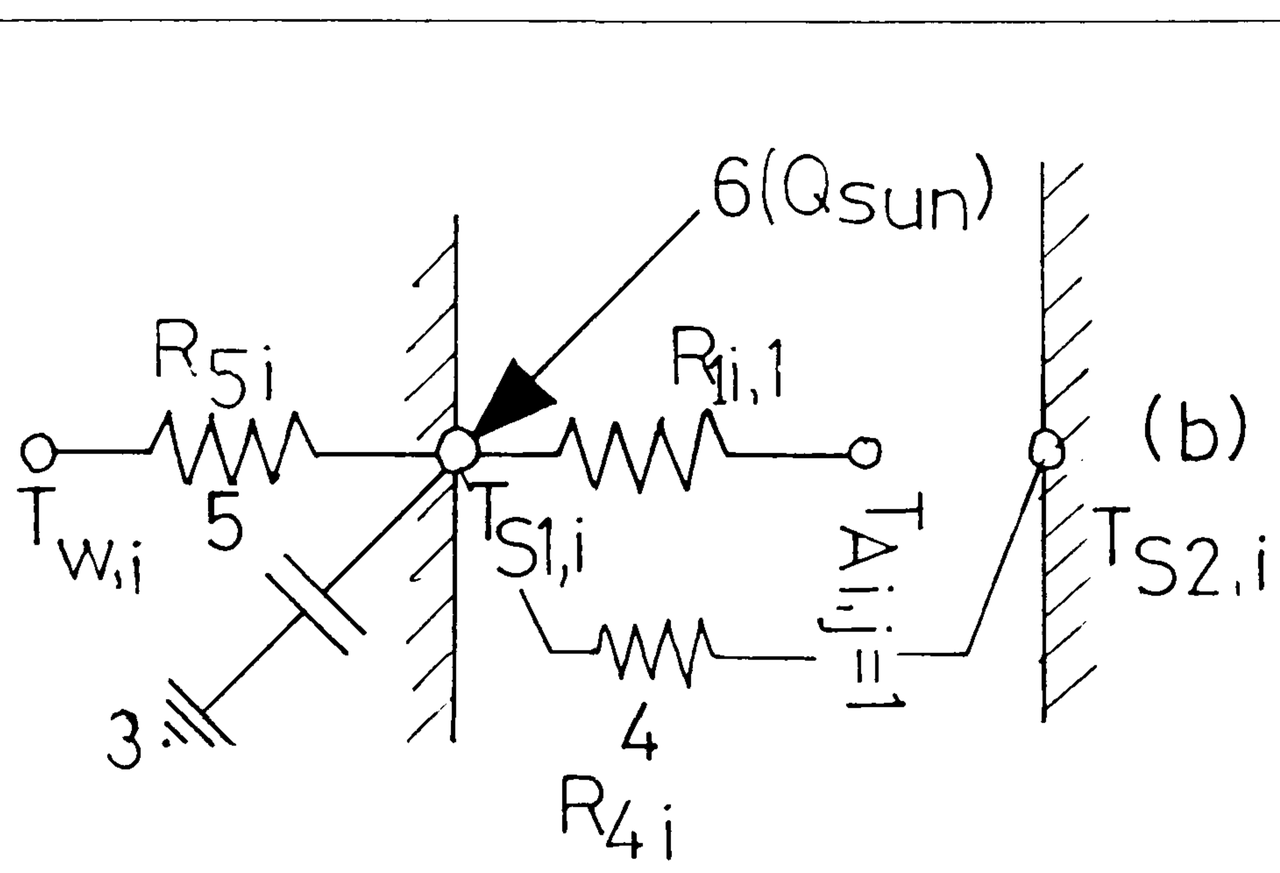

3 - thermal capacitance of solid

4 - radiative resistance

5- solid resistance

6- short wave input

Fig 6.6 - Basic nodes for convection model

be solved using a finite difference technique and will not be included in the following solution. There is no air velocity at such a node but heat is transfered to the air across the boundary layer. A heat balance on these two nodes would give the following two general equations.

$$\frac{1}{R_{1ij}}(T_{Aij} - T_{Aij-1}) + \frac{1}{R_{1ij+1}}(T_{Aij} - T_{Aij+1}) + \rho c v_x dy(T_{Aij} - \overline{T}_{Ai-1j}) = 0 \quad (6.10)$$

$$\frac{1}{R_{5i}}(T_{S1i} - T_{wi}) + \frac{1}{R_{1i}}(T_{S1i} - T_{A1i}) + \frac{1}{R_{4i}}(T_{S1i} - T_{S2i}) = Q_{SUN} \quad (6.11)$$

6.4.2 - Velocity distribution

As mentioned before, Pacetti et al assumed a particular velocity profile, in their case described by a 1/7th power equation, (i.e expressing v_x as a function of y). This or any velocity profile can be used in the model as will be shown below. In general

$$v_x = f(y) \quad (6.12)$$

the average velocity at any interval is

$$\bar{v}_x = \frac{1}{d}\int_0^d v_x \, dy \quad (6.13)$$

The model is solved with average velocities at each vertical interval. The velocity at each node is then found iteratively so that equation 6.10 is satisfied. This is done by guessing a value for the maximum velocity, from this finding the velocity at each node to satisfy 6.9, and

then integrating. The procedure is repeated until convergence of v.

On top of the horizontal distribution there is also a vertical velocity distribution. This is obvious from the continuity equation

$$\rho vA = \text{constant} \qquad (6.14)$$

After an iteration the density distribution can be calculated from

$$\rho_x = \rho_o(T + 273)/273 \qquad (6.15)$$

From this we find the average density. From the previous iteration the average velocity (v) is known. Using continuity gives

$$\rho_x v_x = \rho_o v_o \qquad (6.16)$$

hence the vertical velocity distribution is given by

$$v_x = \frac{\rho_o v_o}{\rho_x}$$

where the subscript x denotes the average velocity at any vertical interval. This velocity can then be distributed horizontally as shown above.

6.4.3 - Horizontal temperature distribution

The resistance network for the model is shown in Fig 6.7. Originally just one node in the air gap was used, but this was misleading. In reality, if the flow is turbulent, then most of the resistance is across the laminar sub-layer and very little across the main body of the boundary layer.

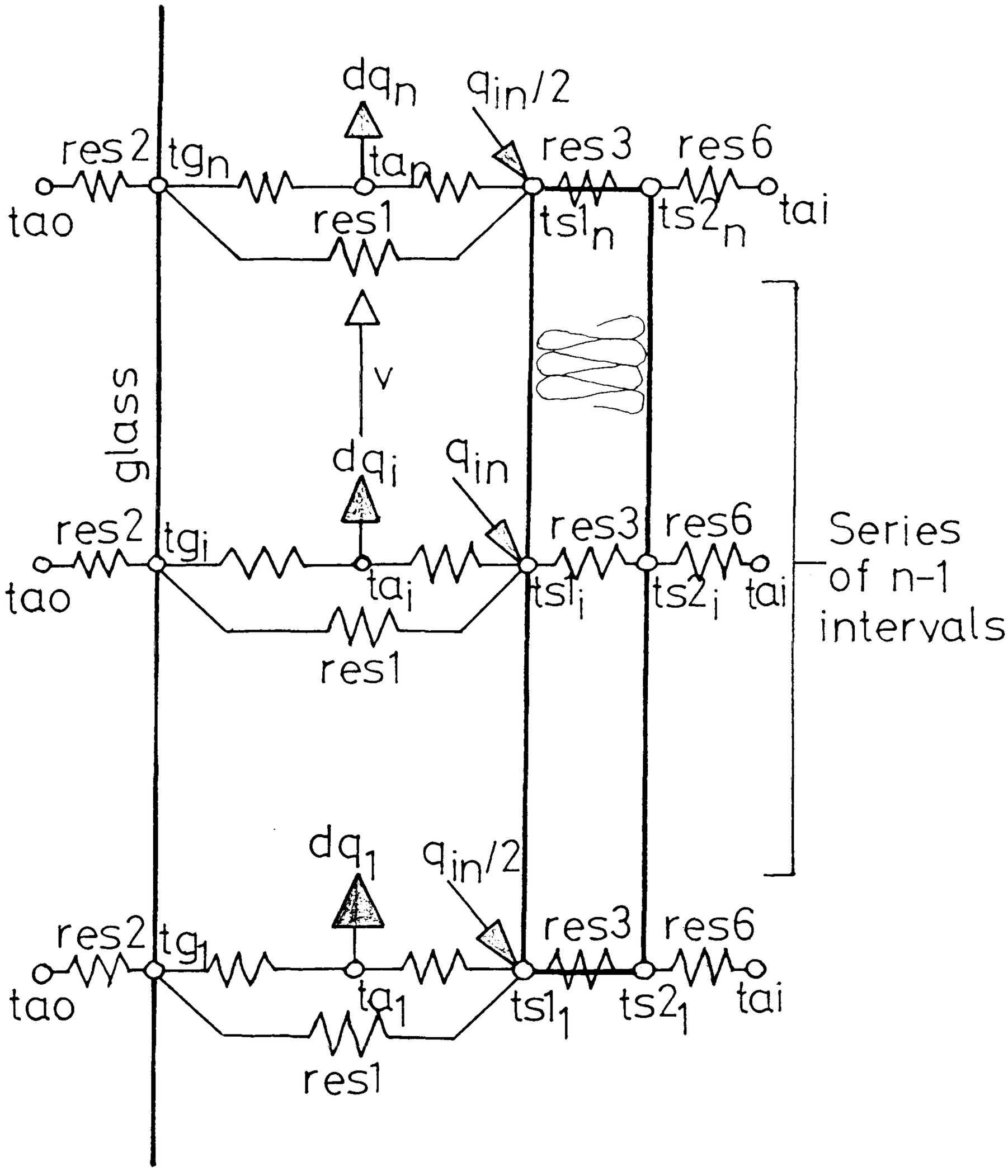

Key: As fig 6.2 with res4 and res5 replaced by a series of m resistances.

dq_i - change in heat content of air.

Fig 6.7- Theoretical model for collector.

If the flow is laminar then there is an parabolic, rather than linear temperature distribution. Hence a series of resistances allow for these effects, although for simplicity the diagram shows only one node. Experience shows that using more than one node increases the overall accuracy only slightly.

The total thermal resistance of the gap is calculated from

$$h_{LAM} = 0.51\left(\frac{dT}{d}\right)^{0.25}\left(\frac{L}{d}\right)^{-0.111} \qquad (6.17)$$

$$h_{TURB} = 0.96 dT^{0.33}\left(\frac{L}{d}\right)^{-0.111} \qquad (6.18)$$

where transition to turbulence is at $dTd^3 = 2*10^{-3}$

This, if necessary, can be continually recalculated in each iterative step, but provided the initial guess of dT is reasonable, the heat transfer co-efficient will not vary much. The heat transfer co-efficient is then distributed, over the whole gap, according to the formula

$$[(y-y_o)/y_o]^{1/7} \qquad (6.19)$$

This is taken from the formula for temperature distribution given by Whitaker in (25). If the flow is laminar the resistances are distrbuted parabolically. Any other distribution can be used according to the flow conditions.

Fig 6.8 shows the nodal network with the number of horizontal nodes equal to m. For laminar flow all the heat at a node is assumed to go only to the node vertically above, hence

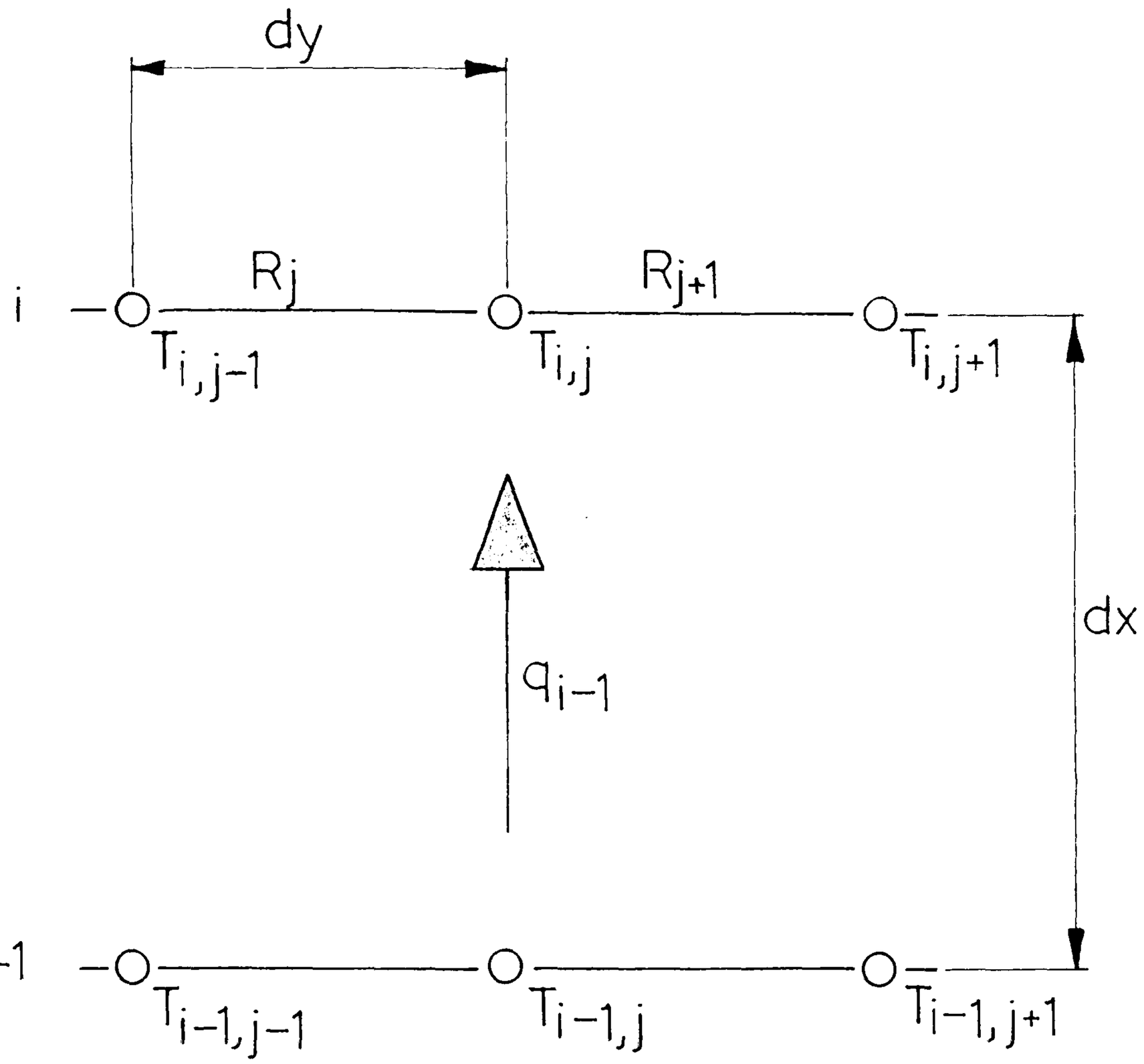

Fig 6.8 - Nodal Network to Calculate Horizontal Temperature Distribution

$$q = \rho cv(dy)(T_{ij} - T_{i-1j}) \qquad (6.20)$$

For turbulent flow, with complete mixing assumed to take place, the average temperature at interval i-1 is used to calculate the heat flow at each node at interval i, hence

$$q = \rho cv(dy)(T_{ij} - 1/m \sum_{j=1}^{m} T_{i-1j}) \qquad (6.21)$$

This gives a realistic temperature distribution, which would need to be justified fully by experiment. In this thesis these equations are used only to demonstrate the potential of the theory. For example, in reality, it is possible that only the immediately adjacent nodes need be summed. As long as the collector can be assumed to be two dimensional, no variation in the z direction need be included.

Due to the high temperature differences (up to 60K), the radiation heat transfer coefficient cannot be calculated by the linearised equation, as shown by figs A3.1 and A3.2 in Appendix 3. Hence the co-efficient is given by

$$h_{RAD} = \frac{\mathcal{F}\sigma(T_1^4 - T_2^4)}{T_1 - T_2} \ W/m^2K \qquad (6.22)$$

where $$\mathcal{F} = \left(\frac{1}{\varepsilon_1} + \frac{1}{\varepsilon_2} - 1\right)^{-1} \qquad (6.23)$$

the surface emittances used will be discussed in chapter 8, when the results are given. As the calculations will be done by computer, this numerically complex equation will not prove difficult. This co-efficient will be continually

recalculated within the program.

6.4.4 - Solution of the model for an overall average velocity

First the solution procedure for a constant velocity and (in the next section) the more general procedure for varying velocity will be outlined.

As can be seen from Fig 6.7 the number of unknowns is one more than the number of nodes,the extra equation comes from the relationship of qo(i) and qo(i-1). At the first interval ta(1) = tai hence

$$q(1) = 0$$

The second and subsequent intervals are solved using the following relationship for q(i) and q(i-1):

$$dq = q(i) - q(i-1) \qquad (6.24)$$

with $$q(i) = \rho\, dcv(ta(i)-tai) \qquad (6.25)$$

where dq is the increase in heat carried by the air. Hence the unknowns are tg(i),ta(i),ts1(i),ts2(i), the solution is simple since q(i) is in terms of ta(i).

The velocity is calculated from the buoyancy pressure arising from the warm air

$$\frac{dp}{dx} = \rho g \qquad (6.26)$$

$$p = 273\ g\rho_o \int_o^h (1/(273+tai)-1/(273+ta))dx \qquad (6.27)$$

The pressure is then used to calculate the velocity, which from D'arcy's equation is

$$p = \frac{4fL(\frac{1}{i}\rho v^2)}{d_e} + \frac{1}{i}k\rho v^2 \qquad (6.28)$$

where $$d_e = d/2(1+d) \qquad (6.29)$$

$$v^2 = p/(\rho(fL/d_e+0.5k) \qquad (6.30)$$

This equation is dependent on the friction factor and the factor k which allows for the pressure lost in going round bends and for entrance and exit losses. Both of these factors are difficult to predict and will be discussed in more detail in chapter 8.

The whole network is solved with an initial guess of velocity. Then from the calculated temperatures , a new value of the velocity is found from the pressure due to buoyancy. The average of the previous velocity and the new velocity is then used to recalculate the network. This is repeated until the values for the velocity converge sufficiently (within 0.01 m/s).

The problem is thus reduced to analysis of a steady state nodal network without using difficult theory, but the details of the solution are not simple. For each interval in Fig 6.6 a heat balance is carried out at each node, giving four equations for the four unknowns, leading to a four by four matrix with a one by four matrix on the right.

Each interval is solved by inversion of the matrix which is repeated many times so that a manual solution is impossible. To obtain solutions a computer program has been written which is described in chapter 7.

6.4.5 - General method of solution

The general method of solution and the equations are as described in sections 6.4.2 to 6.4.4. The following procedure allows for the variation in velocity.

First iteration -

(1) Guess an overall average velocity.

(2) Distribute this horizontally, assuming at each vertical interval the same distribution.

(3) Solve for the temperatures.

(4) Calculate density distribution.

(5) Calculate new average velocity.

Subsequent iterations -

(1) New velocity is given by v = (v1+v2)/2

(2) Calculate vertical velocity distribution.

(3) Distribute these horizontally.

(4) Solve for temperatures.

(5) Calculate density distribution.

(6) Calculate new average velocity.

(7) Have the values of velocities converged If not repeat iteration.

6.5 - Practical Design of Air Collectors

Some idea of the expected performance can be obtained from the gapwidth and the probable values of the temperature difference between the glass and the collector surface. Fig 6.9 shows the variation of Rayleigh number with gapwidth for various temperature differences and some significant Rayleigh numbers. For best performance, the collector should operate between the transition to turbulence and the Rayleigh number found to be a maximum by the procedure described earlier in the chapter.

For example, for a temperature difference of 10 K, (a realistic figure for Britain), a gapwidth of a little over 0.1m will give a Rayleigh number half way between the two figures mentioned above. As described in previous sections, the theory is not capable of giving an accurate optimum value of the gapwidth, due to uncertainty of performance at high Rayleigh numbers.

6.6 - Conclusions

The model described in this chapter is limited, but it is hoped that the underlying theory is capable of wider application. The simplified approach to solving natural convection problems could certainly be applied to other steady state problems. With some modifications the theory could be used with unsteady state conduction theory to

Variation of Rayleigh No. with Gapwidth and Temperature

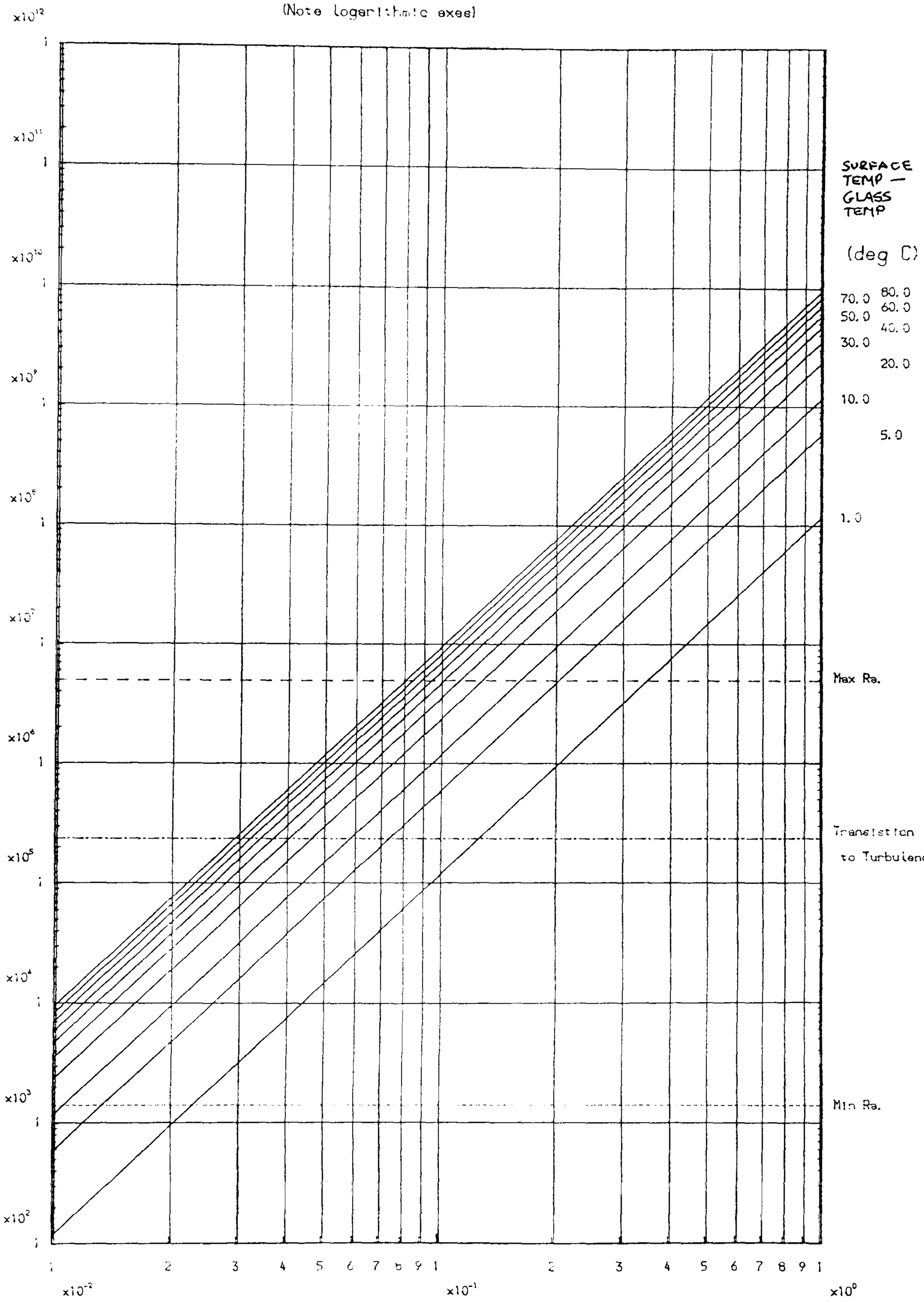

For optimum performance collector should operate between maximum Rayleigh number and the transition to tubulence.

Fig 6.9

extend possible applications to collectors of high thermal capacity, such as the conventional Trombe wall. Chapter 8 describes experiments which show that the model is satisfactory.

Chapter 7

Description of Natural Convection Computer Model

The program, based on theory described in chapter 6, was written on the Leeds University Amdahl VM/470 using the language Algol68 which is more powerful than others such as Fortran66. This greatly reduces the development time. Although Algol68 has a slightly longer runtime the shorter development time more than compensates for this. Since the program was written, other languages such as Pascal and Fortran77 have become available in Leeds which may have both benefits.

There are two versions of the program, 'NATCONV4' and 'NATCONV5', of which the first gives a detailed analysis, including checking whether the flow is fully developed, and iterating for values of the heat transfer coefficients. It was found that the heat transfer coefficients varied very little with temperature, so reasonable average values would give sufficiently accurate results. Once the effect of the gapwidth had been analysed it was no longer necessary to check the condition of flow every time.

'NATCONV5' contains these simplifications and is about ten times faster, although if there were any uncertainty in the performance of the collector, 'NATCONV4' was used.

7.1 - Description

The program can be used to model both natural and forced flow collectors. For the latter, the velocity is specified so that iteration is not necessary, and different heat transfer coefficients are used. It also allows the glass to be replaced by an opaque material. Both of these options are examined in chaper 9.

Fig 7.1 gives a flow chart of the model. The read statements are common whether the analysis is for a forced or natural convection collector. The only difference is for a forced flow collector when the velocity must be specified. A typical datafile is given in Appendix 1.

The main part of the program is the procedure 'tempsolve'. For a given value of velocity this calculates the temperatures in the collector as described in chapter 6. This consists of solving a series of simultaneous equations at each vertical interval, by the NAG routine 'F04DBB' which works by matrix inversion.

In the data file it is specified whether the flow is to be forced or natural. If a natural convection collector is to be analysed an initial guess of velocity is given as a parameter to 'tempsolve', from these temperatures a new velocity is calculated, and this is repeated until convergence.

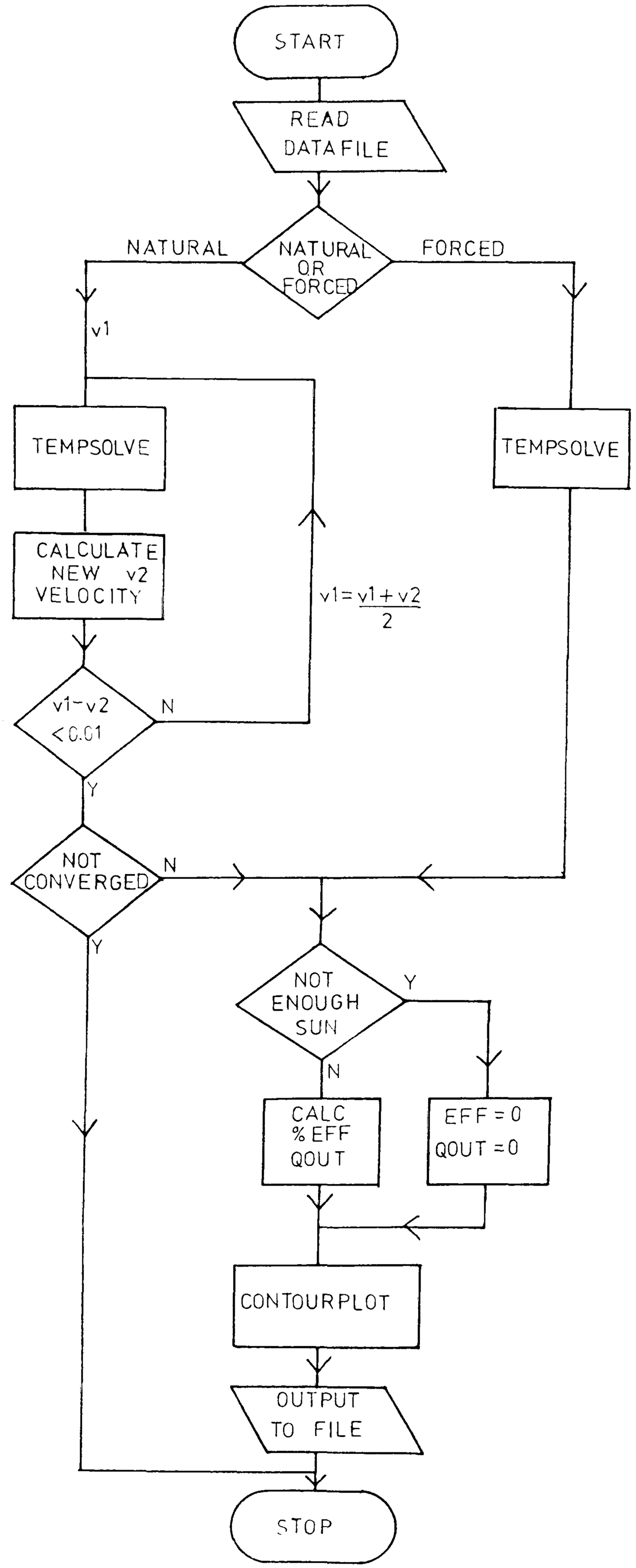

Fig 7.1 - Computer model flow chart

In Fig 7.1 if the criterion 'Not enough sun' is true the efficiency is set to 0. If this test were removed the model would calculate the downward flow.

As with the data, the output is common to both forced and natural collectors. The main output is by computer graphics contained in proceedure 'contourplot', an example of output from this is shown in Fig 8.5. The graphics package used is GHOST80. The interpolation within the contour plotting routines can give poor results if not enough data points are supplied.

Results are also printed into an output file. These can then be displayed on the screen or sent to a line printer. This allows results to be checked before the final graphical output is plotted.

The program can be run once to give a detailed analysis of the performance, or the program can be run, using hourly weather data, to give the total performance over a specified period.

7.2 - Conclusions

To make the program more useful, the calculation of the temperature matrix would need to be more flexible, this is possible using the theory but was not necessary for this work. Results from the program will be discussed in more

detail in chapter 8 (natural convection) and chapter 9 (forced convection).

Chapter 8

Natural Convection Experimental Work and Results

This chapter describes observations of a natural convection collector, and results from the model developed in chapter 6 are compared with the experimental results.

8.1 - Experimental Work

8.1.1 - Description of experiment

Since the work on convection collectors was not begun until later in the project, any complicated experimental work was not possible. Hence it was essential to design any tests to be as simple as possible but at the same time detailed enough to make realistic comparisons with theoretical work.

The collector finally designed is shown in Fig 8.1. Site constraints dictated the dimensions of the collector, but these are realistic sizes. The width of the collector is quite small (1.1m), but since a small gap is used the one dimensional approximation should not be invalidated (1/10 is the maximum allowable ratio of d/b). The overall dimensions are, height = 2.4m, d = 0.11m and b = 1.1m.

Essentially two pieces of information are required:

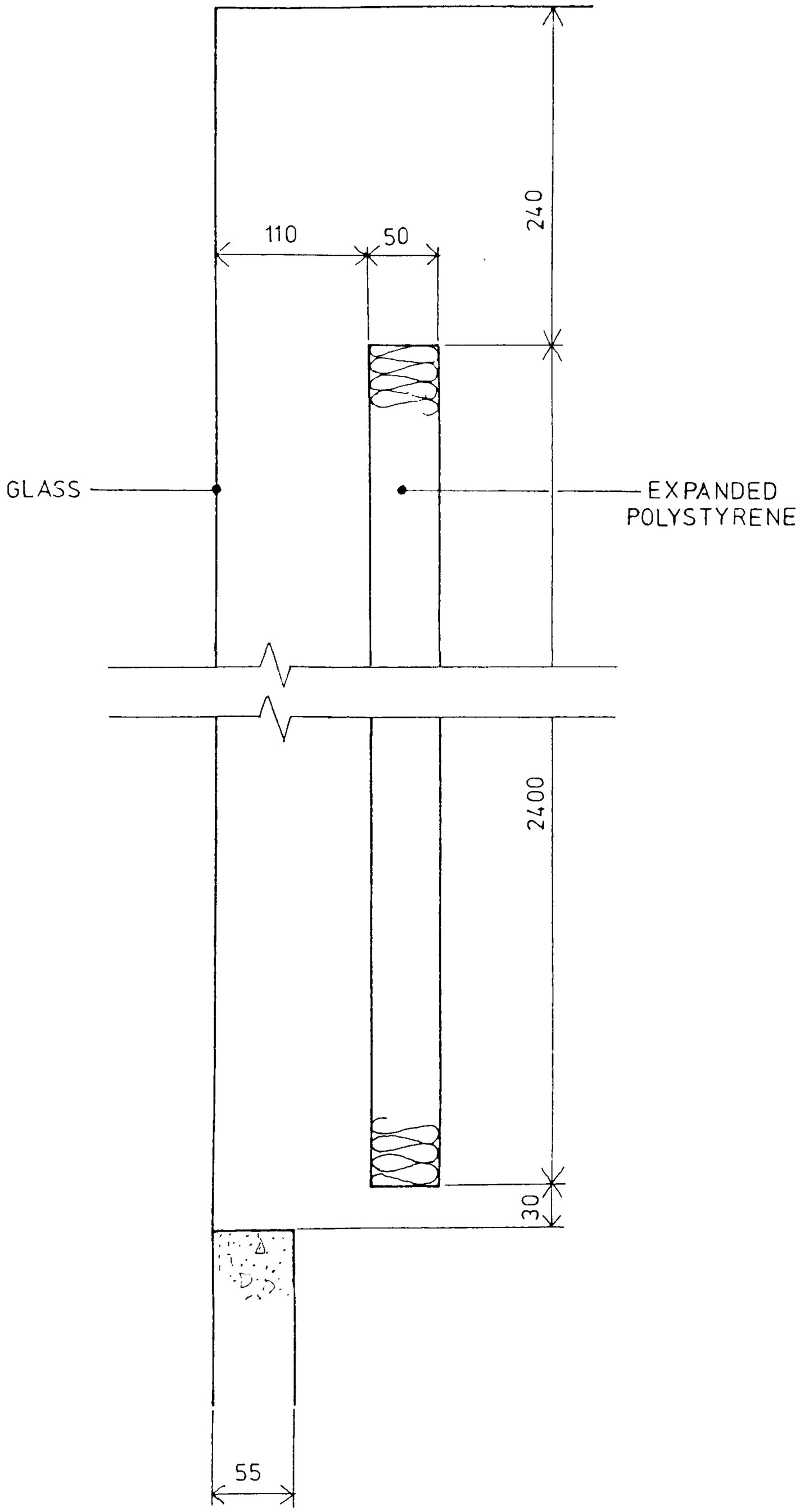

Fig 8.1 - Diagram of air collector

the temperatures and the velocity of the air. The temperatures are measured using thermocouples, monitored by an electronic thermometer. As the thermocouples are in the sun, a radiation screen is needed which needs to be small enough to cause little obstruction to the flow and large enough to give resonable values of temperatures. This meant that temperatures could not be measured at several heights in the collector since this affected the flow too much. It was decided that the temperatures were only to be measured at top and bottom of the wall. The room temperature and the outside air temperature were also measured.

Measurement of the velocity proved much more difficult. Local values could be found with a heated thermistor anemometer but a mean value was also needed. A simple way to obtain this was by timing some object, with high drag co-efficient, as it moved up the collector. The object must be very light and clearly visible. Smoke proved to be unsuitable since it soon dissipated, thus clearly showing the turbulence in the duct. A single object that could be observed was needed. After many trials it was found that the seeds of the Rose Bay Willow Herb (Epilobium angustifolium) were very suitable, but because of the complex shape it was impossible to make any numerical assessment of the drag.

The velocity was measured both by the heated

thermistor anemometer and timing passage of the seeds with a stopclock. The other necessary measurement was the value of the insolation found using the solarimeter described in chapter 3.

As with any real collector, some difficulty was encountered in calculating the friction loss. This is necessary for the theoretical calculations. The bottom is narrower than the top and the air is forced round a bend at both top and bottom. If these effects are allowed for using table C4.39 of the CIBS guide 1970 (26), a k factor of approximately 3 is obtained. This is for a square duct, for parallel plates the k factor should be smaller. Kronwall (27) analysed air flow through various building components including non-square ducts. Kronwall's data gives a k of 2.2 (0.9 for exit and 1.3 for entrance).

It was difficult to estimate the friction loss in the duct, because of the glazing bars, which project about 10 to 15 mm into the gap. It is easy to find a friction factor for the surfaces themselves by finding an approximate Reynold's number and using table C4.1 (Moody Diagram) of the CIBS guide (26) (although of course this table does not strictly apply to natural convection). Estimating the friction loss of any convective system is very difficult. No definite rules can be given here, and each case should be considered separately. For short ducts such as used here, the loss due to bends etc. is larger

than the loss in the duct, so that an accurate value for the pressure loss in the duct itself is not required. Considering the duct to be very rough (to allow for the glazing bars), in the normal operating range, a friction factor of 0.015 was obtained from the Moody diagram given in (27). The function relating pressure drop to velocity is given by

$$p = 0.6v^2(2fL/d + k1 + k2) \qquad (8.1)$$

where k1 = entrance factor, k2 = exit factor

and d is as given by equation 6.19

This function is shown in Fig 8.2, with some observations taken with a micro-manometer. The agreement is very good. The pressure readings are for the total loss over the duct, entrance and exit.

The glazing is ordinary clear window glass. The transmission factor for this varies with the time of year and the time of day. For simplicity an average value of 0.76 is used, as given in table A8.2 of the CIBS guide 1975 (16).

8.1.2 - Surface material of collector

The collector was constructed of 50 mm expanded polystyrene which at first was merely painted matt orange-brown. Both experiment and theory showed this to form a rather inefficient collector. Since the collector

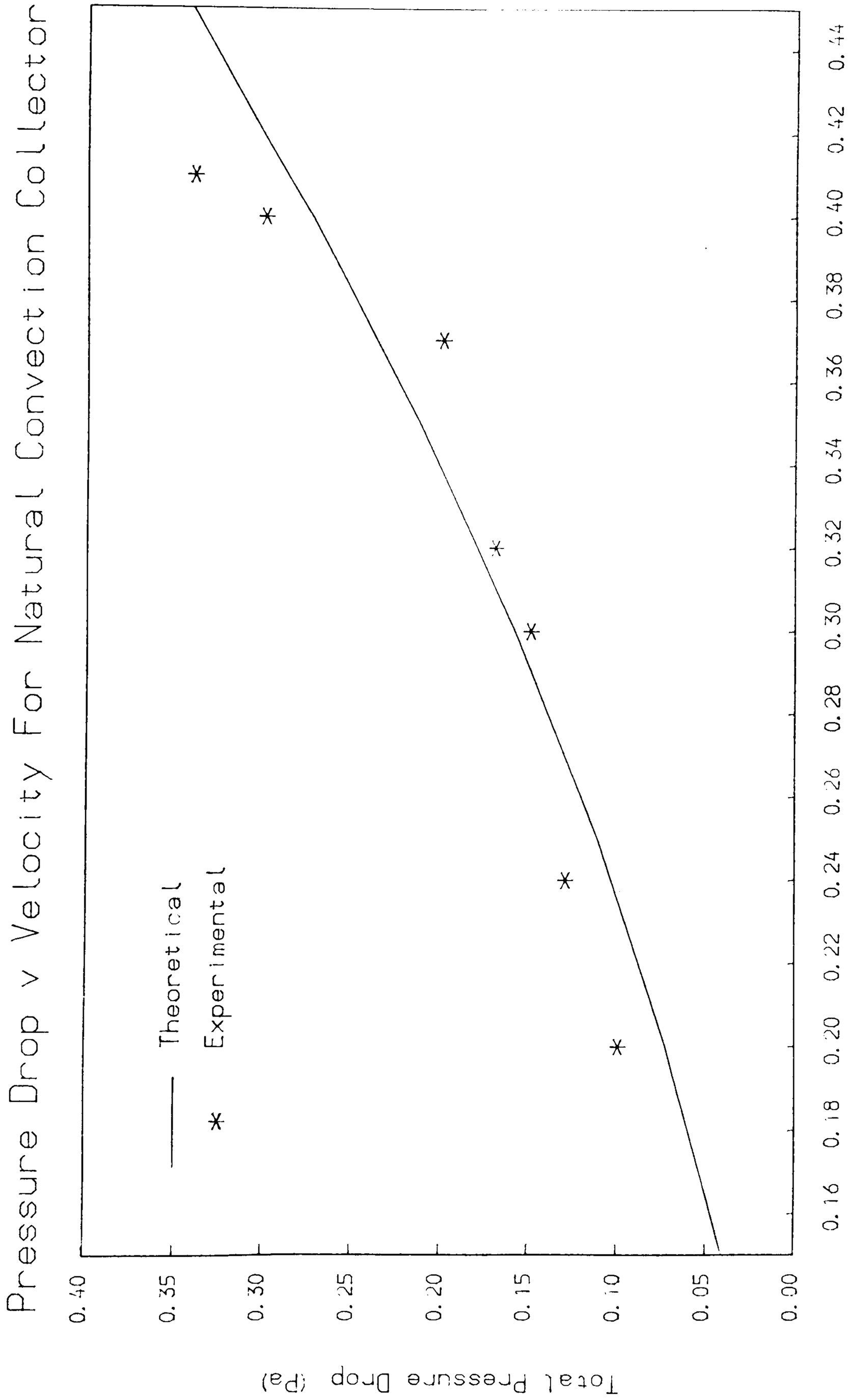
Pressure Drop v Velocity For Natural Convection Collector
Theoretical
Experimental
Total Pressure Drop (Pa)
0.40
0.35
0.30
0.25
0.20
0.15
0.10
0.05
0.00
Velocity (m/s)
0.16
0.18
0.20
0.22
0.24
0.26
0.28
0.30
0.32
0.34
0.36
0.38
0.40
0.42
0.44

Fig 8.2

was not black a value was needed for the surface absorptivity. This was obtained by a simple experiment shown in Fig 8.3. Briefly the box was 500*500*20 mm and was thoroughly sealed to keep the ventilation loss as near zero as possible. Radiation from the monitored centre point to the side walls would be negligible. The total heat transfer co-efficient from the surface was calculated as 4.7 for radiation and 0.6 for convection. The network shown in fig 8.3, is solved for a, tg, tsl and ts2 for various measured values of tao, Q, ta and tai. For this surface an average value of 0.7 was observed. Due to the relative simplicity of this apparatus, the value is quoted to only one significant figure. The average was taken from 25 observations, the maximum scatter was about 0.1.

To improve the performance, painting the surface black would not be sufficient. Hence it was decided to use a selective surface which would cut down the radiation loss from the surface so that more heat is transferred to the air by convection. Some samples of a material 'SKYSORB' were supplied by MPD Technology Ltd.. This is nickel-steel sheet that as been oxidised, the nickel oxide formed is blue-black and forms a selective surface.

The manufacturer's data gives an absorptance of 0.9 and an emissivity of 0.1 at the normal operating temperatures of this collector. This is described by Mason et al. (28) and the figures seem promising. The price of

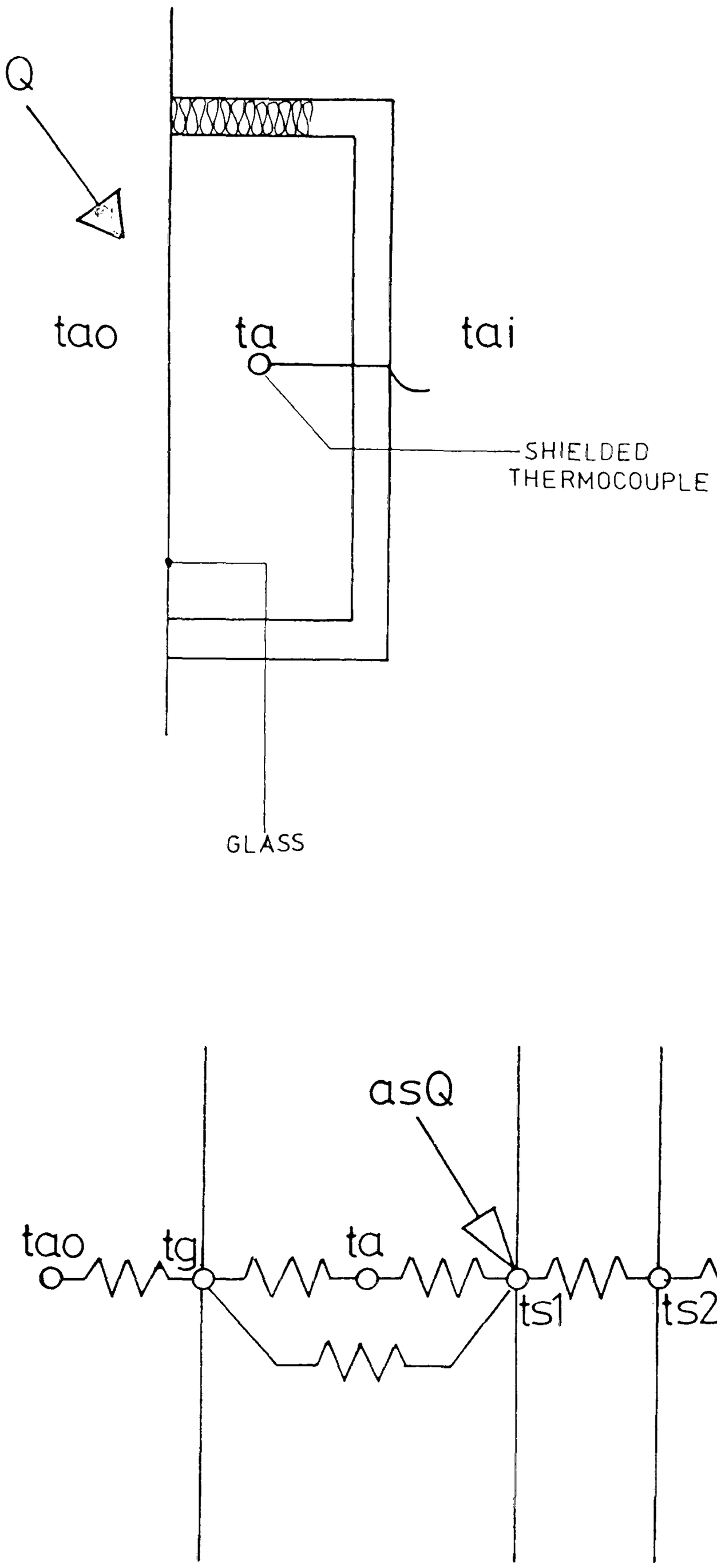

Fig 8.3- Experiment to Determine Surface Absorbitivity

the sheet is not prohibitive (about £10 per m^2) and it may well be that to make natural convection collectors viable in this country these selective surfaces may prove very useful.

8.2 - Description of Results

Both experimental and theoretical results are here described together , the measured weather data being fed into the computer model to give a comparison of results. The results given are a typical example run of the collector, once with a selective surface and once with a non-selective surface. Note that the height of the collector is 2.4m.

8.2.1 - Non-selective surface

Fig 8.4 gives the theoretical results for 15th April 1982. The experimental results for that day are

qout = 490 W

velocity = 0.35 m/s

efficiency = 32.7%

the velocity in these and other experimental runs is found using the Rose Bay Willow Herb seeds, unless otherwise stated. As can be seen the agreement is very good, any inaccuracy is most probably due to the uncertainty of the value of absorptivity used. The value of the friction factor used is 0.015, the insulation surface being quite

TEMPERATURE CONTOURS IN VERTICAL AIR GAP

Theoretical Results for - 1000 hrs on - 15/04/82

Non-selective surface

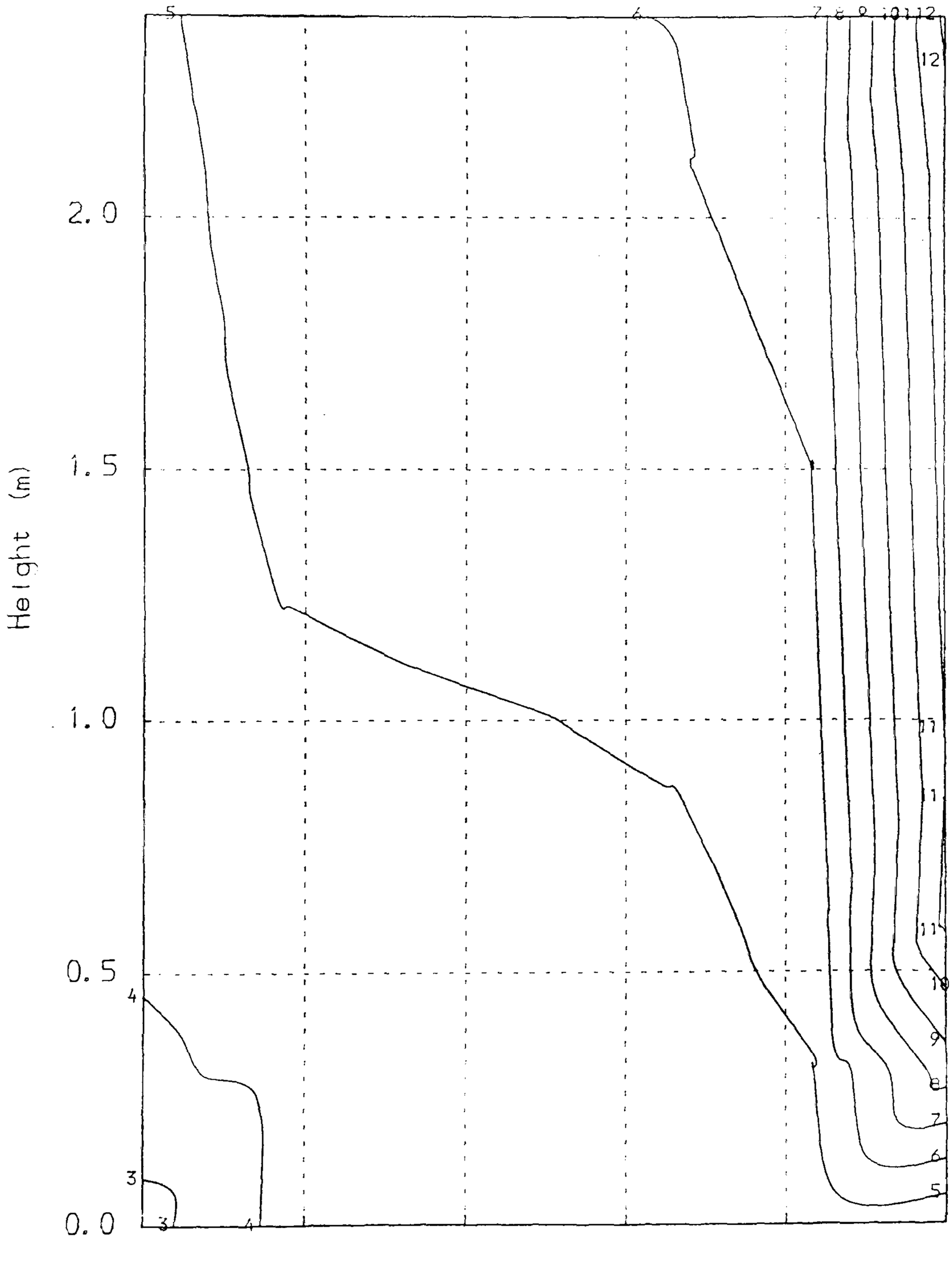

Fig 8.4 VELOCITY CONSTANT EVERYWHERE

rough. The experimental value of velocity is obtained using the seeds. Obviously only one seed could be monitored at any time, but many runs showed these to be very consistent.

8.2.2 - Selective surface

The experimental results are given in Fig 8.6 and the theoretical results in Fig 8.5, for 22nd April 1982. In Fig 8.6 the velocity distributions at the top and bottom of the duct are also given. It is interesting to note that the velocity is higher at the bottom than at the top, this is because the entrance is narrower than the exit although the bottom distribution is measured slightly above the entrance where it has widened out to its full width (Fig 8.1). The average velocity was measured to be 0.41 m/s. The average at the top is 0.40 m/s and at the bottom 0.56 m/s which, if corrected for area, is 0.36 m/s (factor of 7/11).

These profiles agree well with the theoretically calculated veloctiy profiles of Borgers and Akarbi (37). One exception, however, is that the profile at the bottom of the duct, never seems to be of a laminar type. This is due to the air going round a sharp corner, which induces turbulence.

The velocity both from distributions and observation

TEMPERATURE CONTOURS IN VERTICAL AIR GAP

Theoretical Results for - 1015 hrs on - 22/04/82

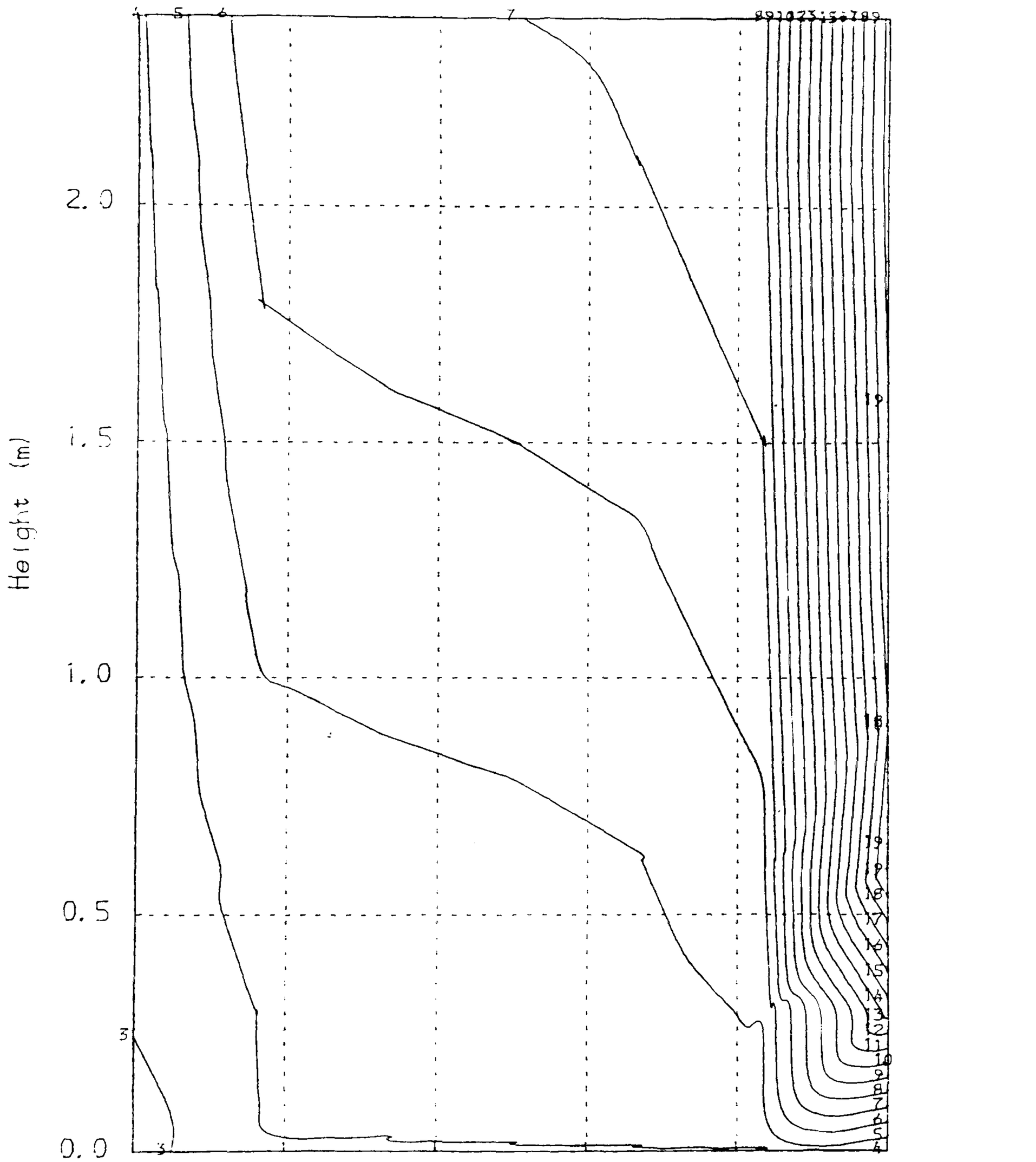

qin =	675.0 W/m2	qout =	773.8 W
eff =	47.8 %	velocity =	0.38 m/s

Fig 8.5(a) - constant velocity

TEMPERATURE CONTOURS IN VERTICAL AIR GAP

Theoretical Results for - 1015 hrs on - 22/04/82

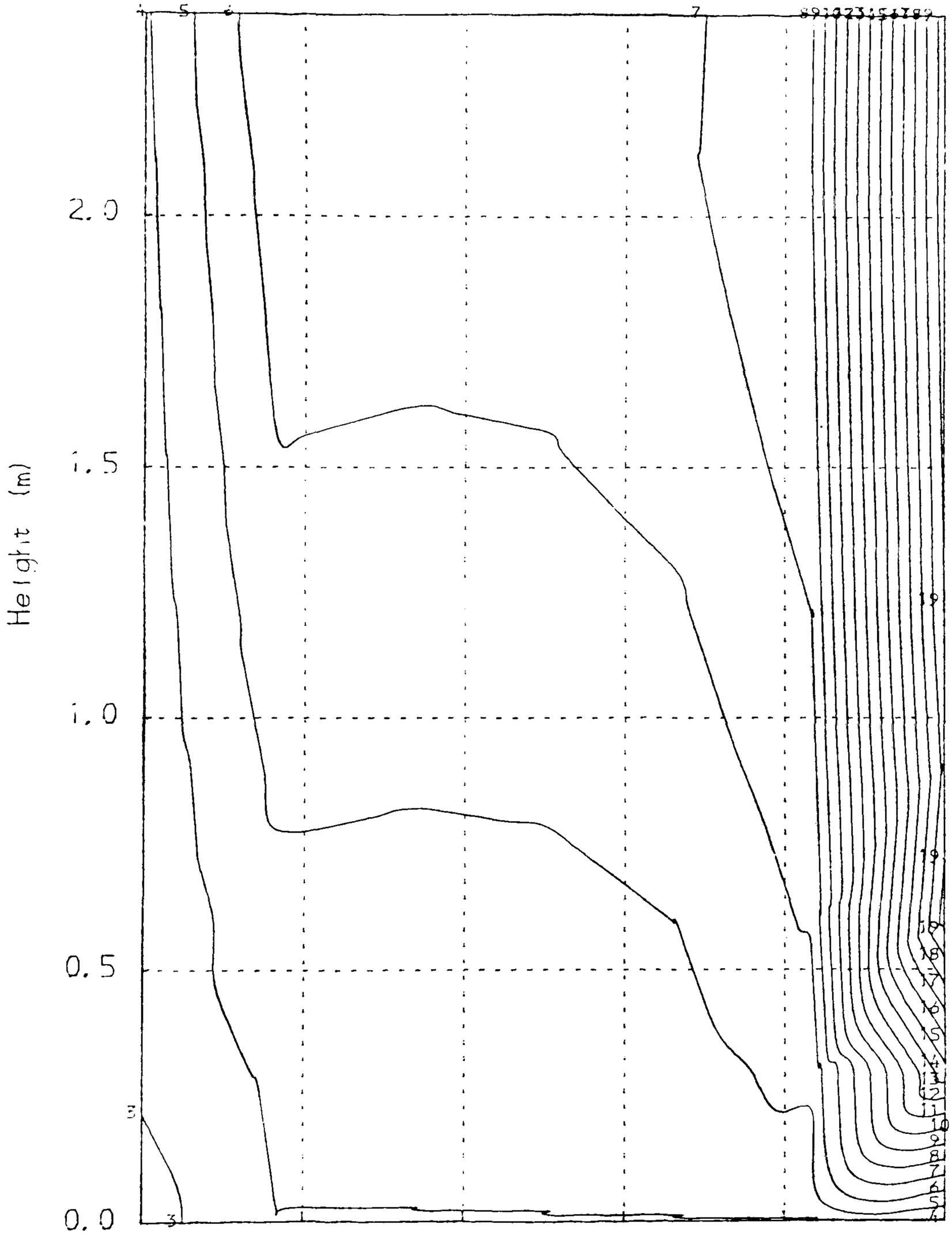

qin = 675.0 W/m2	qout = 730.5 W
eff = 45.1 %	velocity = 0.40 m/s

Fig 8.5(b)- distributed velocity

VELOCITY DISTRIBUTIONS IN VERTICAL AIR GAP

Experimental Results for - 1015 hrs on - 22/04/82

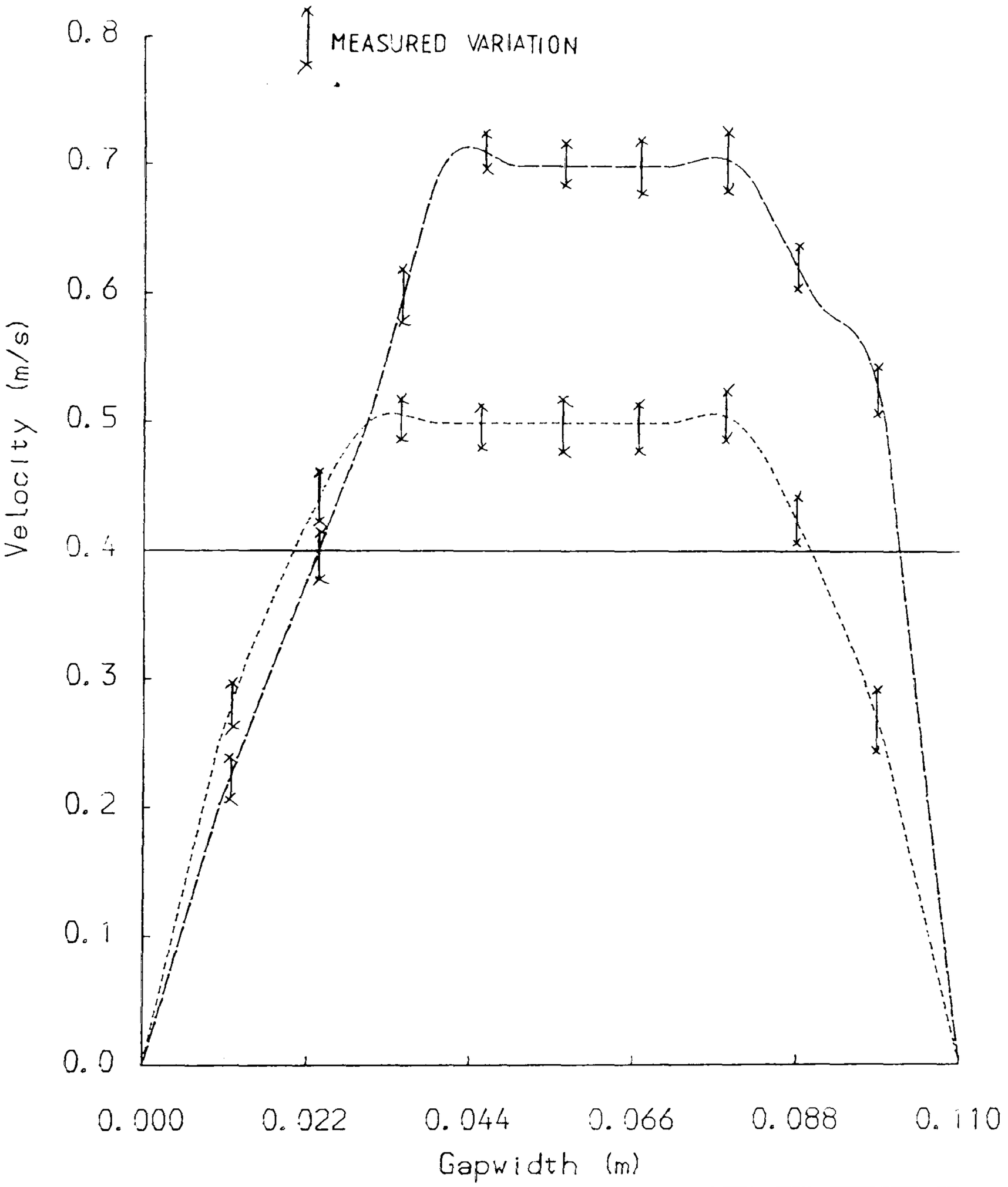

Velocity Profiles

---------- Top distribution

———————— Bottom distribution

———————— Average velocity

tout Experimental 37.4 deg C

tout Theoretical 38.3 deg C

qin = 676.0 W/m2 qout = 837.0 W

eff = 51.6 % velocity = 0.40 m/s

Fig 8.6

is reasonably constant up the height of the collector which makes the assumption in the computer model reasonable. It must be noted that it is very difficult to read a stable value using the heated thermistor, and hence the values are not very reliable.

Fig 8.5 gives the theoretical results using the same weather data and the manufacturer's data on the selective surface. A slightly lower friction factor (0.013) is used since the sheet is very smooth. The results seem reasonable and acceptably close to the experimental results. A maximum variation of about 2% was observed between experimental results and the model. The difficulty in simulating the entrance effects is clearly seen at the bottom right of Fig 8.5, but this does not seem to affect the total result.

The efficiency of about 50% is probably as high as could be expected for the British climate. This gives an output of nearly a kilowatt from a 2.5 sq m collector.

8.2.3 - Annual performance

Having establised the model, it can now be used with any weather data to give an estimate of the annual performance. The theoretical performance for a whole year is given in Fig 8.7, using Irish weather data. The performance is not given for June, July and August since

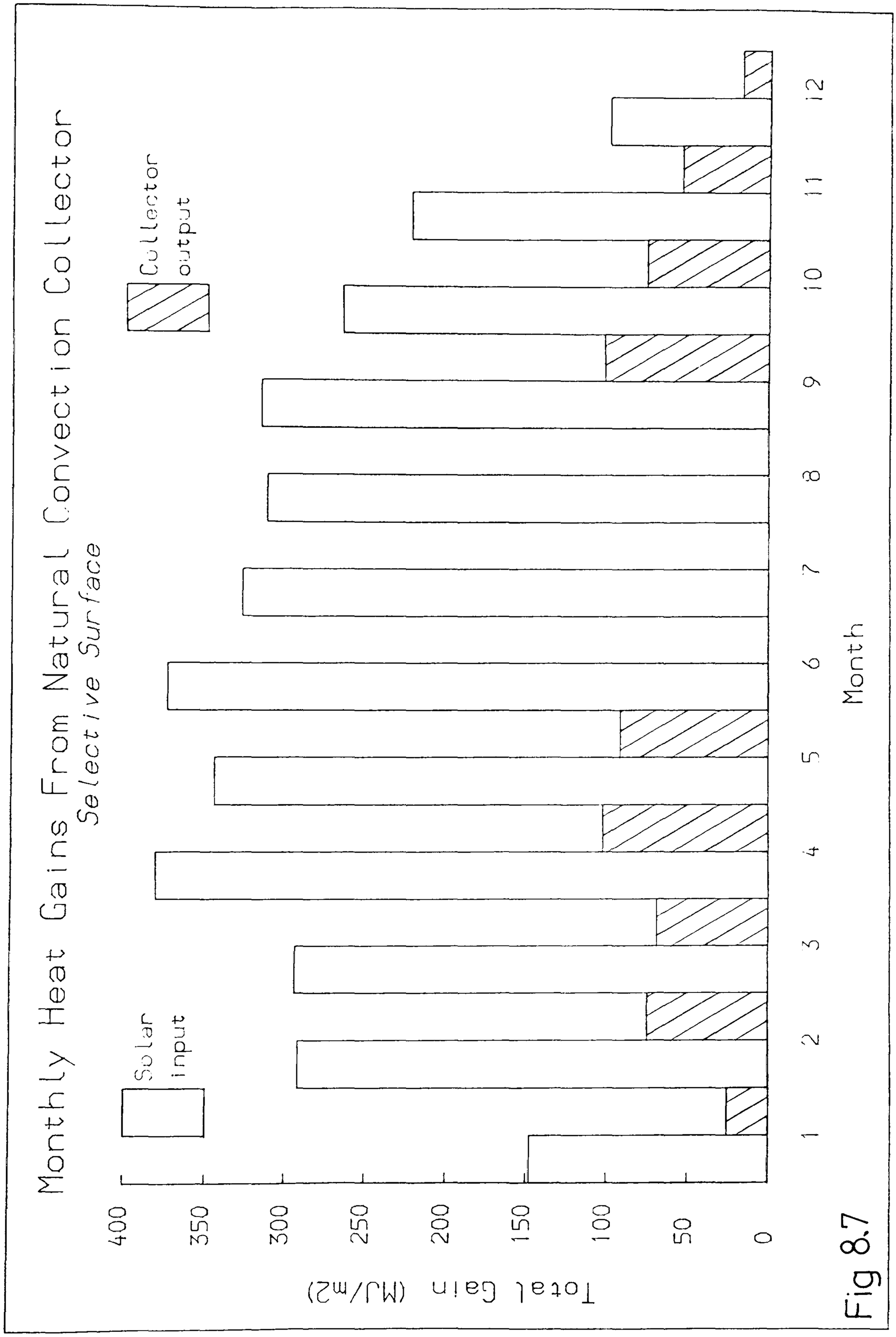

Fig 8.7

Shows monthly total heat outnuts from collector. Predicted by theoretical model.

the collector would not normally be in use. The weather data are averaged from several years and are at hourly intervals. When there is not enough sun, the program assumes the dampers are closed, hence there is zero output. The weather data used are for a single year, not a many year average. The climate of that region of Ireland may not be completely typical of other parts of Britain. The model at present assumes the dampers are closed if the air is too cold, but there is no simple criterion to check whether the air is too hot. This is dependent on the house and hence outside the scope of the model.

8.3 - Other Natural Convection Wall Types

8.3.1 - Introduction

The theoretical model having been shown to be reliable in simulating real collectors, it will be used to model other walls that it was not possible to test experimentally. Such a wall is shown in Fig 6.1 (c). Analysis of such walls cannot be done accurately using the existing model, since the temperature at the collector entrance is not known (e.g not tai), hence strictly the temperature should be found by iteration which would make the model more complicated and increase the run time.

In the following analyses it is assumed that air is drawn into the collector at room temperature, then into the

wall and finally back into the room. This may in fact be more realistic since if the collector were as in Fig 6.1(c), on a sunny day, the collector may well reach equilibrium and the flow cease.

8.3.2 - Theory

The natural convection model is exactly the same as before, except that the pressure losses will be greater (k value = 5.0), calculated as in section 8.1.1. The conduction of heat in the brick wall is calculated using an unsteady state model developed by Lee at Leeds University, and described fully in (14). Briefly it is a finite difference model which calculates two dimensional conduction which can be repeated at intervals along the wall, hence giving a pseudo three dimensional model. The nodes can either be specified as solid or as moving air of a specified velocity for which the model calculates suitable heat transfer coefficients. Originally the model was used for a wall where heat was taken out by cool air. The model as been altered because here warm air flows through a cool wall.

The two models were connected by making the natural convection model a procedure of the conduction model. At any time interval, the output from the collector is in turn supplied as the input for the wall. If the solar radiation is not sufficient to make the collector work, the

conduction model calculates the temperatures as if there were no air flow.

The interface of the two models is not perfect as they were not originally intended to be used together, but the results should show trends although not much weight should be put on the numerical results. With further work it should be possible to make the theory work in conjunction with high thermal capacity components, and hence develop a more suitable model.

Fig 8.8 shows the boundary conditions used for the model. The main complication is the outside condition for the brick wall. Some heat will conduct through the insulation, hence the value of this interface temperature was assumed to be that of the average collector temperature (tai+tout)/2. This may seem rather crude, but the temperature specified makes little difference due to the very high resistance. The resistance the model uses is slightly higher than it should be, since this resistance cannot vary with time, but this effect is negligible. Alternatively, this temperature would have to be calculated by iteration which would increase the computer run time.

8.3.3 - Results

The model was used to simulate the wall over the month of March using the Irish weather data. The

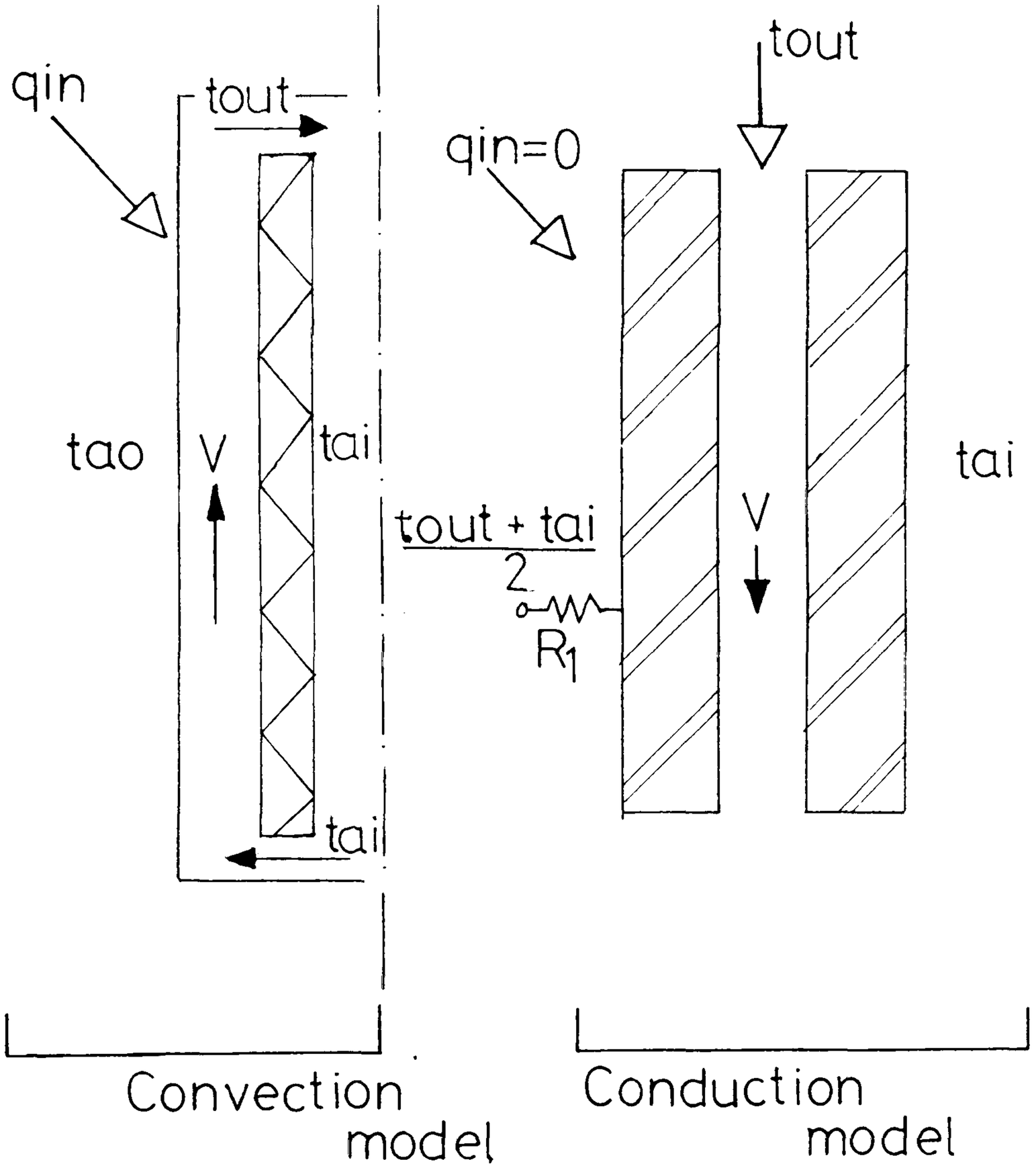

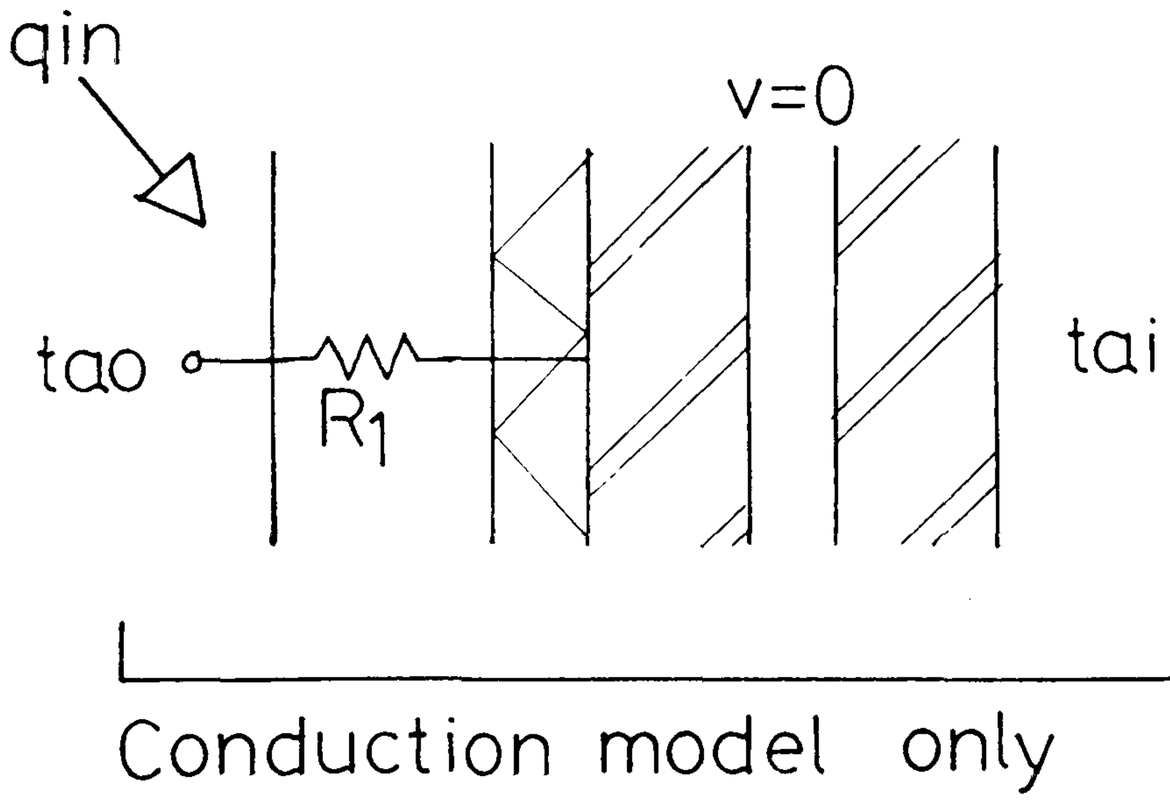

Fig 8.8 - Boundary conditions for model

performance of the collector and the wall, on a typical sunny day, are shown in Fig 8.9, also shown is the performance of the wall predicted by steady state theory. The wall has an average improvement of 10 W/m^2 over the steady state result, this is due to the heat retained in the wall from the previous day plus that from the current day. Clearly in a prolonged dull period this improvement would disappear. The improvement of 10 W/m^2 is, hence, likely to be near the maximum that could be expected.

The performance of the natural convection collector is poorer than described in previous sections, because of the extra pressure loss in the cavity wall. The collector, if considered without the wall, is still producing useful output of up to 600 W.

The major fault with this system is the lack of heat transfer in the cavity wall. For example, for the day summarised in Fig 8.9, of the 594 W the collector is producing at 1100 hrs, only 126 W is being transferred to the wall, the remainder passes into the room. This being so, it would be simpler and more efficient to pass all the air into the room.

8.4 - Conclusions

Natural convection collectors can be made to work in this country if they have selective surfaces and/or 'heat

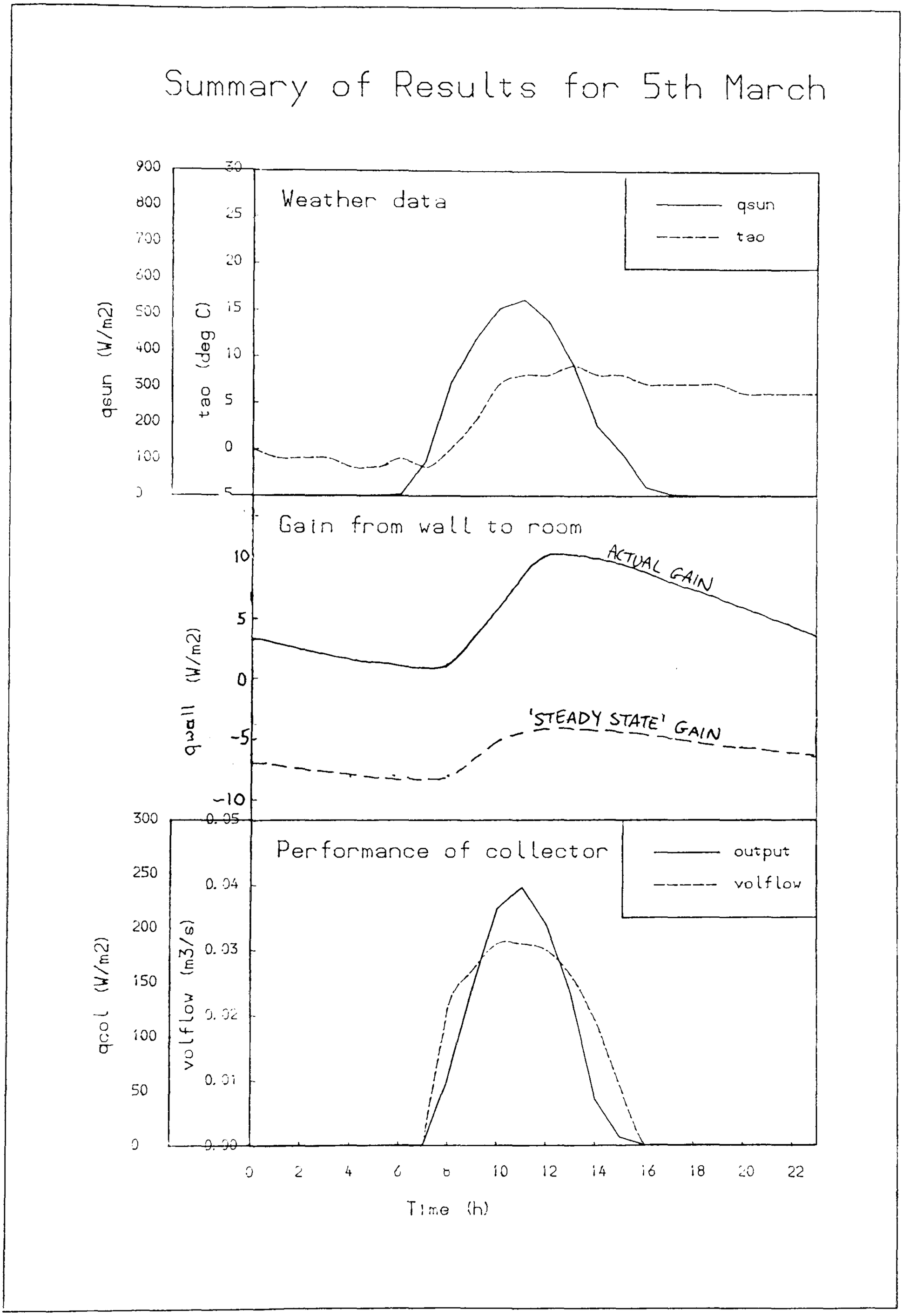

Performance of wall shown in figs6. and 8.8 for a sunny spring day (theoretical calculation).

Fig 8.9

mirror' glazing. Insulating the outside of the masonry wall improves the performance of the collector and also reduces heat loss of the wall during prolonged dull periods.

As was shown in section 8.3, any attempt to store the heat reduces the performance considerably. Hence these collectors seem best suited to buildings occupied in the day only. For dwellings some form of thermal storage is needed. A system requiring storage might be better suited to forced collectors which will be discussed in the next chapter.

Chapter 9

Comparison of Wall Types

This chapter uses the theoretical model described in section 8.3.2 and the theoretical model developed in chapters 6 to 8, to simulate the arrangements that have been tested experimentally and others that could not be so tested because of lack of time. These analyses will be used to compare the various modifications put forward.

9.1 - Justification for Model

The model (described in section 8.3.2) has been well tried and tested in the past by Lee (14), but may be verified further by comparing some results from the experimental walls with the performance predicted by the model. A typical result is shown in Fig 9.1. This is for the glazed, solid wall on 9th Feb 1982. The incident solar radiation for the model is calculated by multiplying the experimental measurement by the solar gain factor and the absorptivity of the wall surface (0.75 and 0.7). The thermal conductivity and specific heat capacity used (0.8 W/mK and 950 J/KgK) are reasonable values taken from the CIBS guide (no experimental values of these could be obtained with any accuracy).

With these values the graphs in Fig 9.1 show a very good correlation the maximum difference being 5 W/m^2 which

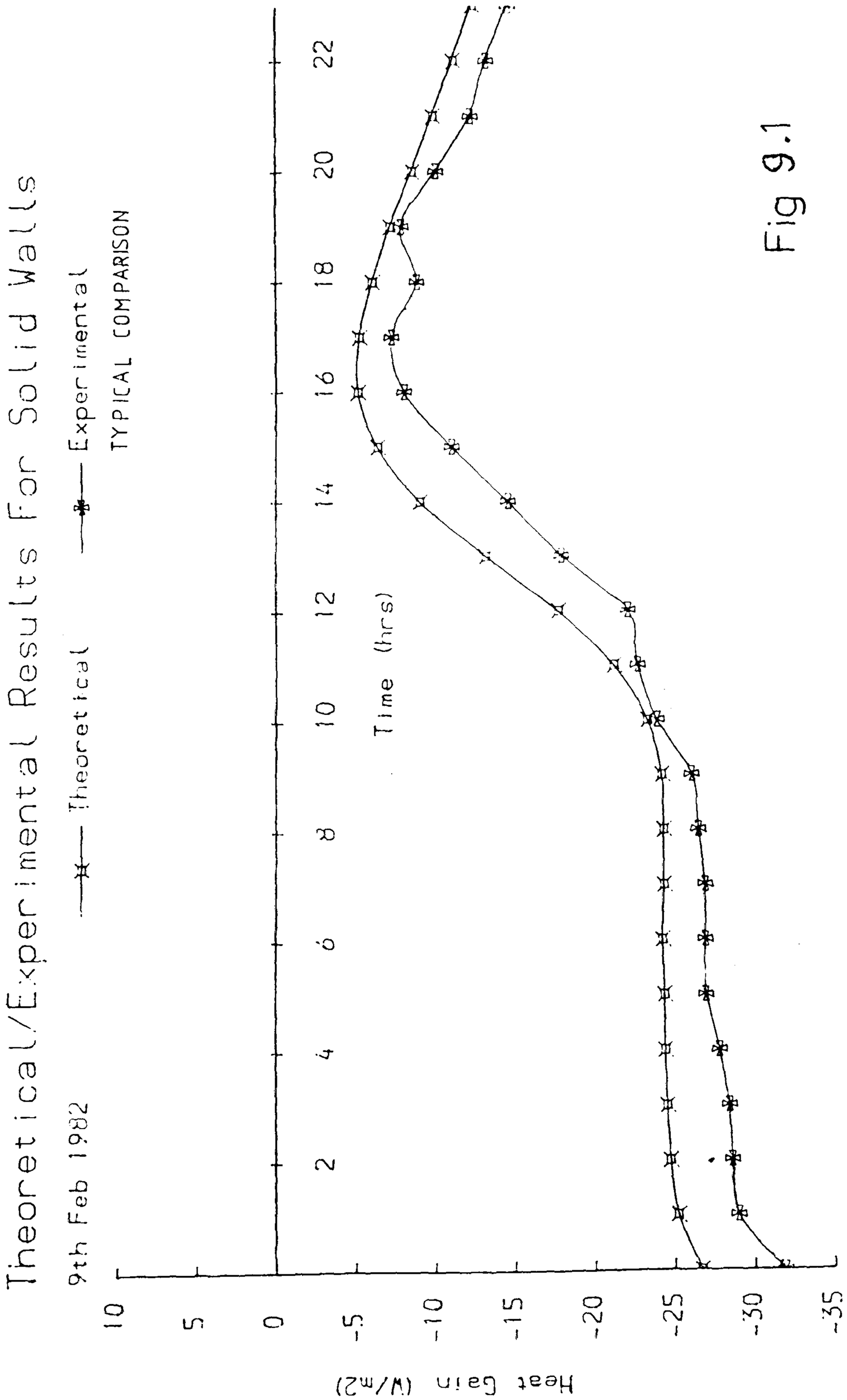
Theoretical/Experimental Results For Solid Walls
9th Feb 1982
Theoretical
Experimental
TYPICAL COMPARISON
Heat Gain (W/m2)
10
5
0
-5
-10
-15
-20
-25
-30
-35
Time (hrs)
2
4
6
8
10
12
14
16
18
20
22

Fig 9.1

corresponds to a temperature difference of 0.5 K at the walls inner suface. Considering a whole month on an hourly basis, the mean difference was 2.8 W/m^1 with a standard deviation of 0.29 W/m^1 . This is very close to the experimental results. More significantly, the graphs show exactly the same trends. This is most important when using the model to compare other walls.

9.2 - Use of a Theoretical Standard Room

In chapter 1 some simple calculations were made to show how a particular wall might behave when part of a whole room. In the light of the various experimental studies, this approach will be repeated, but in more detail. There are two problems which the comparisons so far do not allow for. Firstly it is important to see how the thermal performance of a particular wall affects the overall performance of a building. Secondly, in the case of a collector with no deliberate heat storage, allowance must be made for heat stored in the fabric of the building.

So far all the results discussed have been for collectors attached to rooms with, as far as possible, constant conditions, to allow easy assessment of each collector, without any corrections due to influence of the building itself. The results from earlier chapters will be used, in this analysis, to see how the various collectors inter-relate in a building under varying conditions.

To analyse these effects the wall under consideration is taken as the outside wall of a standard room. This outer wall also has a window. The room itself has a ventilation loss, and the inner walls have no temperature gradient across them, but they can store heat.

Fig 9.2 gives a summary of the properties of this standard room. The room is analysed using the admittance method. This method has many limitations but has the advantage of being very simple. Hence the accuracy of the results is not high, but since the conditions are the same for each wall type the comparisons should be valid.

9.2.1 - The admittance method

The method is described in detail in (29). Its limitations derive from the fact that it is a quasi-steady state technique, i.e the same cycle is repeated for several days. Since the various wall types have been analysed using real weather data and an unsteady state model, this condition is not strictly true, but a good approximation can be made if a day of weather data is selected with the outside air temperature about the same at the start as it is at the end of the day. It is known to be an accurate way of predicting the peak temperature, and is not recommended for calculating hourly inside air temperatures. The modifications outlined below will do this, although as mentioned previously, the accuracy cannot be relied on.

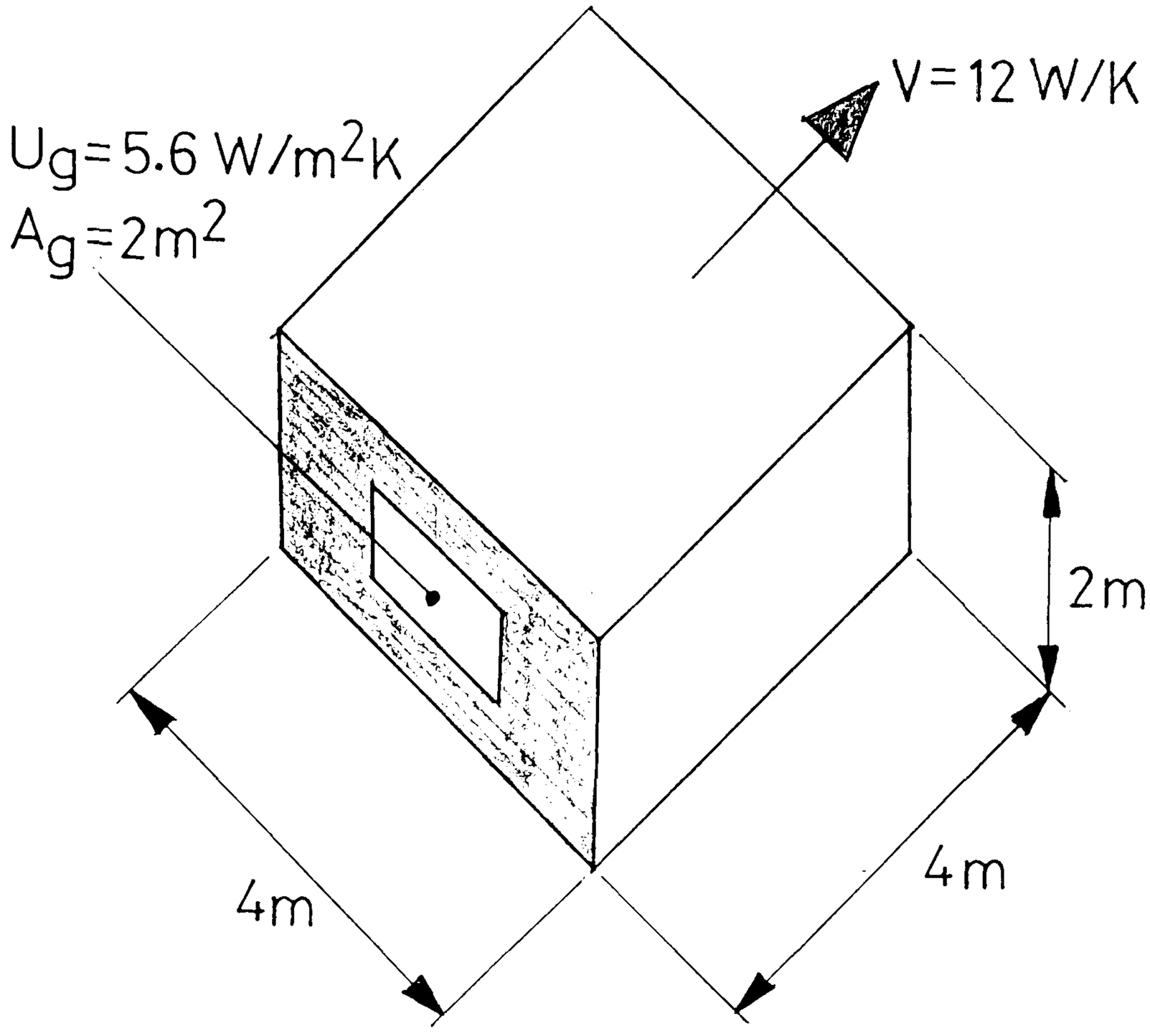

SEE SECTION 9.3

Fig 9.2 (a) – Properties of Standard Room

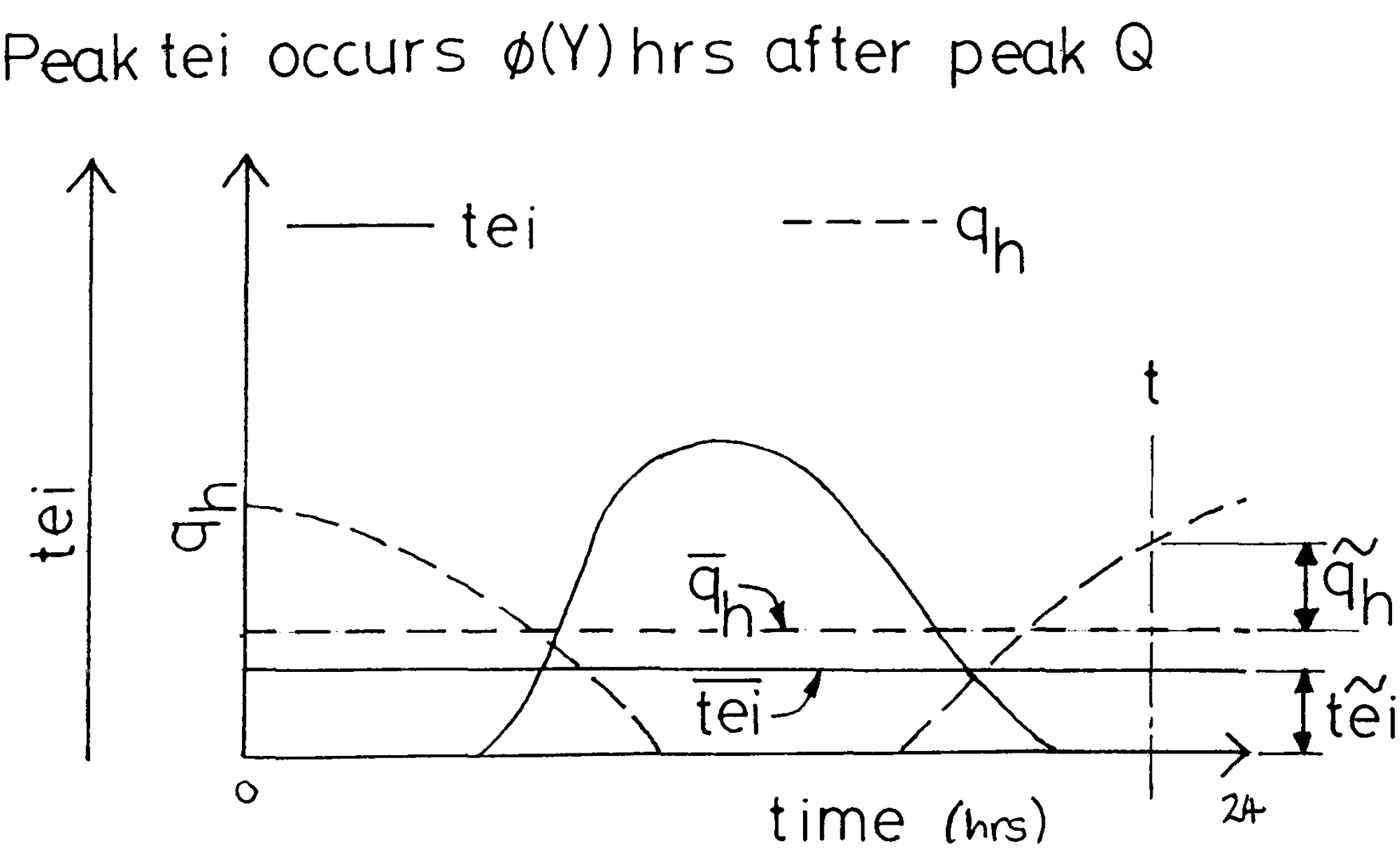

Swings are at any time not only the peak

Fig 9.2(b) – Definition of Admittance Variables

Fig 3.1 of (29) shows that the method is well within an order of magnitude, hence it is accurate enough for the use required in the following analysis. Fig 3.1 of CP 61/74 (29) shows a comparison of hourly variations calculated from the admittance procedure and a more accurate Fourier analysis. For tei>0 the accuracy is better than 10%, for tei<0 the accuracy is less but still well within an order of magnitude.

Certain assumptions can further simplify the method. The inside air temperature is considered to be identical with the inside environmental temperature denoted by tei. The room thermostat is assumed to respond instantly at the set temperature, which for these calculations is 20 C. The inner walls have an admittance (Y) equal to that of the unmodified wall type, i.e cavity or solid brick wall.

Example graphs of tei and the space heating input (q_h) are shown in Fig 9.2 (b). The figure gives the definition of the swing and mean. The mean is a 24 hour mean, and the swing and tei are the value at any time, hence

$$tei = \overline{tei} + \tilde{tei} \qquad (9.2)$$

The value of tei is not known hence this must be solved iteratively. An initial guess slightly larger than the thermostat temperature of 20°C is used. The daily total heat balance gives

$$\overline{q_h} = (U_g A_g + V)(\overline{tei} - \overline{tao}) - \overline{q_i} - A_g s \overline{Q} \quad (9.3)$$

where $\overline{Q}$ = 24h mean insolation (W/m^2)

$\overline{q_h}$ = 24h mean space heating input (W)

$\overline{q_i}$ = 24h mean gain/loss from wall (W/m^2)

It is important to note that the only losses or gains through external elements are $U_g A_g$ and $\overline{q_i}$. The admittance method calculates the wall heat loss q_i using the U value and solair temperature, here this has been replaced by results from the unsteady state model (i.e that of Lee). However

$$\overline{q} = \sum UA(\overline{teo} - \overline{tei}) \quad (9.4)$$

which is the term normally used in the admittance method. The method then uses the concept of the swing to calculate variations around the mean. It is initially assumed that tei is at the thermostat setting and that heating is required, this is given by

$$\tilde{q}_h = -(AY + V)\tilde{tei} - (\tilde{tao}(U_g A_g + V) + A_g s_a \tilde{Q} + \tilde{q}_i) \quad (9.5)$$

If the value of $(\tilde{q}_h + \tilde{q}_h)$ is negative there will be a surplus of heat and the room will tend to overheat, hence the value of tei must be calculated from

$$tei = \overline{tei} + (\tilde{tao}(U_g A_g + V) + A_g s_a \tilde{Q} + \tilde{q}_i)/(AY + V) \quad (9.6)$$

This is done over 24 hours after which the average of tei is found, the whole procedure is repeated with the average

of the new value of tei and the previous guess or calculated value until convergence.

Additionally if the wall in question has a convection collector there will be another term q_c. This will have a mean and swing, and will be similar in format to q_i.

9.3 - Explanation of Wall Type Tables

This section describes figures 9.3-9.20. In these tables the wall analysed is described and defined by various basic parameters. With these are given the thermal transmittance, and the admittance.

The main table, of each figure, gives total monthly gains under various headings. the full daily totals, and the net gain over the evening only for domestic applications. The last totals are those calculated using steady state theory. All the above values are heat flows through the collector wall.

The graph in the lower part of the table shows the daily performance for a typical sunny day in March, this is to show the diurnal effects of solar gain on each wall. It gives also the net gain over the evening and the phase lag of the wall on that day (ϕ), i.e the time between the maximum solar input and the maximum heat flow/ minimum heat loss into the room. This graph in particular shows how the

behaviour of the wall, on a sunny day, affects the heat input to the standard room.

9.4 - Discussion of Theoretical Results

9.4.1 - Solid walls

Figs 9.3-9.12 summarise the performances of solid walls modified in various ways. Figs 9.3 and 9.4 show unmodified walls facing north and south. The combination of the warmer wall and the greater direct gain means the south facing room requires considerably less heat input.

Figs 9.5-9.7 show variations on single glazing. It is interesting to compare these performances with those of the insulated walls Figs 9.11 and 9.12. In the spring and autumn the performance of the glazed walls is not very much greater. In winter the insulated walls are better, and in summer there is a possibility that the glazed walls could cause overheating unless vented. Overall the insulation techniques would probably give greater cost benefit. It would, however, be practicable to use single glazing in a conservatory.

Fig 9.5 shows results for a plain brick wall glazed. These results could apply equally well to a narrow glazed gap or a conservatory. This gives an improvement on the unglazed wall of 0.9 MJ/m^2 over the evening. As shown in

Fig 9.6 the wall can face other than directly south and still give a reasonable performance. Painting the wall dark improves the performance by a further 0.3 MJ/m^2, as shown by Fig 9.7.

It may be possible, for a conservatory, to use movable insulation similar to a concertina folding door, on the outer face of the wall. This would reduce heat loss from the wall to the outside at night, and could be operated either manually or automatically from a timer switch. The results for a wall modified so are shown in Fig 9.8. The performance is very good, but this modification is very much dependent on how it is used by the occupants.

Fig 9.9 shows that single glazing can be thermally effective using selective surfaces. The price of these materials is not prohibitive, but to be effective a good contact must be achieved between the selective sheeting and the wall surface. It is doubtful whether this can be done well and permanently.

Fig 9.10 and 9.11 shows the performance of two types of double glazing. The ordinary double glazing gives a performance as good as the single glazing with selective surface, but does not have the practical difficulties. Fig 9.10 is for Pilkingtons' 'k Insulight Glazing' (31) which claims as a window to have a U value 30% lower than for '

ordinary double glazing. This makes a very efficient solar collector, particularly in the spring and autumn. Clearly to make glazing a solid wall practicable, one of the measures shown in Figs 9.9-9.11 would have to be used.

Figs 9.12 and 9.13 show results for solid walls insulated either on the inside or the outside. Over the year there is little difference between the two, practical considerations would decide which is best. It is interesting to note that the unsteady state model has trouble simulating the wall with outside insulation. This is because very little heat conducts through the insulation, and there are few nodal points to analyse the behaviour within the insulation.

9.4.2 - Cavity walls

Fig 9.14 shows results for an unmodified cavity wall facing south, and Fig 9.15 the same facing north. The performance is much the same as the equivalent solid walls, but the winter losses for the cavity walls are approximately two thirds those of the solid walls, which is proportional to the improvement in U value.

Fig 9.16 is for a cavity wall with polyurethane foam cavity insulation. This is at present readily available, hence it is important to compare any other rehabilitation with this. The performance is very similar to those of the

solid walls with inside and outside insulation. This has the advantage that it does not greatly reduce the wall's admittance.

The cavity wall single glazed with no forced air recovery, Fig 9.17, is not much better in the winter months than the wall with cavity insulation. It is unlikely that this will be economically viable unless better glazing is used, in which case results will be very similar to those of the equivalent glazed solid walls.

The last two cavity walls use forced air recovery in the cavity. Fig 9.18 is for a single glazed cavity wall and Fig 9.19 is for a wall with double glazed heat mirror units. For neither of these has the energy expended by the fan been included in the net result. The fan used in the experimental work described in chapters 3-5, consumed 180 W, which gives a total consumption of 3.2 MJ over a 5 hour period. When the wall with heat mirror glazing gives a slight net gain the energy consumed by the fan is included and the wall with ordinary single glazing gives a net loss. An appropriately sized fan may not give such poor net results.

The poor performance of glazed cavity walls with forced air recovery, combined with practical difficulties (such as the cavity being blocked by mortar and door and window frames) would make such collectors impracticable for

rehabilitation. Even for newly designed buildings, it is unlikely such a technique would be cost effective.

9.4.3 - Convection collectors

Fig 9.20 shows results for a natural convection collector, of the type described in chapters 6-8, here attached to the outside of a solid brick wall. The collector is 2m high by 2m wide. The wall gives a good average performance due to its very low U value, but most of the heat is gained in the day, and little of this heat is stored in the interior fabric. The model shows that the room overheats, but in reality this could be corrected by fitting the collector with a thermostatic control. These results agree with the earlier statement that such a collector would be well suited to a building requiring heating mainly in the day.

9.4.4 - Overall comparisons

Figs 9.21, 9.22 and 9.23 show the total required heat input to the standard room for March, for the periods: 0730-1700 h, 1800-2300 h and full day. The heat inputs for the period 0730-1730 h (Fig 9.21) are approximately in the ratios of the U values of the corresponding walls. For the other two periods, the glazed walls are much better than their U values would suggest, particularly for the period 1800-2300 h (Fig 9.22).

Fig 9.3- SOLID BRICK WALL: UNGLAZED

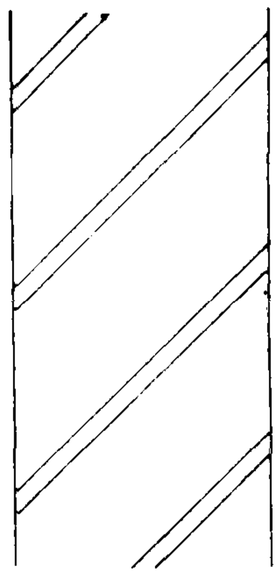

Surface Absorptivity	0.70
Angle to South	180° north
Transmittance	2.19 W/m2K
Admittance Parameters	
Thermal Admittance Y	4.75 W/m2K
Time Lead of Y	1.39 hrs
Decrement Factor	0.46
Time Lag of D.F	-6.93 hrs
Surface Factor	0.50
Time Lag of S.F	-1.64 hrs

Monthly Gains to Room (MJ/m2)

Month	1	2	3	4	5	6	7	8	9	10	11	12
Rad gain Full Day	-78.4	-65.3	-66.1	-50.2	-35.7	-15.5	-13.2	-17.9	-29.9	-46.8	-60.9	-68.1
Conv gain Full Day	0.0	0.0	0.0	0.0	0.0	0.0	0.0	0.0	0.0	0.0	0.0	0.0
Net gain Full Day	-78.4	-65.3	-66.1	-50.2	-35.7	-15.5	-13.2	-17.9	-29.9	-46.8	-60.9	-68.1
Net gain 1800-2300	-15.9	-12.5	-12.1	-8.0	-4.7	-0.4	-0.4	-1.7	-4.5	-8.7	-12.0	-13.7
Steady State With TEO	-76.8	-63.3	-64.5	-50.0	-36.3	-16.8	-14.6	-18.6	-29.9	-46.2	-59.4	-66.4

Daily Performance For 20th March

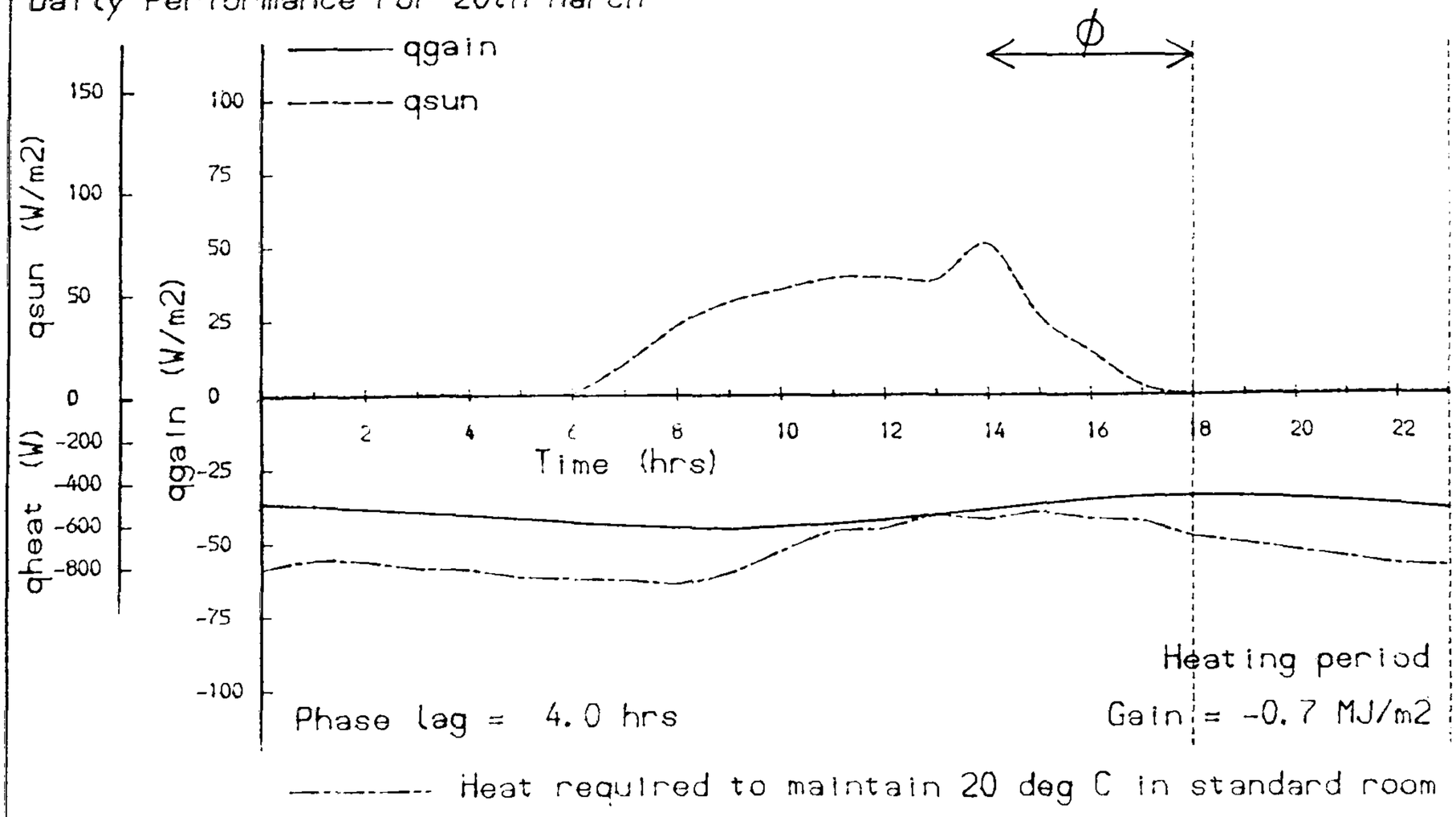

Fig 9.4 - SOLID BRICK WALL: UNGLAZED

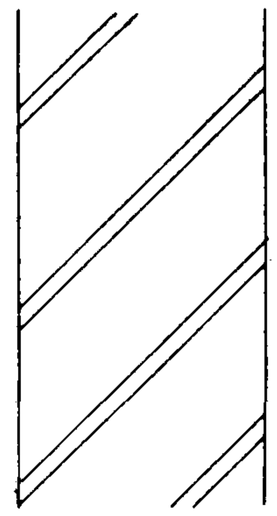

Surface Absorptivity	0.70
Angle to South	0° south
Transmittance	2.19 W/m2K
Admittance Parameters	
Thermal Admittance Y	4.75 W/m2K
Time Lead of Y	1.39 hrs
Decrement Factor	0.46
Time Lag of D.F	-6.93 hrs
Surface Factor	0.50
Time Lag of S.F	-1.64 hrs

Monthly Gains to Room (MJ/m2)

Month	1	2	3	4	5	6	7	8	9	10	11	12
Rad gain Full Day	-68.3	-44.9	-49.1	-31.8	-24.4	-4.4	-4.1	-5.6	-11.9	-29.7	-44.9	-61.2
Conv gain Full Day	0.0	0.0	0.0	0.0	0.0	0.0	0.0	0.0	0.0	0.0	0.0	0.0
Net gain Full Day	-68.3	-44.9	-49.1	-31.8	-24.4	-4.4	-4.1	-5.6	-11.9	-29.7	-44.9	-61.2
Net gain 1800-2300	-12.9	-6.7	-7.1	-2.5	-1.3	2.9	2.4	1.9	0.8	-3.7	-7.3	-11.7
Steady State With TEO	-67.9	-45.5	-49.7	-33.8	-26.3	-7.1	-6.6	-7.7	-14.3	-31.3	-45.3	-60.4

Daily Performance For 20th March

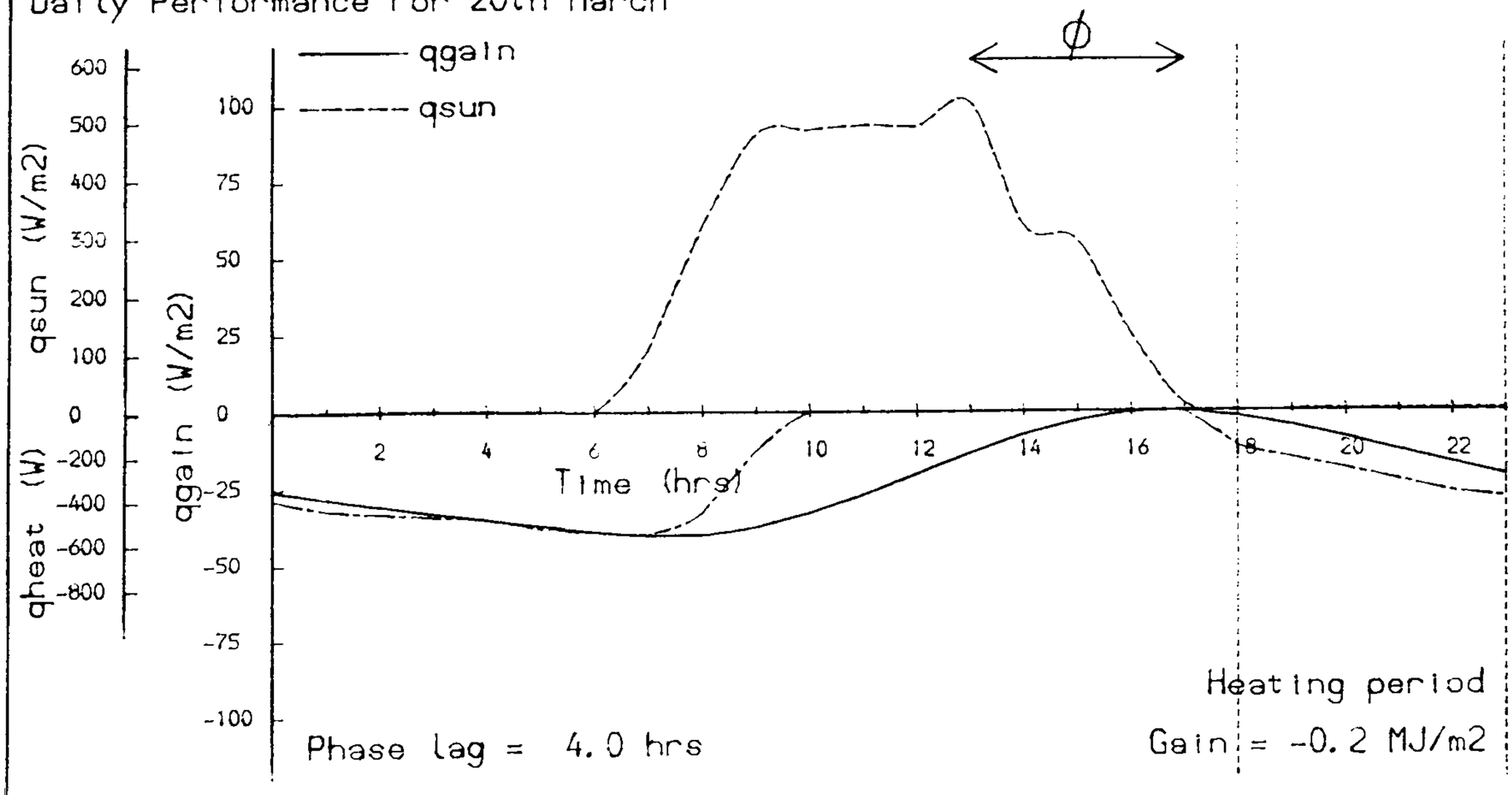

Fig 9.5 - SOLID BRICK WALL: SINGLE GLAZED

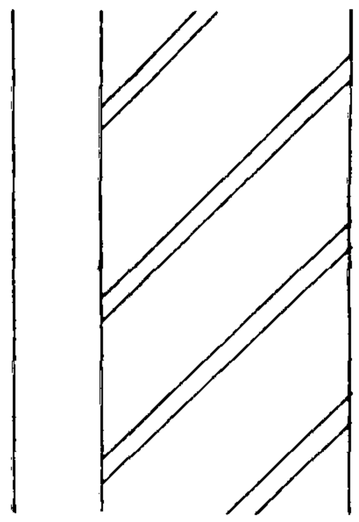

Surface Absorptivity	0.70
Angle to South	0° south
Transmittance	1.62 W/m2K
Admittance Parameters	
Thermal Admittance Y	4.78 W/m2K
Time Lead of Y	1.34 hrs
Decrement Factor	0.30
Time Lag of D.F	-8.03 hrs
Surface Factor	0.49
Time Lag of S.F	-1.62 hrs

Monthly Gains to Room (MJ/m2)

Month	1	2	3	4	5	6	7	8	9	10	11	12
Rad gain Full Day	-26.0	11.5	6.4	22.2	12.8	23.7	23.0	29.1	33.9	18.6	1.8	-28.3
Conv gain Full Day	0.0	0.0	0.0	0.0	0.0	0.0	0.0	0.0	0.0	0.0	0.0	0.0
Net gain Full Day	-26.0	11.5	6.4	22.2	12.8	23.7	23.0	29.1	33.9	18.6	1.8	-28.3
Net gain 1800-2300	-2.7	7.4	6.5	10.5	7.3	9.3	8.8	10.6	12.3	8.4	4.3	-4.0
Steady State With TEO	-29.8	6.9	4.0	27.9	28.4	46.6	40.6	37.8	33.4	13.7	-2.5	-30.8

Daily Performance For 20th March

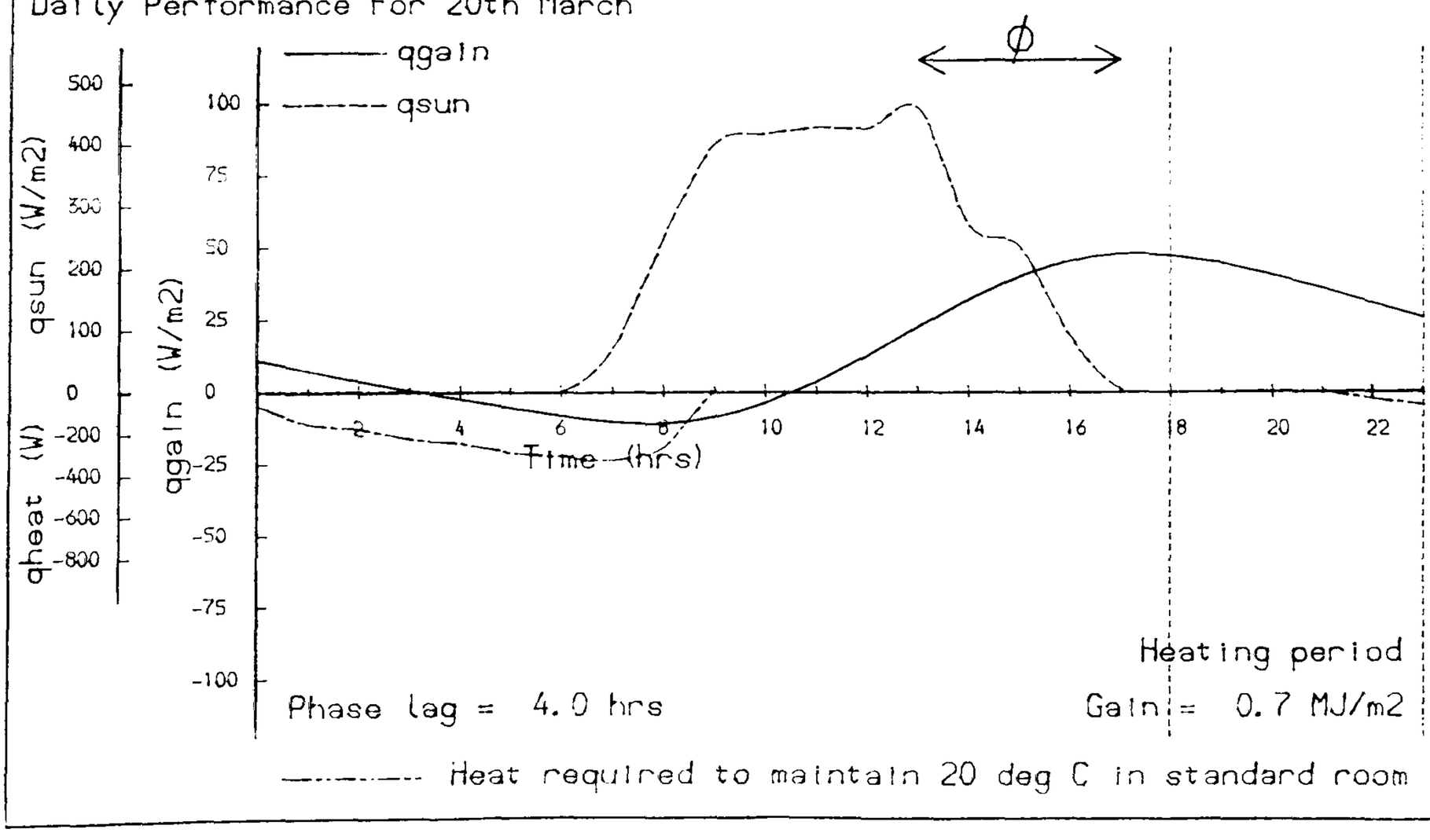

Fig 9.6 - SOLID BRICK WALL: SINGLE GLAZED

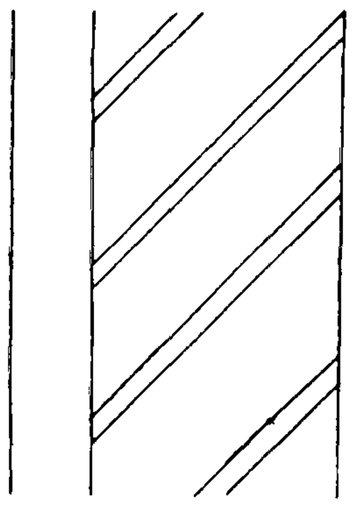

Surface Absorptivity	0.70
Angle to South	33° to east
Transmittance	1.62 W/m2K
Admittance Parameters	
Thermal Admittance Y	4.78 W/m2K
Time Lead of Y	1.34 hrs
Decrement Factor	0.30
Time Lag of D.F	-8.03 hrs
Surface Factor	0.49
Time Lag of S.F	-1.62 hrs

Monthly Gains to Room (MJ/m2)

Month	1	2	3	4	5	6	7	8	9	10	11	12
Rad gain Full Day	-31.5	5.3	-3.5	15.0	11.6	28.0	24.5	28.6	22.1	5.4	-9.1	-32.3
Conv gain Full Day	0.0	0.0	0.0	0.0	0.0	0.0	0.0	0.0	0.0	0.0	0.0	0.0
Net gain Full Day	-31.5	5.3	-3.5	15.0	11.6	28.0	24.5	28.6	22.1	5.4	-9.1	-32.3
Net gain 1800-2300	-4.6	4.7	2.6	6.5	5.1	8.5	7.6	8.7	7.6	3.8	0.6	-5.3
Steady State With TEO	-33.8	3.3	-1.8	23.7	27.3	48.1	40.4	38.7	25.5	4.7	-10.4	-33.7

Daily Performance For 20th March

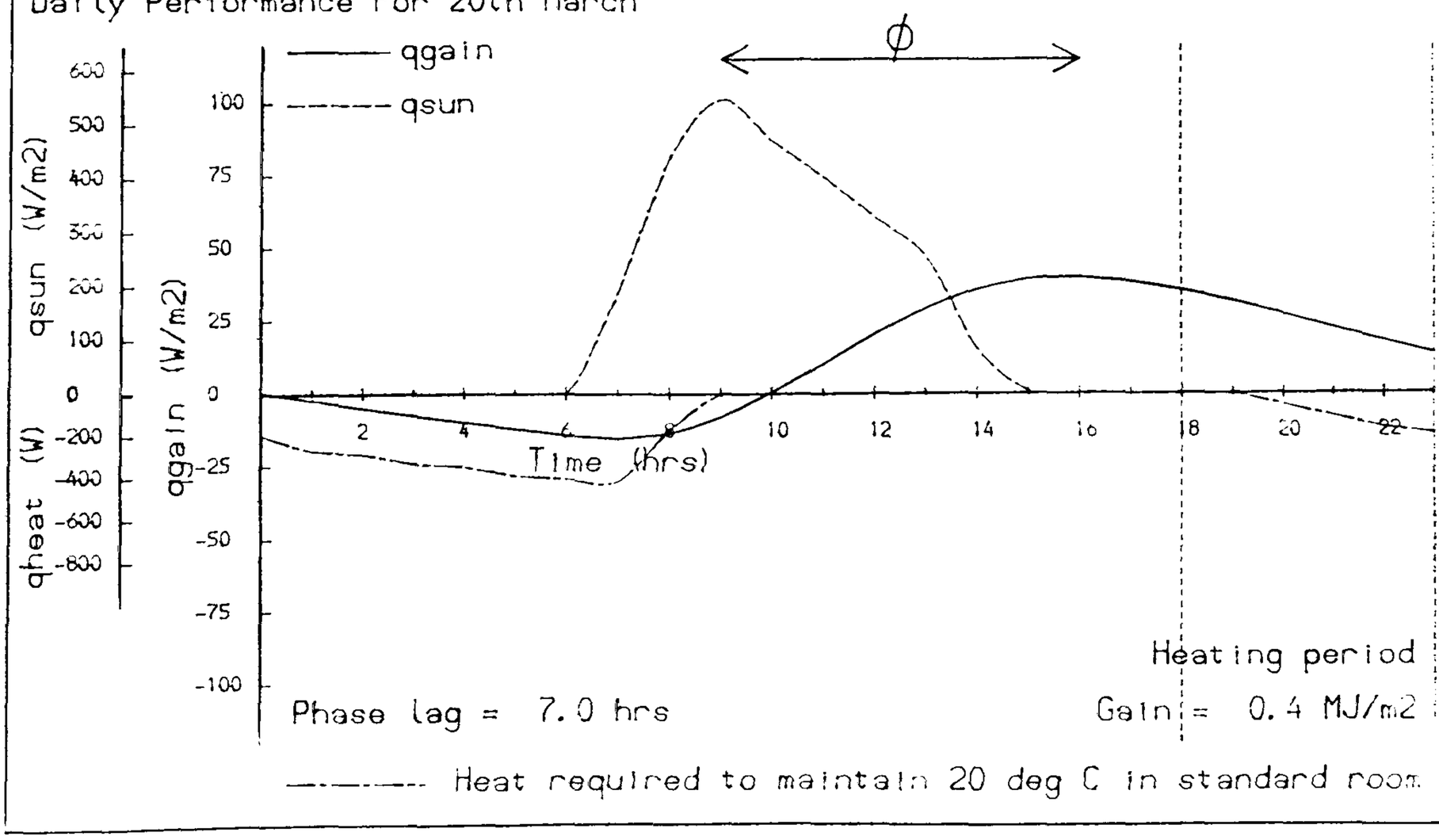

Fig 9.7 - SOLID BRICK WALL: SINGLE GLAZED

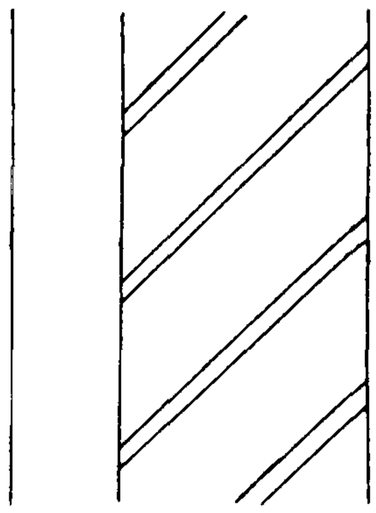

BLACK SURFACE

Surface Absorptivity	0.90
Angle to South	0° south
Transmittance	1.62 W/m2K
Admittance Parameters	
Thermal Admittance Y	4.78 W/m2K
Time Lead of Y	1.34 hrs
Decrement Factor	0.30
Time Lag of D.F	-8.03 hrs
Surface Factor	0.49
Time Lag of S.F	-1.62 hrs

Monthly Gains to Room (MJ/m2)

Month	1	2	3	4	5	6	7	8	9	10	11	12
Rad gain Full Day	-17.0	29.3	23.5	41.8	27.6	38.0	36.2	44.1	51.7	34.7	15.4	-22.1
Conv gain Full Day	0.0	0.0	0.0	0.0	0.0	0.0	0.0	0.0	0.0	0.0	0.0	0.0
Net gain Full Day	-17.0	29.3	23.5	41.8	27.6	38.0	36.2	44.1	51.7	34.7	15.4	-22.1
Net gain 1800-2300	-0.1	12.4	11.5	16.2	11.5	13.4	12.6	14.9	17.4	13.0	8.3	-2.2
Steady State With TEO	-21.6	23.2	20.4	49.2	47.7	67.5	59.0	55.3	51.1	28.6	9.9	-25.2

Daily Performance For 20th March

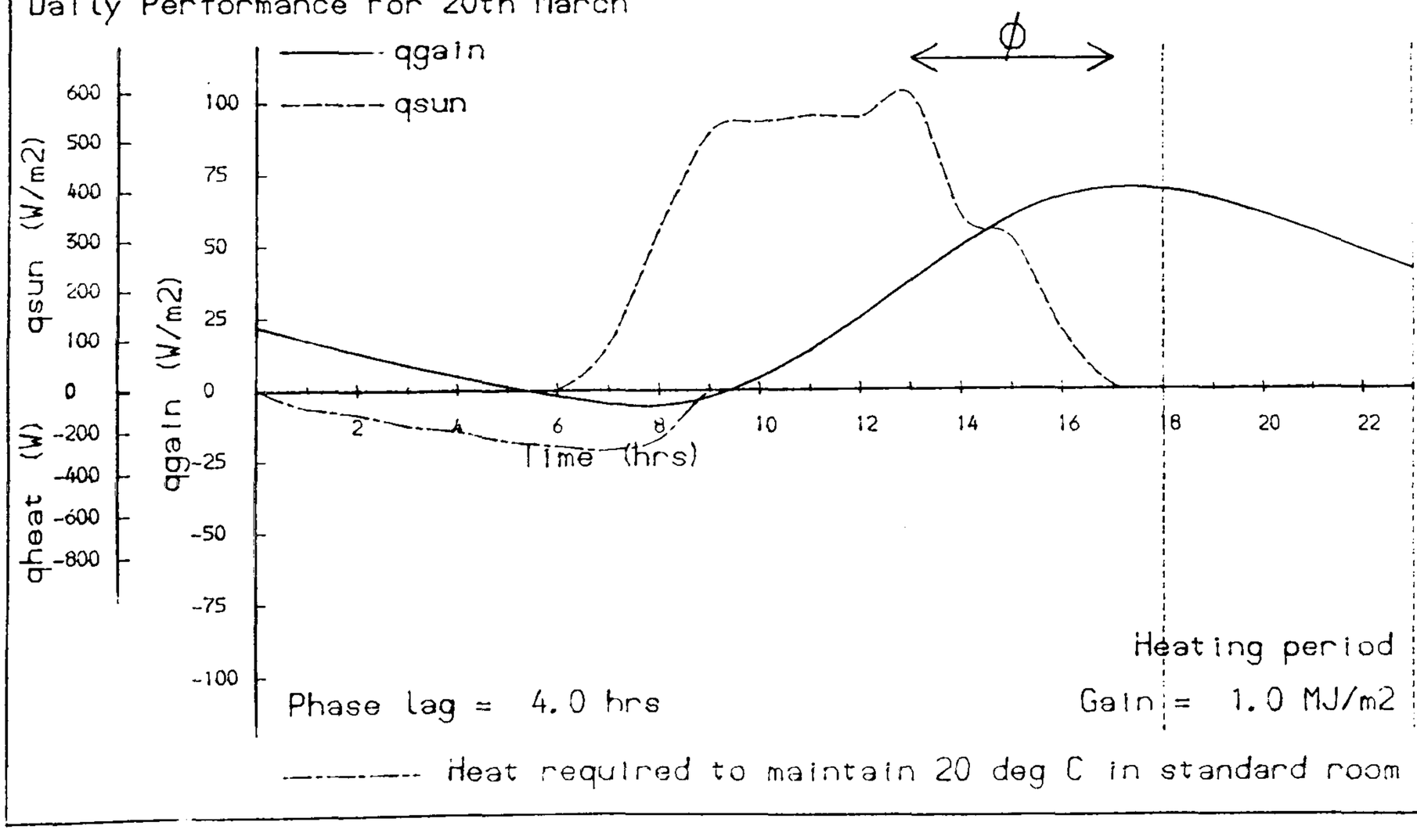

Fig 9.8 - SOLID BRICK WALL: CONSERVATORY, SHUTTERS

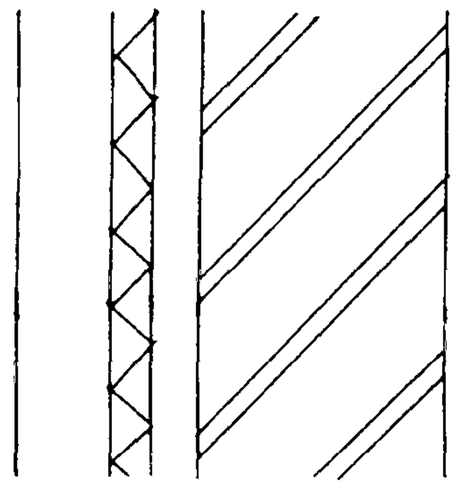

SHUTTERS OPEN 0700
" CLOSE 1800

Surface Absorptivity	0.70
Angle to South	0° south
Transmittance	1.62 or 0.64 W/m2K
Admittance Parameters	
Thermal Admittance Y	4.78 W/m2K
Time Lead of Y	1.34 hrs
Decrement Factor	0.30
Time Lag of D.F	-8.03 hrs
Surface Factor	0.49
Time Lag of S.F	-1.62 hrs

Monthly Gains to Room (MJ/m2)

Month	1	2	3	4	5	6	7	8	9	10	11	12
Rad gain Full Day	3.8	48.8	45.4	62.6	45.6	52.0	47.7	55.9	66.0	50.8	32.8	-4.1
Conv gain Full Day	0.0	0.0	0.0	0.0	0.0	0.0	0.0	0.0	0.0	0.0	0.0	0.0
Net gain Full Day	3.8	48.8	45.4	62.6	45.6	52.0	47.7	55.9	66.0	50.8	32.8	-4.1
Net gain 1800-2300	1.6	12.8	12.2	16.4	12.0	13.4	12.4	14.5	16.9	13.1	8.9	-0.5
Steady State With TEO	-29.8	6.9	4.0	27.9	28.4	46.6	40.6	37.8	33.4	13.7	-2.5	-30.8

Daily Performance For 20th March

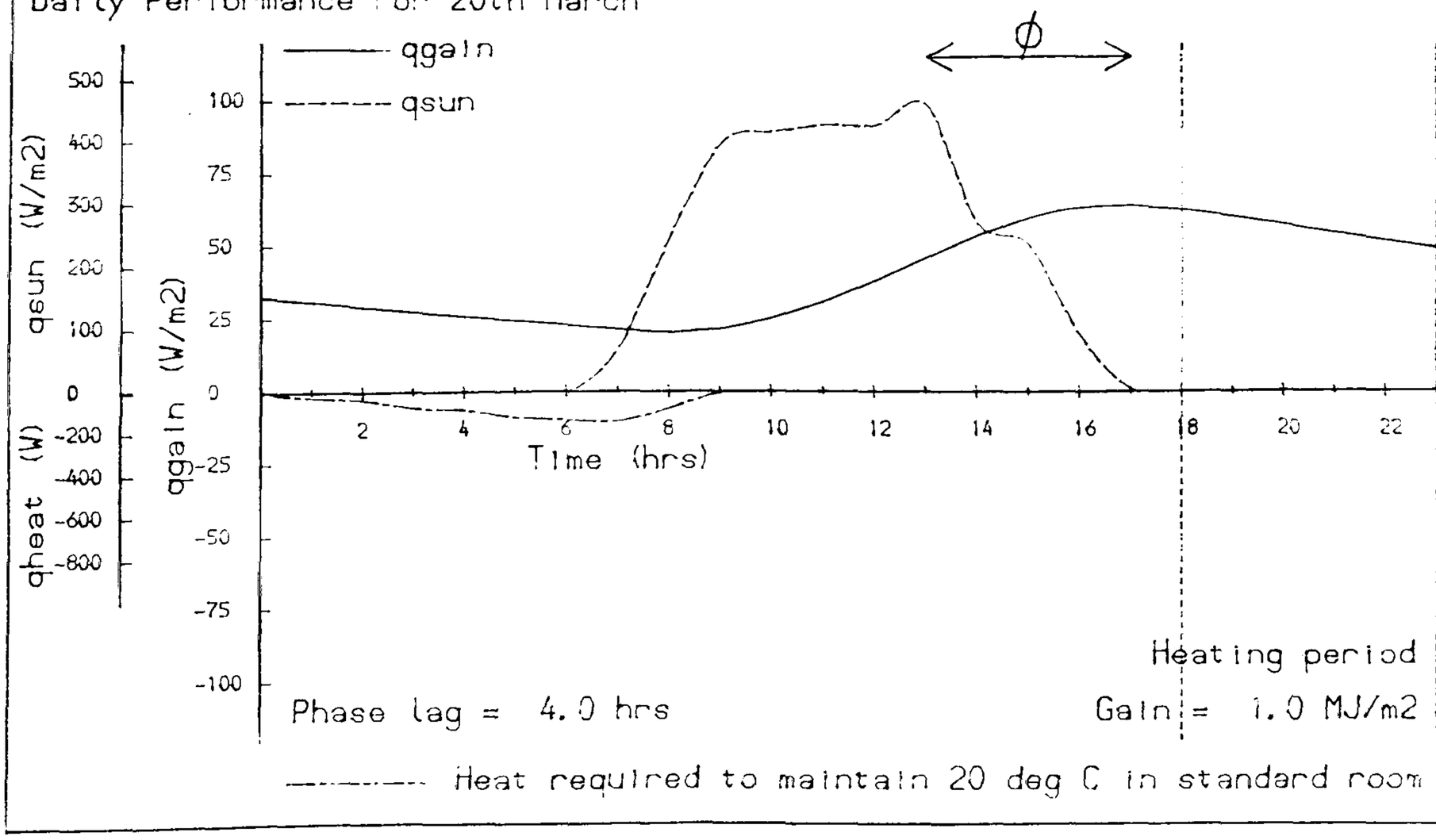

Fig 9.9 - SOLID BRICK WALL: SINGLE GLAZED SELECTIVE

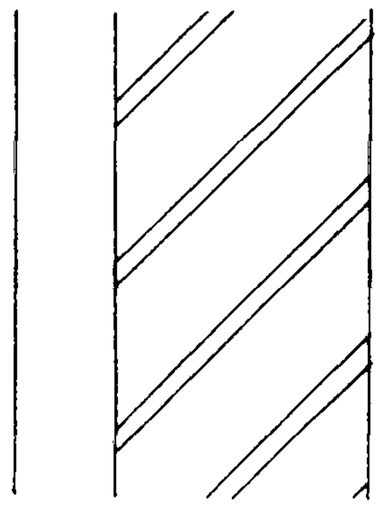

SELECTIVE SURFACE

Surface Absorptivity	0.90 Selective
Angle to South	0° south
Transmittance	1.38 W/m2K
Admittance Parameters	
Thermal Admittance Y	4.78 W/m2K
Time Lead of Y	1.32 hrs
Decrement Factor	0.26
Time Lag of D.F	-8.29 hrs
Surface Factor	0.49
Time Lag of S.F	-1.60 hrs

Monthly Gains to Room (MJ/m2)

Month	1	2	3	4	5	6	7	8	9	10	11	12
Rad gain Full Day	1.8	51.5	46.2	64.3	45.5	52.9	49.5	58.5	69.2	53.5	34.2	-6.8
Conv gain Full Day	0.0	0.0	0.0	0.0	0.0	0.0	0.0	0.0	0.0	0.0	0.0	0.0
Net gain Full Day	1.8	51.5	46.2	64.3	45.5	52.9	49.5	58.5	69.2	53.5	34.2	-6.8
Net gain 1800-2300	3.8	17.1	16.0	20.6	15.1	16.3	15.3	17.8	20.8	16.8	12.2	1.0
Steady State With TEO	-1.8	52.3	50.2	84.3	79.1	99.1	86.7	82.0	78.8	54.0	33.4	-10.2

Daily Performance For 20th March

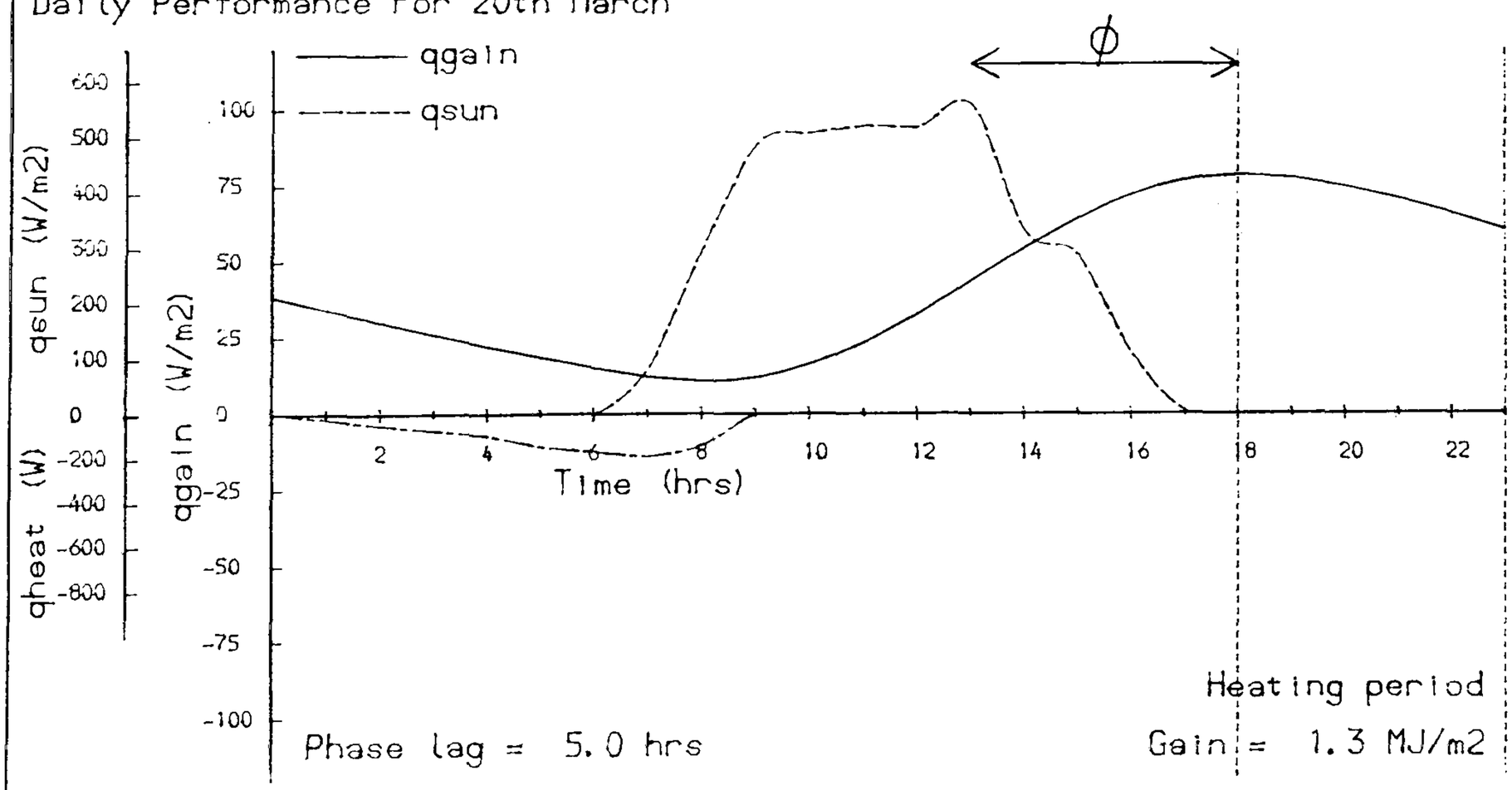

Fig 9.10 - SOLID BRICK WALL: DOUBLE GLAZED

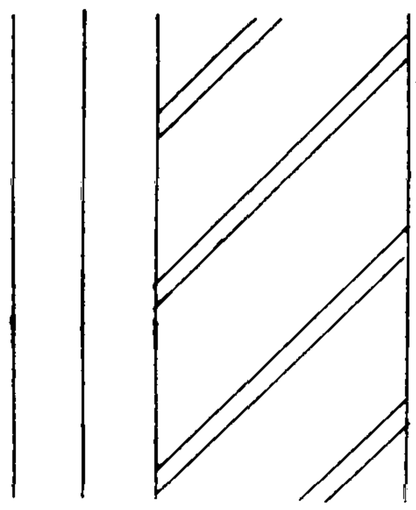

BLACK SURFACE

Surface Absorptivity	0.90
Angle to South	0° south
Transmittance	1.32 W/m2K
Admittance Parameters	
Thermal Admittance Y	4.78 W/m2K
Time Lead of Y	1.32 hrs
Decrement Factor	0.25
Time Lag of D.F	-8.34 hrs
Surface Factor	0.49
Time Lag of S.F	-1.60 hrs

Monthly Gains to Room (MJ/m2)

Month	1	2	3	4	5	6	7	8	9	10	11	12
Rad gain Full Day	3.1	51.3	44.9	59.2	38.9	43.2	42.0	53.0	65.6	52.7	34.5	-5.4
Conv gain Full Day	0.0	0.0	0.0	0.0	0.0	0.0	0.0	0.0	0.0	0.0	0.0	0.0
Net gain Full Day	3.1	51.3	44.9	59.2	38.9	43.2	42.0	53.0	65.6	52.7	34.5	-5.4
Net gain 1800-2300	3.9	16.7	15.3	18.9	13.0	13.5	13.1	16.1	19.6	16.3	12.0	1.1
Steady State With TEO	-8.5	36.9	34.8	63.5	60.2	78.1	68.3	64.4	61.2	39.7	21.9	-14.4

Daily Performance For 20th March

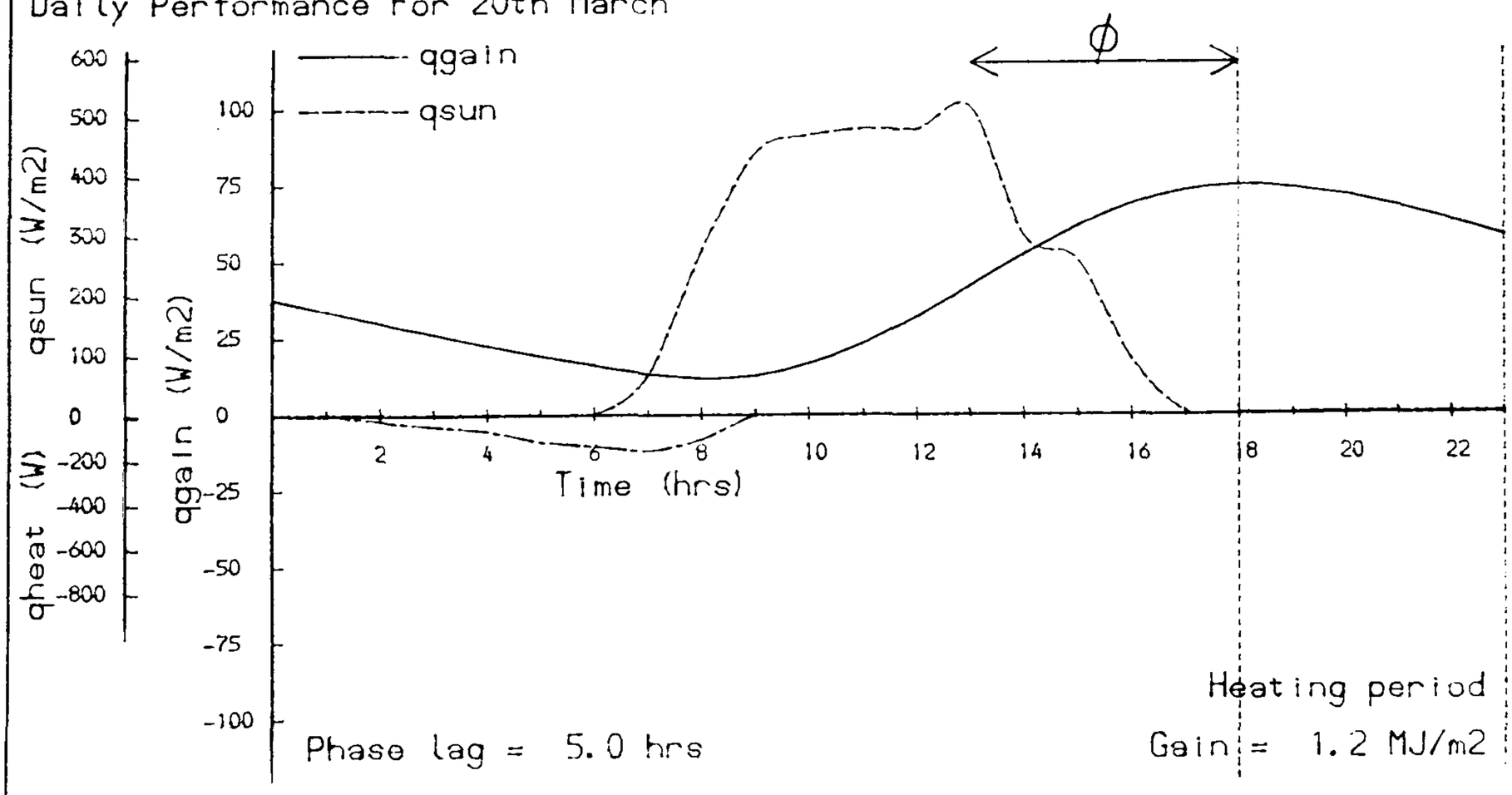

Fig 9.11 - SOLID BRICK WALL: HEAT MIRROR GLAZED

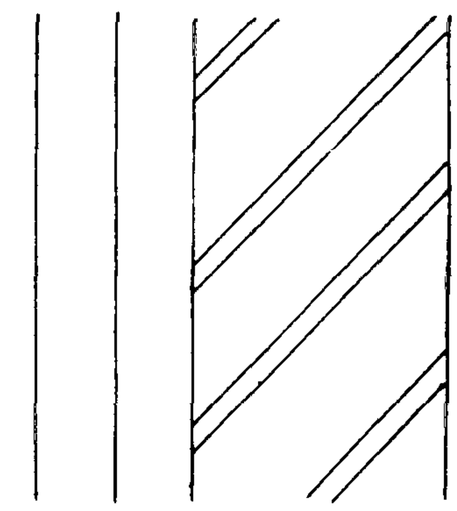

BLACK SURFACE

Surface Absorptivity	0.90
Angle to South	0° south
Transmittance	1.06 W/m2K
Admittance Parameters	
Thermal Admittance Y	4.78 W/m2K
Time Lead of Y	1.31 hrs
Decrement Factor	0.22
Time Lag of D.F	-8.54 hrs
Surface Factor	0.49
Time Lag of S.F	-1.59 hrs

Monthly Gains to Room (MJ/m2)

Month	1	2	3	4	5	6	7	8	9	10	11	12
Rad gain Full Day	16.6	68.3	62.1	76.2	52.1	54.0	51.8	64.0	79.2	67.3	48.8	5.4
Conv gain Full Day	0.0	0.0	0.0	0.0	0.0	0.0	0.0	0.0	0.0	0.0	0.0	0.0
Net gain Full Day	16.6	68.3	62.1	76.2	52.1	54.0	51.8	64.0	79.2	67.3	48.8	5.4
Net gain 1800-2300	6.7	20.1	18.7	22.2	15.6	15.6	15.0	18.2	22.2	19.2	14.8	3.3
Steady State With TEO	5.8	54.3	52.7	83.1	77.4	94.1	82.4	78.0	75.8	54.3	36.4	-3.0

Daily Performance For 20th March

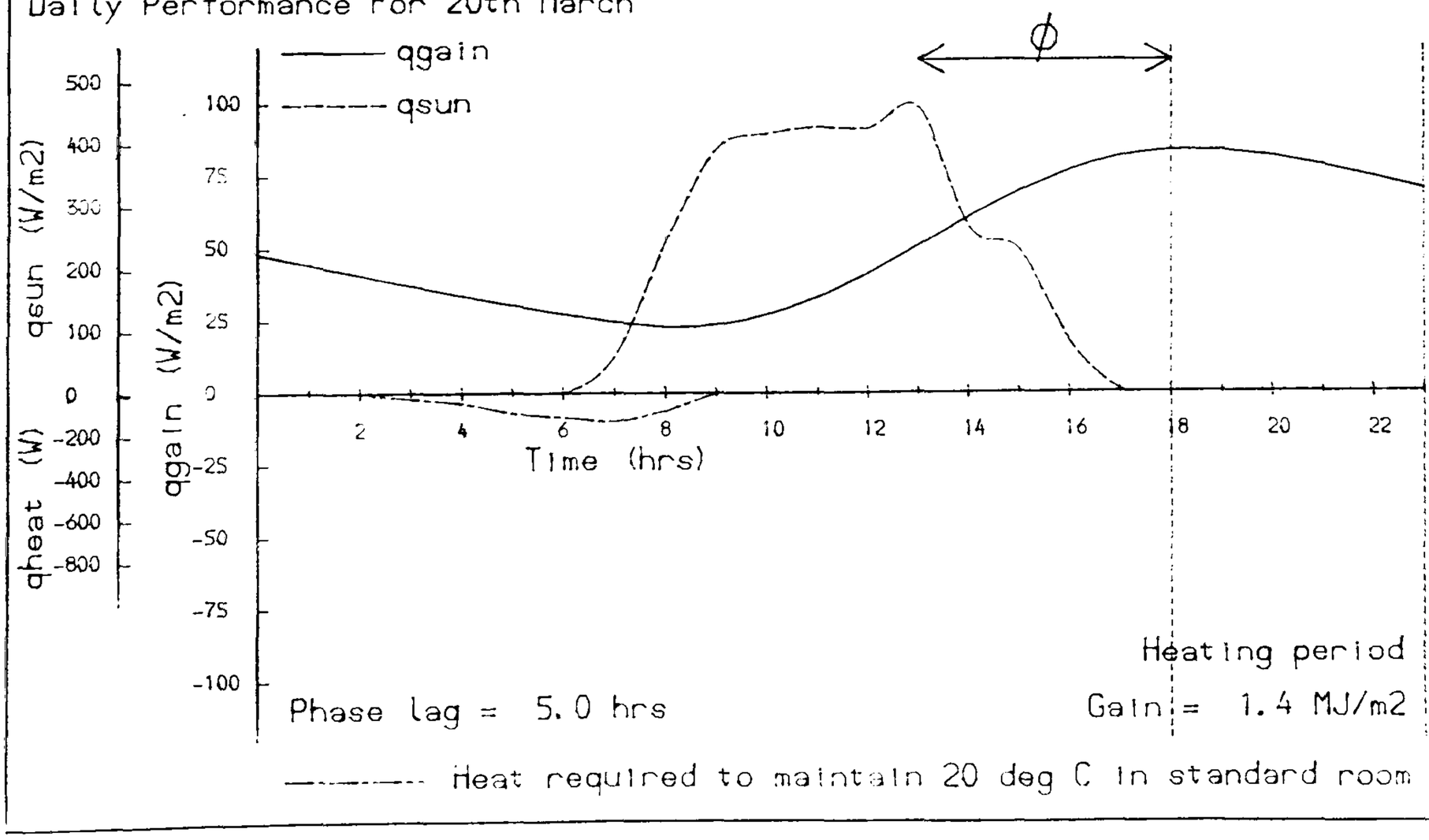

Fig 9.12 - SOLID BRICK WALL: INSIDE INSULATION

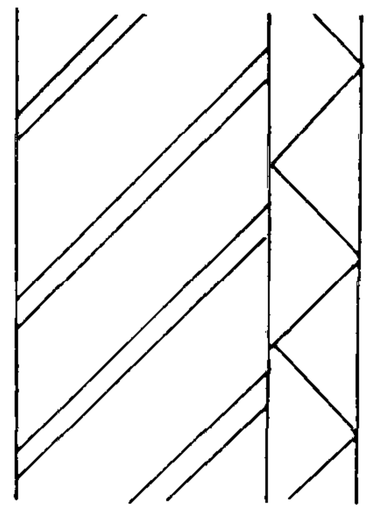

Surface Absorptivity	0.70
Angle to South	0° south
Transmittance	0.41 W/m2K
Admittance Parameters	
Thermal Admittance Y	0.46 W/m2K
Time Lead of Y	0.59 hrs
Decrement Factor	0.24
Time Lag of D.F	-8.47 hrs
Surface Factor	0.94
Time Lag of S.F	-0.04 hrs

Monthly Gains to Room (MJ/m2)

Month	1	2	3	4	5	6	7	8	9	10	11	12
Rad gain Full Day	-12.4	-8.5	-9.3	-6.3	-4.9	-1.3	-1.2	-1.5	-2.6	-5.7	-8.4	-11.1
Conv gain Full Day	0.0	0.0	0.0	0.0	0.0	0.0	0.0	0.0	0.0	0.0	0.0	0.0
Net gain Full Day	-12.4	-8.5	-9.3	-6.3	-4.9	-1.3	-1.2	-1.5	-2.6	-5.7	-8.4	-11.1
Net gain 1800-2300	-2.4	-1.4	-1.5	-0.8	-0.5	0.2	0.2	0.1	-0.1	-0.9	-1.5	-2.2
Steady State With TEO	-12.6	-8.4	-9.2	-6.3	-4.9	-1.3	-1.2	-1.4	-2.7	-5.8	-8.4	-11.2

Daily Performance For 20th March

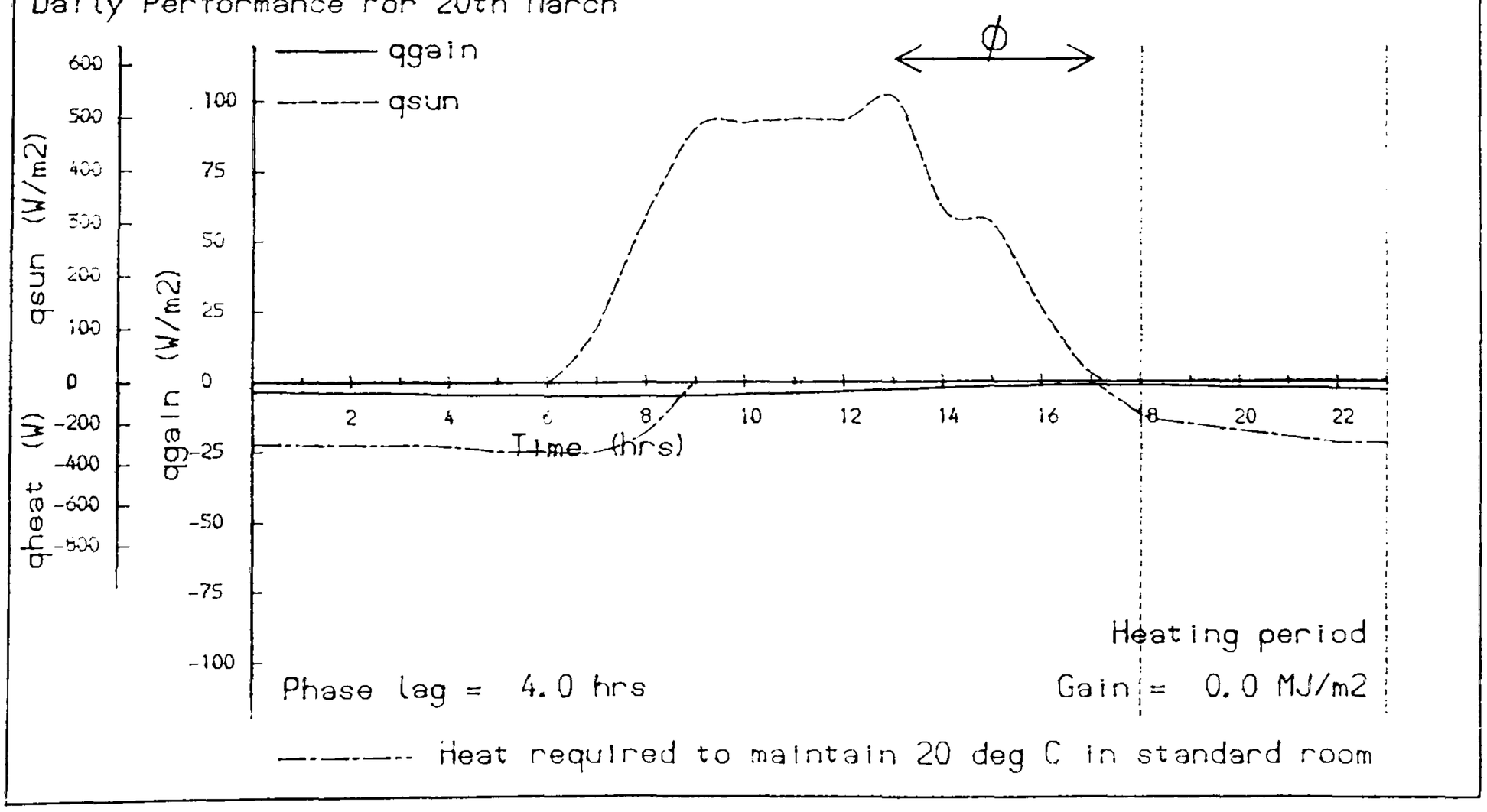

Fig 9.13 – SOLID BRICK WALL: OUTSIDE INSULATION

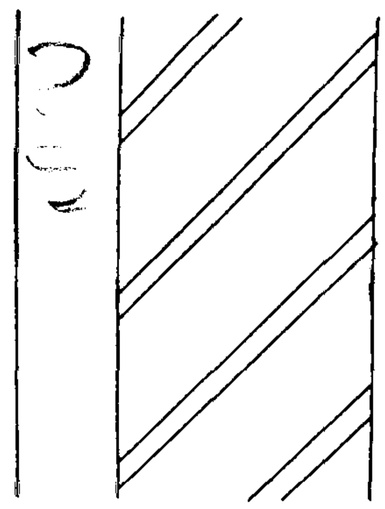

Surface Absorptivity	0.70
Angle to South	0° south
Transmittance	0.41 W/m2K
Admittance Parameters	
Thermal Admittance Y	4.78 W/m2K
Time Lead of Y	1.29 hrs
Decrement Factor	0.16
Time Lag of D.F	-9.12 hrs
Surface Factor	0.49
Time Lag of S.F	-1.57 hrs

Monthly Gains to Room (MJ/m2)

Month	1	2	3	4	5	6	7	8	9	10	11	12
Rad gain Full Day	-23.0	-19.2	-21.2	-18.9	-18.7	-16.1	-16.6	-16.8	-16.9	-19.2	-20.3	-22.5
Conv gain Full Day	0.0	0.0	0.0	0.0	0.0	0.0	0.0	0.0	0.0	0.0	0.0	0.0
Net gain Full Day	-23.0	-19.2	-21.2	-18.9	-18.7	-16.1	-16.6	-16.8	-16.9	-19.2	-20.3	-22.5
Net gain 1800-2300	-4.7	-3.8	-4.1	-3.6	-3.6	-3.0	-3.2	-3.2	-3.2	-3.8	-4.1	-4.6
Steady State With TEO	-12.6	-8.4	-9.2	-6.3	-4.9	-1.3	-1.2	-1.4	-2.7	-5.8	-8.4	-11.2

Daily Performance For 20th March

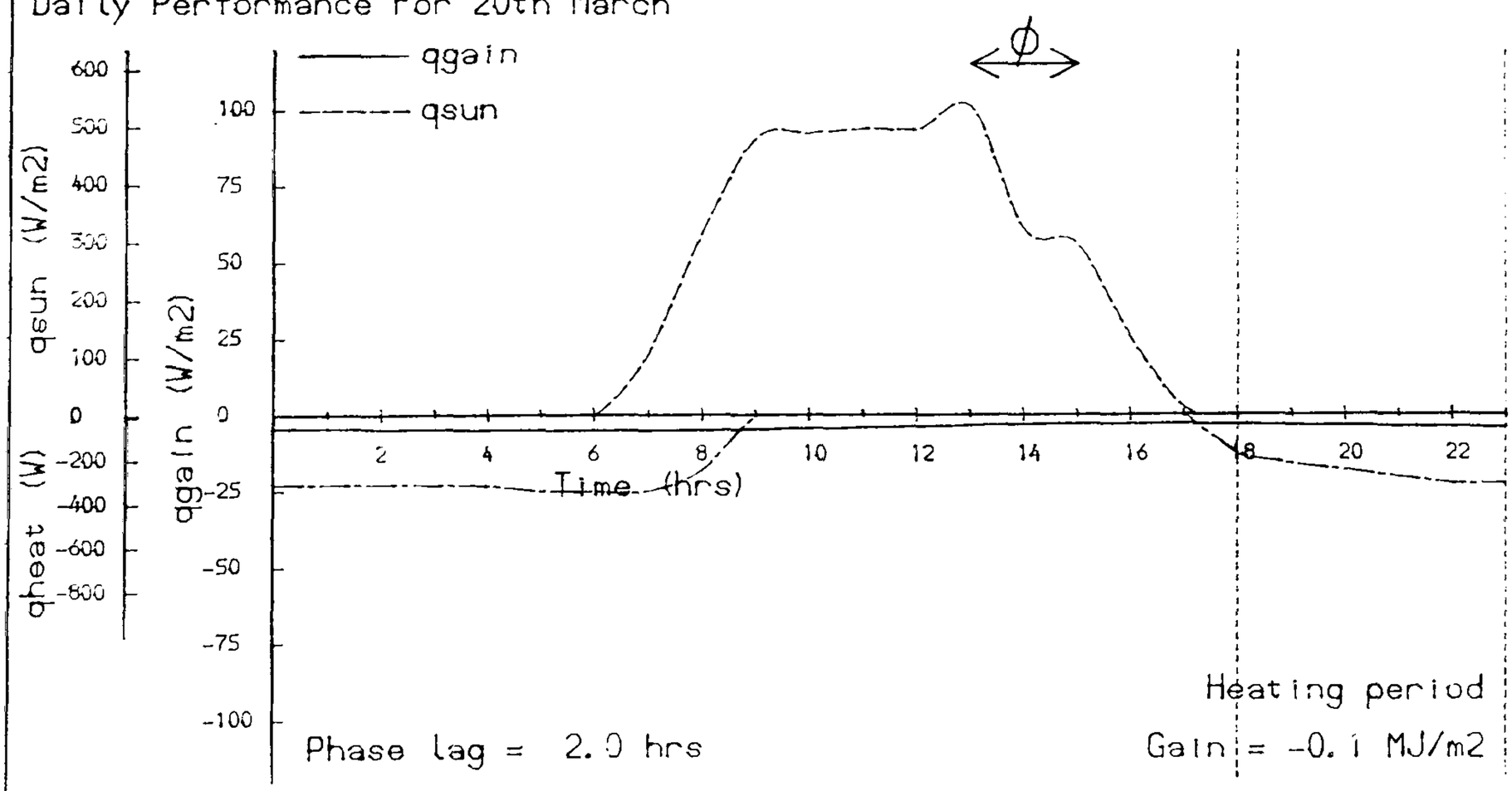

Fig 9.14 - CAVITY BRICK WALL. UNGLAZED

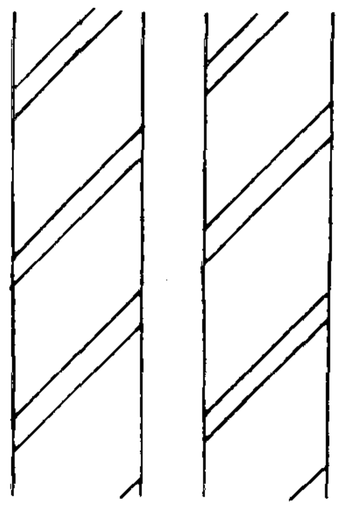

Surface Absorptivity	0.70
Angle to South	0° south
Transmittance	1.57 W/m2K
Admittance Parameters	
Thermal Admittance Y	4.88 W/m2K
Time Lead of Y	1.62 hrs
Decrement Factor	0.39
Time Lag of D.F	-8.19 hrs
Surface Factor	0.52
Time Lag of S.F	-1.91 hrs

Monthly Gains to Room (MJ/m2)

Month	1	2	3	4	5	6	7	8	9	10	11	12
Rad gain Full Day	-46.9	-31.0	-33.9	-21.9	-16.9	-3.0	-2.8	-3.9	-8.2	-20.4	-31.0	-42.2
Conv gain Full Day	0.0	0.0	0.0	0.0	0.0	0.0	0.0	0.0	0.0	0.0	0.0	0.0
Net gain Full Day	-46.9	-31.0	-33.9	-21.9	-16.9	-3.0	-2.8	-3.9	-8.2	-20.4	-31.0	-42.2
Net gain 1800-2300	-8.7	-4.3	-4.7	-1.6	-0.8	2.2	1.8	1.5	0.8	-2.2	-4.8	-7.9
Steady State With TEO	-48.8	-32.7	-35.7	-24.3	-18.9	-5.1	-4.7	-5.5	-10.3	-22.5	-32.6	-43.4

Daily Performance For 20th March

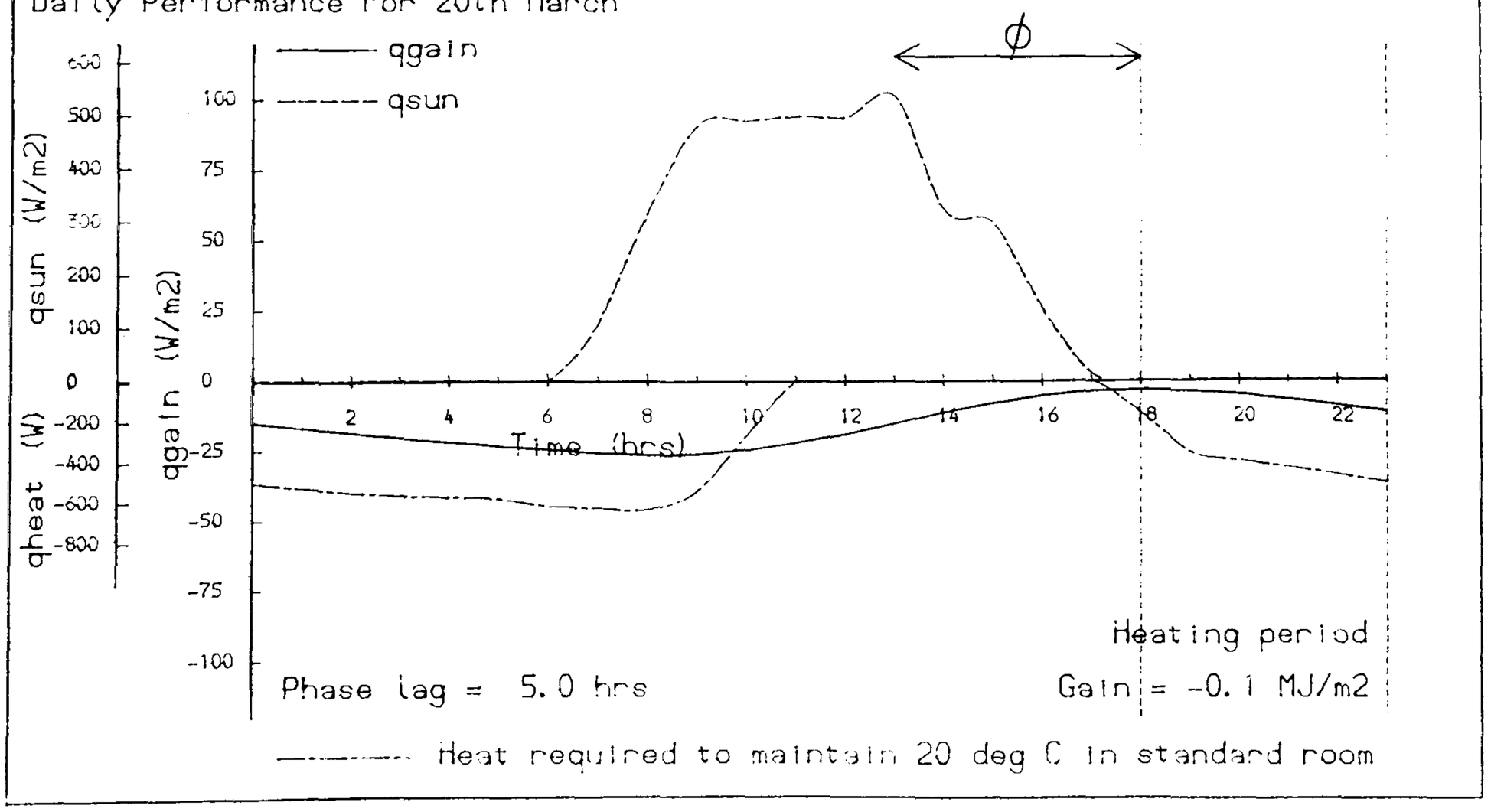

Fig 9.15- CAVITY BRICK WALL: UNGLAZED

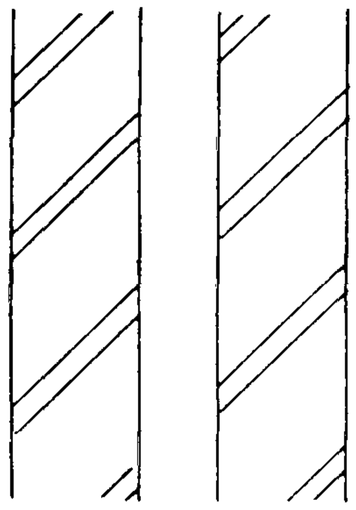

Surface Absorptivity	0.70
Angle to South	180° north
Transmittance	1.57 W/m2K
Admittance Parameters	
Thermal Admittance Y	4.88 W/m2K
Time Lead of Y	1.62 hrs
Decrement Factor	0.39
Time Lag of D.F	-8.19 hrs
Surface Factor	0.52
Time Lag of S.F	-1.91 hrs

Monthly Gains to Room (MJ/m2)

Month	1	2	3	4	5	6	7	8	9	10	11	12
Rad gain Full Day	-53.9	-45.1	-45.6	-34.6	-24.7	-10.7	-9.1	-12.3	-20.6	-32.3	-41.9	-46.9
Conv gain Full Day	0.0	0.0	0.0	0.0	0.0	0.0	0.0	0.0	0.0	0.0	0.0	0.0
Net gain Full Day	-53.9	-45.1	-45.6	-34.6	-24.7	-10.7	-9.1	-12.3	-20.6	-32.3	-41.9	-46.9
Net gain 1800-2300	-10.9	-8.6	-8.4	-5.6	-3.3	-0.3	-0.3	-1.2	-3.1	-6.0	-8.2	-9.4
Steady State With TEO	-55.2	-45.5	-46.4	-35.9	-26.1	-12.1	-10.5	-13.3	-21.5	-33.2	-42.7	-47.7

Daily Performance For 20th March

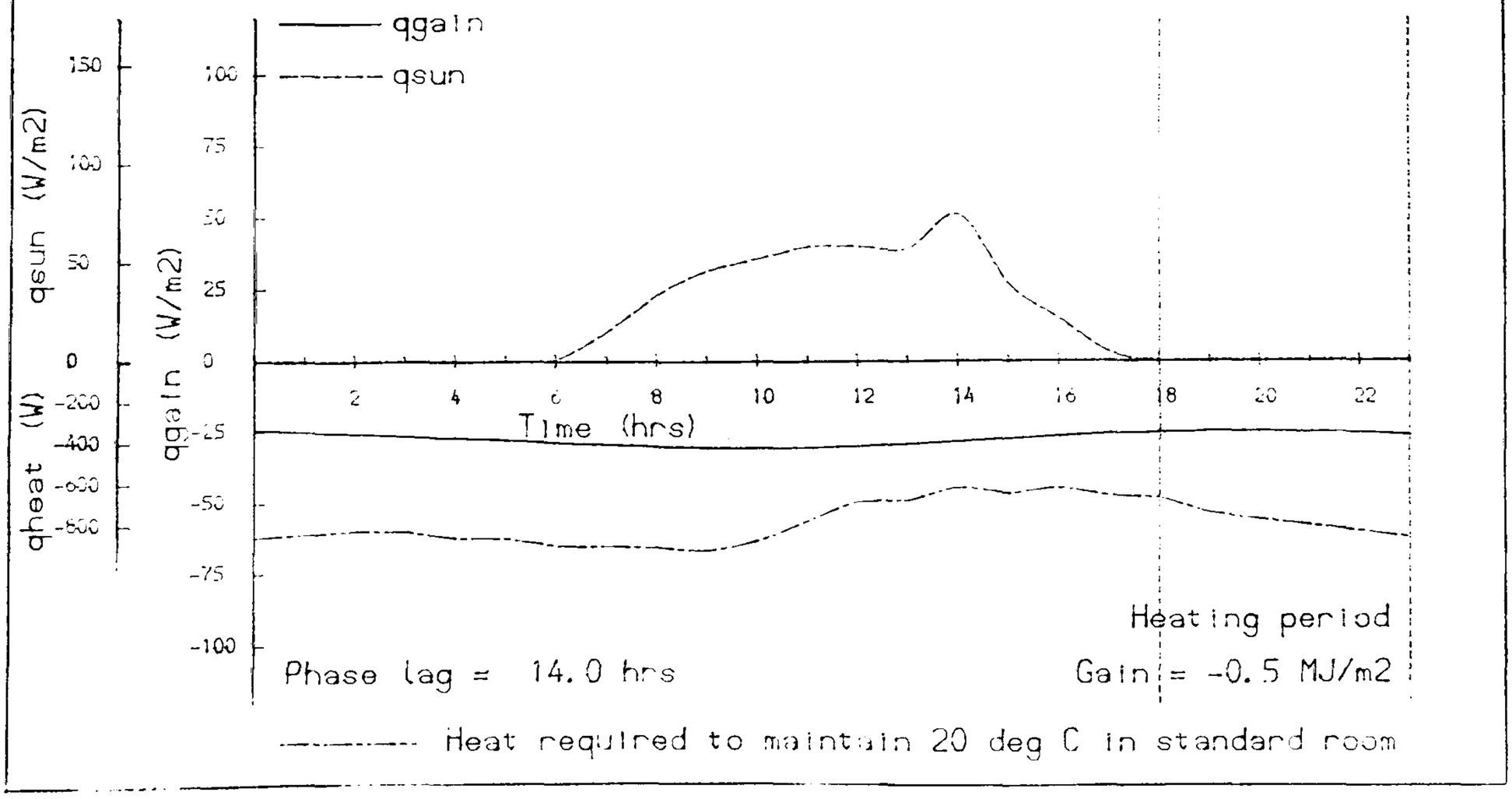

Fig.9.16 - CAVITY BRICK WALL: CAVITY INSULATION

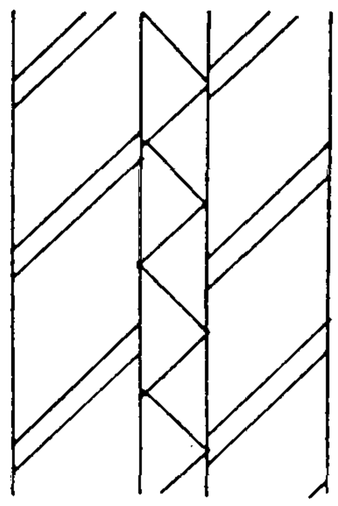

Surface Absorptivity	0.70
Angle to South	0° south
Transmittance	0.41 W/m2K
Admittance Parameters	
Thermal Admittance Y	5.20 W/m2K
Time Lead of Y	1.71 hrs
Decrement Factor	0.27
Time Lag of D.F	-9.86 hrs
Surface Factor	0.51
Time Lag of S.F	-2.22 hrs

Monthly Gains to Room (MJ/m2)

Month	1	2	3	4	5	6	7	8	9	10	11	12
Rad gain Full Day	-10.9	-7.2	-7.9	-5.1	-3.9	-0.7	-0.7	-0.9	-1.9	-4.7	-7.2	-9.8
Conv gain Full Day	0.0	0.0	0.0	0.0	0.0	0.0	0.0	0.0	0.0	0.0	0.0	0.0
Net gain Full Day	-10.9	-7.2	-7.9	-5.1	-3.9	-0.7	-0.7	-0.9	-1.9	-4.7	-7.2	-9.8
Net gain 1800-2300	-2.1	-1.1	-1.2	-0.5	-0.3	0.3	0.3	0.2	0.0	-0.6	-1.2	-1.9
Steady State With TEO	-12.6	-8.5	-9.2	-6.3	-4.9	-1.3	-1.2	-1.4	-2.7	-5.8	-8.4	-11.2

Daily Performance For 20th March

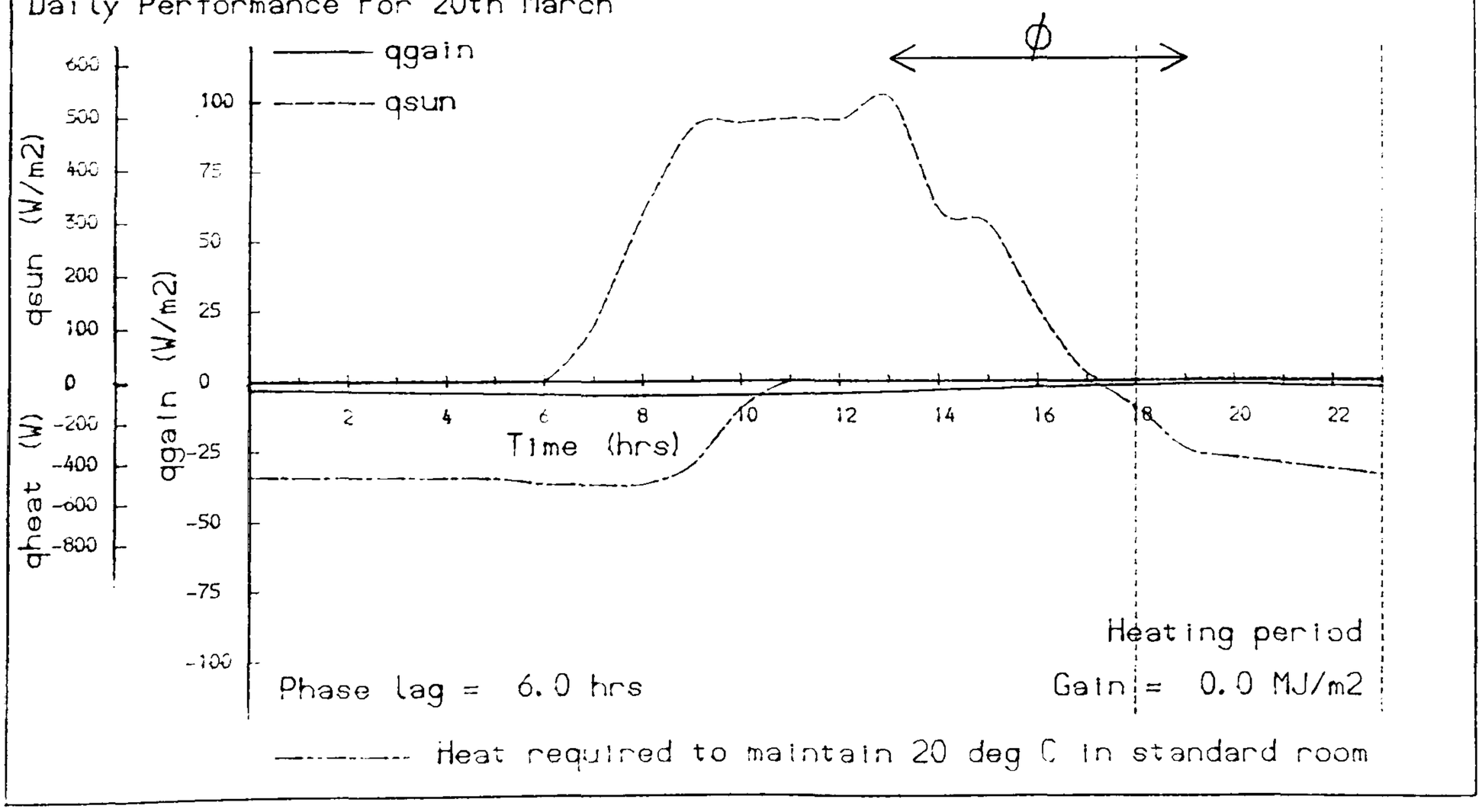

Fig 9.17 - CAVITY BRICK WALL: SINGLE GLAZED

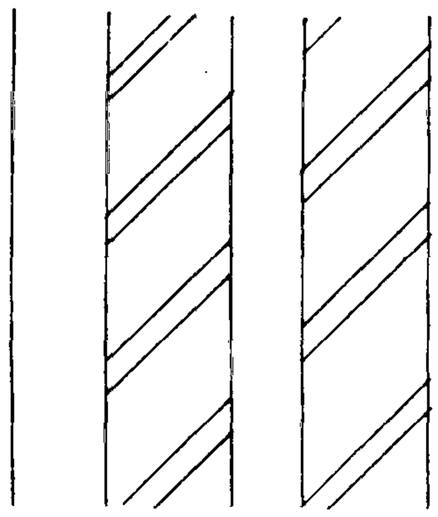

Surface Absorptivity	0.70
Angle to South	0° south
Transmittance	1.26 W/m2K
Admittance Parameters	
Thermal Admittance Y	4.87 W/m2K
Time Lead of Y	1.60 hrs
Decrement Factor	0.24
Time Lag of D.F	-9.50 hrs
Surface Factor	0.51
Time Lag of S.F	-1.89 hrs

Monthly Gains to Room (MJ/m2)

Month	1	2	3	4	5	6	7	8	9	10	11	12
Rad gain Full Day	-19.9	8.8	4.9	17.0	9.8	18.2	17.6	22.2	26.1	14.3	1.3	-21.7
Conv gain Full Day	0.0	0.0	0.0	0.0	0.0	0.0	0.0	0.0	0.0	0.0	0.0	0.0
Net gain Full Day	-19.9	8.8	4.9	17.0	9.8	18.2	17.6	22.2	26.1	14.3	1.3	-21.7
Net gain 1800-2300	-2.2	5.6	4.7	7.8	5.4	7.0	6.6	8.0	9.2	6.3	3.2	-3.1
Steady State With TEO	-23.1	5.3	3.1	21.6	22.0	36.2	31.5	29.3	25.9	10.7	-2.0	-23.9

Daily Performance For 20th March

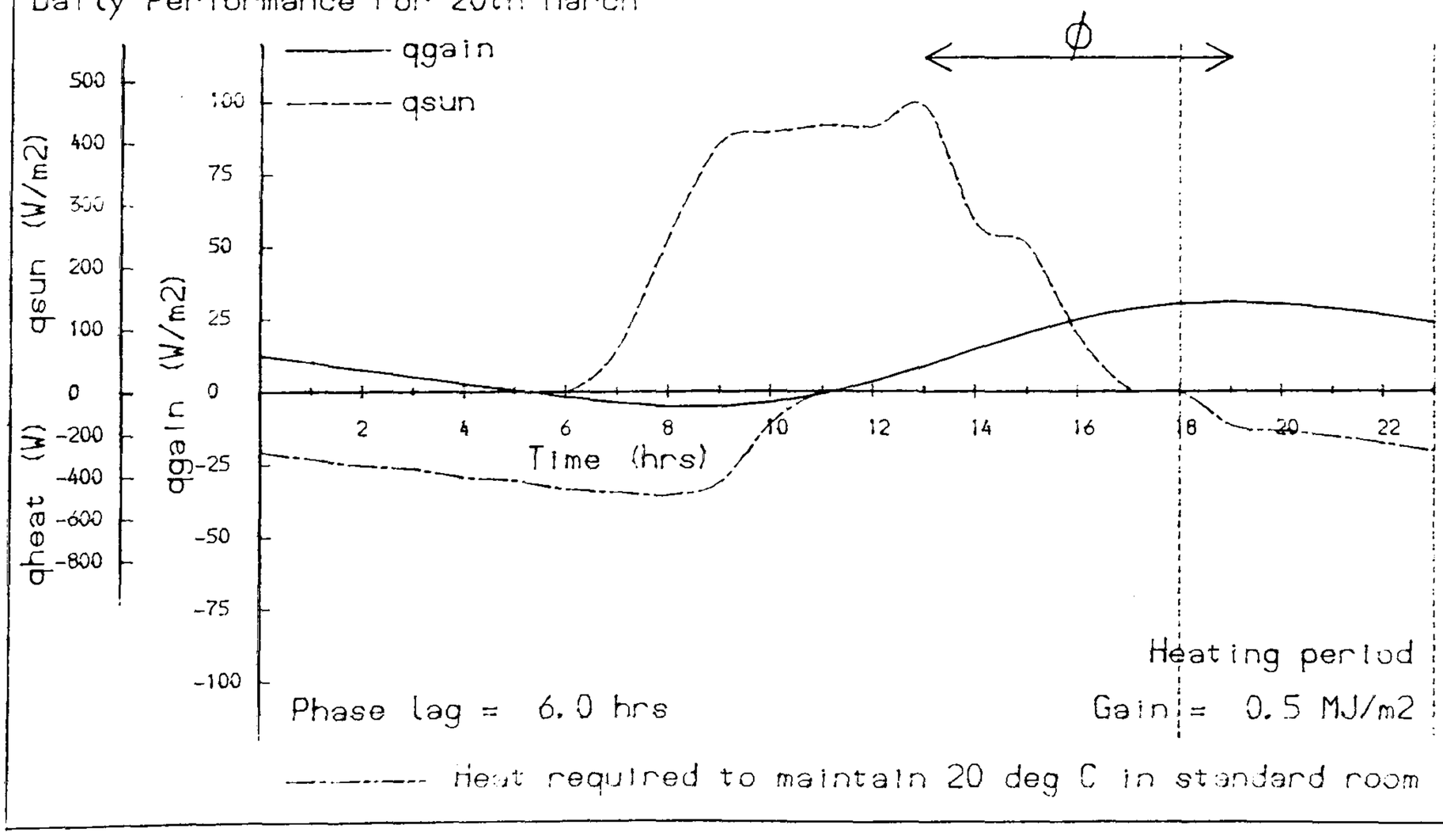

Fig 9.18 – CAVITY BRICK WALL. SINGLE GLAZED AIR

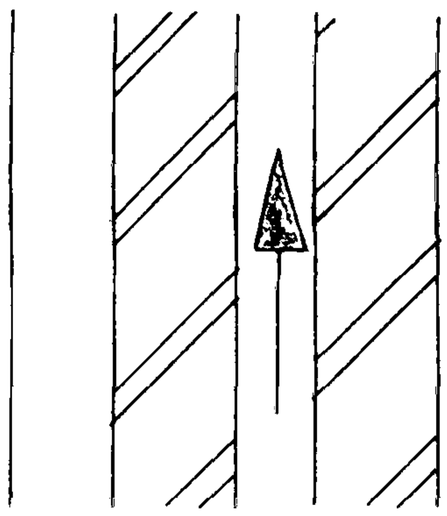

FORCED CONVECTION

Surface Absorptivity	0.70
Angle to South	0° south
Transmittance	1.26 W/m2K
Admittance Parameters	
Thermal Admittance Y	4.87 W/m2K
Time Lead of Y	1.60 hrs
Decrement Factor	0.24
Time Lag of D.F	-9.50 hrs
Surface Factor	0.51
Time Lag of S.F	-1.89 hrs

Monthly Gains to Room (MJ/m2) Convection collector area = 4.0 m2

Month	1	2	3	4	5	6	7	8	9	10	11	12
Rad gain Full Day	-13.6	5.9	2.5	9.5	5.7	10.2	9.7	12.5	14.1	8.0	0.8	-15.5
Conv gain Full Day	4.6	22.9	22.4	31.7	21.8	26.6	25.7	30.4	35.6	25.6	15.9	2.9
Net gain Full Day	-9.0	28.8	24.9	41.2	27.5	36.8	35.4	42.9	49.7	33.6	16.7	-12.6
Net gain 1800-2300	4.0	26.6	25.5	36.3	25.1	30.5	29.3	34.6	40.4	29.3	18.2	1.4
Steady State With TEO	-23.1	5.3	3.1	21.6	22.0	36.2	31.5	29.3	25.9	10.7	-2.0	-23.9

Daily Performance For 20th March

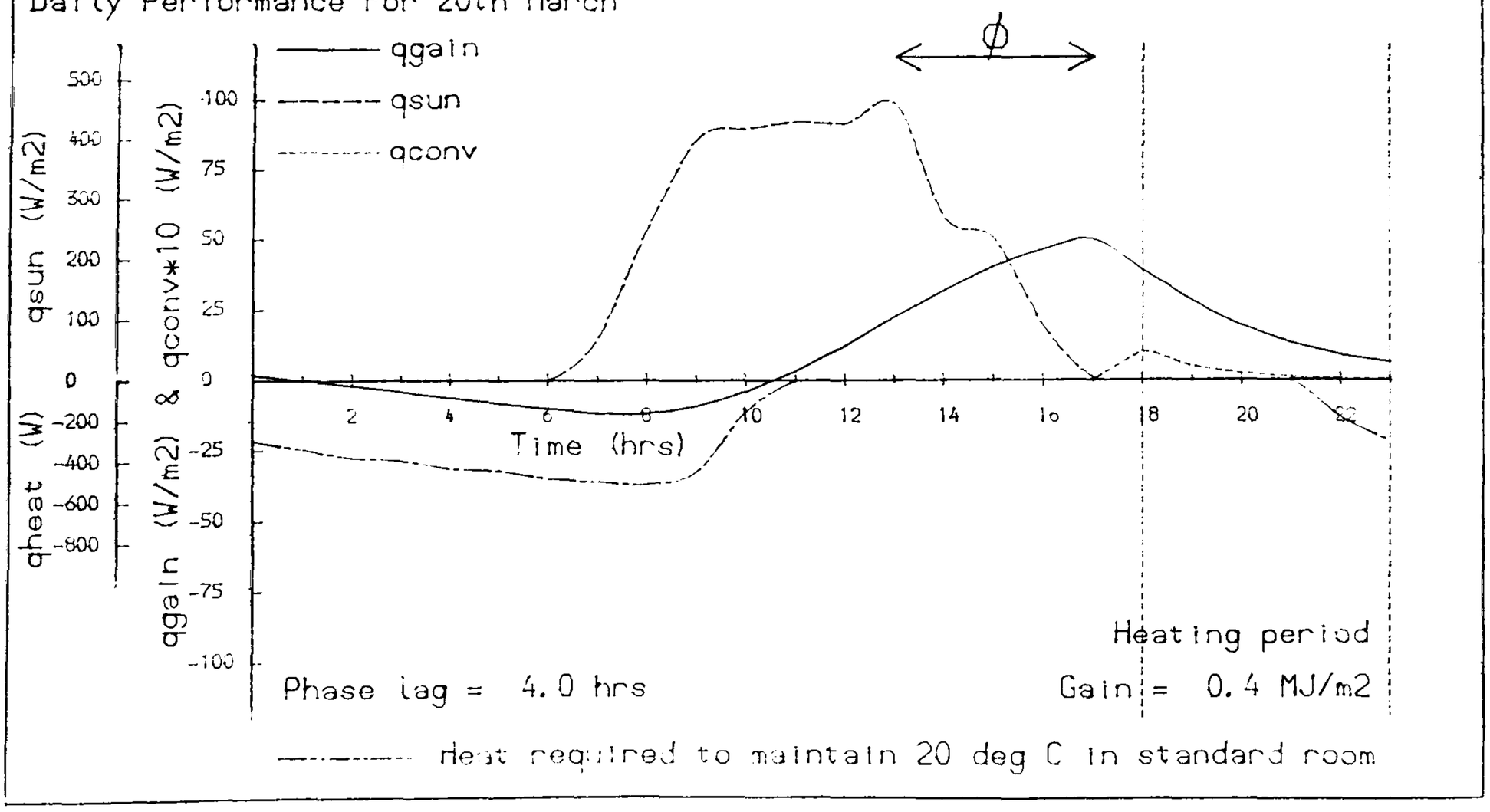

Fig 9.19 – CAVITY BRICK WALL: HEAT MIRROR GLAZED AIR

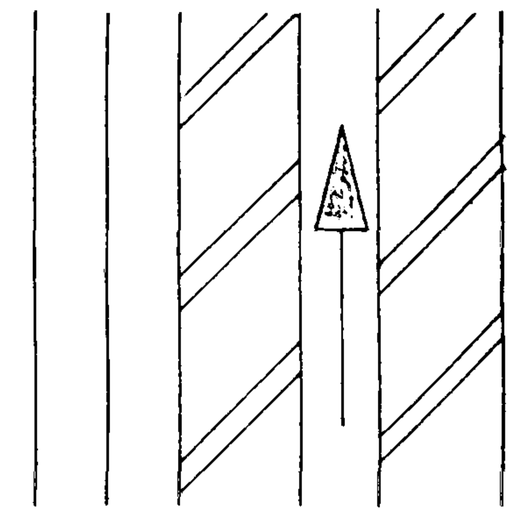

FORCED CONVECTION
BLACK SURFACE

Surface Absorptivity	0.90
Angle to South	0° south
Transmittance	0.89 W/m2K
Admittance Parameters	
Thermal Admittance Y	4.86 W/m2K
Time Lead of Y	1.59 hrs
Decrement Factor	0.16
Time Lag of D.F	-10.11 hrs
Surface Factor	0.51
Time Lag of S.F	-1.87 hrs

Monthly Gains to Room (MJ/m2) Convection collector area = 4.0 m2

Month	1	2	3	4	5	6	7	8	9	10	11	12
Rad gain Full Day	5.6	27.0	23.5	29.0	20.0	20.8	19.9	24.8	29.9	25.5	19.0	0.9
Conv gain Full Day	24.6	63.7	60.4	70.8	49.5	48.6	47.2	57.5	69.9	60.5	47.6	14.7
Net gain Full Day	30.2	90.7	83.9	99.8	69.5	69.4	67.1	82.3	99.8	86.0	66.6	15.6
Net gain 1800-2300	27.3	71.0	67.1	78.7	55.2	54.2	52.5	63.9	77.6	67.3	53.1	16.1
Steady State With TEO	4.8	45.6	44.3	69.9	65.1	79.2	69.3	65.6	63.8	45.6	30.7	-2.5

Daily Performance For 20th March

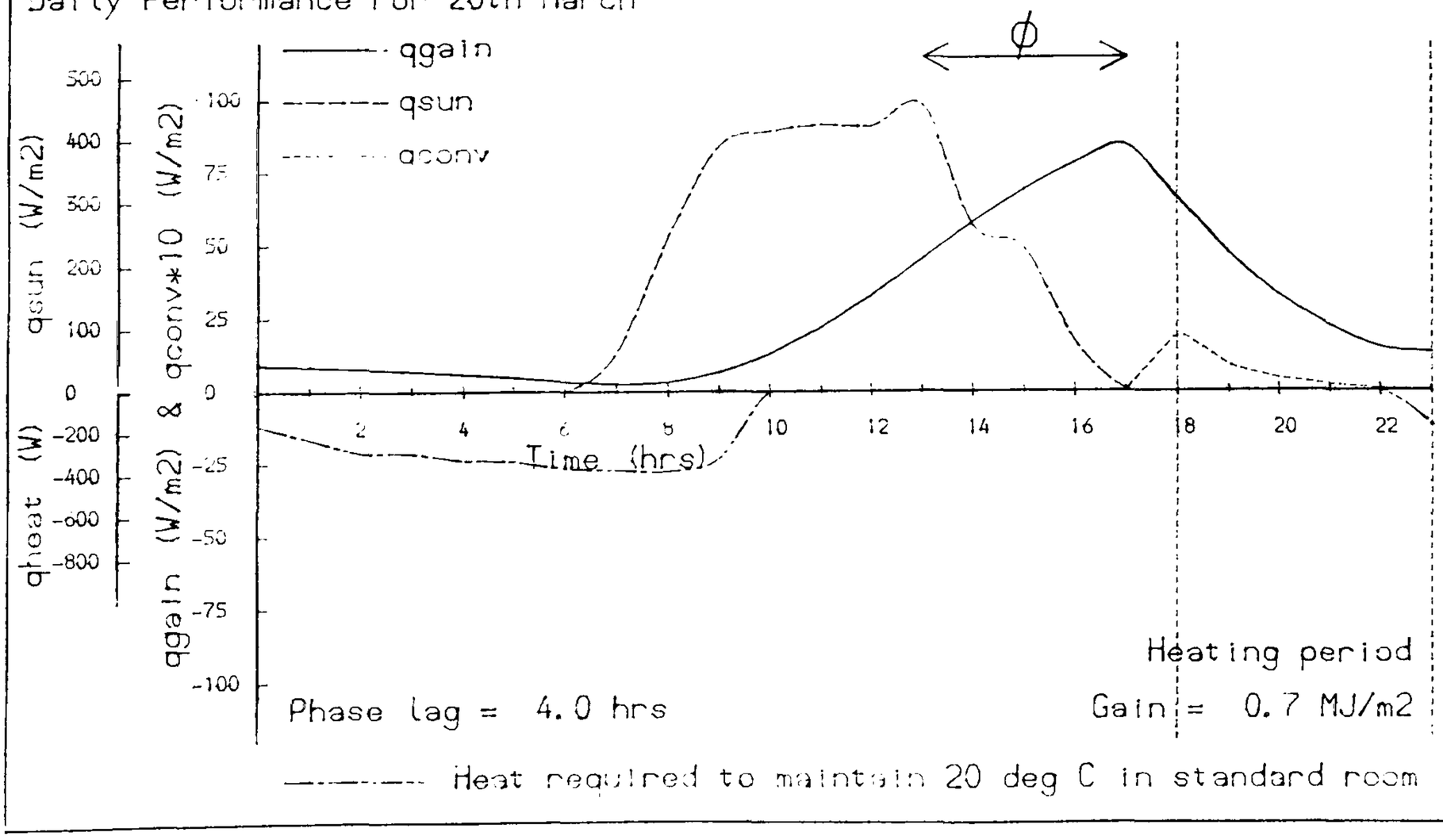

Fig 9.20 - SOLID BRICK WALL: SINGLE GLAZED AIR

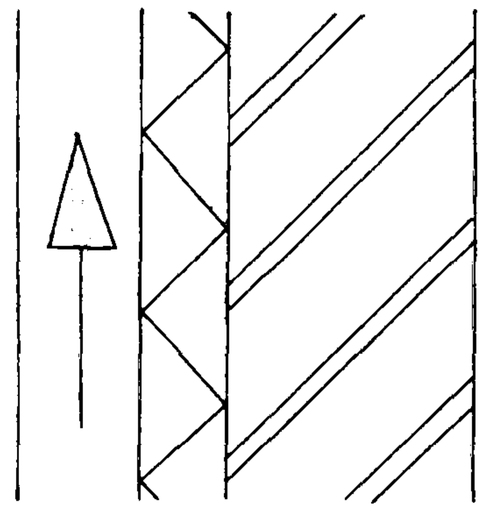

NATURAL CONVECTION
SELECTIVE SURFACE

Surface Absorptivity	0.90 Selective
Angle to South	0° south
Transmittance	0.37 W/m2K
Admittance Parameters	
Thermal Admittance Y	4.77 W/m2K
Time Lead of Y	1.29 hrs
Decrement Factor	0.16
Time Lag of D.F	-9.19 hrs
Surface Factor	0.49
Time Lag of S.F	-1.57 hrs

Monthly Gains to Room (MJ/m2) Convection collector area = 4.0 m2

Month	1	2	3	4	5	6	7	8	9	10	11	12
Rad gain Full Day	-20.4	-17.0	-19.3	-16.7	-16.5	-14.1	-14.4	-14.5	-14.6	-17.0	-18.1	-19.9
Conv gain Full Day	22.2	74.3	72.0	106.4	91.5	0.0	0.0	0.0	103.6	77.2	59.8	18.9
Net gain Full Day	1.8	57.3	52.7	89.7	75.0	-14.1	-14.4	-14.5	89.0	60.2	41.7	-1.0
Net gain 1800-2300	0.0	0.0	0.0	0.0	0.0	0.0	0.0	0.0	0.0	0.0	0.0	0.0
Steady State With TEO	-0.5	13.9	13.4	22.5	21.1	26.4	23.1	21.8	21.0	14.4	8.9	-2.7

Daily Performance For 20th March

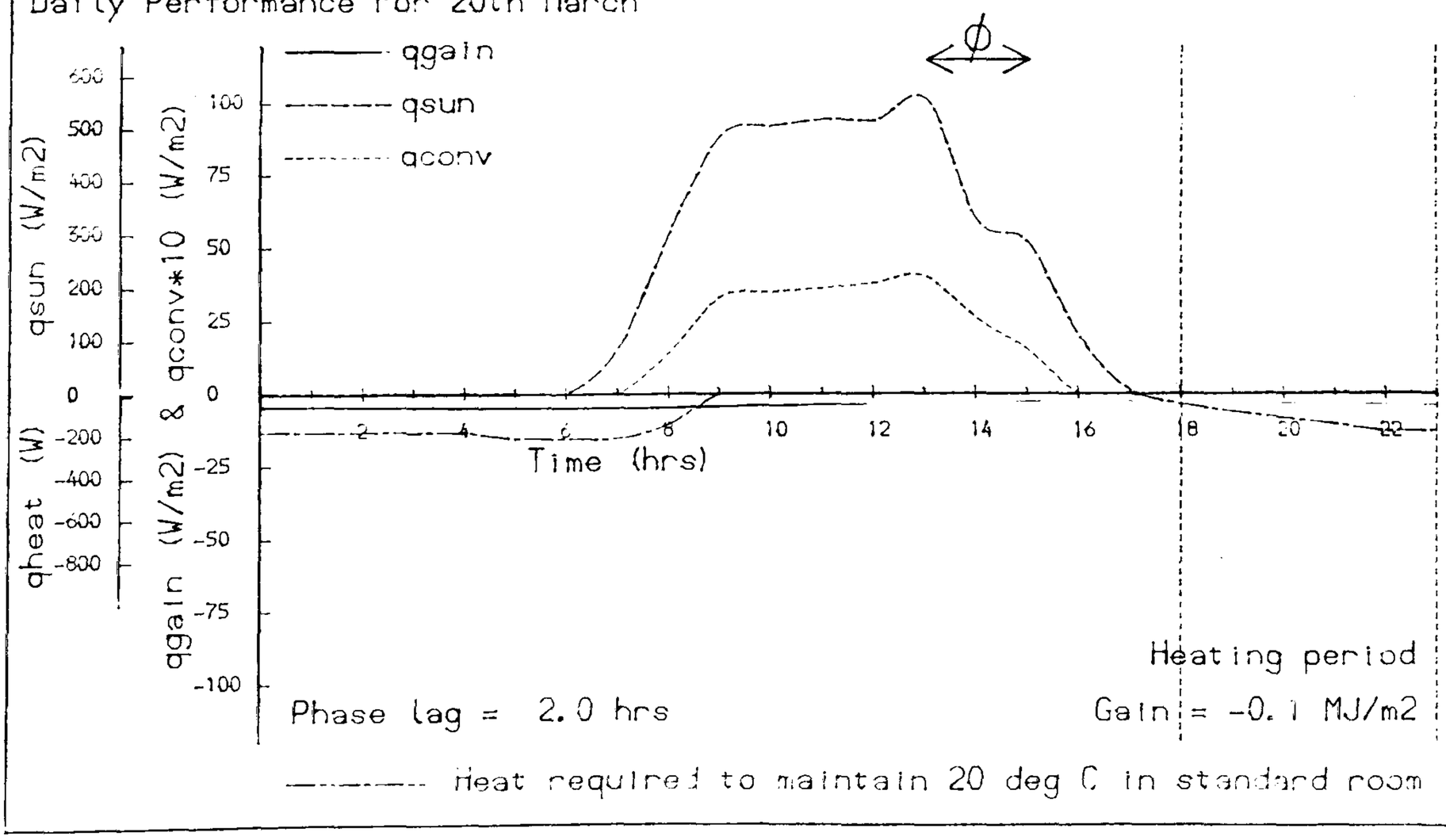

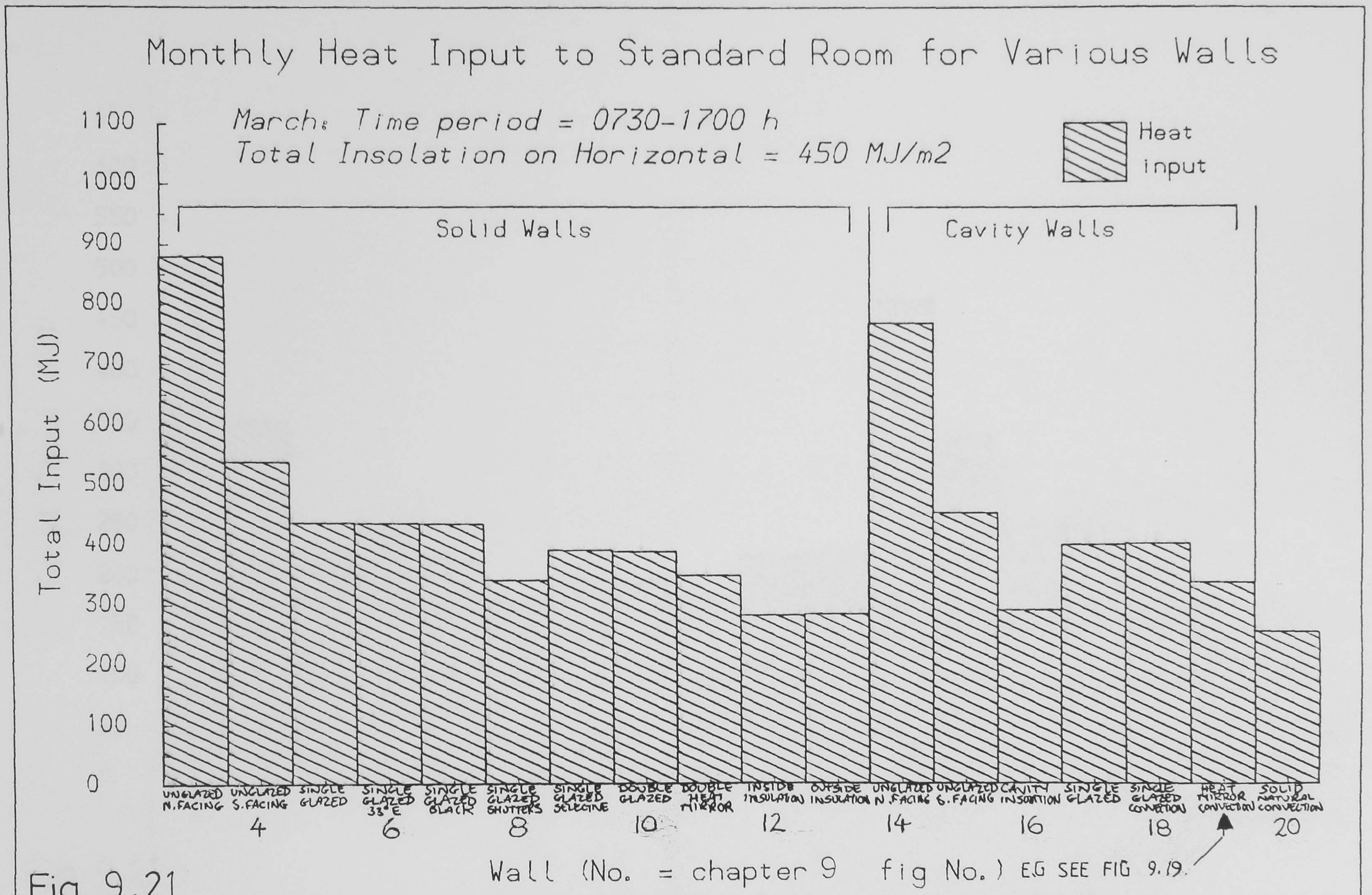
Monthly Heat Input to Standard Room for Various Walls
March: Time period = 0730-1700 h
Total Insolation on Horizontal = 450 MJ/m2
Heat input
Solid Walls
Cavity Walls
Total Input (MJ)
1100
1000
900
800
700
600
500
400
300
200
100
0
UNGLAZED N.FACING
UNGLAZED S.FACING
SINGLE GLAZED
SINGLE GLAZED 33° E
SINGLE GLAZED BLACK
SINGLE GLAZED SHUTTERS
SINGLE GLAZED SELECTIVE
DOUBLE GLAZED
DOUBLE HEAT MIRROR
INSIDE INSULATION
OUTSIDE INSULATION
UNGLAZED N.FACING
UNGLAZED S.FACING
CAVITY INSULATION
SINGLE GLAZED
SINGLE GLAZED CONVECTION
HEAT MIRROR CONVECTION
SOLID NATURAL CONVECTION
4
6
8
10
12
14
16
18
20
Wall (No. = chapter 9 fig No.) EG SEE FIG 9.19

Fig 9.21

Monthly Heat Input to Standard Room for Various Walls

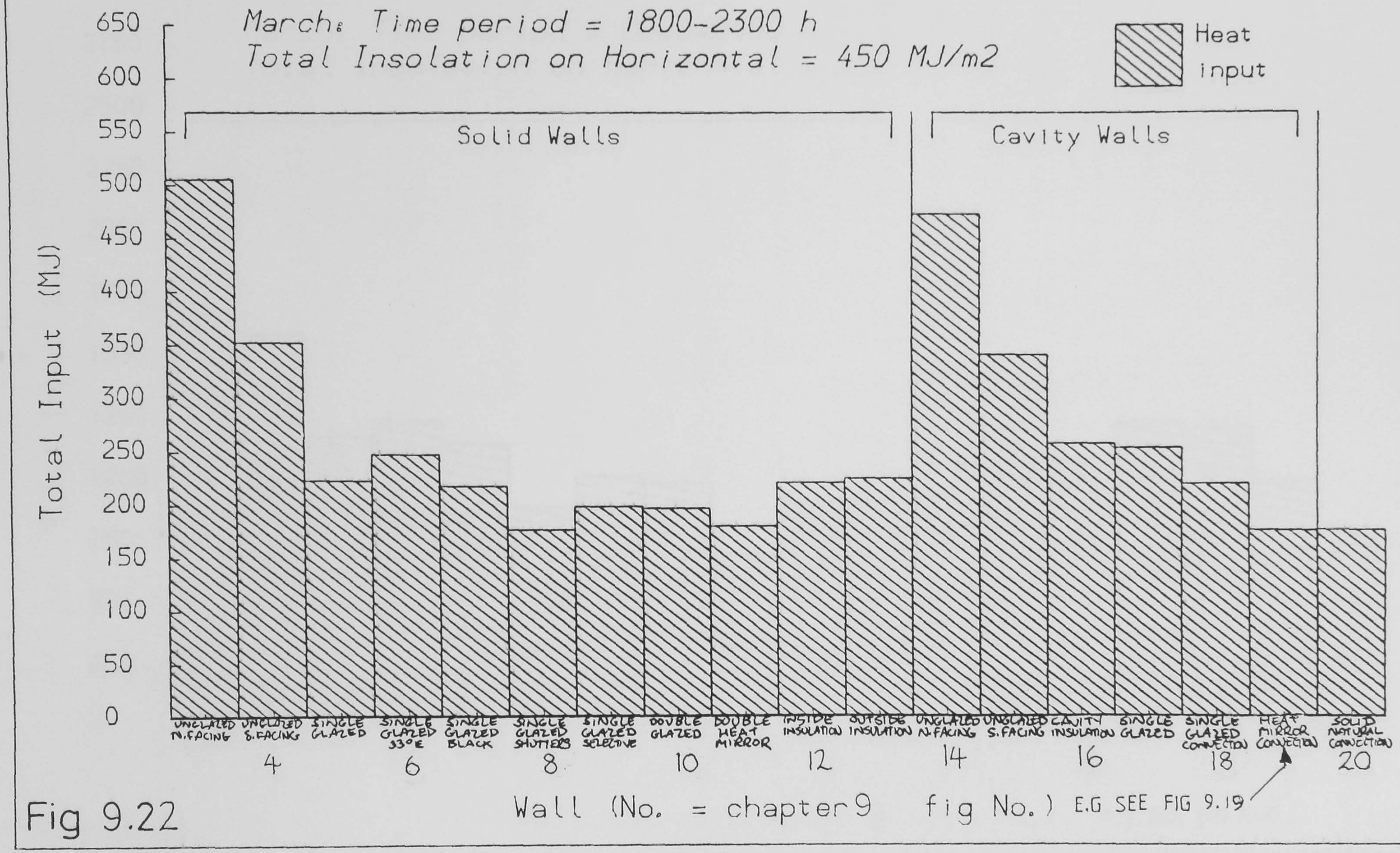

Fig 9.22

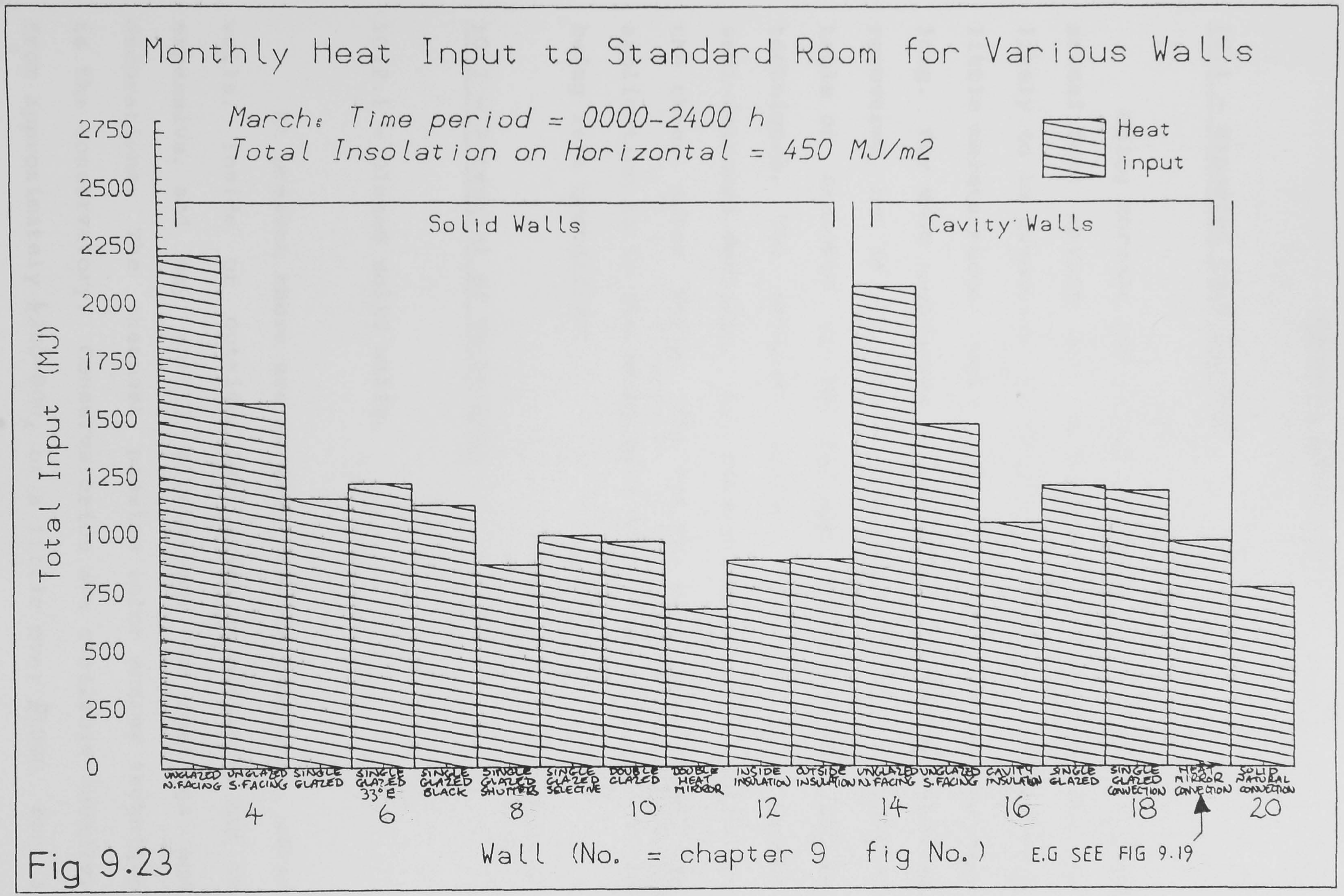
Monthly Heat Input to Standard Room for Various Walls
March: Time period = 0000-2400 h
Total Insolation on Horizontal = 450 MJ/m2
Heat input
Solid Walls
Cavity Walls
Total Input (MJ)
2750
2500
2250
2000
1750
1500
1250
1000
750
500
250
0
UNGLAZED N.FACING
UNGLAZED S.FACING
SINGLE GLAZED
SINGLE GLAZED 33° E
SINGLE GLAZED BLACK
SINGLE GLAZED SHUTTERS
SINGLE GLAZED SELECTIVE
DOUBLE GLAZED
DOUBLE HEAT MIRROR
INSIDE INSULATION
OUTSIDE INSULATION
UNGLAZED N.FACING
UNGLAZED S.FACING
CAVITY INSULATION
SINGLE GLAZED
SINGLE GLAZED CONVECTION
HEAT MIRROR CONVECTION
SOLID NATURAL CONVECTION
4
6
8
10
12
14
16
18
20
Wall (No. = chapter 9 fig No.)
E.G SEE FIG 9.19

Fig 9.23

Chapter 10

General Conclusions

10.1 - Expected Cost Savings

Using current gas prices an estimate of the expected annual fuel saving can be made. The techniques used are likely to be expensive in capital, but will have very little maintainance costs, and the lifetime will be very long. For most techniques, the original investment will be recovered, but it may take a long time. Fig 10.1 gives a table of expected savings for some typical rehabilitation techniques. The maximum saving is for a typical semi-detached dwelling. For insulation, this is applied to the three outer walls, but for the solar techniques, the application is to the south wall only, the other two walls being left unmodified.

10.2 - Potential of Techniques

10.2.1 - Glazed solid walls

At present there are no easy ways of improving solid walls. Inside or outside insulation is possible, but is expensive, and may entail alterations to openings and decorations. The cheapest passive solar energy technique is the conservatory. Conservatories are available cheaply, from approximately £200-800, or a little over £1000 for a

Wall type	Gain/ loss MJ/m²	Improve -ment MJ/m²	Saving £/m²	Maximum saving £
Solid - Full day				
1	-398	0	0	0
2	-501	-103	-0.3	0
3	-17	+381	+1.0	+27
4	+476	+874	+2.2	+58
5	-180	+218	+0.5	+57
Solid - 1800 - 2300				
1	-52	0	0	0
2	-92	-40	-0.1	0
3	+50	+102	+0.3	+8
4	+143	+193	+0.5	+13
5	-35	+17	+0.1	+17
Cavity - Full day				
1	-252	0	0	0
2	-345	-94	-0.2	0
3	+41	+293	+0.7	+18
4*	+642	+893	+2.2	+58
5	-59	+193	+0.5	+57
Cavity - 1800 - 2300				
1	-34	0	0	0
2	-63	-29	-0.1	0
3	+37	+71	+0.2	+5
4*	+513	+548	+1.4	+37
5	-9	+25	+0.1	+17

Fuel cost 0.25p/MJ

1 - Unglazed, facing south
2 - Unglazed, facing north
3 - Single glazed
4 - Heat mirror double glazed
5 - Insulated, outside or cavity

] facing south

* - Forced heat recovery from cavity

Fig 10.1 - Possible Savings for Different Techniques

double glazed conservatory. Conservatories can be justified for other reasons, such as extension of the living area, but with careful positioning will give useful thermal benefits which would enable recovery of the original investment.

The conservatory can only cover a limited area of wall. To cover more wall area and to improve thermal performance further, would require techniques not currently available 'off the peg'. The use of such techniques as heat mirror double glazing, will make a solid wall into a fairly efficient solar collector, but it will be expensive unless it becomes readily available. If available, it would be very suitable for a dwelling, since the phase lag of a brick wall gives the thermal storage necessary for a dwelling.

Unfortunately, however, there will be a tendency for the occupier to use the conservatory as an extra living space at all times of the year. This will require the conservatory to be heated, hence, it will be a poorly insulated room which may increase fuel usage more than a normal house extension.

10.2.2 -Glazed cavity walls

One important difference with cavity walls is that there is already available a relatively cheap and effective

rehabilitation technique, cavity insulation. It is unlikely that any passive solar energy technique, for cavity walls, will become competitive with cavity insulation, although the techniques described in 10.2.1 should be just as effective for cavity walls as they would be for solid walls. Forced air recovery is not likely to be suitable for rehabilitation. This could possibly be improved if the fan were incorporated with a heat pump, but this would need to be tested. There are likely to be very few cavity walls that are suitable for such techniques, because the cavities in most existing buildings are obstructed by ties and mortar and interrupted by door and window openings.

10.2.3 - Natural convection collectors

As shown in chapters 6-8, relatively simple natural convection collectors can be very efficient. The problems are in storing and distributing the collected heat. As described in chapter 8 storing the heat in a cavity or solid wall is very inefficient, hence it would be better to use the conduction gain alone.

If storage is not necessary a natural convection collector would be very effective, provided distribution of the air can be kept to a minimum. The most effective method would be to pass the air straight from the collector into the adjacent rooms. The collector has the advantage

of being simple and almost maintenance free. It would be well suited for schools or offices in old buildings, less so for dwellings (where heat is required in the evening) since the building fabric will not store enough heat for a sufficiently long time.

10.2.4 - Forced convection collectors

Such collectors, analysed briefly in appendix 2, are active and as such are outside the main theme of this work. However, analysis shows that they have potential for rehabilitation, especially because they can be widely applied. There would be the disadvantages that go with active systems of higher maintenance, and shorter life.

Storage is easier with forced flow collectors, since the pressure losses associated with the store can be dealt with by increasing fan performance. This means that the size and position of the store is not so critical. As shown in appendix 2, building components such as the floor, or a wall could be used as a store. If space allowed, a pebble bed store could be used, or the hardcore usually placed below a solid floor might be adopted for use in this way.

Results show that this method has potential, but since the practical difficulties could not realistically be simulated in a small-scale test, a full size demonstration

is needed.

10.3 - General Discussion

Fig 10.2 gives a summary of properties and possible applications of the various rehabilitation methods discussed in section 10.2.

Passive solar energy techniques are theoretically possible for rehabilitation, but in the near future they will be expensive and for this reason they may not become readily available. For new buildings these techniques are begining to become accepted, and as an offshoot they may become available for rehabilitation.

The one exception to the above comments, particularly for dwellings, is the conservatory. These are readily available, cheap and have the additional advantage of extending the living space. The thermal performance of a conservatory is of low efficiency, but given the other benefits, this is not a serious problem. Use of conservatories as heat collectors, undoubtedly needs further research. Apart from providing heat gain by conduction through the wall, heat could also be gained by convection, and also the performance could be improved by using insulating shutters, outside the wall, to reduce heat loss from the wall at night.

	System	Solid wall: glazed	Solid wall: with conservatory	Cavity wall: glazed, forced air heat recovery	Natural convection collector	Forced convection collector
Properties	Phase lag	5-6 h	5-6h	4-5 h	None	None
	Remote storage	Not required	Not required	Not required	Difficult and inefficient	Various possible methods
	Efficiency	Medium	Low	Medium	High	High without store, medium with
	Positioning	Inflexible	Inflexible	Inflexible	Inflexible	Rarely overshadowed
	Capital cost	High*	Low/medium	High*	Medium/high*	High *
	Maintenance	Low	Low	Medium	Low	High
	Life	Long	Long	Fans etc. -limited	Long	Fans etc. -limited
Applications	Dwellings	✓	✓	✓	×	✓ with store
	Offices, schools, etc.	×	×	×	✓	✓ without store
	Additional advantages	None	Extends living space	None	None	None
	Practical problems	None	Needs ground space	Few houses suitable	None	Could disturb house interior

* - NOT GENERALLY AVAILABLE AT PRESENT

Fig 10.2 - Properties and Applications of Passive Solar Rehabilitation Systems

In new houses the wall between the house and the conservatory will be mainly glazed. In older houses, more wall will usually be available for collection and storage of solar gain. One possibility, however, for both cases, is to draw warmed air from the conservatory and use it either for direct heating or to warm a remote heat store (cf Appendix 2).

The major difficulty in any solar technique, is storing the energy. If the occupancy is such that storage is not required, the problem is immediately simplified. Natural and forced convection air collectors, used without heat stores, could therefore be used very successfully for buildings such as schools and offices.

For dwellings, where the owner-occupier has limited money to invest, insulation is probably the best investment, at least for houses with cavity walls. For houses with any wall construction, and favourable orientation, the conservatory provides the cheapest available way of using passive solar energy.

Appendix 1

Data File for NATCONV Programs

```
NATURAL
TRANSPARENT
0
9
5
675.0 11.0 23.0 23.0 2.4 0.11 0.75 0.9
0.0
0.05 0.08 0.04 0.02 0.02 0.04 0.08 2.0 0.12 2.0
0.008 2.9
1015
22/04/82
```

Natural or forced flow

Cover - Transparent or opaque

Debugging parameter (0 = off)

Number of vertical nodes - n

Number of horizontal nodes - m

Insolation - tao - tai - temp. at entry - height - gapwidth

- transmission factor - absorptance

Forced velocity (0 if natural)

Initial resistances (m+5)

f factor - k factor

Time

Date

Appendix 2

Rehabilitation Using Forced Convection

This appendix, although not following the general theme of the thesis, is included to show

(1) a further application of the convection model developed in chapter 6.

(2) to analyse whether the use of forced convection may be more efficient than any passive system.

A2.1 - Description of system

Problems arise from the application of solar energy to existing houses. The orientation is often unfavourable and south walls are often overshadowed. This rarely applies to the roof. The slope of the roof is often less than 45° and rarely over 60° which means the orientation is less critical and in most residential areas there is little chance of the roof being overshadowed.

In this country roofs are usually of timber framing covered with a cladding such as tiles. In such a construction, there is little thermal storage, so that it is necessary to transfer the heat to a separate heat store.

Fig A2.1 shows a possible rehabilitation technique. With the store being below the collector, (and the collector being at an angle), the system would obviously

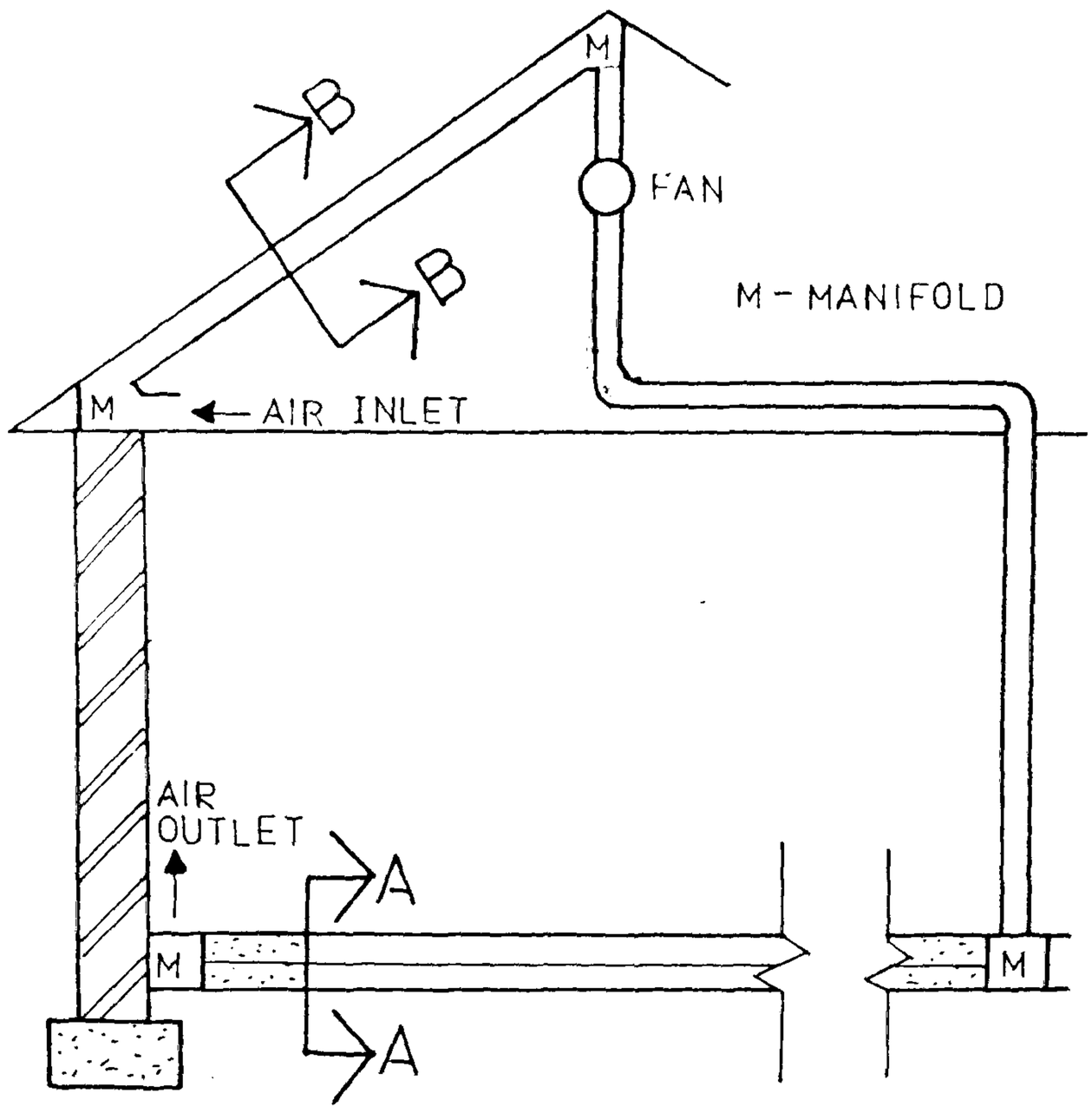

SECTION THROUGH HOUSE

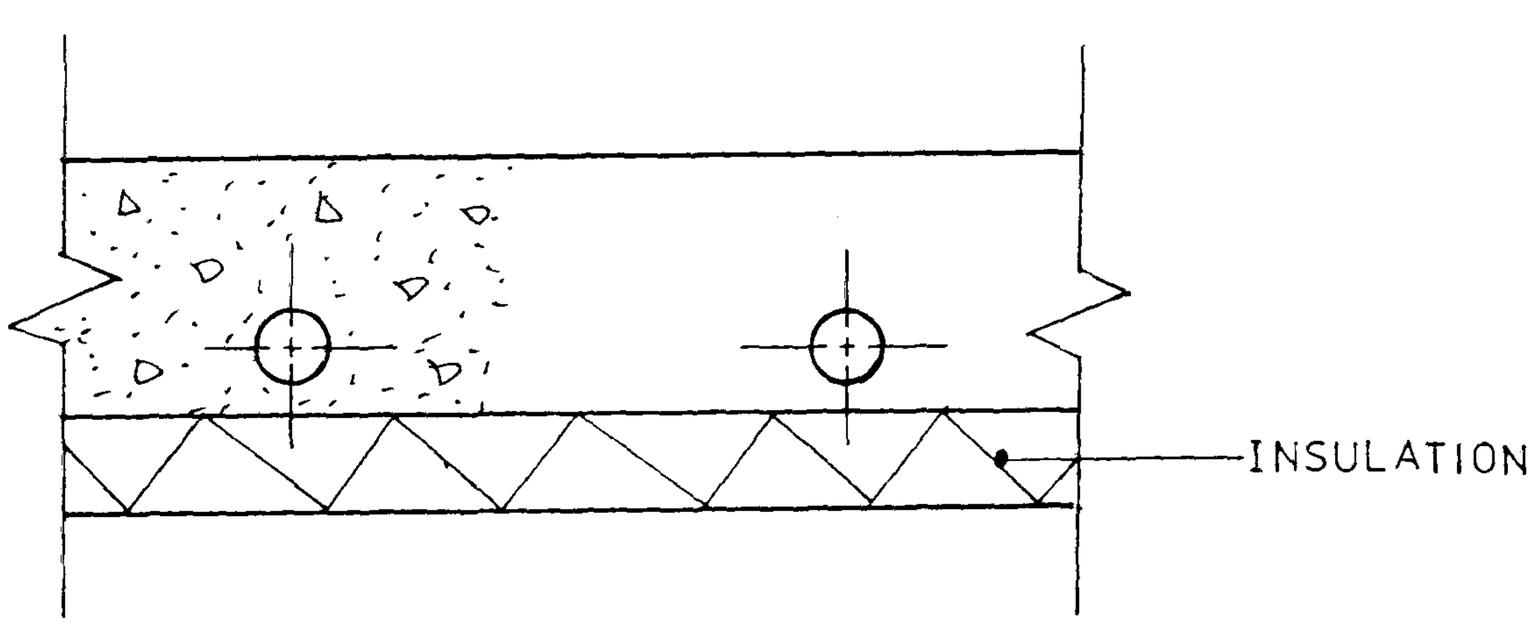

SECTION AA

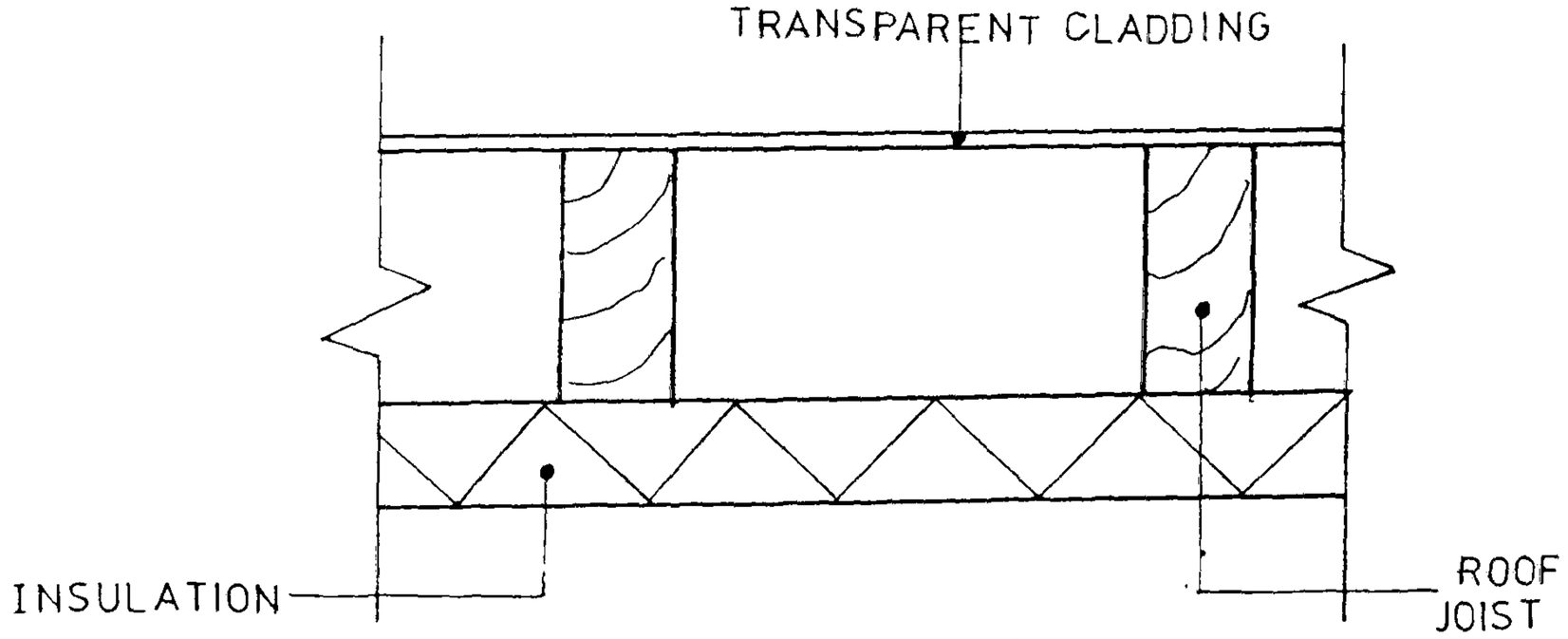

SECTION BB

Fig A2.1 - House Modified with Forced Collector

not work by natural convection so that a fan is needed. Since this system is active it has moved away from the rather simpler passive techniques described earlier but it may well be in practice that this active system has more potential for rehabilitation.

Since in the process of renovating some houses, the roof and ground floor would probably be reconstructed, the capital cost of applying this system would probably not be prohibitive, and since the transfer medium is air, maintenance problems would not be as considerable as with a 'wet' system.

A2.2 - Theory

The theoretical modelling of the forced convection system is similar to that of the natural convection system. A major difference is that in forced convection the velocity is specified, hence there is no need for the iteration that is required for natural convection. The solution of the nodal network is as before, but requires less computer time.

The value of the velocity used is fixed by practical considerations such as the availability of suitable fans hence in these theoretical calculations a volume flow of 0.04 m^3/s per m of collector has been used. There will be an optimum velocity which can be found from pressure losses

and heat transfer, but for this calculation this has not been considered.

A2.2.1 - Optimum gapwidth

To keep friction losses low it is not desirable to make the gapwidth considerably less than the value of 0.1 m that was obtained from the natural convection analysis.

The upper limit again is fixed by whether or not the flow is fully developed. In the case of forced convection there are commonly used rules of thumb for checking whether the flow is fully developed (15)

For gapwidth = 0.1 m

equivalent diameter = 0.2 m

For collector length (L) = 3.0 m

$$L/d = 15$$

For flow to be fully developed $L/d > 20$

As can be seen from this the flow in such a collector is unlikely to be fully developed. But these equations apply to a pipe fed from a large reservoir, with a simple square edged entrance. As can be seen in Fig A2.1 this system is a closed cicuit, with many bends, changes in section etc. Thus for the system analysed here, the flow can be assumed

with reasonable confidence to be fully developed. Hence since the gapwidth is not a critical parameter, a value of 0.1 m will be used.

A2.2.2 - Laminar or turbulent

If the gapwidth is 0.1 m and the volume flow is taken as 0.04 m^3/sm it is possible to make some statement about the condition of the flow.

$$\text{Reynolds' No. (Re)} = \rho vd/\mu \qquad \text{(A2.1)}$$

μ = dynamic viscosity

v = air velocity

= volflow/gapwidth = 0.4 m/s

d = 0.2 m (from section A2.1.2)

Hence Re = 5710

$2000 < Re < 4000$ flow is transitional

As shown in section A2.1.1 there may well be thorough mixing in the collector which would help the development of turbulence. This complicates theoretical calculations but will help heat transfer in the collector in practice.

A2.2.3 - Heat transfer coefficients

From the conditions described the values calculated for the heat transfer coefficients must not be treated as accurate. The equation used to calculate the heat transfer coefficients is that for fully developed turbulent flow given by O'Callaghan (15) as

$$h = 0.023 k_f Re^{0.8} Pr^{0.33} / d \qquad (A2.2)$$

A2.3 - Performance of Collector

A2.3.1 - Glazed collector

The collector simulation was done for one day, for both selective and non-selective surfaces. A plot of solar input, output and efficiency of the collector against time of day is shown in Fig A2.2.

As can be seen the maximum efficiency for the selective surfaced collector is 48% as compared with 33% for the non-selective surface. As with the natural convection collector, the decision whether selective surfaces are worthwhile must be made from financial considerations.

Fig A2.3 shows the variation of efficiency with gapwidth using weather data for noon on the day considered.

GAINS AND EFFICIENCIES FOR FORCED AIR COLLECTOR

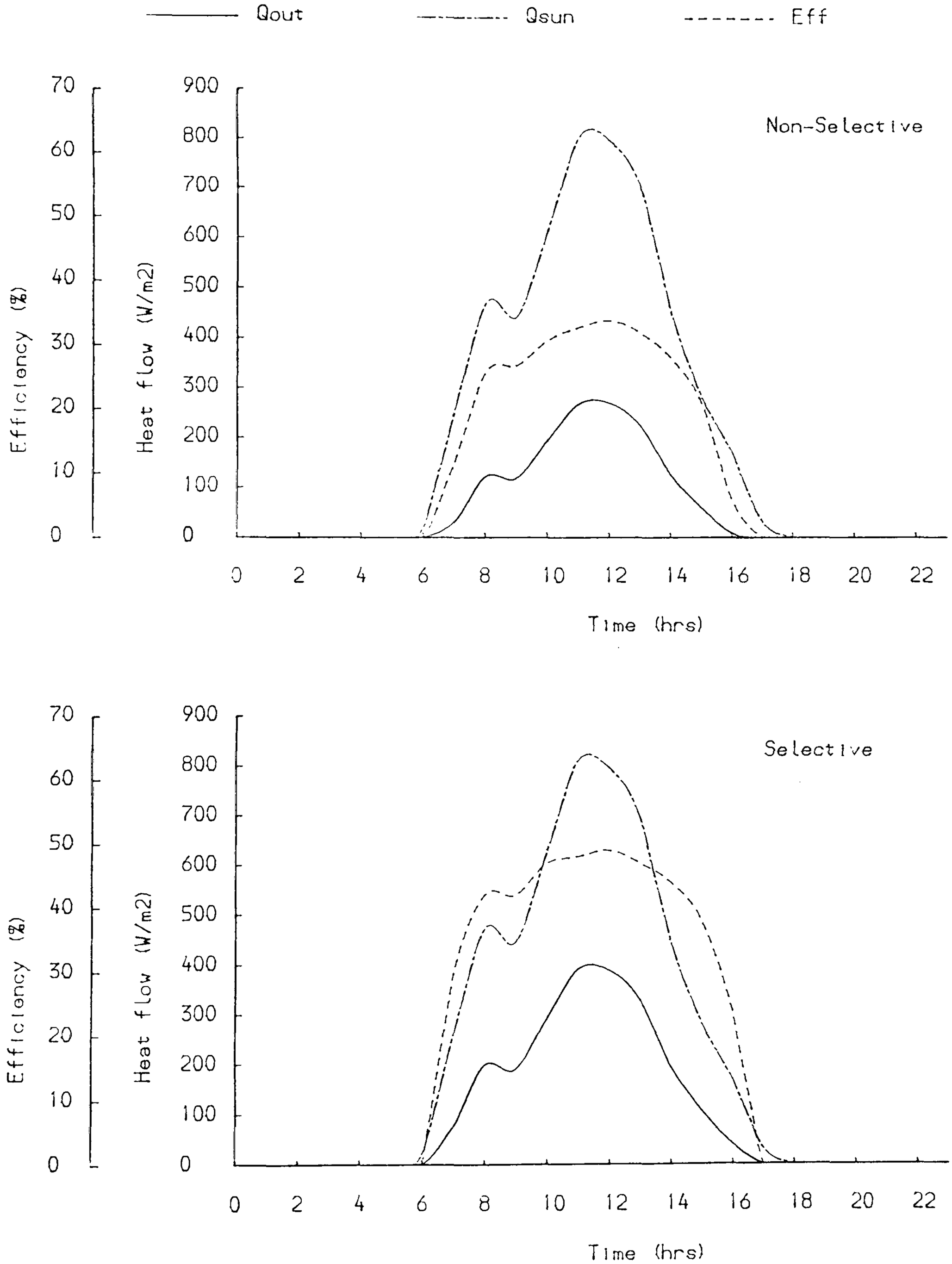

Fig A2.2

PERFORMANCE OF COLLECTOR WITH VARYING GAPWIDTH

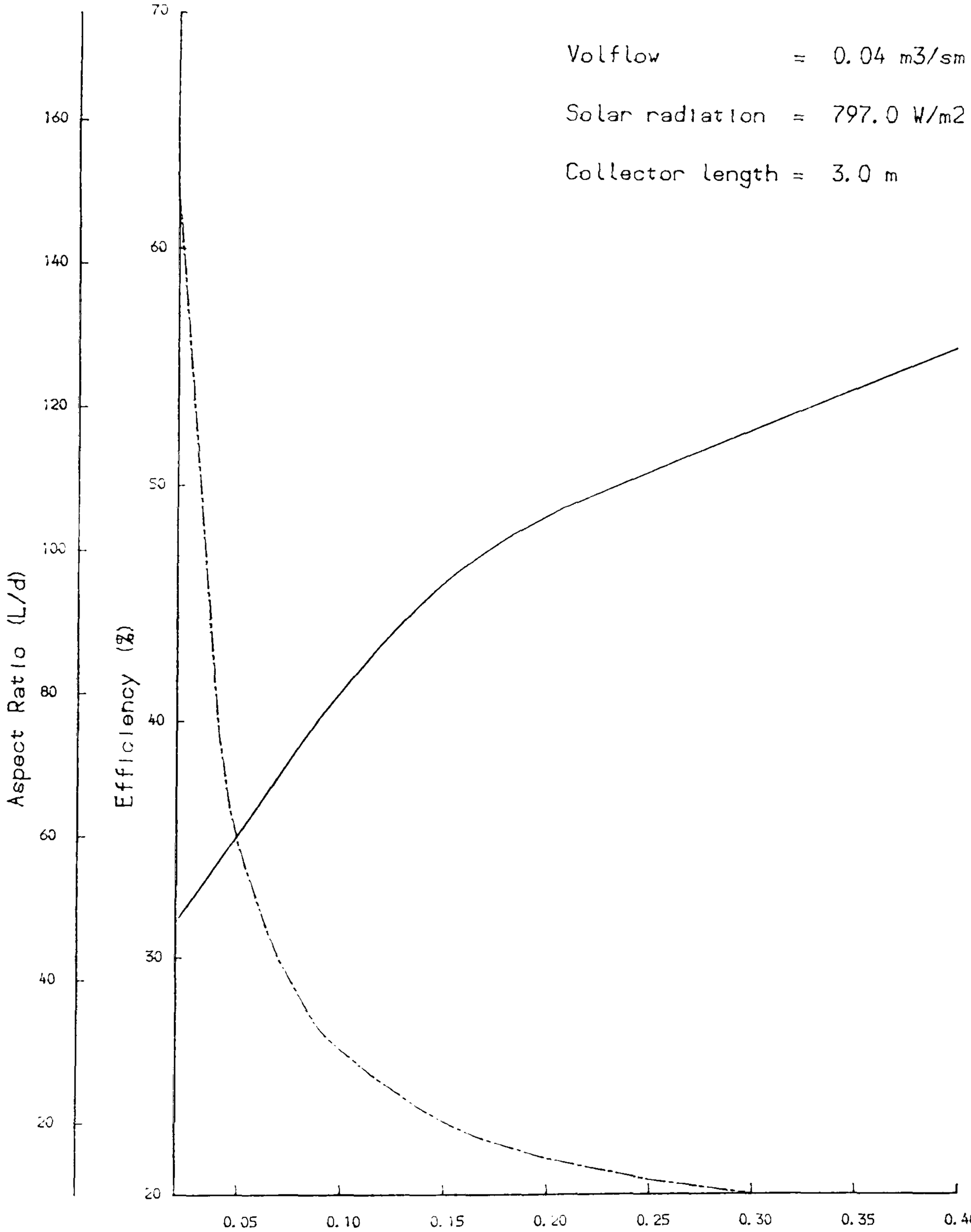

Fig A2.3

The gapwidth of 0.1m (0.2m equivalent diameter) gives a reasonable performance, but the final decision of the best gapwidth must be made from consideration of the friction losses in the whole system and consequently the most practical size of fan.

The temperature contours for noon for both selective and non-selective surfaces are given in figs A2.4 and A2.5. Although these figures are of little significance in themselves, they are useful for comparison with Figs A2.8,A2.9 and A2.10.

A2.3.2 - Opaque collector

Because of the capital cost and maintenance associated with glass it could be more practicable to use an opaque cover such as steel or aluminium cladding. This would certainly not work for the natural convection collector but may function reasonably for a forced convection collector. As discussed in section 2.3 the BRE's Heat Pump House uses an opaque collector, where the construction consists of profiled metal cladding with insulation on its underside.

The modifications necessary in the nodal network of the theoretical model are shown in Fig A2.6. The only difference is that the solar radiation is absorbed by the first layer instead of the insulation surface.

TEMPERATURE CONTOURS IN VERTICAL AIR GAP

Theoretical Results for - 1200 hrs on - 15th MAR

Selective surface

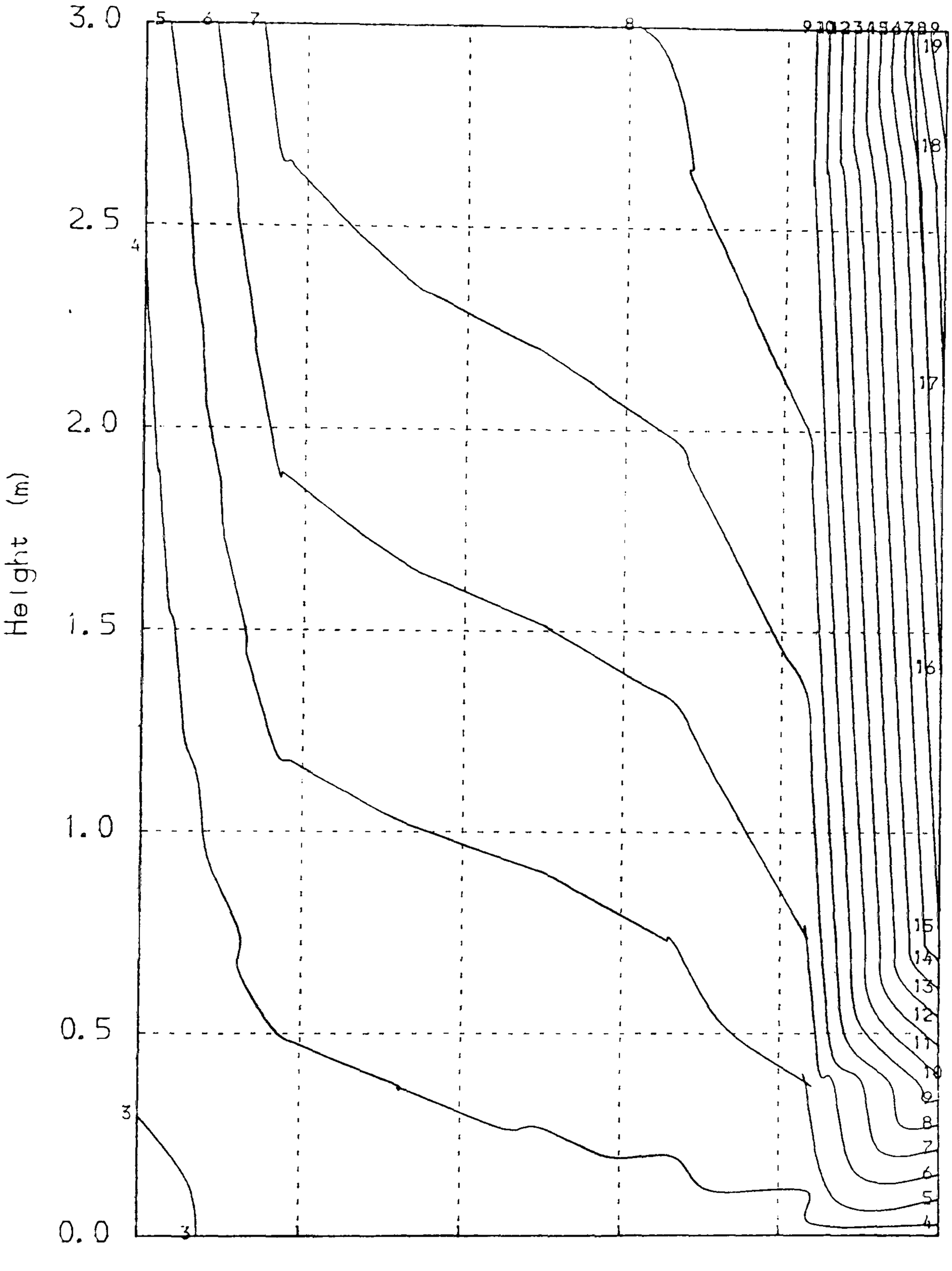

Contour values *5 = deg C

qin =	797.0 W/m2	qout =	1200.8 W
eff =	50.2 %	velocity =	0.40 m/s

Fig A2.4

TEMPERATURE CONTOURS IN VERTICAL AIR GAP

Theoretical Results for - 1200 hrs on - 15th MAR

Non-selective surface

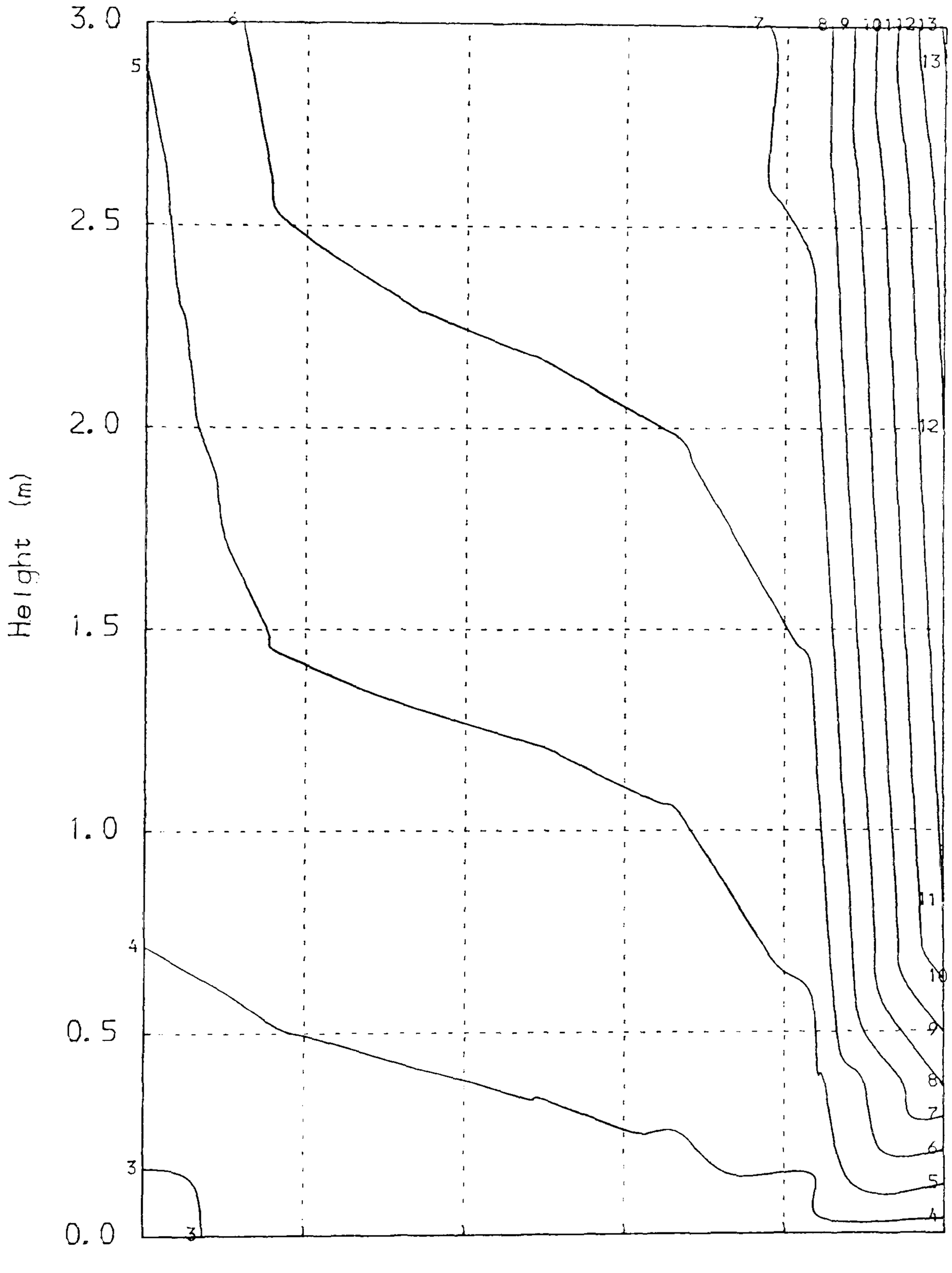

Contour values *5 = deg C

qin =	797.0 W/m2	qout =	835.1 W
eff =	34.9 %	velocity =	0.40 m/s

Fig A2.5

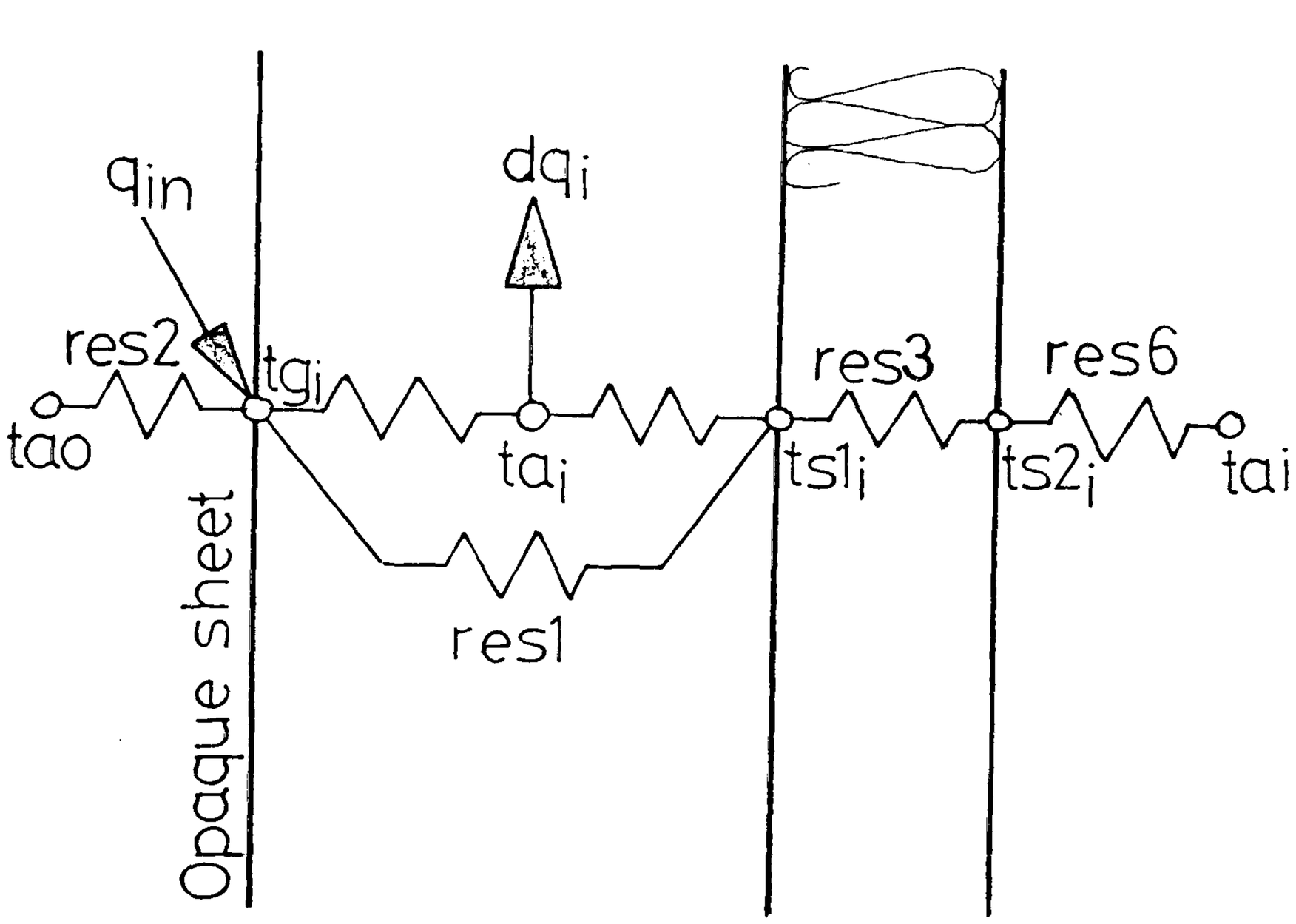

Key: As fig 6.5. Complete collector as fig 6.5

Fig A2.6- Theoretical model for collector with opaque top surface

One unfortunate property of this type of collector is shown clearly in Fig A2.7 which shows the variation of efficiency with varying gapwidth. The collector becomes more efficient with a narrower gapwidth, but this will only be true for an ideal collector. For a real collector, an impossibly large fan would be needed to move the air through a very narrow gap. The sheet used has a selective surface.

For a 0.1m gapwidth the efficiency is 28% , as compared with 48% for the selective surface glazed collector and 33% for the non-selective surface glazed collector. Costs will dictate which system is most practicable.

Figs A2.8,A2.9 and A2.10 show the noon temperature contours for the opaque collector for various gapwidths. Comparison with figs A2.4 and A2.5 shows that more heat is lost to the outside in the opaque collector than in the glazed collector, i.e no advantage is taken of the greenhouse effect. In exactly the same way a double glazed collector would function better than all the systems so far described.

A2.3.3 - Comparison of collectors

A major observation to make about the performance of the two types of collectors is that the efficiency of the

PERFORMANCE OF COLLECTOR WITH VARYING GAPWIDTH

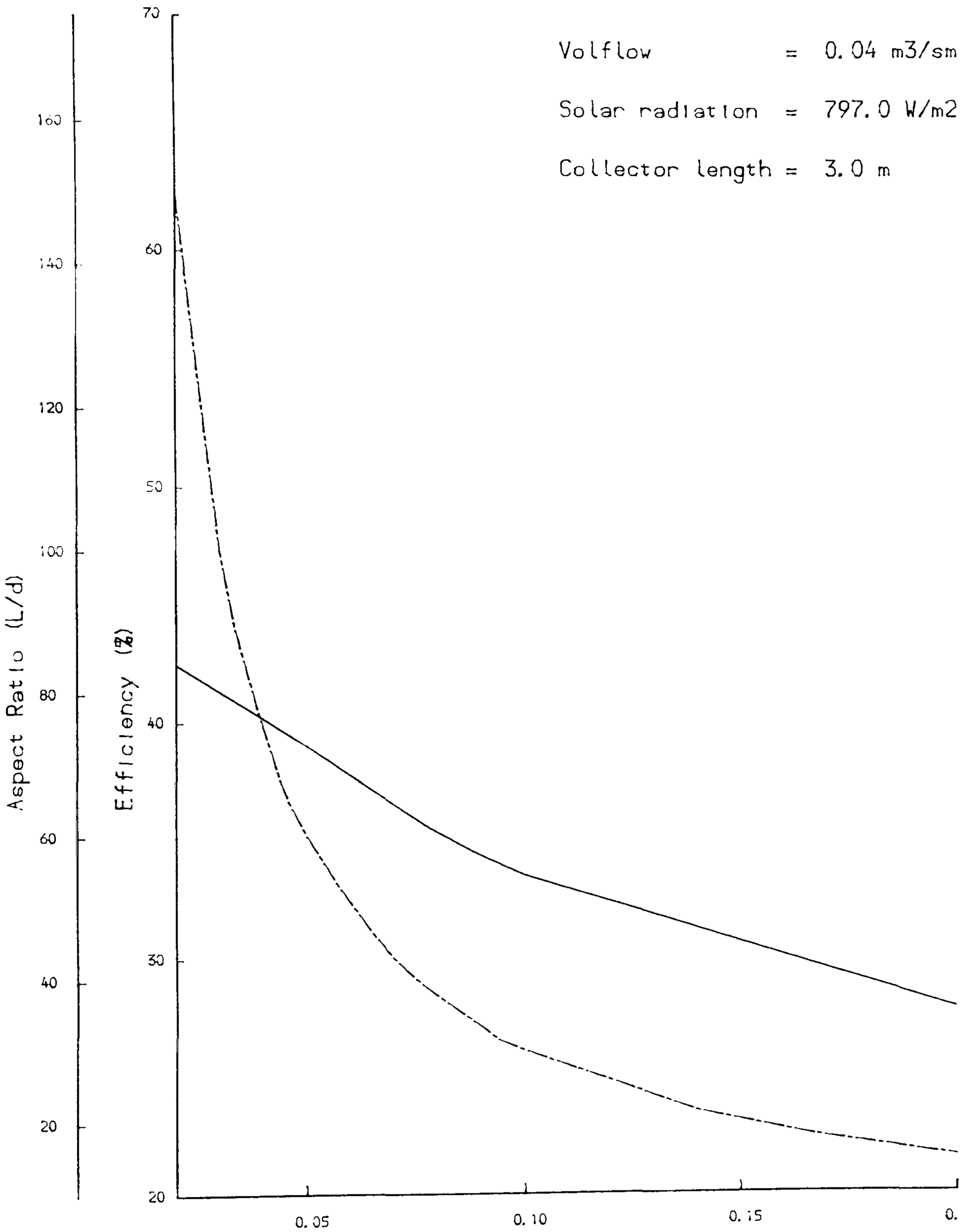

Fig A2.7

TEMPERATURE CONTOURS IN VERTICAL AIR GAP

Theoretical Results for - 1200 hrs on - 15/03/82

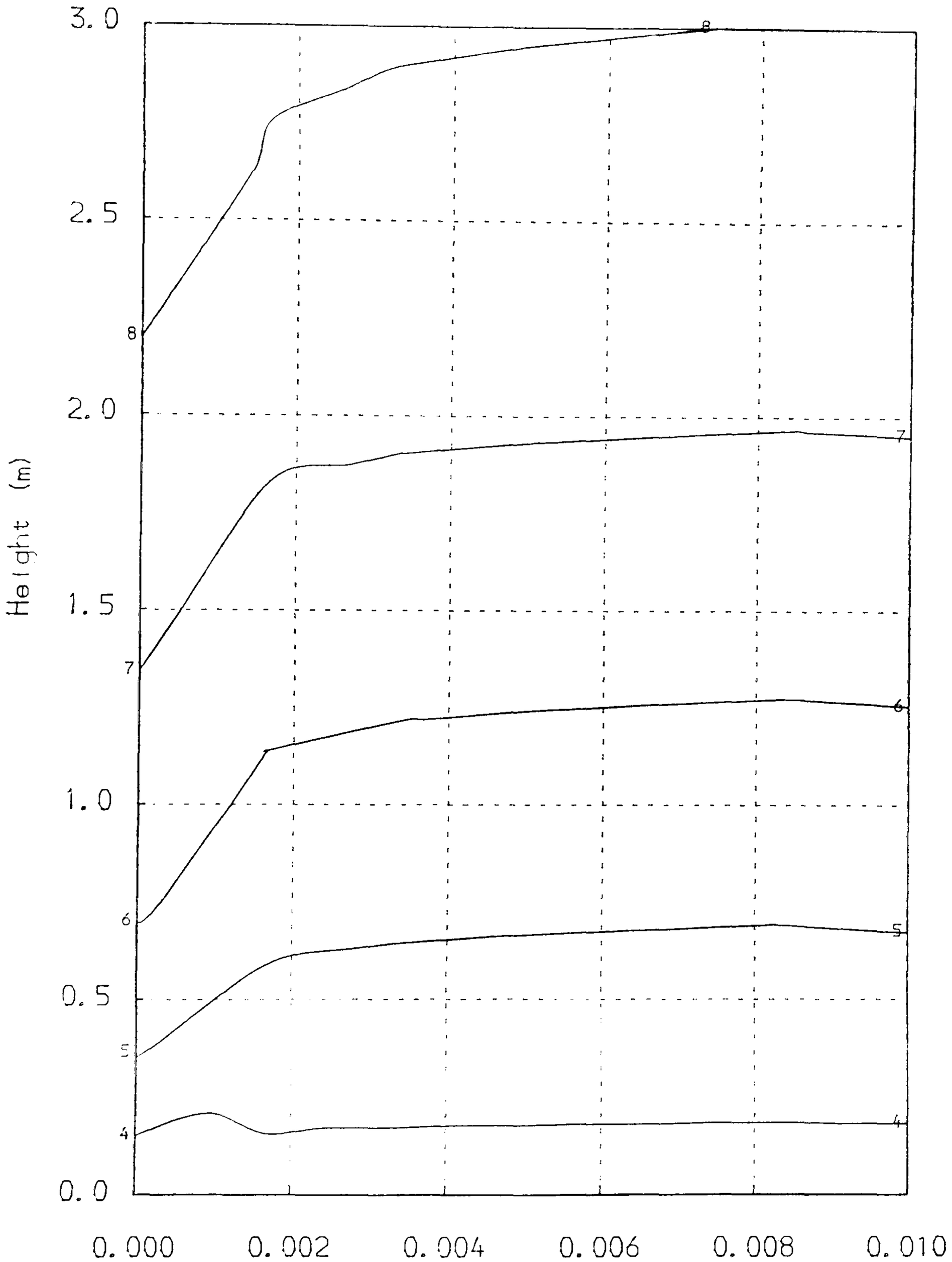

Contour values *5 = deg C

qin =	797.0 W/m2	qout =	1074.5 W
eff =	44.9 %	velocity =	4.00 m/s

Fig A2.8

TEMPERATURE CONTOURS IN VERTICAL AIR GAP

Theoretical Results for - 1200 hrs on - 15/03/82

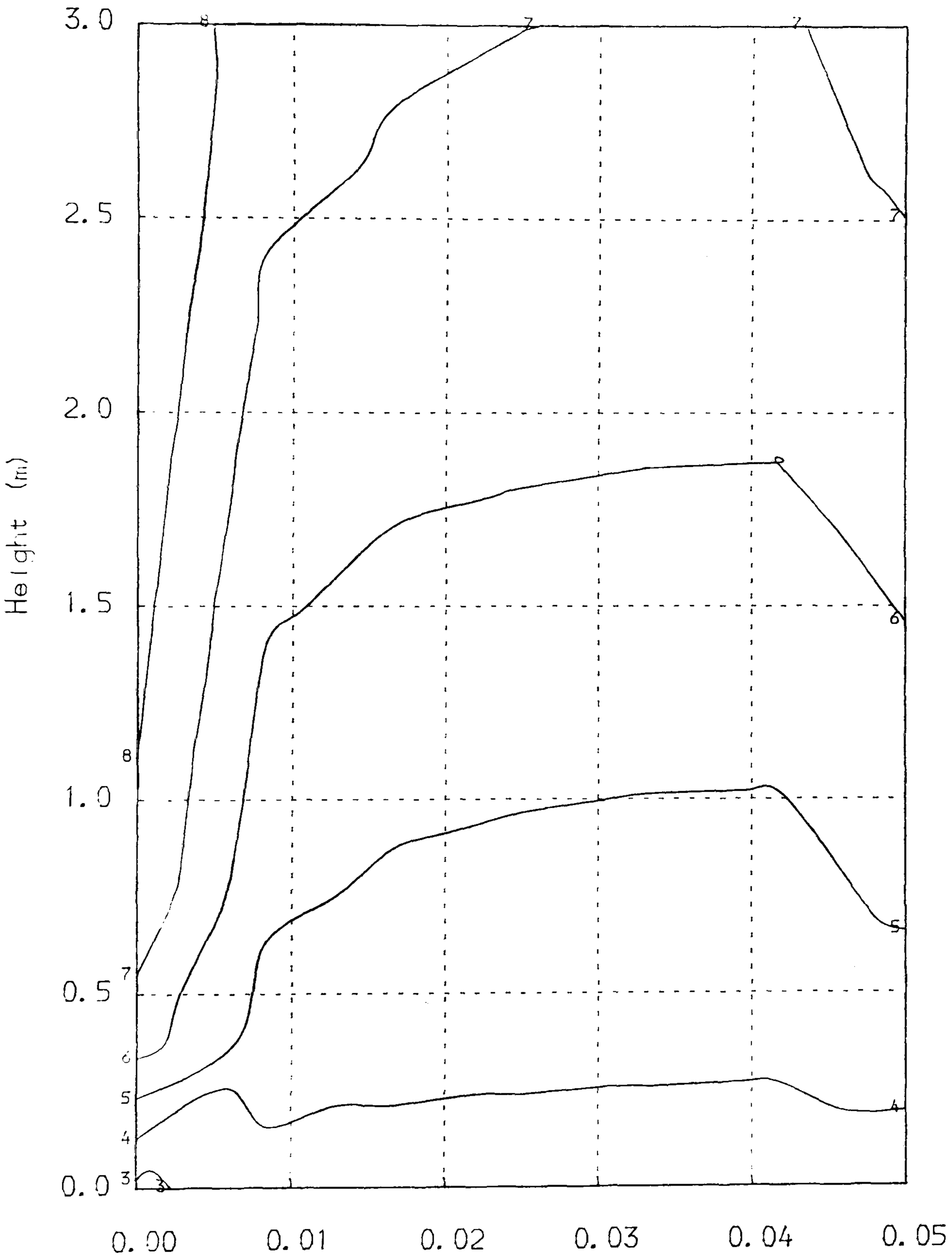

qin =	797.0 W/m2	qout =	873.8 W
eff =	36.5 %	velocity =	0.80 m/s

Fig A2.9

TEMPERATURE CONTOURS IN VERTICAL AIR GAP

Theoretical Results for - 1200 hrs on - 15/03/82

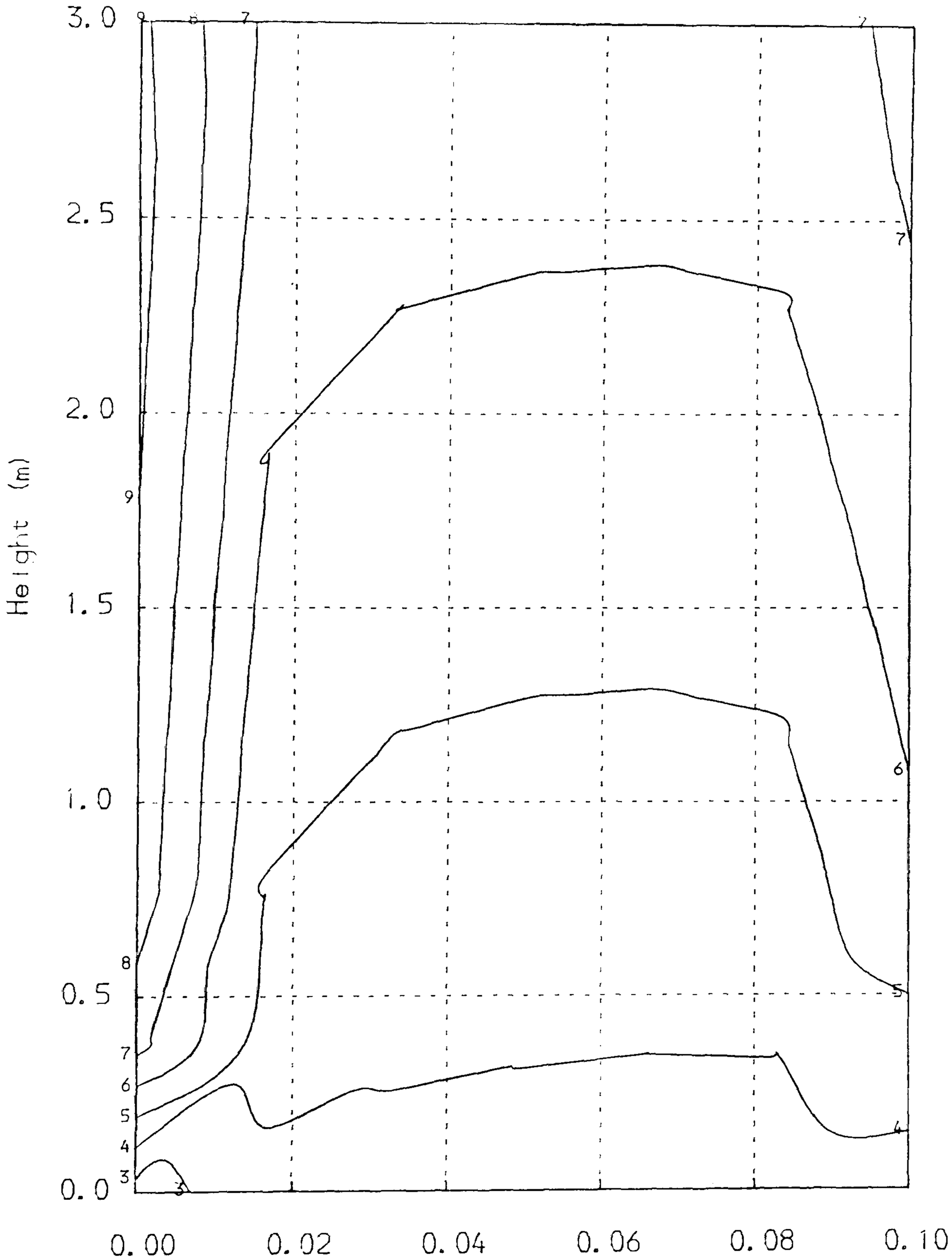

Fig A2.10

glazed collector increases with gapwidth whereas the efficiency of the opaque collector decreases with gapwidth. If the gapwidth for an opaque collector is chosen to give low friction losses, the efficiency will be considerably lower than a glazed collector of equal gapwidth.

For the glazed collector most of the heat collected is transferred to the air in the gap, and is little affected by variation of gapwidth. The convective heat transfer coefficient in the gap is more important for the opaque collector. If the gapwidth is increased, the heat transfer coefficient decreases and more heat is lost to the outside.

A2.4 - Performance of Floor Slab Heat Store

A2.4.1 - Theory

The general layout of the floor is shown in Fig A2.1, warm air from the collector is blown through the ducts in the floorslab. The floorslab analysed is 150 mm thick with pipes 50 mm in diameter. These sizes are merely reasonable guesses and practical considerations may alter them.

The theoretical model described briefly in section 8.3.2 is used to analyse the thermal behaviour of the slab. In this case the model is much more reliable. A major limitation of the model is that for very large nodal grids

the computer time is exceedingly long, hence it is not suitable for analysing the heat flow in the soil below the slab. Consequently the long term performance of the slab cannot be analysed and no benefit can be assumed from the heat stored in the soil.

A2.4.2 - General performance

From a consideration of the performance on a diurnal basis, the first conclusion was that heat gain to the room would be increased if as little heat as possible was lost to the soil. The obvious way to ensure this is to place a piece of insulation between the soil and the slab. The difference in behaviour is shown in the temperature contours in figs A2.11 and A2.12 and also in the daily heat gains in Fig A2.13. For this exercise 75mm diameter pipes are placed at 200mm centres and 100mm depth. Since the insulation considerably improves the performance all subsequent analyses will be for insulated slabs.

The next factors to be considered were the depth and spacing of the pipes. The slab was analysed with the pipe at various depths. A plot of the heat gained to the room in the evening against depth of pipes is shown in Fig A2.14. For a 150 mm thick slab the optimum depth is about 100mm. For less than 100mm, more heat is gained over the day in total, but the phase lag is too short and little heat is recovered in the evening. For pipes deeper than

TEMPERATURE CONTOURS FOR CONCRETE FLOORSLAB

Datafile - FT010A Time - 1200 hrs

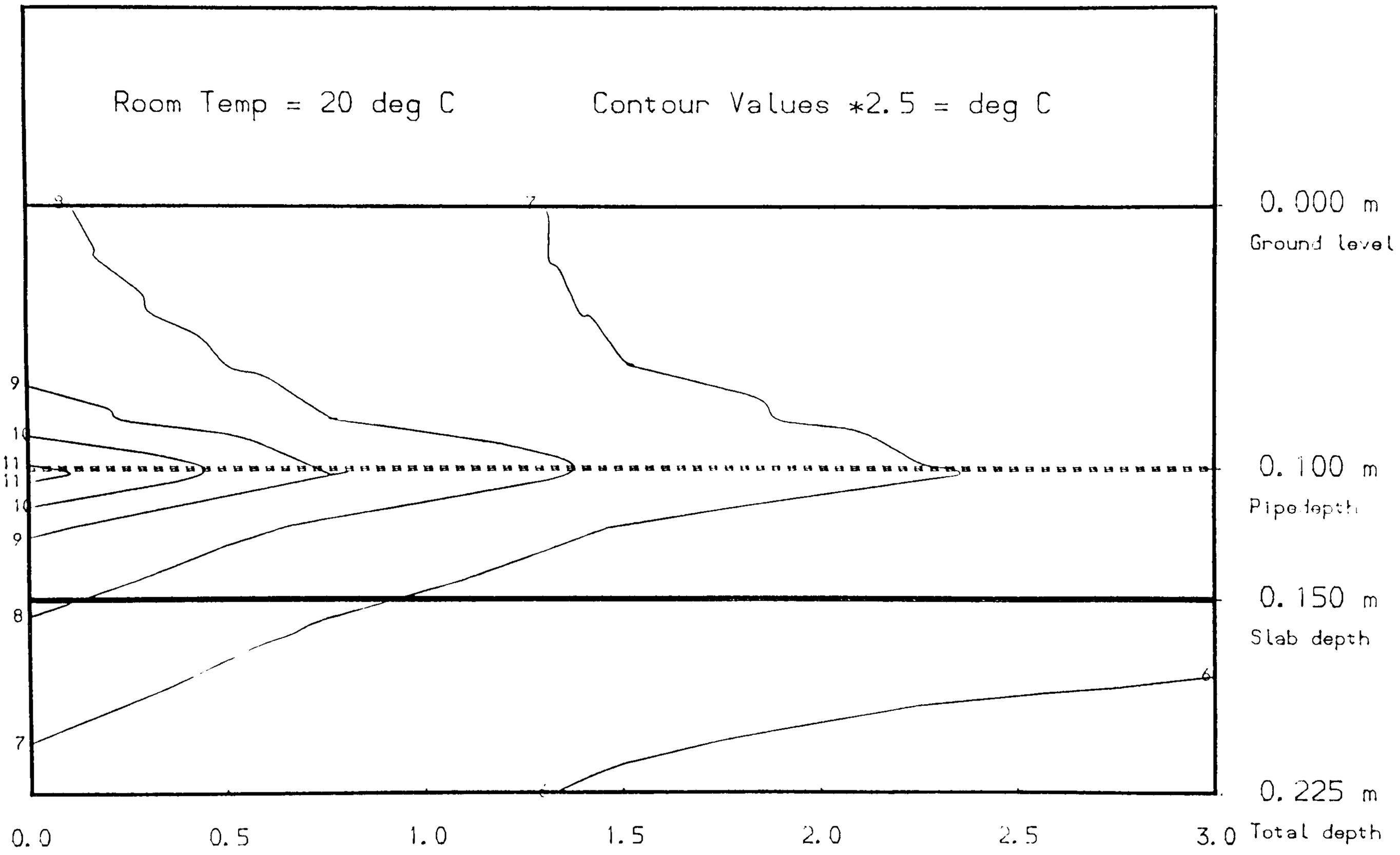

Fig A2.11

TEMPERATURE CONTOURS FOR CONCRETE FLOORSLAB

Datafile - FT015A Time - 1400 hrs

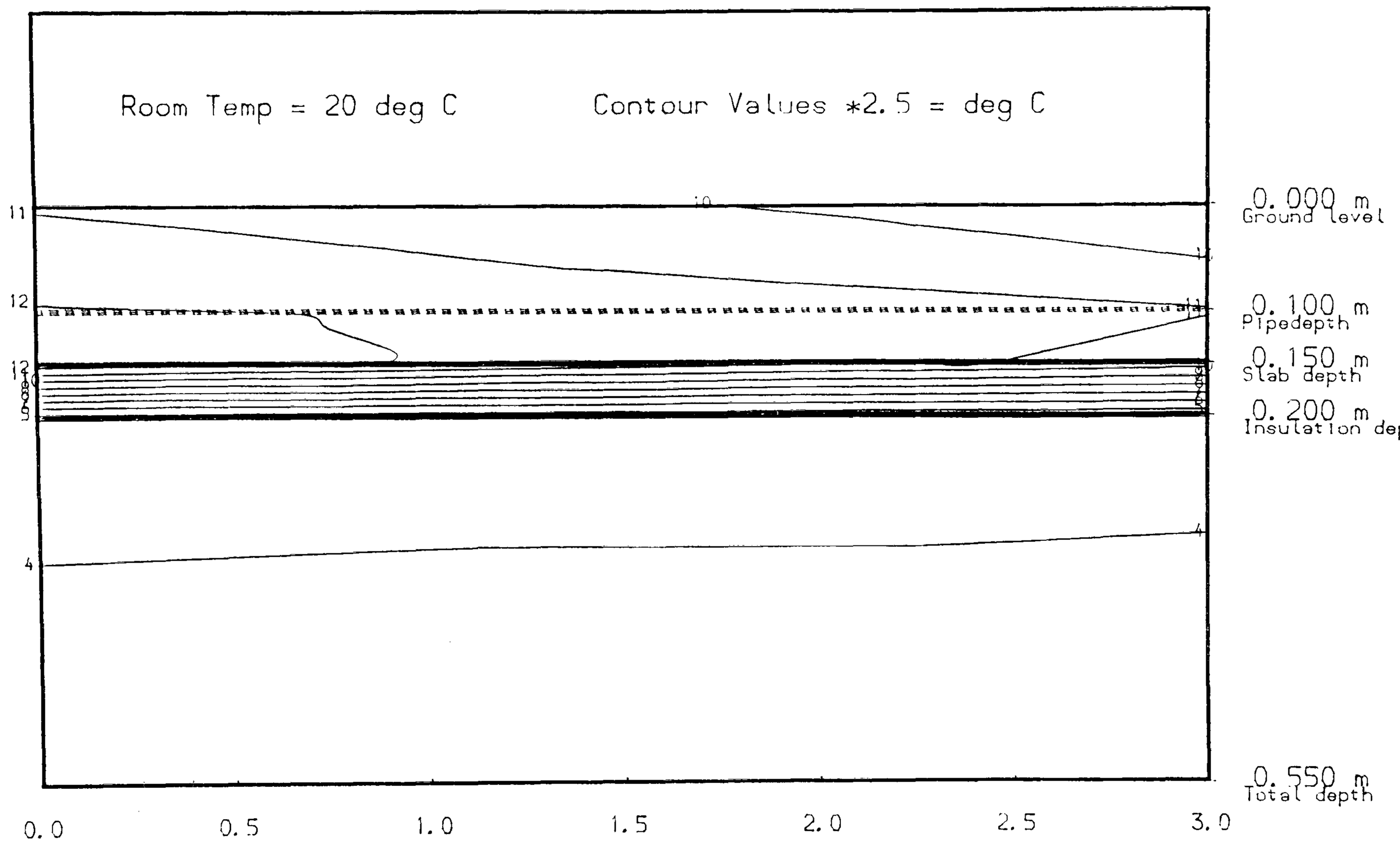

Fig A2.12

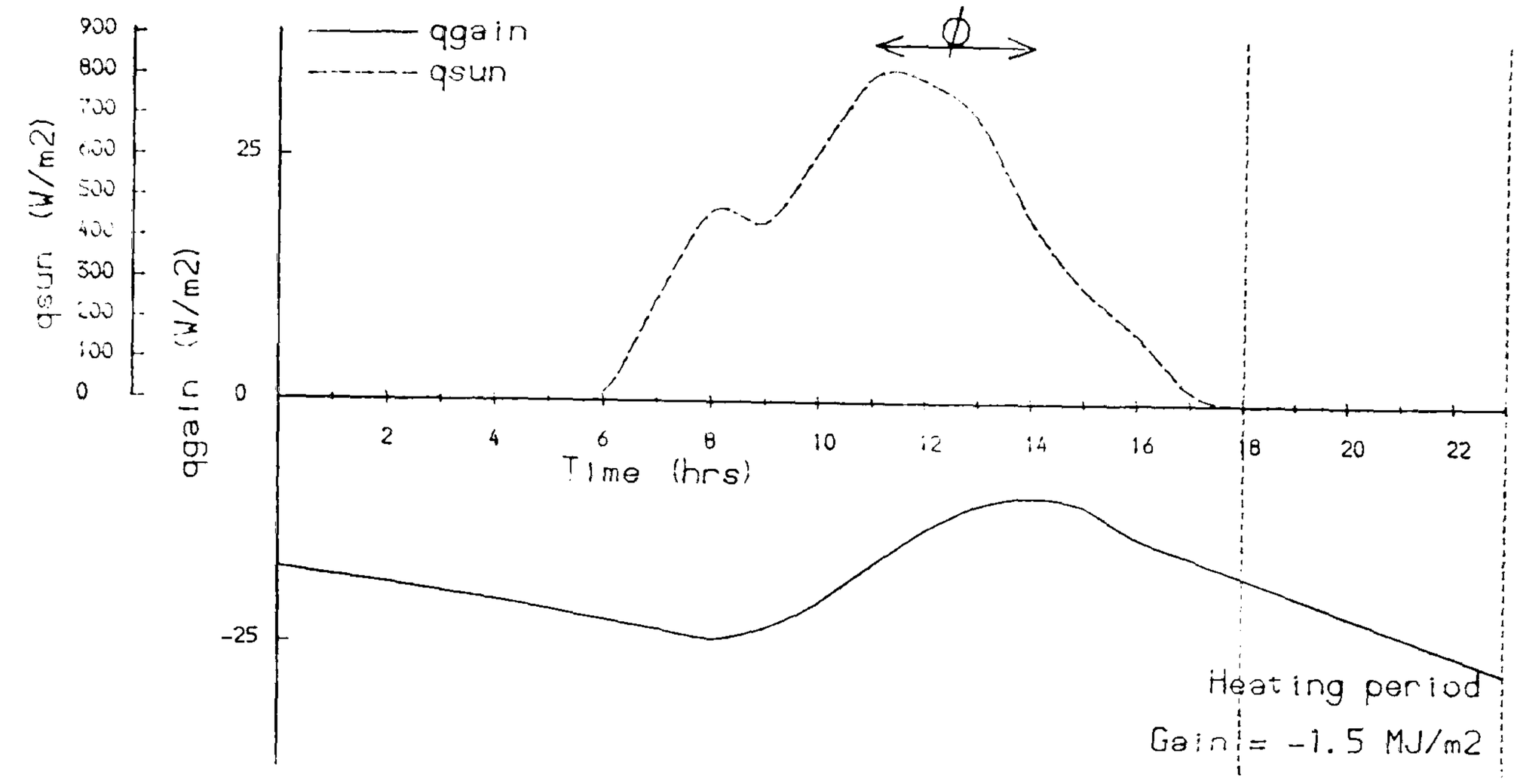

Fig A2.13(a) - Heat gains from unisulated slab

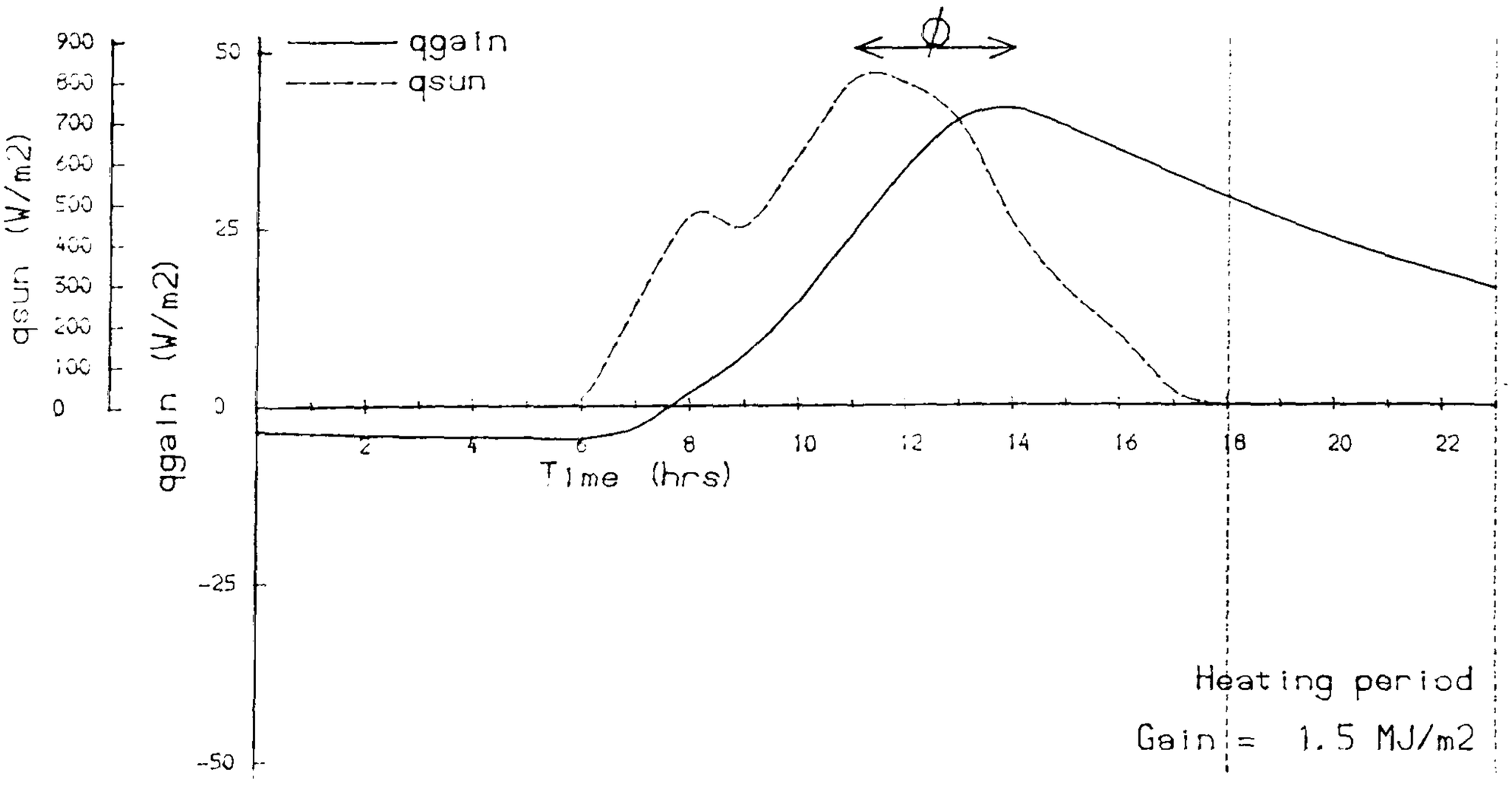

Fig A2.13(b) - Heat gains from an insulated slab

VARIATION OF HEAT GAIN FROM SLAB WITH DEPTH OF PIPE

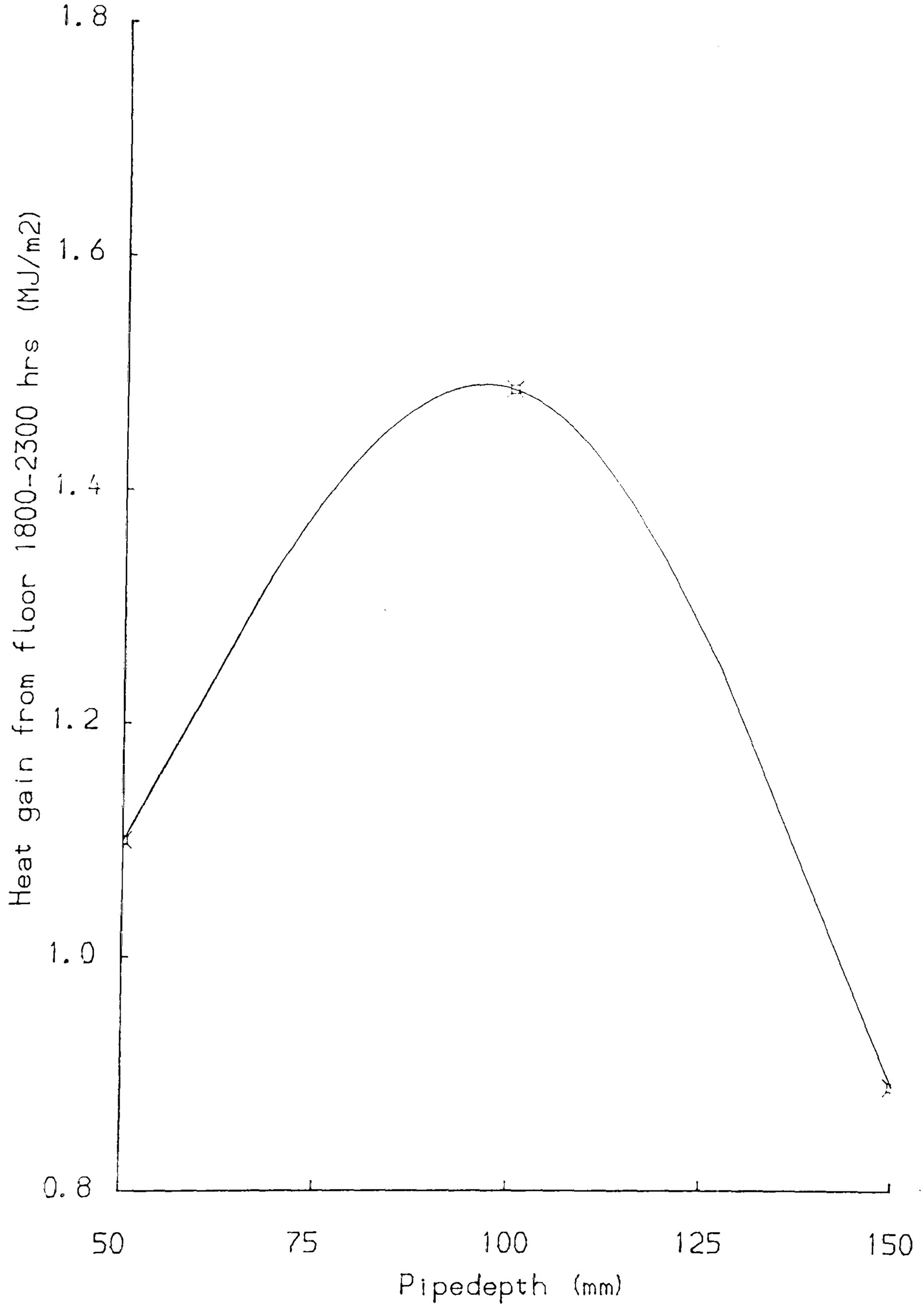

Fig A2.14

100 mm the pipes come in contact with the insulation. Hence heat is conducted through the insulation, is not stored and is lost to the soil below.

As might be expected the spacing of the pipes is not as critical as is the depth. Since the depth is restricted it may be necessary to use pipes of small diameter, and to maintain the volume flow in the pipes the spacing would need to be reduced. With a constant volume flow per m of floor slab, the variation of heat gain with spacing is shown in Fig A2.15. The variation is not great but a spacing of approximately 200 mm is a reasonable compromise.

From the above analyses a gain of about 1 MJ/m^2 could reasonably be expected over the period 1800 - 2300 hrs. This is not much but, as with any rehabilitation system, this must be compared with the heat that the unmodified construction would lose. For an uninsulated solid floor this would be a loss of about 0.1 MJ/m^2 over the same period.

A2.5 - Conclusions

Considering these points a possible practical design is shown in Fig A2.16. The insulation would be laid down followed by a layer of concrete about 25 mm thick. Ducts could be formed from PVC guttering laid on the concrete, then the remainder of the concrete laid to form the floor

VARIATION OF HEAT GAIN FROM SLAB WITH PIPE SPACING

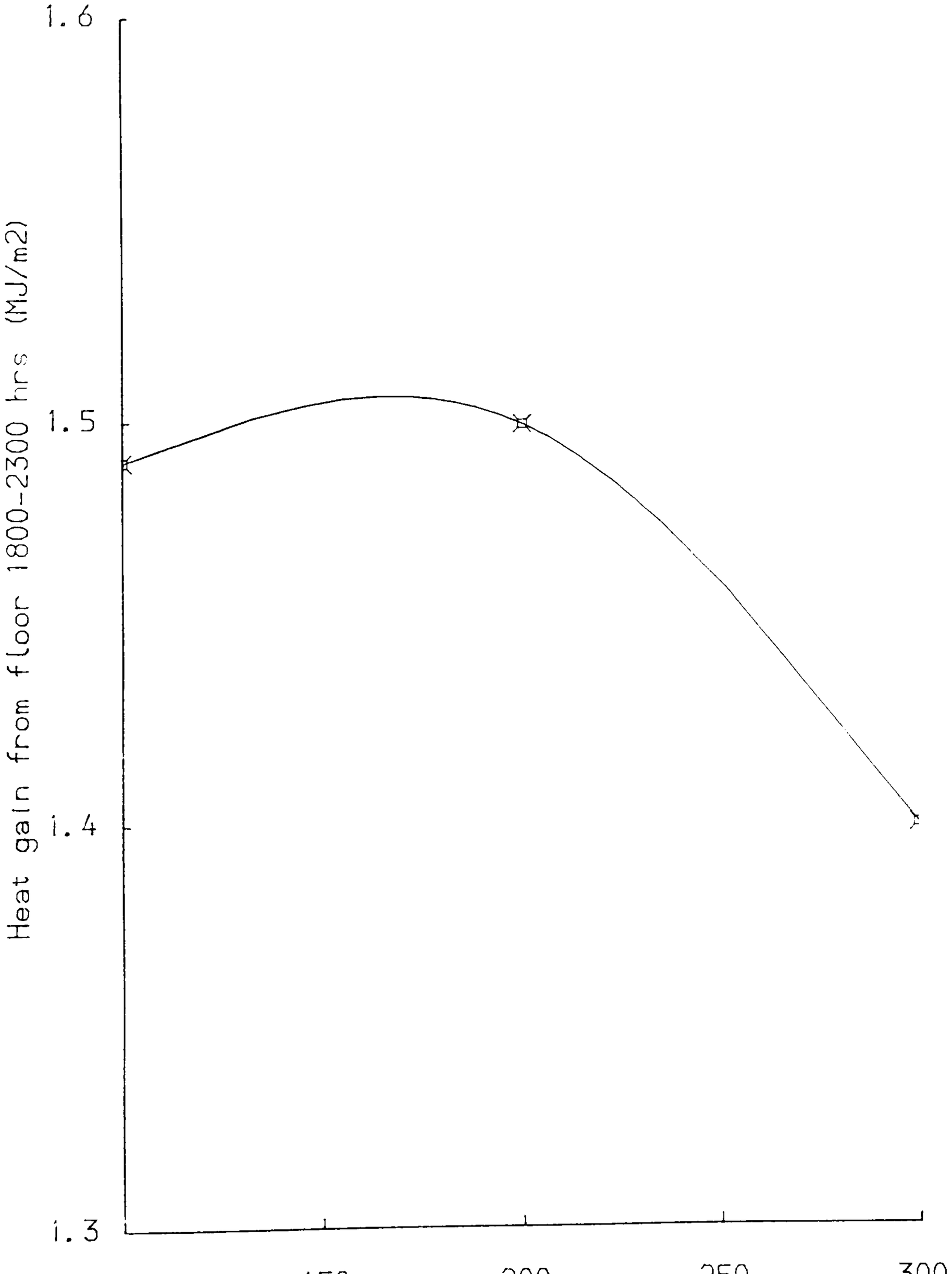

Fig A2.15

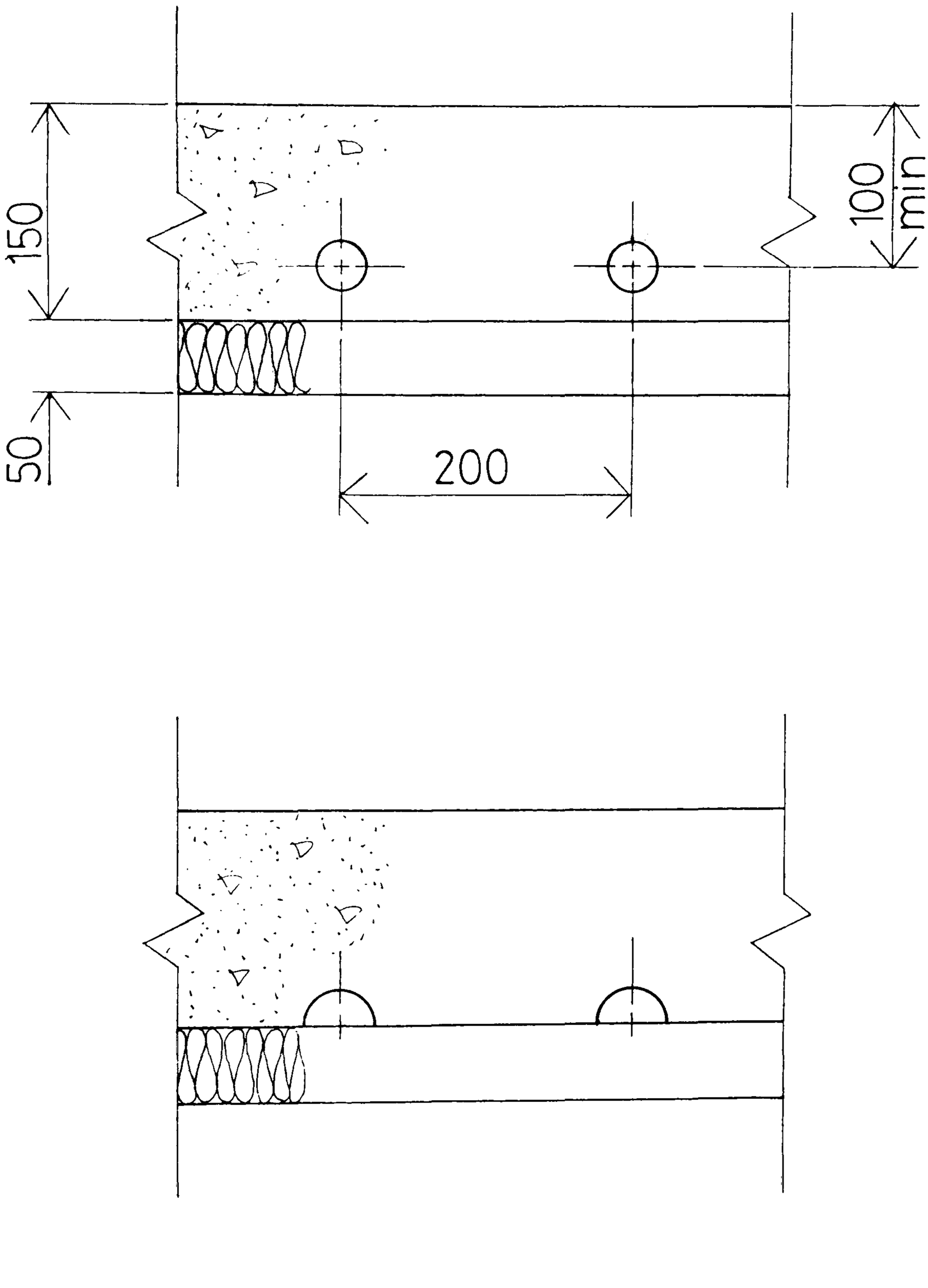

Fig A2.16- Possible Floor Slab Designs.

in the normal way. This procedure should be reasonably simple and cheap, although using insulation in such a way may prove difficult.

This approach needs much more work, including practical tests on an actual house (simulation under laboratory conditions would be difficult). It may well be that this is a practicable method of rehabilitation, possibly in conjunction with some of the techniques described in earlier chapters.

Appendix 3

Calculation of Radiation Heat Transfer Co-efficients

A3.1 - Linearisation of the Fourth Power Equation

In full the radiation heat transfer co-efficient is given by

$$h = \frac{F\sigma\,(T_1^4 - T_2^4)}{(T_1 - T_2)} \qquad A3.1$$

simplyfying equation A3.1 gives

$$h = F\sigma\,(T_1^2 + T_2^2)(T_1 + T_2) \qquad A3.2$$

Fig A3.1 shows the variation of this function with one temperature set at 20 and the other varied. This shows that

$$(T_1^2 + T_2^2)(T_1 + T_2) = 4T_{AV}^3 \qquad A3.3$$

Taking T as 295K, which is an average temperature to be expected in a room

$$\sigma\left(\frac{T_1^4 - T_2^4}{T_1 - T_2}\right) = 5.8 \qquad A3.4$$

The variation of the above function is shown in fig A3.2

Hence $$h = 5.8F \qquad A3.5$$

A3.2 - Calculation of the Configuration Factor

Fig A3.3 shows graphs for calculating the shape factor F, for parallel and perpendicular walls. It can be shown (38) that for radiant heat exchange between two 'non-black' surfaces

$$A_1F_{12} = \frac{1}{A_1}\left(\frac{1}{\varepsilon_1} \quad 1\right) + \frac{1}{A_2}\left(\frac{1}{\varepsilon_2} - 1\right) + \frac{1}{A_1F_{12}} \qquad A3.6$$

For the experimental room described in chapter 3 and shown in fig 3.2 the various configuration factors are (1) wall to ceiling or floor = 0.095, (2) wall to back wall = 0.55, (3) wall to side walls = 0.12.

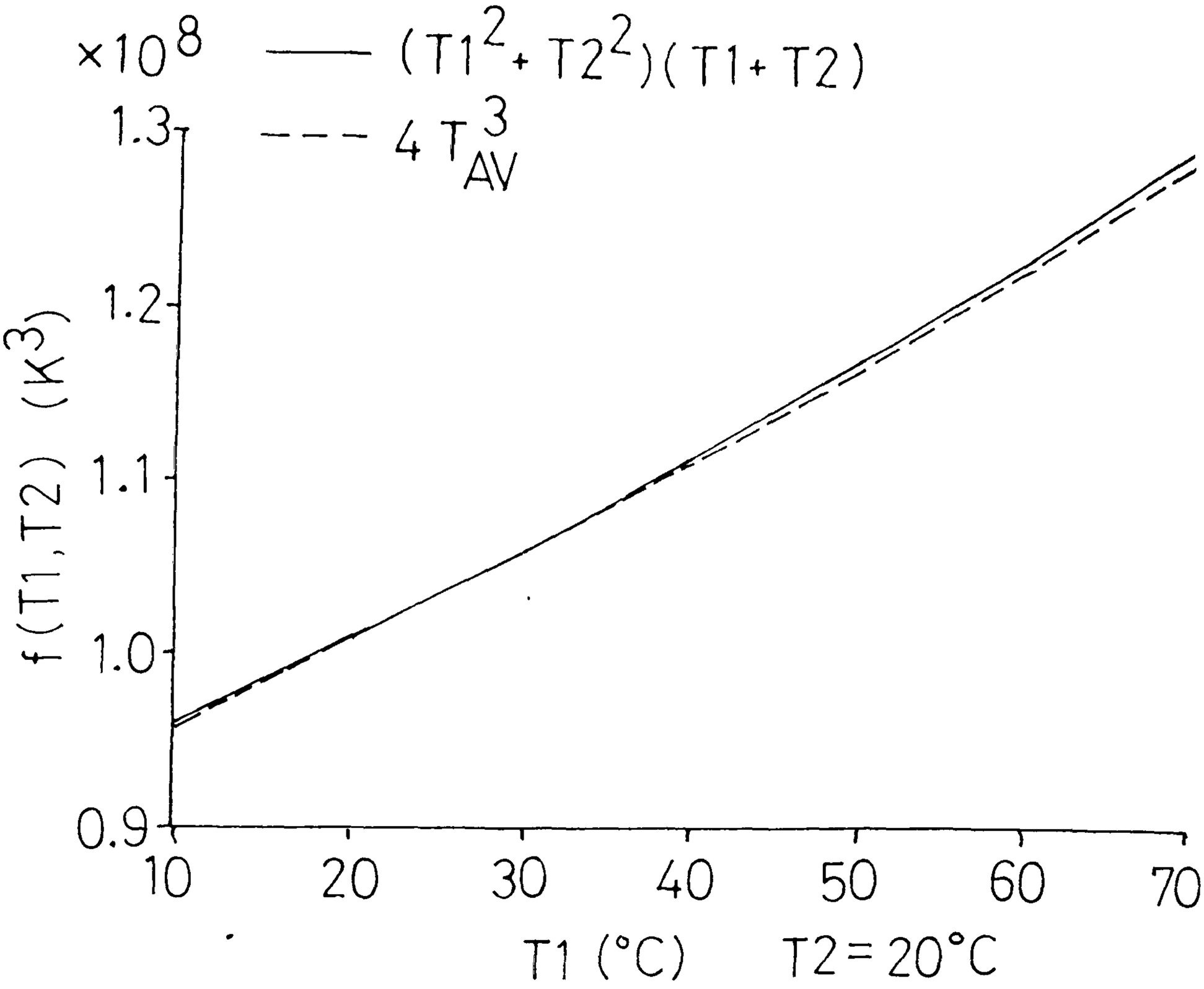

Fig A3.1 - Verification of Linearisation Law

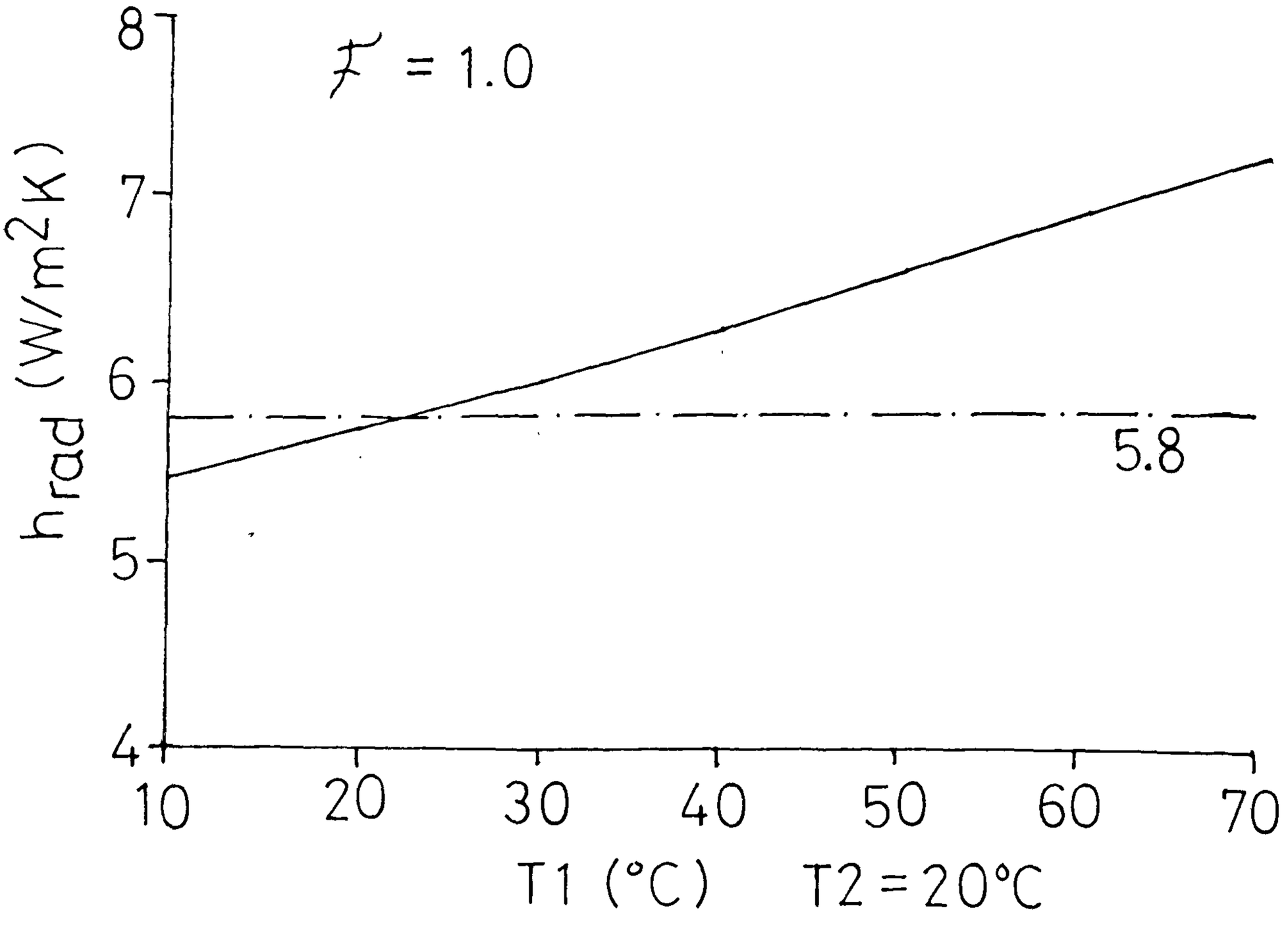

Fig A3.2 - Varition of h_{rad} with Temperature

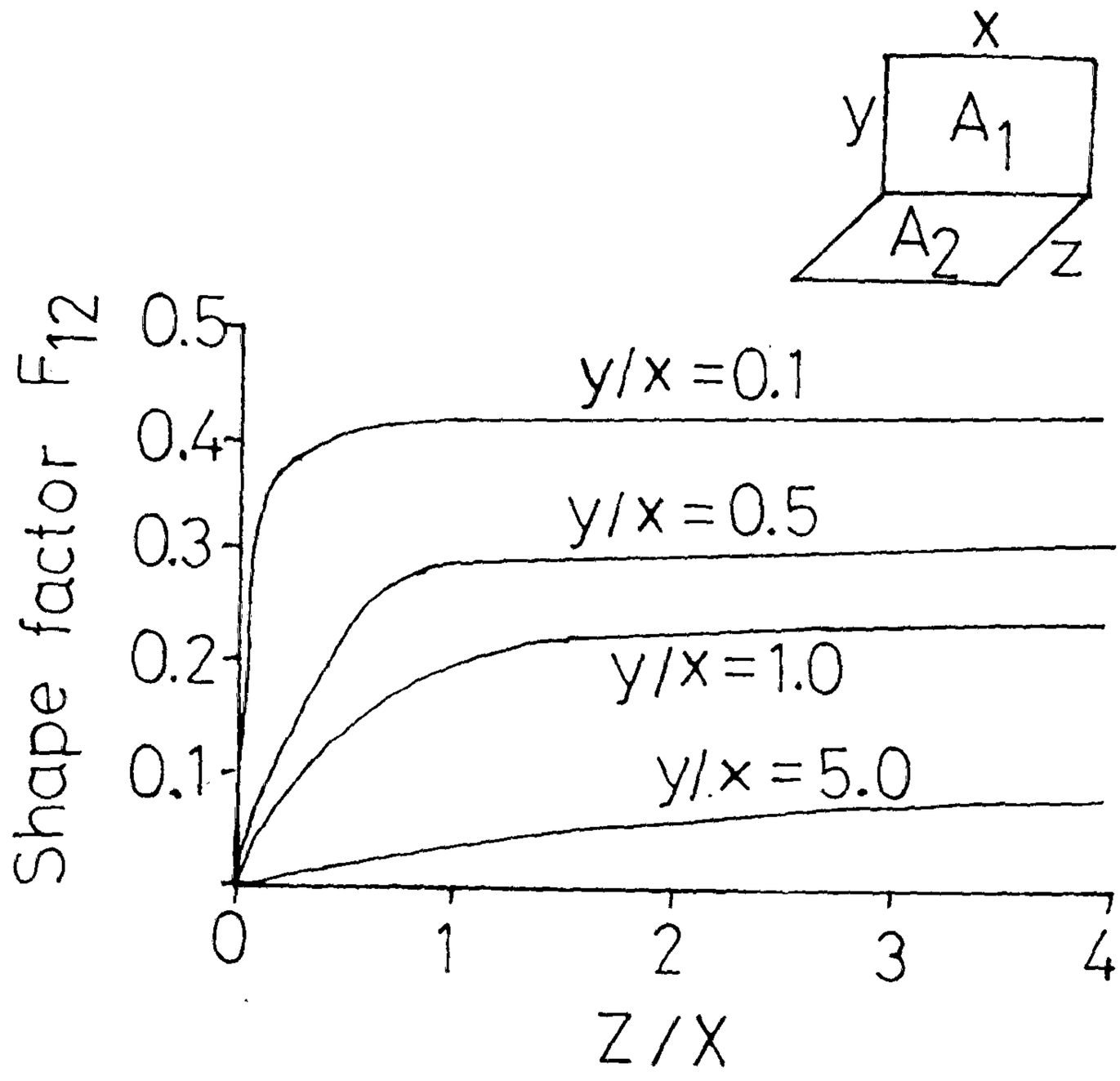

(a) - Adjacent perpendicular planes

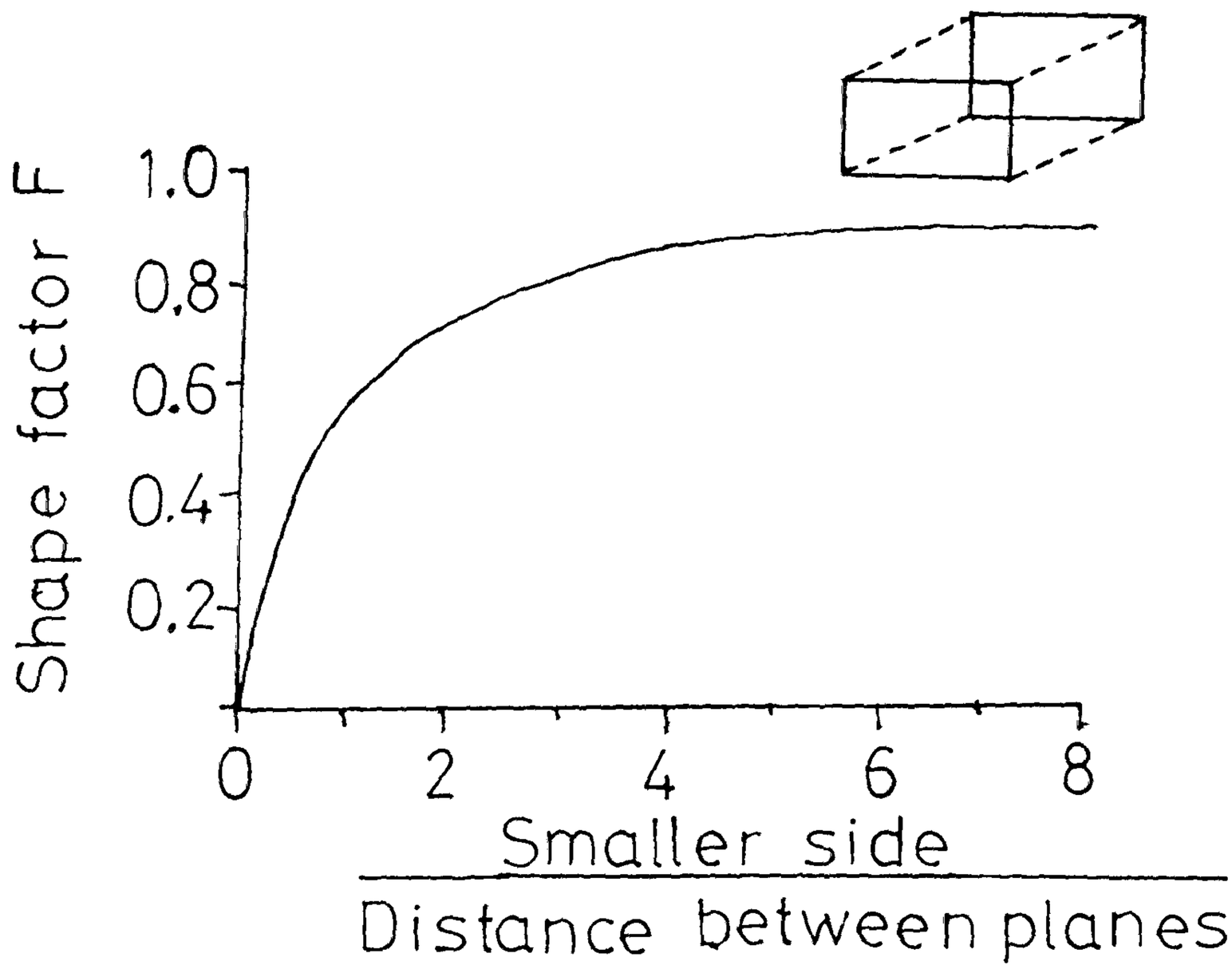

(b) – Parallel identical planes

Fig A3.3 – Calculation of Shape Factors

References

1) Regional Trends, 1984 Edition, Government Statistical Service, HMSO.

2) Paul, J.K. (ed) - Passive Solar Energy Design and Materials, Noyes Data Corporation, 1979.

3) Keller, S.F., Sedrick, A.V. & Johnson, W.G. - Solar Experiments with Passive Retrofit, ASHRAE Journal, Nov 1978, pp.65-68.

4) Lebens, R.M. - Exploring Various Aspects of Passive Solar Energy Collection, With Particular Reference to the Rehabilitation of Ninetenth Century Row Housing in England. MIT M.Arch thesis, Feb.1978.

5) Lebens, R.M. - Passive Solar Heating Design, Applied Science Publishers, 1980.

6) Shurcliff, W.A. - Solar Heated Buildings of North America: 120 Outstanding Examples, Brick House, 1978.

7) The Passive Collection of Solar Energy in Buildings - International Solar Energy Society, UK Section, Conference (C19), London, April 1979.

8) Davies, M.G. - The Contribution of Solar Gain to Space Heating, Solar Energy, 1978, 18 361-367.

9) David, J. - Learning Services, CIBS Journal, 1982, 4(1) 19-22.

10) Performance Monitoring Formats For Solar Heating Systems in Dwellings. Commission of European Communities. Aug.1979. (unadopted)

11) Turrent, D., Doggart, J. & Ferraro, R. - Passive Solar

Heating in the UK. Energy Concious Design, 1980.

12) Houses in the 80's: Energy Systems, Architect's Journal, 16/01/80, pp.143-147.

13) Seymour-Walker, K. - Energy Research and Buildings: Low Energy House Laboratories, BRE News, 46, 1978, p.14.

14) Lee, J. - Development and Optimisation of Trombe's Solar Wall. Leeds University Thesis, Aug.1979.

15) O'Callaghan, P.W. - Building For Energy Conservation. Pergamon, 1978.

16) C.I.B.S. Guide Book A. - The Chartered Institution of Building Services, 1970.

17) Vahid, F. - Theoretical Consideration for the Effect of Rainfall in the Mathematical Models for Simulation of Thermal Behaviour in Houses. Building Services Engineering Research & Technology. 1982, 3 30-34.

18) Basnett, P. - Computer Program - 'HOUSE' User's Guide. Electricity Council Research Centre -, Memorandum, ECRC/MM24, Oct.1974.

19) Jaluria, Y. - Natural Convection Heat and Mass Transfer. Pergamon, 1980.

20) Rohsenhow, W.M & Choi, H. - Heat and Momentum Transfer. Prentice-Hall, 1961.

21) Elder, J.W. - Laminar Free Convection in a Vertical Slot. Journal of Fluid Mechanics, 1965, 23 77-98.

22) Elder, J.W. - Turbulent Free Convection in a Vertical Slot. Journal of Fluid Mechanics, 1965, 23 99-111.

23) Pratt & Karaki - Natural Convection Between Vertical

Plates with External Friction Losses - Application to Trombe Wall. Proceedings of the 3rd National Passive Solar Conference, San Jose, USA, Jan.1979, pp.61-66.

24) Kettleborough, C.F. - Transient Laminar Free Convection Between Heated Vertical Plates Including Entrance Effects. International Journal of Heat and Mass Transfer, 1972, 15 883-895.

25) Whitaker, S. - Elementary Heat Transfer Analysis. Pergamon, 1976.

26) C.I.B.S. Guide Book C., The Chartered Institution of Building Services, 1970.

27) Kronwall, J. - Air Flows in Building Components. Lund Institute of Technology, Sweden, Thesis, 1980.

28) Mason, J.J. & Blower, R. - Selective Conversion Coatings on Nickel and Stainless Steel. Journal de Physique, Colloqium Cl, Supplement 1, 1981, 42 231-245.

29) Milbank, N.O. & Harrington-Lynn, J. - Thermal Response and Admittance Proceedure. BRE Current Paper, CP 61/74, 1974.

30) Duffie, J.A. & Beckmann, W.A. - Solar Energy Thermal Processes. J. Wiley & Sons, New York, 1974.

31) Pilkington 'Insulight' K units. - Trade leaflet, May.1982.

32) Gebhart, B. - Heat Transfer. McGraw-Hill, 1961.

33) Berrett, B. - Passive Use of Solar Energy for Heating Houses. Stephen George & Partners, Sept 1982.

34) Schlicting, H. - Boundary Layer Theory.

McGraw-Hill, 1968.

35) Ashley, S. - Sophisticated Trombe. Journal of CIBS, 1983, 5 No. 6 46.

36) Davies, M.G. - Useful Solar Gains Through a Glazed South Facing Wall in the UK Climate. Building and Environment, 1980, 15 273-282.

37) Borger, T.R. and Akarbi, H. - Free Convective Turbulent Flow Within the Trombe Wall Channel. Solar Energy. 1984, 33 No. 3/4 253-264.

38) Kreith, F. - Principles of Heat Transfer. International Text Book Co. 1965.